# Studies on catalysis by titania

*Thesis submitted to the*
*Cochin University of Science and Technology*
*In partial fulfillment of the*
*requirements for the award of the degree of*

**DOCTOR OF PHILOSOPHY**

**Under The Faculty of Science**

*By*

**Joyes Jacob**

**Department of Applied Chemistry**
**Cochin University of Science and Technology**
**Cochin-682 022, Kerala, India.**

**December 2009**

*To my late parents.....*

DEPARTMENT OF APPLIED CHEMISTRY
COCHIN UNIVERSITY OF SCIENCE AND TECHNOLOGY
KOCHI - 682 022, INDIA
Phone : 0484-2575804, Telex : 885-5019 CU IN, Grams : CUSAT
Fax : 91-484-2575804, E-mail : chem@cusat.ac.in Web: www.cusat.ac.in/dac

14-12-2009

# Certificate

*This is to certify that the research work presented in the thesis entitled "**Studies on catalysis by titania**" is an authentic record of research work carried out by **Ms. Joyes Jacob** under my supervision at the Department of Chemistry, Cochin University of Science and Technology, in partial fulfillment of the requirements for the degree of Doctor of Philosophy in Chemistry and that no part there of has been included for the award of any other degree.*

**Dr. S. Sugunan**
Professor
(Supervising Guide)

# *Declaration*

I hereby declare that the thesis entitled **"Studies on Catalysis by Titania"** is the bonafide report of the original work carried out by me under the supervision of Dr. S. Sugunan at the Department of Applied Chemistry, Cochin University of Science and Technology, and no part thereof has been included in any other thesis submitted previously for the award of any degree.

Joyes Jacob

14-12-2009

Cochin-22

# Acknowledgment

*Joining for Ph.D at the age of 48 was not only a turning point in my life, but also a wonderful experience. I treasured all precious moments shared in the university and would really like to thank all the individual I come across. I wish to express my warm and sincere thanks to all people who have helped and inspired me during my doctoral study. It is a pleasure to convey my gratitude to them all in my humble acknowledgment.*

*I especially want to thank my guide, Prof. Dr.S.Sugunan, for his guidance during my research. His truly scientist intuition has inspired and enriched my growth as a researcher for which exceptionally I am indebted to him more than he knows. It is also a pleasure to mention that I had several opportunities to attend workshops, seminars conducted by eminent scientists just because of my guide's inspiration.*

*I am much indebted to Dr.K.Girish Kumar, present HOD of the Department of Applied Chemistry for his timely help, support and cooperation during the period of this work. Prof. Dr.K.K.Mohammed Yusuff deserves a special thanks as my doctoral committee member and teacher. I am proud to record the meek support given by the former HOD Dr.M.R. Prathapachandra Kurup, Dr.K. Sreekumar and the other faculty members.*

*My heartfelt gratitude to Dr. B.Viswanathan, IIT, Madras for his valuable informations and also for the XPS analysis. I remember with gladness the help I got from the lab of Dr. M.K.Jayaraj of Physics Department and I thank especially Reshmi for the reduction processes.*

*My colleagues at Mar Thoma College ,Tiruvalla have always been a constant source of encouragement during my research . The endless and friendly support when I needed it most, throughout the whole process from my Departmental Colleagues is praiseworthy. Dr.Maries deserves a lot of credit for the success of this research and I am grateful to my friend in every possible way.*

*I gratefully acknowledge your involvement Dr.Sanjay, for your advice, crucial contribution and that intellectual maturity.*

*All my labmates at the Laboratory made it a convivial place to work. In particular, I would like to thank Rajesh for giving me such a pleasant time, his friendship and help in the research period and also to Ajitha teacher, Rose miss,George sir and Dr.Sreedevi who had inspired me in research and life through our interactions during the long hours in the lab. All other folks Reshmi ,Bolie, Ambily,Dhanya, Reni, Nissam ,Mothy ,Temy, Soumini including satheeh and joffrin made me feel young at the age of 50. They offered unlimited help whenever I need them. Many thanks to my students namely Dr. Sreejarani, Sree Prasanth and Joice in Belgium for the analysis, Sreeraj, Neema, Cimi and Noby at the Department of the Applied Chemistry, Sreejith and Swapna of RRL ,Maya for helping me in the literature survey.*

*Furthermore, I owe big gratitude to Dr.Radhika for making me computer-friendly and also Dr.Maya for framing posters, Dr. Kochurani for the visit to IISC Banglore. I would like to thank Dr.Arun, Dr.Ramanathan and Jayakumar for their help in the day-night research in the physical lab. I have also been benefited by the advice and guidance of the present office staff of the Department of Applied Chemistry and of former SO, Mollykutty Sebastian and Librarian Valsala madam.*

*The technical guidance of Dr.Shibu Eapen of STIC, Mr.Suresh of Chemito, Mr.Jose and Mr.Kasmiri of USIC and Mr.Mujeeb for their help during the technical difficulties.*

*Furthermore, I am grateful to come across several life-long friends at work whose names I will never forget. The love and concern of hostel mates, maids and matrons were a comfort and always memorable.*

*Besides, I would like to acknowledge UGC for giving me a chance to do research and support under FIP.*

*My deepest gratitude goes to my family for their unflagging love and support throughout my life; this Ph.D is simply impossible without my husband Reghu, daughters Sharon, Cerene and Zefia. That ray of love is there in me to my sisters and brothers who did a lot in this venture.*

*Last but not least, thanks be to God for my life through all tests in the past few years. You have made my life more bountiful. May your name be exalted, honored, and glorified.*

*Joyes Jacob*

# *Preface*

An earlier Compendium of Chemical Terminology described the notion of catalysis and a catalyst as follows: "*Catalysis is the action of a catalyst*"; and a "*Catalyst is a substance that increases the rate of reaction without modifying the overall standard Gibbs energy change in the reaction*". Some attempts were made in the past to define the term "photocatalysis". Indeed, one of the IUPAC Commissions defined *photocatalysis* as "*a catalytic reaction involving light absorption by a catalyst or a substrate*". In a later revised glossary a complementary definition of a *photo-assisted catalysis* was also proposed: "*catalytic reaction involving production of a catalyst by absorption of light*". Both of these descriptions are less than satisfactory as they lack some, if not many, of the details of the catalytic process. Addition of the extra reactant, namely light, inserts an extra dimension to an otherwise complex issue. The term *photocatalysis* has been characterized in the past by a continued use of labels to describe a variety of mechanistic possibilities for a given process.

Today water resources are the most exploited natural system since man strode the earth.Pollution of water bodies is increasing steadily due to rapid population growth, industrial proliferation, urbanization, increasing living standards and wide spheres of human activities. The large number of water pollutants includes organic like phenolic compounds, dyes, pesticides and synthetic detergents and inorganic, sediments, radioactive materials, thermal pollutants, etc. The World Health Organization (WHO) estimated in 1996 that every eight seconds a child dies from a water-related disease and that each year more than five million people die from illnesses linked to consumption of unsafe drinking water or inadequate sanitation. United Nations declared 2003 as an International Year of Freshwater and also

recommended the proclamation of 2005-2015 as the International Decade on Water for Life.

Briefly narrating, nanocrystalline mesoporous $TiO_2$ catalysts and metal incorporated $TiO_2$ catalysts synthesized by different methods have their unique and often improved mechanical, electrical, optical and chemical properties as compared with conventional catalysts. A comparative activity study is indented in this work to select the best route for the preparation of $TiO_2$ catalysts as well as the best catalytic system among the metal incorporated $TiO_2$ catalysts in pollution abatement such as dye degradation. Thus formulated this thesis into ten chapters including *chemical catalysis* and arrived at the interesting conclusion that metal incorporated $TiO_2$ catalysts give tremendous results in the respective reactions and are eco-friendly catalysts. Last chapter in each section summarizes the investigation and conclusions drawn from the work.

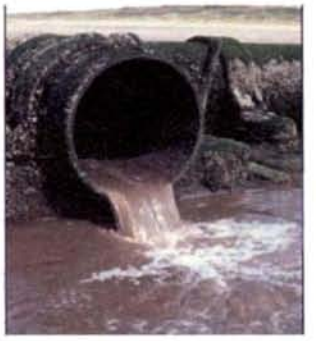

# Contents

## *Chapter* 3

## Physico-Chemical Characterization

## Chapter 4

## Photcatalysis of Ag,Ce and Cu loaded Titania



## Chapter 5

## Photocatalysis of Pt, Pd, Au loaded titania

## Chapter 6

### Summary and Conclusions



## Chapter 7

### Chemical Catalysis



## Chapter 8

### Epoxidation of Cyclohexene



## Chapter 9

### Hydroxylation of Phenol

## *Chapter* 10

## Summary and Conclusions

# Chapter 1

# Introduction

## *Abstract*

Over the years, growing human needs led to industrialization providing amenities to make human life comfortable. However, due to the industrial growth, the pollution of air and water also reached to a degree where new and innovative processes/technologies are required to be developed to check the pollution. Therefore, varieties of techniques have been developed for pollution abatement. Among these processes, photocatalysis systems such as combination of a semiconductor with UV light are a very promising technique. $TiO_2$ nano particles have been extensively studied for oxidative and reductive transformation of organic and inorganic species present as contaminants in air and water. This chapter deals with a brief account of the history of catalysis, photocatalysis, semiconductor photocatalysis, $TiO_2$ and the applications. The oxidation of organic substrates represents one of the most important industrial chemical reactions, explaining the significant efforts invested in the research and development of new heterogeneous catalysts with increased activities and selectivities in these type reactions. Therefore liquid phase reactions like epoxidation of cylcohexene and hydroxylation of phenol were discussed using $CeO_2/TiO_2$and $CuO/TiO_2$ catalysts. The oxidation products of these reactions are important in fine chemical industry, pharmaceuticals etc.

## 1.1.0 Catalysis

Presently we are faced with the challenge of cleaning our natural water and air resources. While we enjoy the comforts and benefits that chemistry has provided us, from composites to computer chips, from drugs to dyes, we are faced with the task of treating wastes generated during manufacturing processes and the proper disposal of various products and byproducts. Catalysis was not a phenomenon which was developed in recent years but which was associated with the life itself. Basic understanding of this phenomenon and its utilization *in vitro* has happened in the last two centuries. Considering our necessities and commodities available, we have to depend on catalytic reactions. Why? Because catalytic processes are more environmental friendly. Needs only low temperature, highly selective to the desired product and/or target our interest, environmentally clean, less expensive compared to other processes and easily controllable.

A clear understanding of the development and utilization of the catalyst and catalysis was possible through the technological advancements in basic spectroscopy and other devices which have thrown light on its structural and mechanistic aspects. Catalysts play key role in the production of clean fuels, the conversion of waste and raw materials into energy, clean combustion engines including control of $NO_X$, soot production and reduction of green house gases, production of clean water and of polymers as well as reduction from polymers to monomers. Tremendous pressure is currently exerted on chemical manufacturing industry to develop new synthetic methods that are environmentally more acceptable in this catalysis field. Photocatalysis play a leading role in this situation and is presently existing in industry front as a pollution abatement technic. It is an

eco-friendly method of producing fine chemicals. Sustainable energy source like sun can be used which leads to the production of hydrogen and oxygen by the conventional redox reaction. A naturally occurring photocatalysis phenomenon is photosynthesis that is known since prehistoric times without any knowledge of the intrinsic mechanisms of plants growth.

### 1.2.0 Photocatalysis

The term *photocatalysis* has been characterized in the past by a continued use of labels to describe a variety of mechanistic possibilities for a given process. Understanding heterogeneous photocatalysis has necessitated a suitable description of (i)what photocatalysis is, (ii) what turnover quantities are (numbers, TON; rates, TOR; frequencies, TOF ) and (iii) how quantum yields $\Phi$ can be established for a seemingly very complex heterogeneous system. The turnover quantities, while being relatively understood in homogeneous photocatalysis, are not simple parameters to estimate and thus have required further considerations in heterogeneous photocatalysis as they necessitate knowledge of the number of photocatalytically active sites for TON and TOR[1]. In the early 1980s, Salomon[2]proposed that the broad description of photocatalysis be subdivided into two main classes: (i) *photogenerated catalysis*, which is catalytic in photons, and (ii) *catalyzed photolysis*, which is non-catalytic in photons. In photogenerated catalysis, ground states of the catalyst and of the substrate are involved in the thermodynamically spontaneous (exoergic) catalytic step. By contrast, in catalyzed photolysis either the nominal catalyst T or the substrate

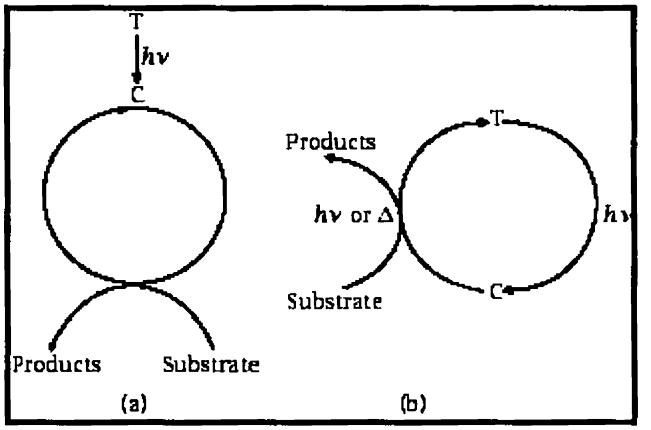


**Fig 1.1** — C is the catalytic entity

or both are in an excited state during the catalytic step. Note that T is the nominal catalyst and C denotes the catalytic entity. Teichner and Formenti [3] described heterogeneous photocatalysis as an increase in the rate of a thermodynamically allowed (G< 0) reaction in the presence of an irradiated solid with the increase (in rate) originating from the creation of some new reaction pathways involving photocreated species and a decrease of the activation energy. In this sense, one could argue that many of the reactions involving irradiated semiconductor photocatalysts belong to the class of photogenerated catalysis. Several photoreactions that take place in the presence of semiconductor particles and that have been claimed to be photocatalytic may in fact be described more appropriately as semiconductor-assisted photoreactions [4]. Thus Photocatalysis can be described as a change in the rate of chemical reactions or their initiation, under the action of light in the presence of substance– called photocatalyst - that absorbs light quanta and takes part in the chemical transformation of the reaction participants or a photocatalyst is a substance that produces

electron-hole pairs by absorption of light quanta and makes chemical transformations of the reaction participants that come into contact with it, and regenerates its chemical composition after each cycle of such interactions. A photocatalytic process occurs via the following steps [**5**]:

- Generation of electron-hole pairs by exciting a semiconductor with radiation of a suitable energy
- Separation of electron-hole pairs by traps that have trapping rate higher than the recombination rate
- Redox reaction by separated electrons and holes with adsorbed substrates, according to thermodynamic and kinetic constraints
- Evolution of products and regeneration of the surface.

This working mechanism for the photocatalytic process can be defined as a chemistry of "redox mechanism" and the role of light is mainly to excite the solid, which must essentially be a semiconductor.

Photocatalytic degradation of environmental contaminants using semiconductor photocatalyst has been studied widely over the past three decades. Historically, the discovery of photo-electrolysis of water directly into oxygen at a $TiO_2$ electrode and hydrogen at a Pt electrode by the illumination of light greater than the band gap of $TiO_2$ (3.2 eV) is attributed to Fujishima and Honda in early 1972 [**6,7**] though photocatalysis by ZnO and $TiO_2$ has been reported much earlier by Markham in 1955. The works of Carry et al. has proved that the semiconductor catalysts have a potential to decompose many organic compounds, conversion of inorganic anions and metal removal [**8**]. Due to faster electron transfer to molecular oxygen, $TiO_2$ is found to be more efficient for photocatalytic degradation of pollutants[**9**].

### 1.2.1 Semiconductor

Semiconductors are electronic conductors with electrical resistivity values generally in the range of $10^{-2}$ to $10^{9}$ ohm-cm at room temperature, intermediate between conductors ($10^{-6}$ ohms-cm) and insulators ($10^{14}$ to $10^{22}$ ohm-cm) [10]. At absolute zero temperature, pure and perfect crystal of most semiconductors will be an insulator. In a semiconductor, the highest occupied energy band is called the valence band (VB) and lowest empty energy band is called the conduction band (CB). These two bands are separated by an energy band called band gap ($E_{BG}$). Figure 1.2 shows the band structure and band filling in metal, insulator, and semiconductor. In intrinsic semiconductor, conduction band is close to the valence band.

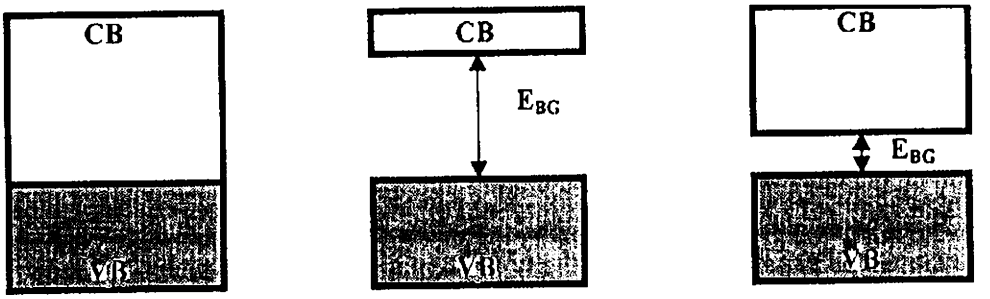


**Fig1.2 Schematic representation of the band structure in (a) metal (b) insulator (c) intrinsic semiconductor**

There are two types of semiconductors, n-type in which majority charge carriers are electrons and p-type in which majority charge carriers are holes. Semiconductors can be made conductive either by putting extra electrons into the conduction bands, or by removal of an electron from the valence band that creates a positively charged hole. The hole can be regarded as the mobile entity because annihilation of a hole by a nearby electron effectively moves the hole over in space. The energy of the most

energetic electrons in the partially filled band is called Fermi level. In a p-type semiconductor, Fermi level lies just above the valence band edge, and in an n-type semiconductor, the Fermi level lies just below the conduction band edge as shown in Figure 1.3.

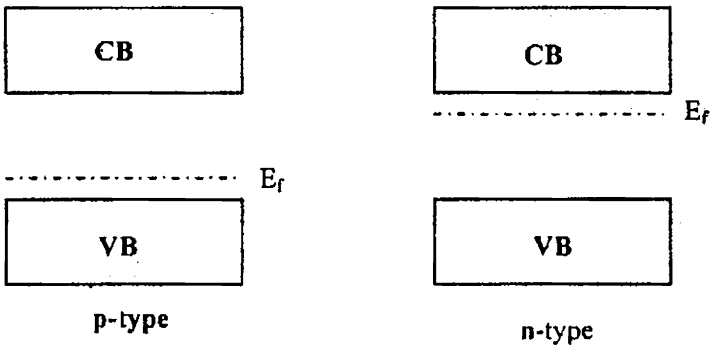


**Figure 1.3: Fermi levels in p- and n-type semiconductors.**

In semiconductors, mobile charge carrier can be generated by three different mechanisms:

1) **Thermal excitation**: If the band gap energy is sufficiently small (less than half an electron volt) thermal excitation can promote electron from valence band to the conduction band.
2) **Photoexcitation**: In this case, an electron can be promoted from the valence band to the conduction band upon absorption of a photon of light, provided that the photon energy is greater than or equal to the band gap energy.
3) **Doping**: It is a process of introducing new energy level into the bandgap. Two types of doping can be distinguished. For n-type doping (with group III elements like B, Al, Ga, and In), occupied donor levels are created near the conduction band edge where current is carried mainly by negative charge carriers. Likewise, p-type doping (with group V elements like P, As, Sb, and Bi)corresponds to the formation of empty

acceptor levels near the valence band, creating positive charge carriers where current is carried mainly by positive charges. The surface defects and impurities in n type or p-type semiconductors are responsible for the change in bandgap of the semiconductor.

### 1.2.2 Semiconductor Photocatalysis

A single particle of semiconductor can provide both oxidizing and reducing species for the reaction. Semiconductors like $TiO_2$, ZnO, $Fe_2O_3$, CdS and ZnS can be used as photocatalyst for the waste water treatment and polluted air purification [**11-20**].Semiconductors can act as sensitizer for light-induced processes. Absorption of a photon of energy greater than the bandgap energy leads to the formation of an electron-hole pair. In the absence of suitable scavengers, the stored energy is dissipated within few nanoseconds by recombination [**21**]. If a suitable scavenger or surface defects state is available to trap electron or hole, recombination is prevented and subsequent redox reaction may occur. The valence band holes are powerful oxidants (+1.0 to +3.5V vs. NHE depending on the semiconductor and pH), while the conduction band electrons are good reductants (+0.5 to -1.5V vs. NHE) [**22**]. Most organic photodegradation reactions utilize the oxidizing power of the holes either directly or indirectly. Semiconductor photocatalysis is an emerging technique valuable for water and air purification and remediation. Fundamental and applied research on this subject has been performed extensively during the last 30 years all over the world [**23-27**]. Nowadays, the main goal of research and development in semiconductor heterogeneous photocatalysis which is a part of Advanced Oxidation Processes (AOPs) used for air and wastewater treatment [**5**].

### 1.2.3 Semiconductor Photocatalysts

Metal oxides and sulphides represent a large class of semiconductor materials suitable for photocatalysis [**24-26**]. Fig 1.4 lists some selected semiconductor materials, which have been reported to be used for photocatalytic reactions,with their VB and CB potentials, bandgap energy.

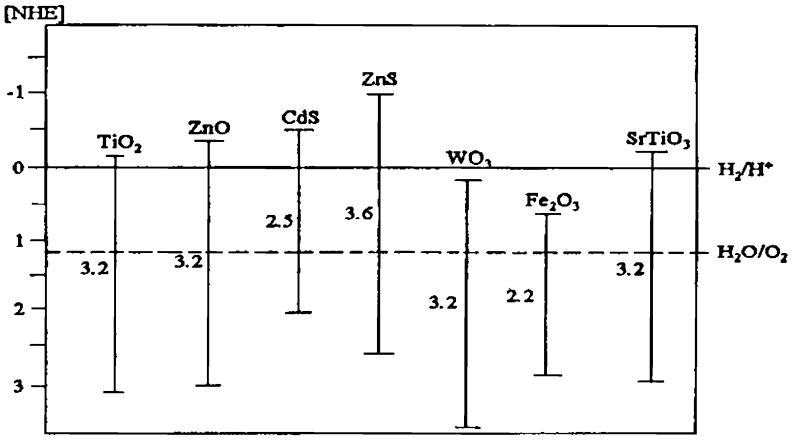


**Fig 1.4. Energy levels of various semiconductors**

Among these listed semiconductors, $TiO_2$ has proven to be the most suitable for wide spread environmental applications [**11,15,18,28**].In spite of this vigorous activity and the search for the "ideal" photocatalyst for more than two decades, titania has remained as a benchmark against which any emerging material candidate will be measured. Titanium dioxide is biologically and chemically inert; it is stable to photo- and chemical corrosion and is inexpensive. Furthermore, $TiO_2$ is of special interest since it can use natural (solar) UV radiation. This is because $TiO_2$ has an appropriate energetic separation between its valence and conduction bands, which can be surpassed by the energy of a solar photon. The VB and CB energies of the $TiO_2$ are estimated to be +3.1 and -0.1 volts, respectively, which means that its band gap energy is 3.2eVand therefore absorbs the

near UV light ($\lambda$<388nm). Due to faster electron transfer to molecular oxygen, $TiO_2$ is found to be more efficient for photocatalytic degradation of pollutants [**29**]. The band position of some common semiconductor photocatalysts in aqueous solution at pH =1 are shown

| Semiconductor | Valence Band ( V vs. NHE) | Conduction Band (V vs.NHE) | Band gap (eV) | Band gap Wavelength (nm) |
|---|---|---|---|---|
| $TiO_2$ | +3.1 | -0.1 | 3.2 | 388 |
| $SnO_2$ | +4.1 | +0.3 | 3.9 | 318 |
| ZnO | +3.0 | -0.2 | 3.2 | 388 |
| ZnS | +1.4 | -2.4 | 3.7 | 335 |
| $WO_3$ | +3.0 | +0.2 | 2.8 | 443 |
| CdS | +2.1 | -0.4 | 1.4 | 496 |
| CdSe | +1.6 | -0.1 | 1.7 | 729 |
| GaAs | +1.0 | -0.4 | 1.4 | 886 |
| GaP | +1.3 | -1.0 | 2.3 | 539 |

**Table 1.1 Band Position of Common Semiconductor Photocatalyst atpH=1**

Although ZnO has characteristics similar to $TiO_2$ and seems to be a suitable alternative to $TiO_2$, it dissolves in acidic solutions and therefore cannot be used for technical applications [**30**].Other semiconductor particles (CdS or GaP) absorb larger fractions of the solar spectrum than $TiO_2$ and can form chemically activated surface-bond intermediates, but unfortunately, such catalysts get degraded during the repeated catalytic cycles usually involved in heterogeneous photocatalysis.

### 1.2.4 The Structure of $TiO_2$

There are four polymorphs of $TiO_2$ found in nature; rutile (tetragonal), anatase (tetragonal), brookite (orthorhombic), and $TiO_2$ B (monoclinic). Other structures exist as well, for example cotunnite $TiO_2$ has been synthesized at high pressures and is one of the hardest polycrystalline materials [31].In 1982 Rosemeyer ;1993, Morad and Aldahan have found the co-existing nature of rutile, anatase and brookite [32]. In 1986 Post and Burnham calculated that the rutile is more stable than anatase by less than 4 KJ/mole and more stable than brookite by approx 20 KJ/mole at low temps [33]. Particle size experiments suggest that, in $TiO_2$ crystals less than a few tens of nanometers in diameter, the anatase is more stable than rutile due to surface energy effects in 1997 by Gribb and Banfield [34]

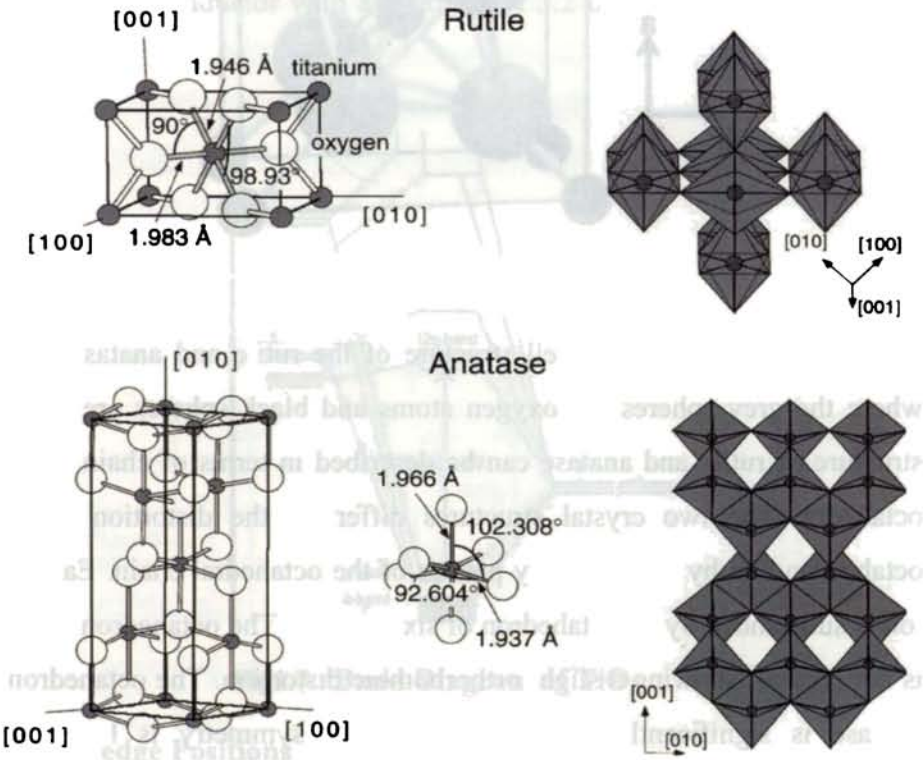


**Fig1.5 Bulk structures of Rutile and Anatase $TiO_2$.**

However, only anatase and rutile play role in all the applications of $TiO_2$. Figure 1.5 shows the bulk structures of rutile and anatase $TiO_2$. The energy bandgap of anatase (3.2 eV, 388 nm) and rutile (3.02 eV, 411 nm) combines with the valence band position to generate highly energetic holes at the interface giving rise to easy oxidation reactions. Anatase has been found, in most of the cases, to be photocatalytically more active than rutile [25,35-38] .

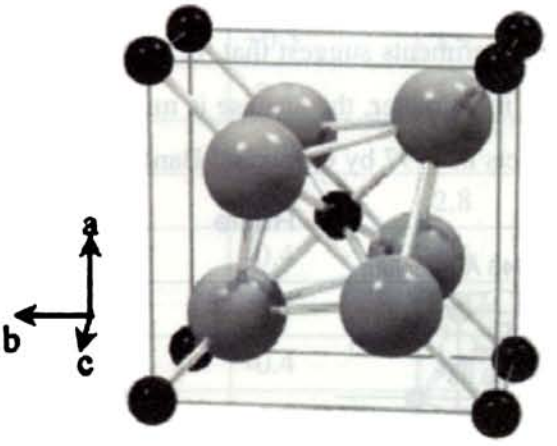


**Fig 1.6 Unit cell of $TiO_2$**

Figure 1.6 shows the unit cell structure of the rutile and anatase crystal where the grey spheres are oxygen atoms and black spheres are Ti. The structure of rutile and anatase can be described in terms of chain of $TiO_6$ octahedra. The two crystal structures differ by the distortion of each octahedron and by the assembly pattern of the octahedral chain. Each $Ti^{4+}$ ion is surrounded by an octahedron of six $O^{2-}$ ions. The octahedron in rutile is not regular, showing a slight orthorhombic distortion. The octahedron in anatase is significantly distorted so that its symmetry is lower than orthorhombic. In rutile structure each octahedron is in contact with 10 neighbour octahedron each (two sharing edge oxygen pairs and eight

sharing corner oxygen atoms) while in the anatase structure each octahedron is in contact with eight neighbours (four sharing an edge and four sharing a corner) [39]. Among the two crystalline phases of anatase and rutile, anatase is believed to possess enhanced photocatalytic and photoelectrochemical conversion performances probably because of its open structure compared with that of rutile [25,40].

### 1.2.5 Electronic Properties of $TiO_2$

The titanium has no electrons in its valence shell when it is in the oxidation state of +4, resulting in an empty $t_{2g}$-band. The band gap is the gap between the filled p-band(valence band) and the empty $t_{2g}$-band (conduction band). The empty $t_{2g}$ and completely filled p-band of $TiO_2$ makes the semiconductor with a bandgap of 3.2 eV which falls in the UV region.

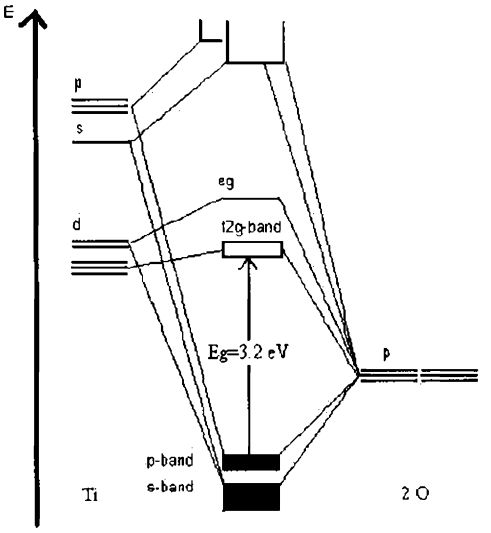


**Fig1.7 Band Diagram of $TiO_2$**

### 1.2.6 Band edge Positions

The indication of the thermodynamic limitation for the photoreaction that can be carried out with the charge carrier will be

understood by knowing the band positions or flat band position of the semiconductors. In order to photo-reduce a chemical species, the conduction band of the semiconductor must be more negative than the reduction potential of the chemical species and to photo-oxidise a chemical species, the potential of the valence band of the semiconductor must be more positive than the oxidation potential of the chemical species. The ordinate in Figure 1.8 denotes the internal energy and not free energy. The free energy of an electron-hole pair is smaller than the energy of the band gap. The reason for this behaviour is that the electron-hole pairs have significant configurationally entropy arising from the large number of translational states accessible to mobile carriers in the conduction and valence band. $TiO_2$ has it band edge at -0.1 V and +3.1 V with respect to NHE. The band gap and band edge position with reference to NHE for a number of ionic and covalent materials in the bulk state are given Figure1.8. The data refer to the conditions where the semiconductor is in contact with the aqueous redox electrolyte at pH=1.

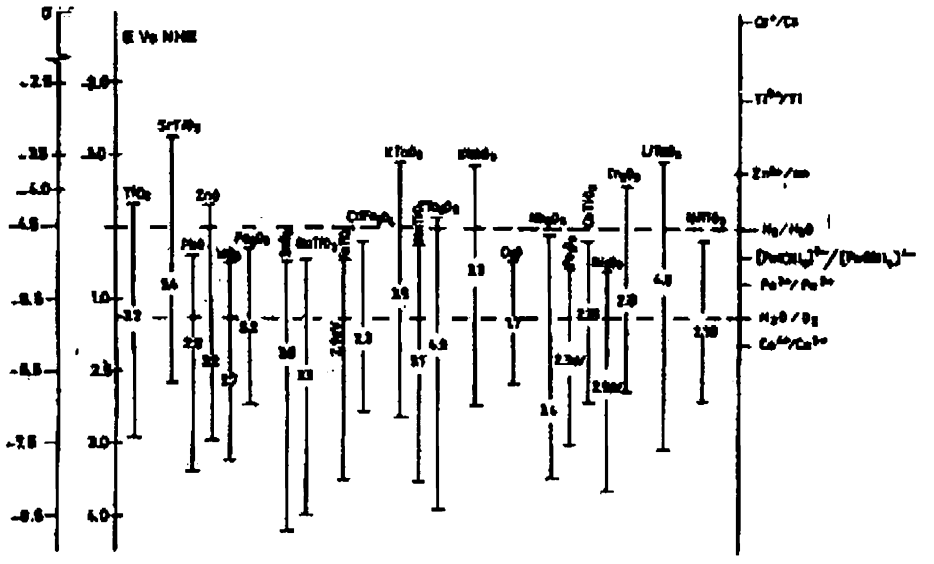

Fig 1.8 The positions of bands of semiconductors relative to the standard potentials of several redox couples (shown at the right hand side of the figure). The positions of the valence and conduction band of semiconductors appear favourable for one or the other of the redox reaction of the cleavage of water.

### 1.2.7 Space charge Layer and Band Bending

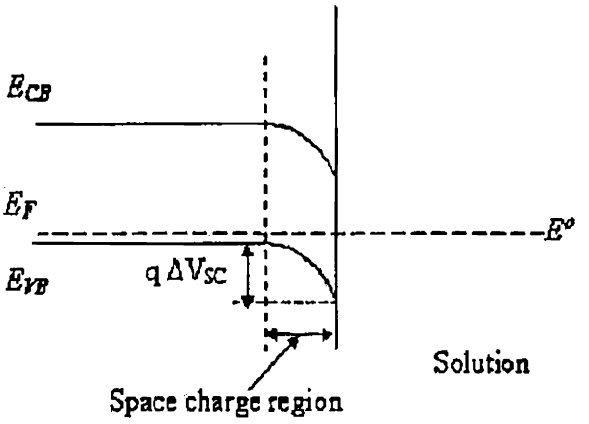


**Fig 1.9 Space charge region on the semiconductor**

Space charge layer plays a crucial role in photocatalytic reactions. The generation of a space charge layer requires the transfer of mobile charge carriers between the semiconductor and the electrolyte. For bulk semiconductor in contact with liquid medium, the charge transfer can only take place in the presence of an electroactive species acting as electron donor or acceptor. Thus, an interfacial redox reaction is required to produce the electric field within the semiconductor. The term space charge layer is used to define an electrically charged region of narrow width, typically $10^{-5}$- $10^{-3}$ cm, extending from the surface of semiconductor into its bulk phase. Often such a layer forms spontaneously as a consequence of charge between the semiconductor and the electrolyte. Or unlike metals, semiconductors have energy gap, which restricts the recombination of photgenerated electron–hole pair. The field is penetrated into the bulk to a few angstroms called space charge layer. Within the space charge layer, the valence and conduction bands are bent. When the semiconductor is placed in vacuum the bands are usually flat. When the semiconductor is allowed to contact with solution or the metal, band bending occurs. The double layer is formed at the semiconductor-solution interface and the transfer of mobile

charge carrier between semiconductor and solution produces the space charge layer. If there is no space charge layer, the electrode is at the flat band potential. When the semiconductor is doped with the transition metals or any other species, it will affect not only the Fermi energy level but also the thickness of the space charge region. The thickness of the Garrett space charge region is inversly proportional to the carrier concentration. ie..as carrier concentration increases the thickness of the space charge region decreases [41]. Normally lower activity is observed when semiconductor is used alone; this is due to the high recombination rate of the electron–hole pair. When the semiconductor surface is doped with an appropriate metal, the rate of recombination reduces to a greater extent and the photocatalytic activity is correspondingly enhanced. Depending upon the redox potential of the substrate, one can tune the redox properties of the semiconductor by doping with metals. In the case of n-type semiconductor, the surface was enriched by negative charge .In order to maintain the electrical neutrality positive space charge layer has been formed in the semiconductor, which results in band bending. The direction of band bending depends on the nature of the excess charge present on the surface of the semiconductor [42].In band bending, four different situations may arise [43]. These are illustrated in Figure1.10and 1.11 for a n-type semiconductor in contact with the electrolyte. If charges are accumulated at the semiconductor side which have the same sign as the majority charge carriers, one obtains an accumulation layer. If on the

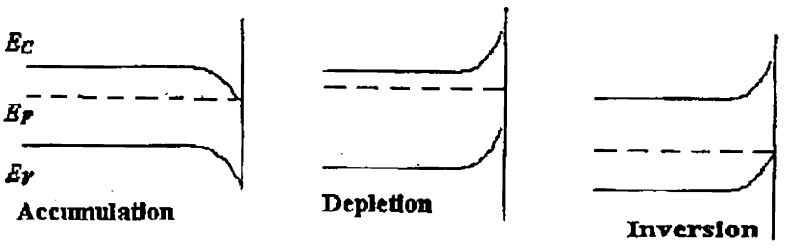


**Fig 1.10 Band bending at the interface**

other hand, majority charge carrier deplete into the solution, a depletion layer is formed. The excess space charge within this layer is given by immobile ionized donor states. The depletion of majority carrier can go so far that their concentration at the surface decreases below the intrinsic level. If the electronic equilibrium is maintained, the concentration of holes in this region of the space charge layer exceeds that of electrons. As a consequence, the Fermi level is closer to the valence band than the conduction band and the semiconductor is p-type at the surface and n-type in the bulk called an inversion layer. When the semiconductor is in contact with an electrolyte containing a redox couple, the Fermi level adjusts to equilibrate with potential of redox species. Contact between the semiconductor and electrolyte results in Schottky barrier. The electric field of this barrier induces spatial separation between electron and hole by driving the photo generated electron and hole in opposite directions, resulting band bending at the interface or for efficient photocatalytic reaction, the electron- hole pair recombination must be suppressed either trapping the photogenerated electron or hole or both can lead to this. When semiconductor particle is exposed to light with energy greater or equal to band gap (the energy difference between the minimum of conduction

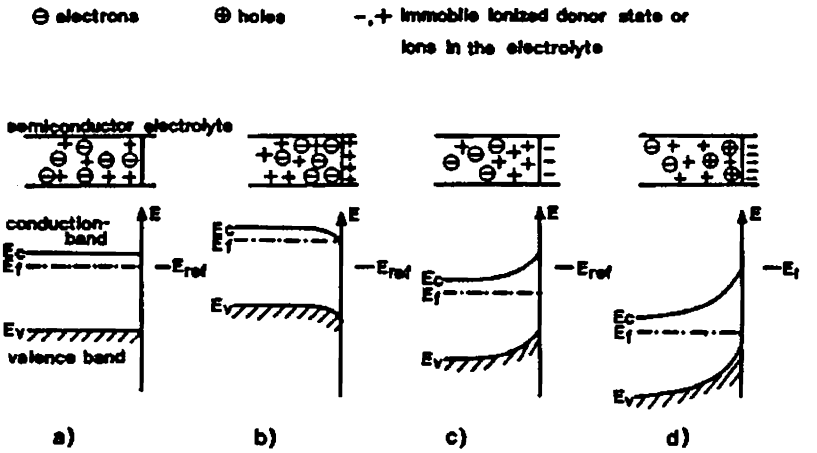


**Fig 1.11** Space charge layer formation at the n-type semiconductor-Solution interface: (a) flat band potential (b) accumulation layer (c) depletion layer (d) inversion layer.

band edge and the maximum of valence band edge) it leads to the creation of electron-hole pairs. Under the influence of the electric field, this electron-hole pair moves into the surface of the conduction and valence band respectively. The electron in the conduction band moves to the surface and reduction reaction takes place either with adsorbed molecule or the surface groups. The depletion layer at the semiconductor-solution interface, sometimes referred to as Schottky barrier, plays an important role in light induced charge separation which is discussed in detail in this chapter.

### 1.2.8 Mechanism of Semiconductor Photocatalysis

When semiconductor photocatalyst is irradiated with light having energy hv higher than the bandgap energy, $E_{BG}$, light absorption process creates an electron in the conduction band (CB) and a hole

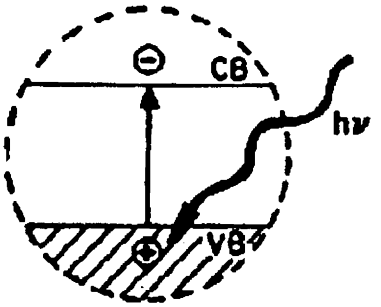


**Fig 1.12 Mechanism of Photocatalysis on a semiconductor**

in the valence band (VB), which can then diffuse and/or migrate to the semiconductor's surface and react as depicted in the Fig 1.12.The possible events these photogenerated electron–hole pairs may undergo are given in Fig1.13

(a) recombination in the bulk

(b) recombination at the surface

(c) reduction of a suitable electron acceptor , A adsorbed on the surface by the photogenerated electron

(d) oxidation of a suitable electron donor , D adsorbed on the surface by the photogenerated hole.

The electron hole pairs recombine to generate heat and if this is the only process that occurs, the semiconductor will show no photoactivity. Electron hole recombination is promoted by defects in the semiconductor material and thus most amorphous semiconductor materials show little photoactivity. If, however, the photogenerated electron and hole are able to make their separate ways on to the surface of the semiconducting material then it is possible for these to interact with surface species.

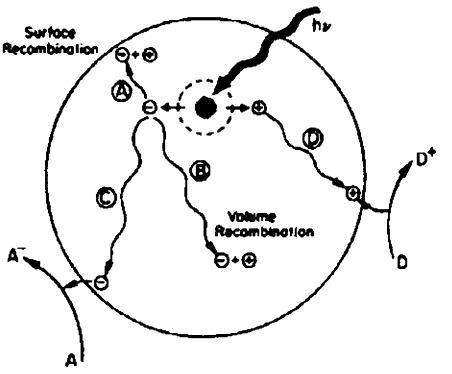


**Fig1.13 Processes on the Photo-excited semiconductor Surface and Bulk [44]**

Under these circumstances, if an electron donor D molecules such as ethanol, methanol and EDTA (Ethylene diamine tetra acetic acid), is present at the surface, then the photogenerated hole can react with these molecules to generate an oxidized product, $D^{+}$. Similarly, if there is electron acceptor A molecules present at the surface, such as oxygen or hydrogen peroxide, then the photogenerated electrons can react with them

to generate a reduced product, $A^-$. The overall reaction can be summarized as follows:

$$A + D \xrightarrow[h\upsilon \geq E_{BG}]{\text{Semiconductor}} A^- + D^+ \qquad \textbf{Reaction 1.1}$$

The above basic electron–hole generation, transport and transfer processes are also illustrated in Figure 1.14[**45**]. Many of the current commercial systems that utilize **Reaction 1.1** employ the semiconductor photocatalyst such as $TiO_2$ to drive oxidation of organic pollutants by oxygen i.e. photomineralization of pollutants. $TiO_2$

Organic pollutant + $O_2$ $\rightarrow$ $CO_2 + H_2O +$ mineral acids **Reaction 1.2**

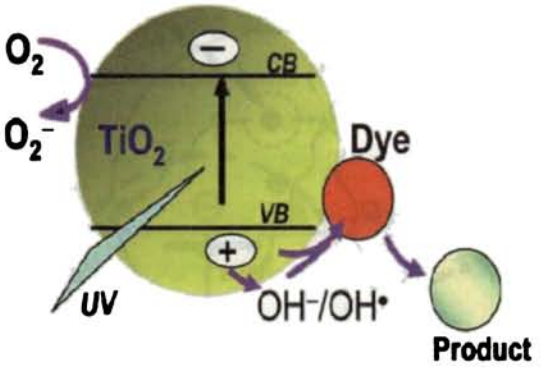


**Fig 1.14 Schematic illustration of the major processes on $TiO_2$**

It may be noted that, for **Reaction 1.2** only mineral acids are generated, if there are any hetroatoms such as sulphur, nitrogen or chlorine present in the original organic pollutant. In photomineralisation, ultra-bandgap light generates electron-hole pairs. Photogenerated holes that make it to the surface can react with surface hydroxyl groups to generate adsorbed hydroxyl radicals ($OH^•$) which in turn can oxidise the pollutant molecules such as dyes. Photogenerated electrons that make it to the surface can react with adsorbed oxygen to generate superoxide anion ($O_2^{•-}$)

which can be subsequently reduced to hydrogenperoxide and then water. The intermediate species hydroperoxides($HO_2^{\bullet}$)produced can act as a further source of hydroxyl radicals ($OH^{\bullet}$). In photomineralisation of organic materials sensitized by $TiO_2$ as depicted by **Reaction 1.2**, the photogenerated electrons reduce water to oxygen and the photogenerated holes mineralise the organics. The latter process appears to involve the initial oxidation of surface hydroxyl groups on the $TiO_2$ to hydroxyl radicals which then oxidise the organics and any subsequent intermediate or intermediates [**23-25,30,45**]. The reduction of oxygen by photogenerated electrons generate superoxide anion($O_2^{\bullet -}$) as an initial reduction product. The latter species can be further reduced to hydrogen peroxide, which is intermediate in the overall reduction of oxygen to water. Hydrogen peroxide is, of course, also a possible source of hydroxyl radicals and it appears likely that during the course of **Reaction 1.2** some of the mineralisation of the organic pollutant is brought about by oxidising species such as hydroxyl radicals generated via the reduction of oxygen by photogenerated electrons [**23-25,30,45**].

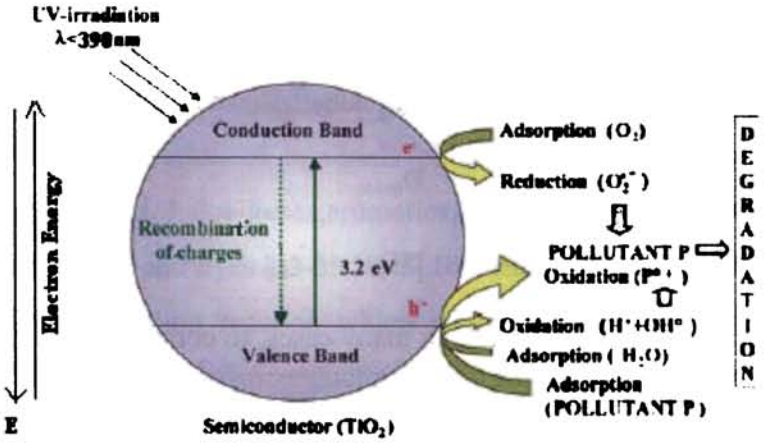


**Fig 1.15 Photocatalytic redox reactions**

As shown in Figure 1.15 When a photon of energy higher or equal to the bandgap energy is absorbed by a semiconductor particle, an electron from the valence band (VB) is promoted to the conduction band (CB) with simultaneous generation of a hole ($h^+$) in the valence band (VB). The electrons in CB ($e^-_{cb}$) and the holes in the valence band ($h^+_{vb}$) can recombine on the surface or in the bulk of the particle in a few nanoseconds or can be trapped in surface states where they can react with donor (D) or acceptor (A) species adsorbed or close to the surface of the particle. The energy values of the valence band and conduction band are standard redox potential (NHE). The efficiency of a photocatalyst depends on the competition of different interface transfer processes involving electrons and holes and their deactivation by recombination. The semiconductor photocatalytic process is a complex sequence of reactions that can be expressed [**46,47**] by the following set of equations:

$$TiO_2 \xrightarrow[h\upsilon \geq E_{BG}]{\text{Semiconductor}} TiO_2(e_{cb}^-, h_{vb}^+) \rightarrow \text{recombination}$$

$$TiO_2(h_{vb}^+) \rightarrow H_2O^-_{ads} \rightarrow TiO_2 + HO^{\cdot}_{ads} + H^+$$

$$TiO_2(h_{vb}^+) + HO^-_{ads} \rightarrow TiO_2 + HO^{\cdot}_{ads}$$

$$TiO_2(h_{vb}^+) + D_{ads} \rightarrow TiO_2 + D^+_{ads}$$

$$HO^{\cdot}_{ads} + D_{ads} \rightarrow D_{oxide}$$

$$TiO_2(e^-_{cb}) + A_{ads} \rightarrow TiO_2 + A^-_{ads}$$

The oxidative pathway leads, in many cases, to complete mineralisation of an organic substrate to $CO_2$ and $H_2O$. Generally, A is dissolved $O_2$, which is transferred in superoxide radical anion ($O_2^{\cdot-}$) and can lead to the additional formation of $HO^{\cdot}$.

$TiO_2$ ( $e^-_{cb}$) + $O_{2ads}$ + $H^+$ → $TiO_2$ +$HO_2^{\cdot}$ ↔ $O_2^{\cdot -}$ + $H^+$

$HO_2^{\cdot}$ + $TiO_2$ ( $e^-_{cb}$) + $H^+$ → $HO_2$

$2HO_2^{\cdot}$ → $H_2O_2 + O_2$

$H_2O_2 + O_2^{\cdot -}$ → $HO^{\cdot} + O_2 + HO^-$

$H_2O_2$ + hν → $2HO^{\cdot}$

$H_2O_2$+ $TiO_2$ ( $e^-_{cb}$) → $HO^{\cdot} + HO^-$

In general, it is usually assumed that the organic pollutant in water or air does not undergo direct hole transfer, although there is some evidence that this process does occur in some cases (at least to some extent) but rather that oxidation takes place through a surface-bound hydroxyl radical ($Ti^{IV}OH^{\bullet +}$) **[50]**. Electron-hole recombination on most semiconductor materials is usually very fast, e.g. typically less than 10 ns for $TiO_2$. However, if a hole scavenger is added to a semiconductor colloid, it is possible to remove some of the photogenerated holes and effectively trap the photogenerated electrons for a sufficient time to allow their transient absorption spectrum to be recorded. Similarly, if an electron scavenger is added, the transient absorption spectrum of trapped photogenerated holes can be determined. The semiconductor photocatalysis proved effective in the complete mineralisation of hundreds of organic materials including many alkanes, alkenes, haloalkenes,aromatics, haloaromatics, insecticides, pesticides, detergents and dyes [**23-25,30,45**].**Reaction 1.2** is an example of a photocatalytic oxidation reaction which is often abbreviated as PCO. Although there are many semiconducting materials, only a few are very effective as semiconductor photocatalysts. Ideally, a semiconductor photocatalyst should be chemically and biologically inert, photocatalytically active, easy to produce and use, activated by sunlight and cheap. In fact, not

surprisingly, no semiconductor fits this list of ideal specifications, although semiconductor, titanium dioxide, $TiO_2$, comes close to them. Thus, $TiO_2$ displays features of an ideal semiconductor photocatalyst with the exception that it does not absorb visible light.$TiO_2$ has a large bandgap 3.2 eV and therefore, is only a UV light absorber and as a consequence is limited to absorbing a small fraction, ca. 10% of the solar spectrum . Despite this limitation, its positive features far outweigh this, and so $TiO_2$ has become the semiconductor material widely studied in the field of semiconductor photochemistry. Most of the early work in semiconductor photocatalysis, focused mainly on the photomineralisation of organics dissolved in aqueous solution as explained by **Reaction 1.2** while usually employed semiconductor is in the form of a powered dispersion. As a result, a number of commercial devices currently in market utilize $TiO_2$ in the form of powder dispersion.

### 1.3.0 Synthesis of Nanocrystalline Mesoporous $TiO_2$

The advancement in this field of photocatalysis is the synthesis of nanostructured mesoporous oxides with improved catalytic efficiency. Recently much attention was drawn to the preparation of titania powders with mesopores ,namely mesostructured titania which was proved to have high catalytic activity . The advent of supra-molecular chemistry has given a new thrust to this field of porous solids. The mesoporous materials with different compositions, new pore systems, and novel properties have attracted considerable attention because of their remarkably large surface areas and narrow pore size distributions, which make them ideal candidates for catalysis[48].Nano particle is a challenge as the material properties change drastically resulting from the particle size[49]. Nanocrystalline mesostructured $TiO_2$ photocatalyst can be synthesized by using different

surfactant templating methods with a narrow meso pore size distribution and controlled pore structure **[50–52].** Most of the earlier studies of photocatalytic degradation of pollutants in air and water were carried out with standard P25 Degussa $TiO_2$. Some of the researchers had tried to synthesize the $TiO_2$ by various methods to enhance the photocatalytic activity. Factors considered in photocatalysis are band gap and band positions ,redox level of the substrate, solution pH etc.. It has also been reported that the photocatalytic activity depends on the physical properties such as surface area **[53,54]**,crystal structure**[55]**, crystallite size**[56]** and surface hydroxyl groups**[57]**.It is reported that anatase phase of $TiO_2$ as compared to rutile phase is more active for the photocatalytic degradation of organic pollutants in wastewater and air**[58-60]**.

### 1.4.0 Metal Doped Semiconductor

Several attempts has been made to lower the band-gap energy of $TiO_2$,but no appreciable change in the band-gap energy of $TiO_2$ was observed**[61-63].** Though, $TiO_2$ is more photoactive among the studied catalytic materials, it is less active in the visible region due to its high band gap(3.2 e V).For the same reason ,the light absorption will take place at < 390 nm (UV region).Since the solar spectrum consists of only 10 % UV light , the efficiency of the process is very poor. Inorder to overcome this, various attempts have been made to activate the $TiO_2$ in the visible region. Normally lower activity is observed when semiconductor is used alone, this is due to high recombination rate of electron–hole pair. When semiconductor surface is doped with an appropriate metal, the rate of recombination reduces to a greater extent and the photocatalytic activity is correspondingly enhanced**[64-68]** as the rate of electron transfer from semiconductor to metal is faster than self-recombination rate. According to Frank–Condon principle the electron transfer reaction takes place faster

than any other reaction and the rate depends on the density of the energy states on both sides of the interface. The photocatalytic activity varies with respect to parameters like nature of the metal (higher electron affinity metal), method of metal loading, extent of metal loading and nature of the semiconductor. Mainly there are two methods followed for metal loading on semiconductor namely impregnation method[**69-71**]and photocatalytic deposition method [**72**].The amount of metal loading should be optimum for better photocatalytic activity .The higher loading of the metal results in the formation of a very narrow space charge region, so that the penetration of light into the semiconductor is greately hindered in the space charge layer ,thereby increasing the recombination rate[**73**].Usually the metal should have high electron affinity and it should have suitable work function to form ohmic contact with the semiconductor. This can be explained on the basis of metal-semiconductor interface. Two types of contacts are possible for metal-semiconductor interface like(1). Schottkey barrier (2).Ohmic contact

### 1.4.1 Schottkey Barrier

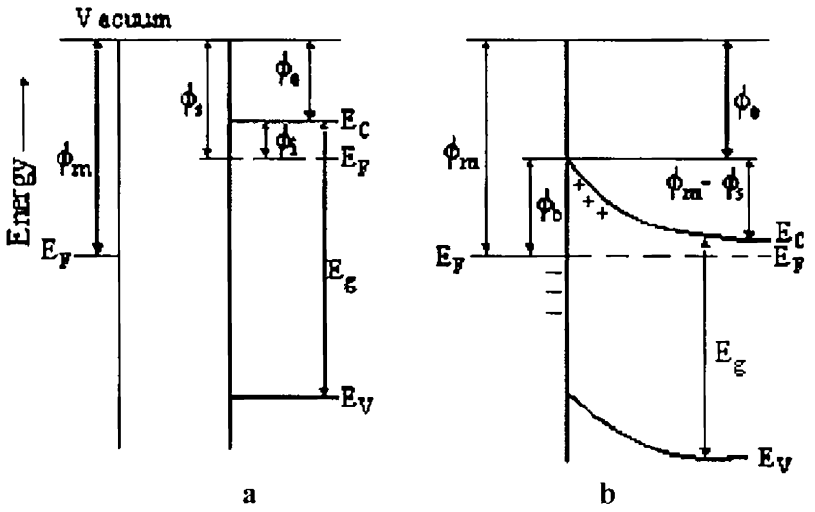


**Fig. 1.16 Formation of Schottkybarrier on metal-semiconductor interface**

If a metal and semiconductor are brought together the energy levels of both metal and semiconductor are readjusted. If the work function of the metal is greater than the semiconductor, the electrons will flow from the semiconductor to the metal until fermi levels of both becomes equal. Energy levels of the semiconductor and the metal before and after the contact made are shown in fig 1.16 a and b. $\Phi m$ and $\Phi s$ are the work functions of the metal and semiconductor respectively. $\Phi s = \Phi e + \Phi i$ ($\Phi e$ is the electron affinity measured from the bottom of the conduction band and $\Phi i$ is energy difference between Fermi level and conduction band)[74].Excess positive charge is accumulated in the semiconductor due to the electron transfer from semiconductor to metal, the distribution of this positive charge results in creation of Schottkey barrier. The barrier restricts the flow of electrons from semiconductor to metal.

### 1.4.2 Ohmic Contact

In ohmic contact, when the work function of the metal is less than that of the n-type semiconductor ($\Phi m < \Phi s$) the contact behaves in a different manner. In this case electron flow from metal to semiconductor resulting in accumulation of negative charge in semiconductor and downward bending of conduction band occurs as shown pictorically in fig 1.17 a and b. The electron can then move in either direction depending on the applied potential (positive or negative).

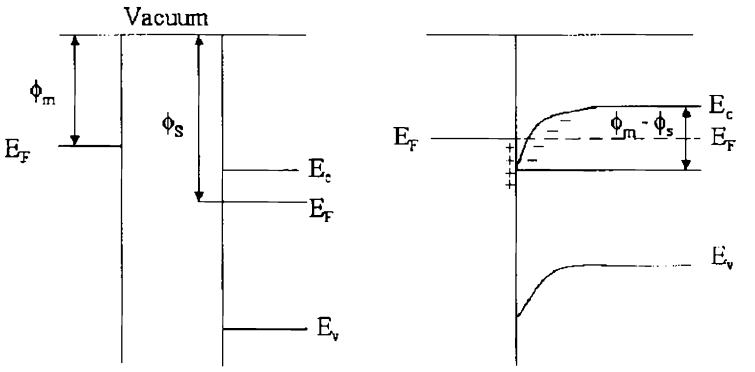


**Fig.1.17 Formation of Ohmic contact**

### 1.5.0 Factors Affecting Semiconductor Photocatalysis

### 1.5.1 Catalyst Concentration

In semiconductor photocatalysis, the reactions are carried out either in static or in slurry or dynamic flow photoreactor. The initial reaction rates are directly proportional to the catalyst mass (m) indicating a true heterogeneous catalytic regime. However, above a certain m limit value, the reaction rate levels off and becomes independent of m. This limit depends on the nature of the compound to be treated and on the geometry and working conditions of the photoreactor corresponding to the maximum $TiO_2$ concentration in which all the particles (i.e. the entire surface exposed) are totally illuminated. At higher catalyst concentration, a screening effect of exceeding particles masks part of the photosensitive surface. The optimal catalyst concentrations that ensure a total adsorption of efficient photons for $TiO_2$ range from 0.1 to 5.0 g $l^{-1}$ [75-78].

### 1.5.2 Initial Substrate Concentration

Generally, the degradation kinetics of compounds follows a Langmuir-Hinshelwood mechanism with a reaction rate ($r$) varying

proportionally to the fraction of surface covered by the substrate (θ) as follows:

$$r = k\,\theta = k\,(KC / 1 + KC)$$

where $k$ is the reaction rate constant, $K$ is the compound adsorption constant and $C$ the initial compound concentration. For diluted solutions, $KC$ becomes << 1 and the reaction is of apparent first order whereas for higher concentrations, KC >>1 and the reaction rate is maximum and of zero order [**79-81**].

### 1.5.3 Temperature and pH

Most of the photocatalytic reactions are not sensitive to small variations in temperature. Very few cases have shown Arrhenius dependence during detoxification [**19**]. However the pH of the aqueous solution significantly affects the particle size, the surface charge, and the band edge positions of the $TiO_2$ due to its amphoteric character [**82**]. The Zero Point Charge (pH pzc) or pH at which the surface of an oxide is inert, for $TiO_2$ is known to be close to 6.8. Above and below this value, the catalyst is negatively or positively charged according to Equations 1.13 and 1.14 respectively. In consequence the photocatalytic degradation of organic compounds is affected by the pH.

$$TiOH_2^+ \leftrightarrow TiOH + H^+ \qquad \text{Reaction 1.13}$$

$$TiOH \leftrightarrow TiO^- + H^+ \qquad \text{Reaction 1.14}$$

### 1.5.4 Light intensity

It has been reported that degradation rate is proportional to light intensity which confirms the photo-induced nature of the catalytic process activation with the participation of photoinduced electrical charges in the

reaction mechanism [**83**]. However, at high light intensity, the degradation rate becomes proportional to the square root of this parameter [**84**].

### 1.5.5 Oxygen

The rates and efficiencies of photo-assisted degradation of organic substrates are reported as significantly improved in the presence of oxygen or by the addition of several oxidizing species such as peroxydisulfate or peroxides [**11, 85**]. The oxygen concentration dependence has been reported due to the involvement of $O_2$ adsorption and depletion, both in the dark and during illumination at the photocatalyst surface. Molecular oxygen acts as a conduction band electron trap, suppressing totally or partially the surface electron-hole recombination. The superoxide anion ($O_2^{\bullet -}$) formed is an effective oxidant agent.

### 1.5.6 Adsorption of Substrate Molecules on Semiconductor

One important consideration in the $TiO_2$ photocatalyzed reactions is the adsorption of the organic compounds on the surface of the semiconductor particles. The Langmuir type relationship between degradation rates and initial organic compound concentrations indicates that adsorption plays a role in the photocatalytic reaction. However, this role on the photocatalyzed degradation rate is still uncertain.

### 1.5.7 Inorganic ions

Some anions commonly found in natural or polluted waters (e.g., chloride, bromide, sulphate, phosphate) have an inhibiting effect on the photodegradation process if they are bound to $TiO_2$ or are close to its surface [**19,86**]. Consequently, the pH and pH pzc should be the determining properties for the ions effect, as well as the chemical affinities of the ions for $TiO_2$. Significant inhibition in the degradation rate of

different compounds has been observed in presence of chloride at pH=3 [85]. According to Equation 1.15 at acidic pH, $TiOH^{2+}$ and TiOH are the main species on the catalyst surface and the chloride ions compete with organic compounds for active sites lowering the degradation rates. At higher pH, the negatively charged catalyst surface Equation 1.16 repulse the approach of chloride ions and no inhibiting effect is observed. Nitrate ions with charge similar to that of chloride, only slightly inhibit the reaction at pH=3, indicating the role of individual ions.

### 1.6.0 Application of Semiconductor Photocatalysis

Semiconductor photocatalysis is unequivocally accepted as best technology for the complete mineralization of organic pollutants and it is adopted by many chemical industries for waste water treatment. The highlighting aspect of semiconductor photocatalysis is that a wide spectrum of pollutants can be mineralized by this method. Researchers had applied this technique over a variety of commonly known organic pollutants. Textile finishing mills discharge waste water containing a great variety of organic contaminants in a wide range of concentration. The release of this colored waste waters poses a major problem for the industry as well as threat to the environment[87,88].The number of dyes presently used in dye industry is about 10,000.Among these dyes, azo dyes constitute the largest and the most important class of commercial dyes[89].For the treatment of these dyes common treatment processes as well as biological process is ineffective. Air pollutants are present in the atmosphere in concentrations that disturb the dynamic equilibrium in the atmosphere and thereby affect man and his environment. This may cause skin cancer and eye irritation, affects central nervous system etc., [90].Thus industrial wastes or exhausts, combustion of fuels, petro chemical complexes and storage and usage of

organic solvents are the root cause of environmental pollution. $TiO_2$is a protective against environmental damages and used as air cleaners, self cleaning ceramic tiles, side-view mirrors, car body coating [91]. One of the earliest examples of the application of semiconductor photocatalysis as a method of disinfection as effective in sensitizing the photokilling of bacteria was the work of Matsunaga et al. [30]. However, under UV light irradiation the super-hydrophilic property of $TiO_2$ where the contact angle becomes smaller depending on the irradiation time surfaces never become cloudy, even in the rain. This remarkable function can also be applied for the production of new mirrors that can be used in bath areas and the side mirrors of cars. Researchers in Japan and Hong Kong are testing construction materials coated with titanium dioxide to see how well they can fight pollution. In Hong Kong, concrete slabs coated with titanium dioxide removed up to 90 percent of nitrogen oxides from older cars and diesel trucks and a contributor to smog, acid rain and other environmental headaches are some of the recent applications.

### 1.7.0 Literature Survey

Heterogeneous photocatalysis is an advanced oxidation process (AOP), which can be successfully used to oxidize many organic pollutants present in aqueous systems. During the past 30 years of research and development in the area of semiconductor photocatalysis have been very tremendous. Photocatalytic degradation involves the use of certain semiconductors as catalysts for the production of the radicals mentioned in the mechanism and has proven to be an effective method for mineralizing commercial dyes without having any of the drawbacks. This research is aimed on the degradation of dyes because they represent an increasing market share and a large fraction of the applied reactive dye is wasted due

to dye hydrolysis in the alkaline dye bath, and finally, conventional wastewater treatment plants have low removal efficiency for reactive and other anionic soluble dyes [**92**]. Experimental observations indicate almost complete oxidation of most of the organic compounds to $CO_2$, $H_2O$ and inorganic anions via photocatalytic processes.[**93,94**]. A new class of reactive adsorbents obtained by pyrolysis of individual and mixed industrial sludges were used as media for the removal of cationic(Basic Fuchsin) and anionic (Acid Red 1) dyes [**95**]. Due to indestructibility of some of the organics, a post treatment is necessary to remove the organics from the contaminated environment [**96**].Izumi *et al.* (1980) have used platinised (10% by weight) $TiO_2$ to decompose benzoic acid and adipic acid. They proposed a photo-Kolbe type reaction mechanism for the oxidation process [**97**].

Photocatalysis of anatase thin film coated PAN fibers prepared at low temperature is a very interesting piece of work[**98**].Photocatalytic oxidation of natural materials such as glucose, ethanol, cellulose, food stuffs and wood have been studied by Kawai and Sakata [**99**].Photocatalytic degradation of eight azo dyes was conducted in basic medium, by Maria S.T.Gonqalves *et al.* studying the influence of various amounts of $TiO_2$ and different light sources, a medium pressure (400 W) and a low pressure (16 W) Hg vapour lamps and lamps for household purposes. Decolourisation extents ,observed ,are related to dye structure [**100**]. A. Fujishima and X. Zhang briefly discussed some fundamental studies on $TiO_2$ photocatalysis, summarize the present commercialization of $TiO_2$-based products, and highlight several points for the future development of $TiO_2$ photocatalysis in their paper[**101**]. It reports that a significant number of pesticides,[**102,103**] photocatalytic degradation of atrazine on nanoparticulate films, dye compounds and surfactants can be completely oxidized (mineralized) and a

variety of bacteria and viruses have been killed by irradiation with near ultraviolet light in the presence of $TiO_2$.

Several reviews have been published[**19,104,105**] discussing the underlying reaction mechanisms and illustrating examples. A report of D. M. Blake provides a comprehensive bibliography of work available in the open literature for scientists and engineers interested in the use of heterogeneous photocatalytic oxidation or reduction processes in environmental remediation, This reports also includes properties and application of photocatalytic chemistry in organic synthesis [**106**]. Several semiconductors such as CdS, CdSe, WO3, ZnO, $SnO_2$ and $TiO_2$ have been used for environmental cleanup [**12-13, 15-20, 107**]. A kinetic study on photocatalytic degradation of C.I. Acid Yellow 23 by ZnO photocatalyst has been effective[**108**].Metal-doped titania systems are effective in enhancing the photocatalytic activity, Nano-Ag particles doped $TiO_2$ for efficient photodegradation of Direct azo dyes is given[**109**].In a recently published work, Synthesis, characterization and of different Metal-doped titania systems with improved photocatalytic activity is discussed [**110-112**] .Enhancement of photo induced hydrogen production from irradiated $Pt/TiO_2$ suspensions with simultaneous degradation of azo-dyes is informative.[**113-115**]. Different metal ions such as Fe, Cu, Co, Cr, Mo, Ce, V, W, Mn, Ag, Nd, Pd and Ni were doped on the surface of $TiO_2$ [**116-126**].A large number of articles are available on the photocatalytic activity and decolorization and degradation of dye solutions and wastewaters in the presence of $TiO_2$ .

### 1.8.0 Aim and Scope of the Present work

Irradiation of $TiO_2$ can initiate the oxidation of most organic molecules and the final product of such oxidation is normally $CO_2$, $H_2O$,

and inorganic ions. Commercial P25 $TiO_2$(Degussa P-25) is most commonly used for photocatalytic degradation of organic compound in water. This catalyst has limitations like

1. Wide bandgap of 3.23 eV .
2. Smaller surface area (50±15 $m^2gm^{-1}$).
3. Difficult to separate from treated water.
4. Photo-oxidation of aromatic compounds is not so fast

The main objective of the present work is to develop a more active catalyst to overcome some of the above mentioned limitations with special thrust to

1. Development of highly photoactive (visible) photocatalyst by a simpler method.
2. Development of catalyst with higher surface area.
3. Enhancement of prepared catalyst by impregnation of metal ions exchange.
4. Study of the photocatalytic activity in pollution abatement especially dyes.

In photocatalytic degradation, the size of the catalyst is an important factor affecting the catalytic activity of the catalyst[**127-129**]. A crystal size of about 10-11 nm is believed to be the optimum size for photocatalytic application[**130**].The structural and electronic properties of the semiconductor photocatalyst can undergo significant changes as the particles size decreases, whereby the properties of planar, edge and corner sites changes as the size of catalyst become smaller, these structural changes can directly affect catalyst activity. The $TiO_2$ photocatalyst, being a semiconductor, also exhibits discretion of its electronic band structure as

the particle size shrinks [131,132]. This is known as quantum size effect and has been observed for nanometre-sized $TiO_2$ particles [134].

Therefore most of the research has been focused on reduction of $TiO_2$ particle size. Different preparation methods such as sol-gel, Hydrothermal, self-assembly, Impregnation, co-precipitation, Deposition-precipitation, Chemical vapour deposition are reported by several researchers [135-140] to synthesize nanoparticles of titania. Nowadays researchers have developed techniques to prepare anatase $TiO_2$ nanorods and nanofibers [141,142]. Work had been reported in which the absorption band of $TiO_2$ is shifted to visible region by incorporating noble metals. [143,144]. Enhanced photocatalytic activity has been achieved by using Pt and Pd metals for the degradation [145]. This research work aimed at developing catalyst through a best method whichcould satisfy all the above requirements to produce efficient catalytic activity. Thus the present work in photocatalysis includes

1. Selection of a route by loading metals like Ag, Ce, Cu .
2. Incorporation of noble metals in the selected route .
3. Degradation studies in different Dyes.

Three routes selected for the preparation of the catalysts were sol-gel, hydrothermal and Evaporation Induced Self Assembly (EISA)and a comparative study of the catalysts in these different routes were carried out using the degradation of Methylene Blue dye after incorporating metals like Ag, Ce and Cu. The best route which satisfy the above requirements of the catalyst is selected and the noble metals like Pt, Pd and Au are incorporated in to the titania matrix and the effect of degradation in the dyes like methylene blue(MB), malachite green(MG), Acid Orange7(AO7), Acidblue 25(AB25)and Acid Red-1(AR1)were studied. The catalysts like

$TiO_2$-$CeO_2$ and $TiO_2$-CuO were used in some reactions in chemical catalysis .Thus liquid phase reactions like Epoxidation of Cyclobenzene and Phenol Hydroxylation were conducted using the mentioned catalysts.

### 1.9.0 Methods of Preparation

The correct sampling, sample preparation, choice of the support and appropriate method are important in heterogeneous catalysis and are one of the major challenges in today's research [**146**]. According to Ardson, "catalyst preparation is the secret in achieving the desired activity, selectivity and life time" [**147**]. In recent years, major advances have been made on techniques for physically and chemically characterizing supported catalyst and on the quantitative and qualitative aspects of catalyst preparation, so that the design of supported catalysts has become a feasible activity [**148-151**] .The preparation methods of catalysts have been reported to affect the activity of the mixed oxide systems [**152-154**]. Some of the methods are discussed below.

### 1.9.1 Sol-Gel Process

The Sol–Gel (SG) technique has emerged as a promising processing route for the synthesis of nano-sized particles [**155-166**]. The process involves first the formation of a sol followed by that of a gel. A sol, which is a liquid suspension of solid particles ranging in size from 1nm to 1 micron, can be obtained by the hydrolysis and partial condensation of molecular precursors, such as an inorganic salt or a metal alkoxide. The hydroxylation is achieved either by varying the pH or by hydrolyzing alkoxide precursors in an organic solvent. Further condensation of sol particles into a three-dimensional network produces a gel, which is a diphasic material with a solid encapsulating a solvent. The encapsulated liquid can be removed from a gel by either evaporative drying with

supercritical extraction and the resulting solid products are known as a xerogel and an aerogel respectively. Increased chemical homogeneity in multicomponent systems is the advantage of sol-gel method. The disadvantages of this process are long processing time, large shrinkage, and possibility of large agglomerate formation.

### 1.9.2 Hydrothermal Treatment (HT)

Low-Temperature routes have attracted a great deal of interest for a number of years now [167-170].This method is also called the autoclave method. Subcritical conditions are often used in hydrothermal synthesis, typically temperatures less than $250^0$ C, and the use of a sealed autoclave produces mild, autogeneous pressures (around 20 atm). This pressure is to nucleate and regulate the growth of the particles. In this method the reaction path is very sensitive to the experimental conditions such as temperature, pH, duration of treatment [171]. A surfactant is used as the shape controller or template. Shape evolvement was elucidated by quenching the reaction at different stages. Microemulsion hydrothermal treatment route is advantageous over the other routes as the size of the particles can be affected by the ratio of surfactant to water [172].

### 1.9.3 Evaporation Induced Self Assembly Method (EISA)

Thermally stable mesoporous titania can be synthesized following a different synthesis route ie. Evaporation induced self assembly method. Mesoporous materials have high surface areas and high pore volumes because of the large dimensions of the pores. But one of the major drawbacks in the synthesis of mesoporous titania is the high reactivity of the the initial titanium compounds toward hydrolysis and condensation. If this reactivity is not tempered, a poorly organized structure will be formed .The high reactivity of the precursors can be efficiently be controlled by pH

adjustment and complexation effects. Controlled amount of water is added to a non-aqueous solvent, leading to a specific formation of the mesoporous structure. Such a combination was first reported by P.Yang et al [173].

### 1.9.4 Impregnation

One of the most frequently used methods to achieve deposition of the active component precursor over high surface area support is impregnation. This technique consists of introducing, into the pore space of a support, a solution of an inert precursor, i.e. one that does not interact with the solid surface. In principle, the precursor thus remains in the dissolved state in the solution and does not become fixed on the surface at this stage of preparation. Incipient wetness impregnation is used for precious control of the amount of the deposition.

### 1.10.0 Chemical catalysis

### 1.10.1 Heterogeneous Catalytic Oxidation

Catalytic oxidation is widely employed in the manufacture of bulk chemicals from aromatics and more recently, as an environmentally attractive method for the production of fine chemicals. The oxidation of organic substrates represents one of the most important industrial chemical reactions, explaining the significant efforts invested in the research and development of new heterogeneous catalysts with increased activities and selectivities in these type reactions. Compared with other chemical processes the oxidation process is complex and difficult to be controlled or to be stopped at a certain stage. For these reasons the selective oxidation is an attractive field of research. Organic compounds such as phenols and phenolic derivatives are amongst the most common chemicals which form a major threat to the ecological balance on account of their poor biodegradability. A possible solution to this problem consists in using

technology based on catalytic oxygen transfer from "clean" oxygen donors, such as hydrogen peroxide ($H_2O_2$). Mixed oxides containing transition metal oxides are becoming popular in heterogeneously catalyzed oxygen transfer reactions in the liquid phase using hydroperoxides. The use of hydrogen peroxides in the oxidation of organic molecules is a major goal, both in academic and in industry, because of the environmental acceptability of this oxidant, which depends mainly on the nature of its by-product, water. Among commonly used oxidants such as dioxygen, $H_2O_2$ and alkyl hydroperoxide(TBHP), $H_2O_2$ is an attractive one since it is easy to handle, have high content of active oxygen, non-toxicity, and non-polluting property and produces only water as the co-product**[174-179]**. TBHP can oxidize organic compounds effectively and is a waste-avoiding oxidant when it is used in a controlled manner without organic solvents and other toxic compounds. In fact, there is a trend to use $H_2O_2$ as an oxidant for large volume processes such as caprolactam synthesis and propylene oxidation. One of the major advantages of the $H_2O_2$ oxidation is the high tenability of the reaction parameters**[180-182]**. In this work, catalytic oxidation reactions like epoxidation of cyclohexene and hydroxylation of phenol were dealt with. The products of these reactions are important in fine chemical industry, pharmaceuticals etc., Cyclohexene epoxide is of great technical importance as it is applied in the modification of epoxy resin properties and the synthesis of new polymers, copolymers and solvents. Catechol and hydroquinone are two of the many phenolic derivatives of high value. They are widely used as photography chemicals, anti-oxidants and polymerization inhibitors and are also used in pesticides, flavoring agents, and in medicine. Oxidation reactions were carried out in liquid phase using hydrogen peroxide as well as alkyl hydrogen peroxide as oxidants. Effect of change in catalyst composition, temperature and duration on oxidation has been discussed thoroughly.

## References


1. N. Serpone, A. Salinaro, A. V. Emeline, V. K. Ryabchuck, J. Photochem &Photobiol. A: Chem. 130 (2000) 83.
2. R. G. Salomon, Tetrahedron. 39 (1983) 485.
3. S. J. Teichner, M. Formenti, Photoelectrochemistry, Photocatalysis andPhotoreactors, M.Schiavello (ed.), Reidel,Dordrecht,(1985) 457.
4. L. P. Childs, D. F. Ollis, J. Catal. 66 (1980) 383.
5. M. Schiavello , Photocatalysis and environment, Kluwer Academic Publishers, London.
6. A.Fujishima, Hashimoto K, Watanabe T. $TiO_2$ photocatalysis: fundamentals and applications. Tokyo: BKC, Inc., (1999).
7. A. Fujishima, K. Honda, Nature. 238 (1972) 37.
8. J.H. Carey, J. Lawrence, H. M. Tosine, Bull. Environ. Contam. Toxicol. 16 (1976) 697.
9. (9)N.Daneshvar,, D.Salari, A.R.Khataee, J.Photochem .Photobiol. A 162(2004) 317.
10. C. Kittle, Introduction to Solid State Physics, Wiley Eastern Limited, New Delhi(1976).
11. O. Legrini, E. Oliveros, A.M. Braun, Chem. Rev. 93 (1993) 671.
12. A. P. Davis, C.P. Huang, Wat. Res. 24 (1990) 543.
13. C.Kormann, D..Bahnemann, M. R..Hoffmann,J.Photochem. Photobio A:Chem. 48 (1989) 161.
14. D. F. Ollis, A. L. Pruden, Environ. Sci. Technol. 17 (1983) 628.
15. R. W. Mathews, Wat. Res. 24 (1990) 653.
16. A. Scalfani, L. Palmisano, E. Davi, New J. Chem. 14 (1991) 265.
17. J. -M. Herrmann, Catal. Today 24, (1995) 157.
18. J. -M. Herrmann, Trends Photochem. Photobiol. 3, 2 (1994) 633.
19. J. -M. Herrmann, C. Guillard, P. Pichat., Catal. Today 17, (1993) 7.
20. D. H. Kim, M. A. Anderson, J. Photochem. Photobiol. A: Chem. 94 (1996)221.
21. G. Rothenberger , J. Moser, M. Gratzel, N. Serpone, D.K. Sharma, J. Am.Chem.. Soc. 107 (1985) 8054.

22. M. Gratzel Heterogeneous Photochemical Electron Transfer. CRC Press,BocaRaton, FL.

23. T. Fujishima, N. Rao, D. Tryk, J. Photochem. Photobiol. C: Photochem .Rev. 1 (2000) 1.

24. A. L. Linsebigler, G. Lu, J. T. Yates, Chem. Rev. 95 (1995) 735.

25. M. R. Hoffmann, S.T. Martin, W. Choi, D.W. Bahnemann, Chem. Rev.95 (1995) 69.

26. J. Peral, X. Domenech, D. F. Ollis, J. Chem. Technol. Biotechnol. 70 (1997) 117.

27. J. Gimenez, D. Curco, M. A. Queral, Catalysis Today, 54 (1999) 229.

28. World Resources Institute 1994-95, N.Y.O., 1994.

29. N.Daneshvar,, D.Salari, A.R.Khataee, J.Photochem .Photobiol. A 162(2004) 317.

30. T. Matsunaga, R. Tomoda, T. Nakajima, H. Wake, FEMS Microbiol. Lett. 29 (1985) 2 L

31. G. V. Samsonov, The Oxide Handbook, IFI/Plenum Press, New York, (1982).

32. Rosemeyer 1993 ; Morad and Aldahan have found the co-existing nature of $TiO_2$.

33. Post and Burnham.

34. Gribb and Banfield in 1997.

35. N.Negishi,T. Iyoda, K.Hashimoto, A.Fujishima. Chem. Lett. 841 (1995).

36. P.V. Kamat, Nanoparticles and Nanostructured films, InJ.H. Fedlerwiley-VCH,New York (1998.)

37. M. Anne Fox, M. T. Dulay Chem. Rev. 93 (1993) 341.

38. M. 1. Litter, Appllied Catalysis B: Enviromental 23 (1999) 89.

39. A. Mills, A. Beghazi, D. Rodman, Wat. Res. 30 (1996) 1973

40. Y.T.Kwon,K.Y.Song,W.I.Lee, G.J.Choi, Y.R.Do, J.Catal. 191 (2000)192.

41. A.J.Bard,M.Stratmann,S.Licht(2002)"Encyclopaedia of Electrochemistry" Vol6. Semiconductor electrodes & Photoelectrochemistry Wiley-VCH

42. M.Gratzel,A.Hagfeldt, Chem.Rev.95(1995)49.

43. W. J. Albery, P.N.Barlett , J. Electrochem. Soc. 131 (1984) 315.

44. A. Mills, S. L. Hunte, J. Photochem. Photobiol. A: Chem. 108 (1997)1.

45. Prashant V. Kamat, Dan Meisel ,C. R. Chimie. 6 (2003) 999.

46. D.Hufschmidt, L.Liu, V.Seizer,D.Behnemann,Water Sci Technol. 49 (2004) 135.

47. Martin. S. T., Herrmann. H., Choi. W., Hoffmann. M. R. Trans. Faraday Soc. 90 (1994) 3315.

48. D.Trong On, D. Desplantier-Giscard, C. Danumah,S. Kaliaguine, Appl. Catal. A 222 (2001) 299.

49. H. Zhang, M. Finnegan, J. F. Banfield, Nano Lett. 1 (2001) 81.

50. A. Sayari, P. Lui, Micropor. Mater. 12 (1997) 149.

51. J.Y. Ying, C.P. Mehnert, M.S. Wong, Angew. Chem. Int. Ed.Engl.38 (1999) 56.

52. W.Yu-de, M. Chun-lai, S. Xiao-dan, L. Heng-de, Appl. Catal.A246 (2003) 161.

53. J. Peral, X. Domenech, D. F. Ollis, J. Chem. Technol. Biotechnol. 70 (1997) 117.

54. B.Ohtani,S.-W.Zhang, S.Nishimoto, Kagiya, Photochem. Photobiol. A64(1992)23.

55. A. Mills, G. Porter, J. Chem. Soc. Faraday Trans.78(1982) 3659.

56. A.Sclafani,L.Palmisano,M.Schiavello,J.Phys.Chem.94(1990)829.

57. Y.Oosawa,M.Gratzel,J.Chem.Soc.Chem.Commun.(1984)1629.

58. M. Seredych, T. J. Bandosz J. Am. Chem. Soc. 46 (2007) 1786.

59. O. Carp, C.L. Huisman, A. Reller, Prog. Solid State Chem. 32 (2004)33.

60. A. Mills, S.-K. Lee, Platinum Met. Rev. 47 (2003) 2.

61. W.Choi,A.Termin,M.R.Hoffmann,J.Phys.Chem.98(1994)13 669.

62. A.Fuerte,m.d.Hernandez-Aionso,A.J.Moura,A.Martinez-Arias,J.Soria

63. K.E.Karakitoou;X.E.Verykios,J.Phys.Chem.97(1993)1184.

64. J.C.Escudero,S.C.MarchJ.Gimenez,R.Simarro J. Catal. 123 (1990) 319

65. H.Courbon ,J.M.Hermann,P.Pichat, J. Catal.72(1981)129.

66. M.Matsumura,Y.SatoH.Tusbomura, J. Phys. Chem. 87 (1983) 3807.

67. D.W.Bahnemann, J.Monig,R.Chapmann, J. Phys. Chem.91 (1987) 3782.

68. J.Papp, H.S.Shen,R.Kershaw,K.Dwight,A,Wold, Chem. Mater.5 (1993) 284.

69. W.Zou,R.D.Gonzalez,Catal.,Lett.,12(1992) 73.

70. A.L.Bonivardi, M.A.Baltanas, J. Catal.125(1990)243.

71. I.Alt-Ichou, M.Formenti, B.Pommier, S.J.Teichner, J.Catal.91 (1985)293.

72. Bucher et al., (1990)

73. N.J.Renault, P.Pichat,A.Foissay,R.Mercier, J. Phys. Chem. 90 (1986) 2733.

74. B.Viswanathan(2002)'Photocatalysis'.Chapter 20in a hand book of catalysisprinciples and applications.

75. J. Gimenez, D. Curco, M. A. Queral, Catalysis Today. 54 (1999).229.

76. D. Chen, A. K. Ray, Applied Catalysis B: Environmental. 23 (1999) 143.

77. G. Al-Sayyed, J. C. D'Oliveira, P. Pichat, Journal of Photochemistry and Photobiology A: Chemistry. 58 (1991)99.

78. J. P Percherancier, R. Chapelon, B. Pouyet, Journal of Photochemistry and Photobiology A:Chemistry. 87 (1995)261.

79. J. M. Herrmann, Catalysis Today. 53 (1999) 115.

80. Y. Inel, A. N. Okte, Journal of Photochemistry and Photobiology A: Chemistry. 96 (1996)175.

81. I. Arslan, I. A. Balcioglu, D. W. Banheman, Applied Catalysis B: Environmental. 26 (2000)193.

82. I. P. Fernandez, F. J. de las Nieves, S. Malato, Journal of Colloid and Interface Science. 227 (2000) 510.

83. D.F.Ollis, Solar-assisted photocatalysis for water purification: (1991) Kluwer Academic Publishers.

84. G. Al-Sayyed, J. C. D'Oliveira, P. Pichat, Journal of Photochemistry and Photobiology A: Chemistry. 58 (1991) 99.

85. M. S. Wrighton, Acc. Chem. Res. 12 (1926) 97.

86. E. Pelizzetti, Solar energy materials and solar cells. 38 (1995) 453.

87. G.M.Colonna,T.Caronna,B.Marcandalli,Dyes Pigments. 41 (1999) 211.

88. C.S.Poon,Q.Huang,P.C.Fung,Chemosphere .38 (1999) 1005.

89. M.Neamtu, I.Siminiceanu,A.Yediler ,A.Kettrup,Dyes Pigments.53 (2002)93.

90. R. Cai, K. Hashimoto, K. Itoh, Y. Kubota, A. Fujishima, Bull. Chem. Soc. Jpn.64 (1991) 1268.

91.

92.

93.

94.

95.

96.

97.

98.

99.

100.

101.

102.

103.

104.

105.

106.

107.

108.

109.

110

111

91. Y. Paz, Z. Luo, L. Renberg, A. Heller, J. Mater. Res. 10 (1995) 2842.

92. P.C. Vandevivere, R. Bianchi, W. Verstraete, J. Chem. Technol. Biotechnol.72 (1998) 289.

93. J. Sarasa, M.P. Roche, M.P. Ormad, E. Gimeno, A. Puig, J.L. Ovelleiro,Water Res. 32 (1998) 2721.

94. I.K. Konstantinou, T.A. Albanis, A review, Appl. Catal. 49 (2004) 1.

95. M. Seredych, T. J. Bandosz J. Am. Chem. Soc. 46 (2007) 6 1786.

96. Mills G. Hoffman, M.R. Environ. Sci. & Techno. 27 (1993) 1681.

97. Izumi. I., Dunn. W.W. Wilburn. K.O, Fan. F.F, Bard. A. J, J. Phys. Chem. 84 (1980) 3207.

98. Zhang Liuxue, Liu Peng, Su Zhixing Materials Chemistry and Physics 98 (2006) 111.

99. Kawai. T, Sakata.T. Nature. 286 (1981) 474.

100. M. S.T.Gonqalves, A. M.F.Oliveira-Campos, E. M.M.S. Pinto, P. M.S. Plasencia,M. J. R.P. Queiroz Chemosphere .39 (1999) 781.

101. Akira Fujishima, Xintong Zhang C. R. Chimie .9 (2006) 750.

102. T.A. McMurray, P.S.M. Dunlop, J.A. Byrne Journal of Photochemistry& Photobiology A: Chemistry .182 (2006) 43.

103. E. Bizani a, K. Fytianos a, , I. Poulios b, V. Tsiridis c Journal of Hazardous Materials .136 (2006) 85.

104. P. V. Kamat , Chem. Rev. 93 (1993) 267.

105. M. A. Fox, M. T. Dulay, Chem. Rev. 93 (1993) 341.

106. D. M. Blake, Bibliography of Work on the Photocatalytic Removal of Hazardous CompoundsFrom Water and Air, National Renewable Energy Laboratory, January (1997).

107. D. F. Ollis Environmental Sci. Technol. 19 (1985) 480.

108. M.A. Behnajady, N. Modirshahla, R. Hamzavi Journal of Hazardous Materials B.133 (2006) 226.

109. N. Sobana, M. Muruganadham1, M. Swaminathan ,Journal of Molecular Catalysis A: Chemical. 258 (2006) 124.

110. J.C. Colmenares, M.A. Aramendı´a, A. Marinas, J.M. Marinas, F.J. Urbano Applied Catalysis A: General .306 (2006) 120.

111. G. Colon, M. Maicu, M.C. Hidalgo, J.A. Navıo Applied Catalysis B: Environmental .67 (2006) 41.

112. Huaming Yang, Jing Ouyang, Aidong Tang, Yu Xiao, Xianwei Li, Xiaodan Dong, Yongmei Yu Materials Research Bulletin.41 (2006) 1310.

113. Alexia Patsoura, Dimitris I. Kondarides, Xenophon E. Verykios Applied Catalysis B: Environmental. 64 (2006) 171 .

114. Chun He, Dong Shu, Ya Xiong, Xihai Zhu, Xiangzhong Li Chemosphere. 63(2006) 183.

115. Chun He, Ya Xiong, Dong Shu, Xihai Zhu, Xiangzhong Li Thin Solid Films .503 (2006) 1.

116. C. H. Kwon, J. H. Kim, In Sun Jung, Hyunmin Shin, Ki Hyun Yoon, Ceramics International .29 (2003) 851.

117. H. Jiang, L. Gao, Mater. Chem. Phys. 77 (2002) 878.

118. M. I. Litter, Appllied Catalysis B: Enviromental. 23 (1999)89.

119. M.I.Litter,J. A.Navio, J. Photochem. Photobio.A: Chem.98 (1996) 171.

120. A. Fuerte, M. D. Hernández-Alonso, A. J. Maira, A. Martínez-Arias, M. Fernández-García, J. C. Conesa , J. Soria, Chem. Commun. 24 (2001) 2718.

121. M. Anpo, Y. Ichihashi, M. Takeeuchi, H. Yamashita, Science and Technology in Catalysis.(1998) 305.

122. Y. Fu, C. Shearwood, Scripta Materialia. 50 (2004) 319.

123. Y. Wang, H. Cheng, Y. Hao, J. Ma, W. Li, S. Cai, J. Mater. Sci. 34 (1999) 3721.

124. (124) M. S. Jeon, W. S. Yoon, H. K. Joo, T. K. Lee, H. Lee, Appl. Surf. Sci. 165 (2000) 209.

125. E. Traversa, M. L. D. Vona, P. Nunziante, S. Licoccia, T. Sasaki, N. Koshizaki, J. Sol–Gel Sci. Technol. 19 (2000) 733.

126. A. Burns, W. Li, C. Backer, S.I.Shah Mat.Res Soc Symp. Proc Vol. 703.

127. M. Anpo, T. Shima, S. Kodama, J. Phys. Chem., 91 (1987) 4305.

128. P. Pivera, K. Tanaka, T. Hisanaga, Appl. Cat. B: Environ. 3 (1993) 37.

129. Z. Zhang, C.-C. Wang, R. Zakaria, Y. Ying, J. Phys. Chem. 102 (1998)10871.

130. Y.Q.Wang and J.Y.Ying,Chem.Mater.11,3113(1999).

131. L. Bruce, J. Phys. Chem. 90 (1986) 2555.

132. T. Kariyone, M. Anpo, K. Chiba, M. Tomonari, Hyomen, Surface. 29 (1991) 156.

133. A. J. Maira, K. L. Yeung, C. Y. Lee, P. L. Yue, C. K. Chan, J.Catal. 192 (2000) 185.

134. S. Yin, Q. Zhang, F. Saito, T. Sato, Chem. Lett. 32 (2003) 4.

135. E.Vigil, J.A.Ayllon,A.M.Perio,R.R.Clemente,Langmuir 17(2001) 891.

136. H. Zhang, M. Finnegan, J. F. Banfield, Nano Lett. 1 (2001) 81.

137. E. Scolan, C. Sanchez, Chem. Mater. 10 (1998) 3217.

138. V. Chhabra,V. Pillai,B.K. Mishra,A. Morrone, D.O. Shah, Langmuir .13 (1995) 3307.

139. R. R. Basca, M. Gratzel, J. Am. Ceram. Soc. 79 (1996) 2185.

140. P. D. Cozzoil, A. Kornowski, H. Weller J. Am. Chem. Soc. 125 (2003)14539-14548.

141. W. Sigmund,W. J. Yuh, H. Park, V. Maneeratana, G. Pyrgiotakis, A. Daga, J.Taylor, J. C. Nino J. Am. Ceram. Soc. 89 (2006) 2 395.

142. Thammanoon Sreethawong,Yoshikazu Suzuki, SusumuYoshikawa, C.R. Chimie .9 (2006) 307.

143. R.S. Sonawane, M.K. Dongare, Journal of Molecular Catalysis A: Chemical. 243 (2006) 68.

144. Chun He, Dong Shu, Ya Xiong, Xihai Zhu, Xiangzhong, Li Chemosphere .63 (2006) 183..

145. J.G. Goodwin, Jr. Koranne, M.M. Marcelin G, J. Catal. 148 (1994) 369.

146. .T.Richardson,PrinciplesofCatalDevelop,Plenum Press, NY (1989) 134.

147. B. Imelik, J.C. Vedrine (Eds), Catalyst Characterization: Physical Techniques for Solid Materials, Plenum Press, New York (1994).

148. K. Morikawa, T. Shirsaki, M. Okada, Adv. Catal. 20 (1969) 97.

149. J.J. Burton, R.L. Garten (Eds.) L.L. Murrell in Advanced Materials in Catalysis, Chap. 8, Academic Press, New York (1977).

150. D.L. Trimm, Design of Industrial Catalysts, Elsevier, New York. (1980).

151. K. Foger, Catalysis, Science and Technology, JR. Anderson, M. Boudart. (Eds.) Springer, New York. 6 (1984) 227.

152. Q. Fu, A. Weber, M. Flytzani-Stephanopoulos, Catal. Lett. 77 (2001) 87.

153. P. Moriceau, B. Grzybowska, Y. Barbaux, G. Wrobel, G. Hecquet, Appl. Catal. A: Gen. 168 (1998) 269.

154. M.J.Holgado,S.SanRoman,P.MaletV.Rives,Mater.Chem.Phys89(2000) 49

155. X. M. Wu, L. Wang, Z.C. Tan, G. H. Li, S. S., Qu, J. Solid State Chem. 156(2001) 220.

156. S. Sakka, Am. Ceram. Soc. Bull. 64 (1985) 1463.

157. M. S Ahmed, A. A. Yosry, J. Non-Cryst. Solids .186 (1995) 402.

158. C. Anderson, A. J. Bard, J. Phys. Chem. 99, 24 (1995) 9882.

159. K. Kato, Y. Torii, H. Taoda, T. Kato, Y. Butsugan, K. Niihara, J. Mater. Sci . Mt. 10 (1996)913.

160. K. Kato, H. Togeda, K. Gijutsuin, Japan Patent, 08099041 A2. 1996.125:66102 CA.

161. M. Mikula, V. Brezova, M. Ceppan, L. Path, L'. Karpinsky, J. Mater. Sci. Lett. 9 (1995) 615.

162. S.Nakamura, K.Suzuki, JapanPatent, 08187433A2. 125 (1996) 208277 CA.

163. N.Nobuaki,T.Iyoda,K.Hashimoto,A. Fujishima,Chem. Lett. 9 (1995) 841.

164. K. T Ranjit, B. Viswanathan, T. K. Varadarajan, J. Mater. Sci. Lett. 10 (1996) 874.

165. S. Sitkiewitz, A. Heller, New J. Chem. 20, 2 (1996) 23341.

166. B. R. Weinberger, R. B. Garber, Appl. Phys. Lett. 66, 18 (1995) 2409.

167. Rouxel.J, Tournoux.M, Brec.R Soft Chemistry Routes to New Materials;Trans Tech Publications:Uetikon-Zuerich , Switzerland. (1994).

168. Rouxel.J, Tournoux.M,Solid State Ionics.84 (1996)141

169. Gopalakrishnan.J,Chem.Mater.7(1985)1265.

170. Rao.C.N.R, Gopalakrishnan.J, New Directions in Solid State Chemistry,Cambridge University Press, Cambridge.(1997).

171. WangFumin,ShiShengZhan,GongFeng,JieuJuitin,Adachi Motonari,J. chem.eng.15(2007)754.

172. M. Anderson, L. Osterlund, S. Ljungstrom, A. Palmqvist J. Phys. Chem.B 106(2002) 10674.

173. P.Yang,Z.zhao,D.Margolese,D.I.Chmelka,B.F.Stucky.G.D.Nature.396(199 8) 152.

174. G.D. Vulpescu, M. Ruitenbeek, L.L. van Lieshout, L.A. Correia, D. Meyer, PaulP.A.C. Pex, Catal. Commun. 5 (2004) 347.

175. K.M. Choi, S. Ikeda, S. Ishino, K. Ikeue, M. Matsumura, B. Ohtani, Appl. Catal.A: Gen. 278 (2005) 269.

176. N. Ma, Z. Ma, Y. Yue, Z. Gao, J. Mol. Catal. A: Chem. 184 (2002) 361.

177. C. Palazzi, L. Olivia, M. Signoretto, G. Strukul, J. Catal. 194 (2004) 286.

178. S. Biella, M. Rossi, Chem. Commun. (2003) 378.

179. J.E. Remias, T.A. Pavlosky, Ayusman, J. Mol. Catal. A: Chem. 203 (2003) 179.

180. R. Noyori, M. Aoki, K. Sato, Chem. Commun. (2003) 1977.

181. U.R. Pillai, E.S. Demessie, Green Chem. 6 (2004) 161.

182. T. Iwahama, G. Hatta, S. Sakaguchi, Y. Ishii, Chem. Commun. (2000) 163.

# Chapter 2

# Experimental Methodology

## *Abstract*

The development of ecologically friendly technologies is currently one of the most important goals in industrial chemistry research. The physical and photochemical characteristics of semiconductor catalysts appear to be highly dependent on the exact experimental conditions used in the preparation. Nanostructured mesoporous $TiO_2$ can be prepared by several methods namely sol-gel method (SG), Hydrothermal method(HT), Evaporation Induced Self Assembly Method(EISA) and by controlled crystallization of an amorphous precursor. This chapter gives a detailed description of the catalyst preparation and pretreatment conditions, materials used, the techniques used to characterize the catalysts, the experimental set up and measures used for the catalytic activity study.

### 2.1.0 Catalyst preparation

In particular, $TiO_2$ presents interesting properties for the photocatalytic reactions. Among the common crystalline forms of titania, anatase is generally recognized to be the best support. However, the use of $TiO_2$ as a catalyst is limited by the fact that it possesses a relatively low specific surface area. Therefore, many attempts have been performed in order to synthesize mesoporous titania with a high surface area and high stability using a variety of different templates **[1-3]** .The catalytic activity strongly depends on the methods of preparation and pretreatment conditions apart from the reaction parameters. Small variations in the preparation conditions radically alter the performance of the catalyst. Therefore intense care must be taken during the selection of materials and preparation of the systems.

### 2.1.1 Sol-Gel Method

The sol–Gel (SG) technique has emerged as a promising processing route for the synthesis of nano-sized particles because of the simplicity of sol–gel processing in addition to its high purity resulting from the availability of high purity chemicals as raw materials

A sol is a dispersion of solid particles in a liquid phase where the particles are very small (1-1000nm) so that gravitational forces are short-range forces like vanderwaals attraction and surface charges. Hence the particles remain suspended indefinitely. Since the moment of inertia is so small they undergo continuous Brownian movement. They are classified as lyophobic if there is a relatively weak solvent-particle interaction, and lyophilic if this interaction is relatively strong **[4-6]**. Sols are thermodynamically unstable due to the large surface area volume ratios. So

it has a tendency to agglomerate to reduce the surface area. This process is called flocculation and if it is irreversible it is called coagulation. Sols can be made kinetically stable by the imposition of the energy barrier on the particle to overcome before getting agglomerated. The three origins of this barrier are the development of surface charge, steric hindrance, and solvation. A surface charge can develop either the preferential dissociation of one of the lattice ion of the sol particle or the preferential adsorption of the charged species from solution. An equal and oppositively charged diffused layer is developed in solution adjacent to the charged surface. The overlap of these diffused layers surrounding two approaching sol particles produces repulsion **[8-10].** Steric hindrance is by the adsorption of short chain polymers on to the surface of the particles. As the particles approach one another, adsorbed polymers lose their configurational entropy and it causes a repulsive force. Energy of solvation is most effective in the case of aqueous systems. It is the energy required disrupting the ordered layer of water surrounding the sol particles and allowing it to come closer.

Gel is a three dimensional inter-connected solid network that expands in a stable fashion through out the liquid medium. If the solid net work is made up of colloidal sol particles, gel is colloidal. If the solid net work is made up of sub colloidal chemical units, the gel is polymeric **[11-13].** The continuous net work makes the gel soluble, in shape but with low strength. Gelation is a process in which a sol or a solution forms to a gel. Inorganic gels comprise of two phases in the thermodynamic sense, the solid network and liquid phase. Polymeric gels are composed of only one thermodynamic phase, the solution. An important criterion for gel formation from a sol is that there should be a strong particle –solvent interaction so that at least a portion of the solvent is bound by chemical

bonding. Sol- gel process is a colloidal route and includes the following steps

1. The preparation of homogeneous solution of easily purifiable precursor in an organic solvent miscible with water or the reagent.
2. Converting the homogeneous solution to a sol by treatment with a suitable reagent.
3. Allowing the sol to change into a gel by self polymerization and condensation.
4. Shaping the gel to the desired form such as thin films, fibres, spheres etc.
5. Heat treatment of the shaped gel.

### 2.1.2 Mechanism of Sol-gel Route

In Sol-gel synthesis of titania, the precursor usually used is the metal alkoxides. Alkoxide is a combination of metal cation with alcohol groups. In these alkoxides there exists metal oxygen bonds. Since there is a large difference in electronegativity between titanium and oxygen, the Ti-O bond is highly polar and extremely reactive, especially towards water. The different routes adopted for obtaining nanocrystalline titania sol are

1. Polymeric route – Hydrolysis and condensation of stabilized titanium alkoxide to give titania sol.
2. Colloidal route- Precipitation of titanium oxy hydroxide followed by peptisation using electrolytes such as $HCl/HNO_3$.
3. Polymeric route[14]

The replacement of OR groups depends on factors such as

1. Nature of alkyl group.
2. Nature of solvent.

3. Concentration of each species in the solvent.
4. Water to alkoxide molar ratio.
5. Temperature.

The mechanism can be represented as follows:-

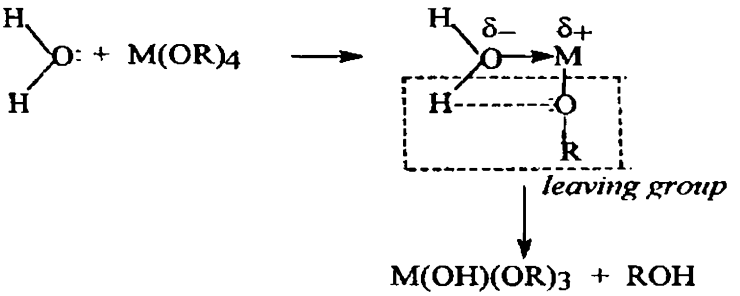


Condensation involves the removal of a molecule of water and forms a metal-oxygen-metal bond.

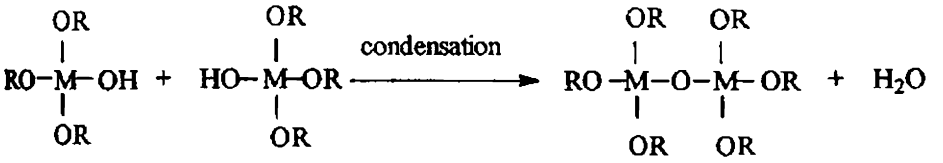


Colloidal route

This involves a precipitation –peptisation process. The hydrolysis and condensation reactions proceed to form clusters and after a particular stage the gel gets precipitated [15]. The precipitate is again dispersed in the medium to get a stable sol. Precipitate is loosely bound agglomerate of colloidal particles. The $H^+$ ions from $HNO_3$will get adsorbed on the surface of these colloidal particles forming the adsorbed layer. The development of surface charge will stabilize the particle resulting in a stable sol. Eletrophilic proton will attack the oxygen atom and bridge between titanium atoms and thus electron density is withdrawn from Ti atoms making it more electrophilic. Under these conditions, Ti atom can attack

the electron density from the oxygen atom in water more easily. Consequently the oxolation bonds are broken and $TiO_2$ particles are peptized to light blue sols. These sols will remain stable for a long time.

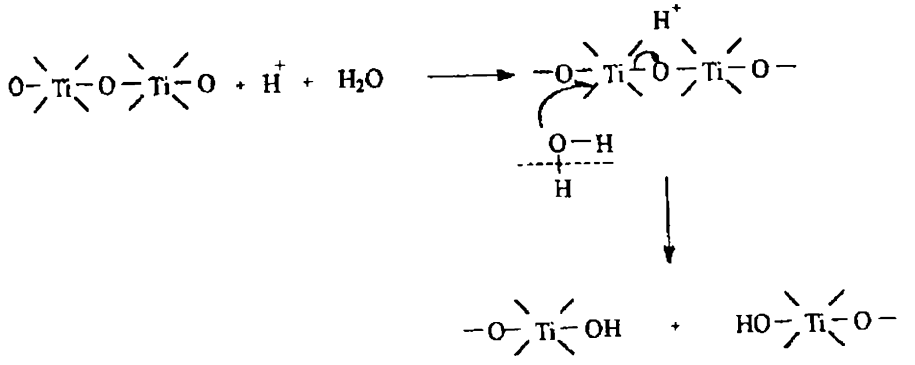

### 2.1.3 Preparation of titania Catalysts by sol-gel route

In Sol-Gel route, the precursor is titaniumisopropoxide. TTIP: $HNO_3$: $H_2O$ in the molar ratio 1:0.1:12 is stirred for 3days in a pH of about 4. After ageing for 5 days it was dried at 60°c to get the gel. The samples after overnight drying at 110°C were powdered and calcined at 723 K for 5 h in a muffle furnace in air atmosphere. Calculated amount of metallic nitrate solutions such as 6 wt % of Ag, Ce and Cu were added by wet impregnation method. Thus obtained catalysts were further reduced in a current of $H_2$ for 6 hrs at 723 K in a tubular furnace. The catalysts were labeled as T1 for pure $TiO_2$, T2 silver metal loaded, T3 ceria metal and T4 copper metal loaded $TiO_2$.

Two sets of catalysts were also prepared at calcination temperatures of 673 K and 773 K, incorporating 6 wt% of metals and carried out the physico-chemical characterization to obtain a qualitative idea regarding the formation of anatase phase in the prepared catalysts and to optimize the calcination temperature.

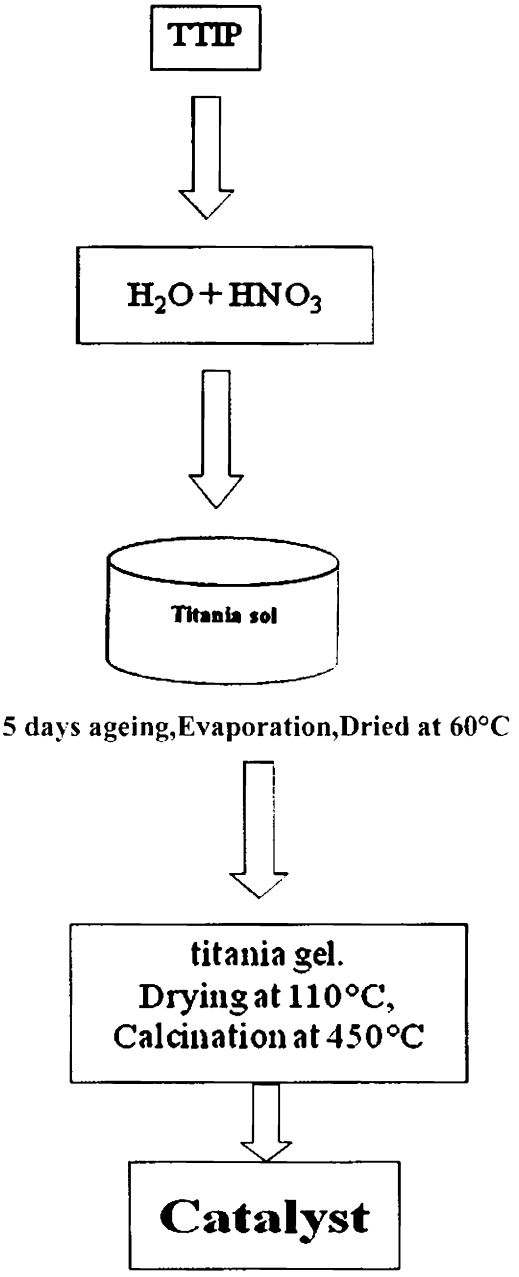
TTIP
$H_2O + HNO_3$
Titania sol
5 days ageing,Evaporation,Dried at 60°C
titania gel.
Drying at 110°C,
Calcination at 450°C
Catalyst

| Catalyst | System 1 (Calcination temp-673K) | System 2 (Calcination temp-723K) | System 3 (Calcination temp-773K) |
|---|---|---|---|
| Pure $TiO_2$ | T1 400 | T1 | T1 500 |
| $Ag/TiO_2$ | T2 400 | T2 | T2 500 |
| $Ce/TiO_2$ | T3 400 | T3 | T3 500 |
| $Cu/TiO_2$ | T4 400 | T4 | T4 500 |

### 2.1.4 Preparation of titania Catalysts by Hydrothermal route

In general, hydrothermal synthesis is a prospective method to obtain nanocrystalline titania particles, where polymorphism, particle size and crystallinity could be controlled by the hydrothermal conditions **[16,17]**. Moreover, it is a low temperature technique for materials development, widely applied in industrial processes for ceramic synthesis **[18]**. The hydrothermal technique requires autoclave instrumentation and relies on the extensive heating of the nanoparticles diluted over an aqueous solution or slurry. Fine-tuning of the semiconducting nanoparticle size and specific active area critically affects the desired properties of the photocatalysts by varying the surface to volume ratio, by affecting the photo excited charge transfer and by influencing the surface hydroxyl concentration. Recent research activity in the field of materials chemistry reveals the crucial role of water on the final properties of titanium dioxide nanoparticles **[19]**. Water molecules express their nucleophile character, inducing the semiconductor particles decrease under elevated temperature and pressure conditions, similar to those achieved in an autoclave. In this way, the energy band structure becomes discrete and titania nanoparticles exhibit

optical and photocatalytic properties superior to those of the source material [20]. Furthermore, it is well established that amorphous titania develops its photocatalytic properties after heating at temperature 450°C in an ambient environment. Surprisingly, the crystallization temperature for the anatase crystalline phase under hydrothermal conditions is only 200 °C [21,22]. This observation proves that water molecules can induce structural changes more efficiently, consuming less energy. Control of the factors like increased roughness and complexity of the photocatalyst surfaces, and amplified hydroxyl content per unit area can be combined with improved interconnection of the nanoparticles and adhesion to the substrate by fine tuning of the autoclave parameters can lead to efficient immobilized titania photocatalysts. The solution based hydrothermal treatment assures flexibility of the synthetic procedure, as time consuming steps of paste preparation are reduced by dissolving necessary reagents prior to heating. Thus the catalysts can be easily produced and subsequently they are expected to present uniformity, adherence and sufficient photocatalytic activity [23].

Ethanol and water are stirred well and to it titanium isopropoxide is added in drops stirred for another 2 hrs at room temp and the suspension was transferred into an autoclave, heated at 353K for 20 hrs. The pH was 6.6 slightly higher than the iso electric point of titania (IEP) which is 5.8. Warm seed suspension was mixed into a neutral aqueous soln of Pluronic P123($EO_{20}PO_{70}EO_{20}$) under vigorous stirring at 313K for 1 hr and transferred into an autoclave and kept for 20hrs at 353K. It is then filtered ,dried and calcined at 723 K for 5 h in a muffle furnace in air atmosphere. TTIP: EtOH: P123:$H_2O$ is in the molar ratio 1:10.55:0.034:430 [24]. Calculated amount of metallic nitrate solns such as 6 wt % of Ag, Ce and Cu were added and stirred by wet impregnation method. Thus obtained

catalysts were further reduced in a current of $H_2$ for 6 hrs at 723 K in a tubular furnace.

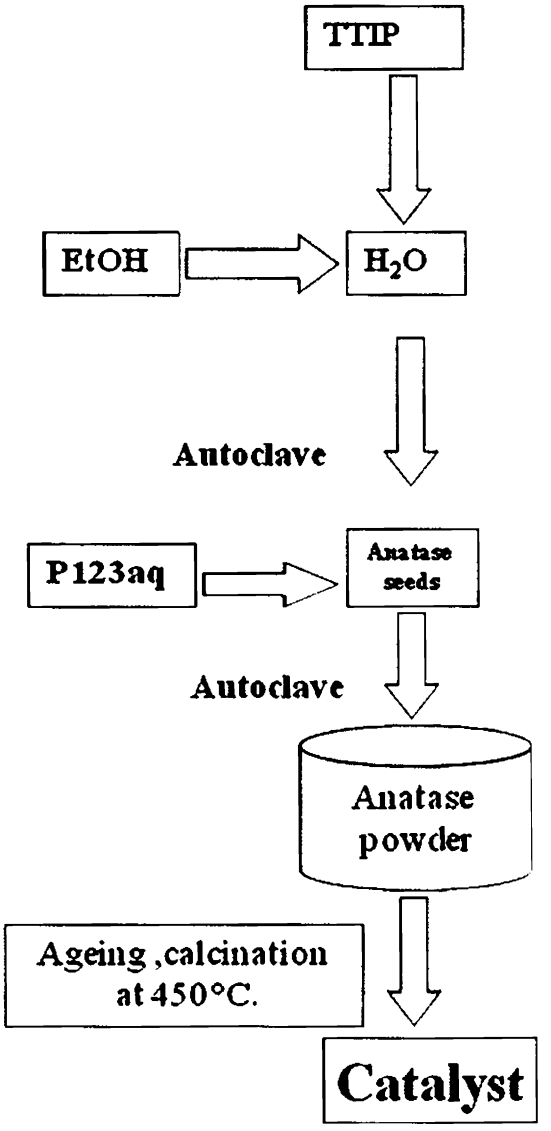

| Catalyst | Systems |
|---|---|
| Pure $TiO_2$ | THT1 |
| $Ag/TiO_2$ | THT2 |
| $Ce/TiO_2$ | THT3 |
| $Cu/TiO_2$ | THT4 |

### 2.1.5 Preparation of titania Catalysts by EISA route

Mesoporous materials have high surface areas and high pore volumes because of the large dimensions of the pores. But one of the major drawbacks in the synthesis of mesoporous titania is the high reactivity of the initial titanium compounds toward hydrolysis and condensation. If this reactivity is not tempered, a poorly organized structure will be formed .The high reactivity of the precursors can be efficiently be controlled by pH adjustment and complexation effects. Controlled amount of water is added to a non-aqueous solvent, leading to a specific formation of the mesoporous structure. Such a combination was first reported Stucky *et* al **[25].** ie. thermally stable mesoporous titania can be synthesized following a different synthesis route ie. Evaporation induced self assembly method (EISA) **[26].** Mesoporous titania was prepared using cetyltrimethylammoniumbromide (CTABr) **[27]** as a surfactant and titanium tetraisopropoxide (Ti $(OPr)_4$) as the titanium source. $Ti(OPr)_4$ was added to an ethanolic HCl, resulting in a titanium precursor solution, which was added to an ethanolic CTABr solution. pH was observed to be 6.1 slightly higher than the iso electric point of titania (IEP).After vigorous stirring, the resulting solution was transferred in an open Petri dish for 7 days at 333K to evaporate the solvent. The molar ratios were

Ti:CTABr:HCl:H2O:EtOH as 1:0,16:1,4:17:20 **[28].** Catalysts were further reduced in a current of $H_2$ for 6 hrs at 723 K after incorporating the metals.

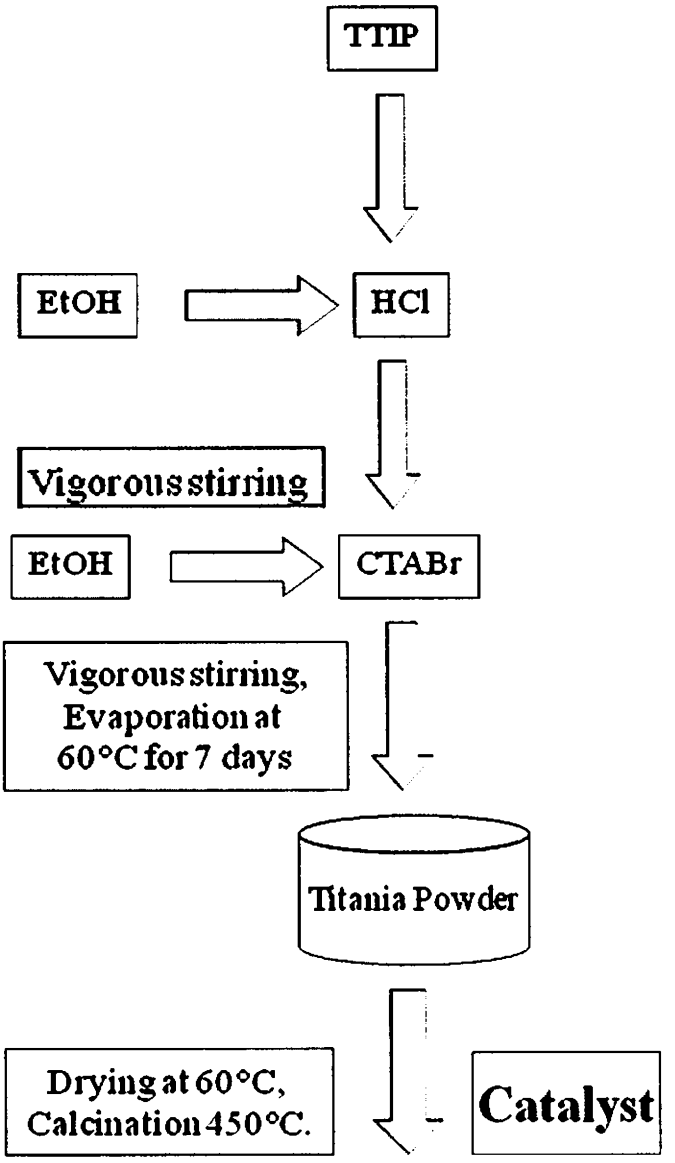


A synthetic approach to mesoporous metal oxides is introduced by the so-called evaporation-induced self-assembly process (EISA). By slow

alcohol evaporation, a controlled building of an inorganic network with nanocrystalline domains around the voids of the liquid-crystalline interphase results in a hexagonally ordered $TiO_2$ mesophase. A controlled thermal treatment in order to remove the template is crucial as it often results in a collapse of the mesoporous structure. Recently, Cassiers *et* al. [29]developed the new synthesis step that controls the transformation into the anatase phase without loss of porosity, by treating the titania hybrid with an aqueous $NH_4OH$ solution. This treatment results in a thermally stable mesoporous titania structure with anatase nanoparticles in the walls. The obtained mesoporous titania samples exhibit a high surface area, which could reach 600 $m^2 g^{-1}$, and pore volumes up to 0.30 $cm^3 g^{-1}$. Moreover, the mesoscale order of $NH_3$- treated titania was stable after thermal treatment up to 500 °C. Although in the literature, an extensive research has been done on vanadia-silica materials systems, mesoporous transition-metal oxides have been rarely studied as a support. In this work, mesoporous titania was prepared following the post $NH_3$ treatment, based on its porosity characteristics, a large potential as a catalytic support. And the support material gets converted into the metal oxide form after calcination [30-33].Some metal oxides were deposited on the mesoporous titania by wet impregnation method. This method allows the metal oxide to be spread out on the titania support material. After deposition, a careful and controlled calcination is performed in order to remove the organic ligands, without collapsing the mesostructure of the support[34].

It is known that the catalytic activity of catalysts not only depends on the loading but also on the structure and dispersion of the species. These factors are highly influenced by the nature of the oxide support. Therefore, it is important to investigate the properties of the transition metal oxide supports.

The stabilizing effect of $NH_3$-treatment on mesoporous titania is also reported. All samples are $NH_3$ treated for 48 hrs in a reflux system. One gram of solid was treated with 50 ml of basic water by the addition of 30% $NH_3$ keeping the pH between 10-11 and all the samples were calcined at about 723K for 5hrs [35[.

| Catalyst | System 1 | System 2 (Ammonia treated) |
|---|---|---|
| Pure $TiO_2$ | TEA1 | TEA1 $NH_3$ |
| Ag/ $TiO_2$ | TEA2 | TEA2 $NH_3$ |
| Ce/$TiO_2$ | TEA3 | TEA3 $NH_3$ |
| Cu/$TiO_2$ | TEA4 | TEA4 $NH_3$ |

### 2.1.6 Wet impregnation method

Metals like Ag, Ce, Cu were incorporated into titania catalyst by adding about 6 wt.% of the metallic salt solutions to $TiO_2$ powder to get a 0.05 molar soln. of the metal. The resulting slurry was heated slowly at $70^0$C under continuous stirring and maintained at that temperature until nearly all the water gets evaporated. The solid residue was dried at 110 $^0$C for 24 h [36-38] .Finally, ground, sieved and labeled. The incorporation of metals like Pt ,Pd and Au were also carried out by adding about 0.2-1% metallic salt solutions to $TiO_2$ powder. Thus obtained catalysts were further reduced in a current of $H_2$ for 6 hrs at 723 K in a tubular furnace.

### 2.2.0 Materials

The materials used for the preparation of catalysts are given below. Analar grade from Merck were used as such, without further purification.

| Materials | Suppliers |
|---|---|
| Titanium(iv)isopropoxide | Aldrich |
| Pluronic P 123 | Aldrich |
| CTABr | Aldrich |
| Hexa chloro platinate | Aldrich |
| Tetra Chloro aurate | Aldrich |
| Palladium nitrate | Aldrich |
| methylene blue(MB) | Aldrich |
| malachite green(MG) | Aldrich |
| Acid Orange7(AO7) | Aldrich |
| Acid blue- 25(AB25) | Aldrich |
| Acid Red-1(AR1) | Aldrich |
| Conc. Nitric Acid | Merck |
| Silver nitrate | Merck |
| Ceria nitrate | Merck |
| Copper nitrate | Merck |

### 2.2.1 Preparation of different composition of Catalysts

The catalyst systems developed for the present investigation were denoted as given below. Three different routes were selected for the preparation of the catalysts and three different metals were incorporated in the first part of the work. About **3**,**6** and **9**% composition of metals incorporated catalysts were also prepared. Selecting HT route as the best route, about **0.2**,**0.6** and **1**% of noble metals were incorporated in the selected route.

| Notation | Systems |
|---|---|
| T1, THT1,TEA1 | Pure titania catalysts where T is sol-gel, THT is HydroThermal and TEA is EISA Route. |
| T2,THT2,TEA2 | Titania containing metals such as **Ag** and weight % of **3, 6** and **9** is denoted as such. |
| T3,THT3,TEA3 | Titania containing metals such as **Ce** and weight % of **3, 6** and **9** is denoted as such |
| T4,THT4,TEA4 | Titania containing metals such as **Cu** and weight % of **3, 6** and **9** is denoted as such |
| $TiO_2$/M-y | Titania containing metals (M) like Pd, Pt, and Au having weight % (y) of **0.2, 0. 6** and **1.0** . |

### 2.3.0 Catalyst characterization

All the prepared catalysts were characterized by different physico-chemical techniques[39] such as X-ray diffraction (XRD), Fourier Transform Infrared spectroscopy (FTIR) , surface area &pore diameter measurements (BET&BJH), thermogravimetric analysis (TG/DTA),energy dispersive X-ray analysis (EDX), scanning electron microscopy (SEM),Transmission electron microscopy(TEM), X-ray photoelectron spectroscopy (XPS),Diffuse Reflectance UV-Vis Spectroscopy(UV-DRS) , acidity-basicity determination by the method temperature programmed desorption of ammonia(TPD), Diffuse Reflectance UV-Vis Spectroscopy (UV-Vis DRS)and chemical catalytic studies such as liquid-phase reactions

analyzed by gas chromatography (Chemitto 1000 GC, FID detector). A brief discussion of the various methods followed is presented below.

### 2.3.1 X-Ray Diffraction analysis (XRD)

X-Ray Diffraction analysis (XRD) is the one of the widely used and versatile techniques for the qualitative and quantitative analysis of the solid phases[40]. Diffraction from microcrystalline and amorphous powder can be studied by this technique. Compared to the three dimensional location of each reflection in a single crystal diffraction experiment, the powder diffraction pattern can give only one dimensional data due to the rotational projection of the randomly oriented reciprocal lattices. Powder XRD is a long-range order technique sensitive to the basic periodic structure of a solid sample. The purity of the substance, transition to different phases, allotropic transformation, lattice constants and presence of foreign atoms in the crystal lattice can also be recognized by this technique. The XRD method involves the interaction between the monochromatic X-rays (like Cu $K_\alpha$ or Mo $K_\alpha$) with family of planes (identified by a system of Miller Indices, hkl) in the polycrystalline material. A fixed wavelength is chosen for the incident radiation and the Bragg's peaks are identified as a function of scattering angle $2\theta$. The interplanar distances (d spacing) are calculated from the Bragg's equation,

$$n\lambda = 2d \sin\theta,$$

Where $\lambda$ is the X-ray wavelength and n is an integer called order of reflection.

The mean crystallite size of a material can also be determined from the broadening of an X-ray diffraction peak, which is inversely proportional to crystallite size and this can be achieved by following the Scherrer method using the formula,

$$d = 0.9 \lambda / \beta \cos\theta$$

which is derived from Bragg's equation. 'd' is the thickness of the crystal and $\beta$ = FWHM (full width at half maximum intensity).

One can calculate the crystallinity with respect to a standard material by determining the integrated area under the peaks between a set $2\theta$ limits in the sample ($A_S$) and compared with the area obtained for a standard or reference material ($A_R$) in the same $2\theta$ limits [% crystallinity = ($A_S$ x 100)/$A_R$]. Research workers have set their own ways of measuring crystallinity for relative comparison, for example, doing integration of the peaks by gravitation methods or integrating the area of several strong peaks in the region $2\theta_1$ - $2\theta_2$ and dividing it by the total area in the same $2\theta_1$-$2\theta_2$ region or routinely taking the intensity of the strongest peak as a faster route to know the crystallinity of the sample. Quantifying the number of phases and their concentration is invariably done using the comprehensive libraries (ASTM and JCPDS or PDF indices) of available characteristic *d* spacing and intensities of previously studied solids.

One cannot detect an impurity phase of less than 2-3 % when a XRD profile is scanned for routine analysis. If there is an impurity phase detected on fast scanning, one has to do a slow step scanning for sufficiently long time to maximize the detection of minority or impurity phases by accumulation of intensity counts and refine the profile if necessary for phase quantification. The quantitative analysis can also be done by Rietveld refinement method, which requires the knowledge of the crystal structure of all the phases present in the mixture.

The XRD patterns of the catalyst samples were taken using Philips diffractometer (PW 1710). Ni filtered Cu $K_\alpha$ radiation ($\lambda$ = 1.5404 Å) and a movable detector, which measures the intensity of diffracted radiation as a

function of 2θ are the main parts of the instrument. The X-Ray diffraction patterns of the catalysts were recorded using a Rigaku D-max C X-ray diffractometer using Ni filtered Cu Kα radiation source (λ =1.54056$A^0$). The anatase peaks of the systems were confirmed by comparing with JCPDS data files.

### 2.3.2 Infrared Fourier Transform spectroscopy (FTIR)

Infrared spectroscopy (IR) is widely used in the field of characterization of heterogeneous catalysts. Identification of the structural features of the catalysts such as adsorbed and dispersed species and their structure, metal-metal interaction, reaction intermediates on the catalyst surface etc. are some of the important information obtained from infrared spectral studies.

Information can be well assigned by the appearance of two IR bands[41,42]. Usually these two IR bands are hidden in ordinary FTIR spectroscopy. The infrared spectra of the prepared samples were recorded by a DR-IR (Shimadzu, model 8300) in the range 400-1400 $cm^{-1}$. FT-IR spectra (Infra red spectra) were obtained by the KBr technique over the wave number range 400-4000$cm^{-1}$ by using ABB BOMEM (MB Series) FT-IR spectrophotometer[43].

### 2.3.3 $N_2$ adsorption/ desorption analysis

**Surface area determination method** (BET)

The Brunauer, Emmett and Teller method (BET) [44] has been adopted as a standard procedure for surface area determination and is ideally suited for the determination of surface areas of finely divided solids [45]. By the introduction of a number of simplifying assumptions, this theory extends Langmuir model to multilayer adsorption. In BET theory, it

is assumed that the solid surface possesses uniform, localized sites and the adsorption at one site does not affect adsorption at neighbouring sites. It is further assumed that the adsorption is multiplayer and the heat of adsorption of the second and the subsequent layers are identical and is equal to the liquefaction of the adsorbate. The BET equation can be represented as,

$$\frac{P}{v(p_0-p)} = \frac{1}{C\,v_m} + \frac{(C-1)\,P}{C\,v_m\,p_0}$$

Here, C = a constant for a given system at a given temperature and is related to the heat of adsorption, v = volume adsorbed at equilibrium pressure p, $v_m$ = volume of the adsorbate necessary to form a monolayer on the surface and $p_0$ = saturation vapour pressure of the adsorbate.

The BET equation demands a linear relation between $p/[v\,(p_0-p)]$ and $p/p_0$, where slope = $(C-1)/C\,v_m$ and y intercept = $1/C\,v_m$. From the slope and y-intercept, $v_m$ can be calculated. The specific surface area of the sample is then calculated using the relation,

$$\text{Surface area } (m^2g^{-1}) = \frac{v_m N_0 a_m}{22414 \times \text{weight of the catalyst}}$$

Where $a_m$ = average area occupied by the nitrogen molecule (1.62 $Å^2$) and $N_0$ = Avagadro number.

Although in principle any gas or vapour may be chosen as the adsorbate, the usual choice is nitrogen as it is inexpensive, easily obtained, inert towards most of the solids and is able to penetrate even the finest pores. Most solids are inherently porous, and many techniques have been developed to characterize the porous structure of solids. Among them the

nitrogen adsorption technique is the most popular one that can obtain the data on total pore volume, the BET surface area and the pore size distribution.

**BJH Method**

Before we intrude into the characterization of the pore structure, it's noteworthy to discuss the types of isotherms and hysteresis loops. According to the International Union of Pure and Applied Chemistry (IUPAC), the majority of adsorption-desorption isotherms may be grouped into six types[46] as shown in Figure 2.1 below.

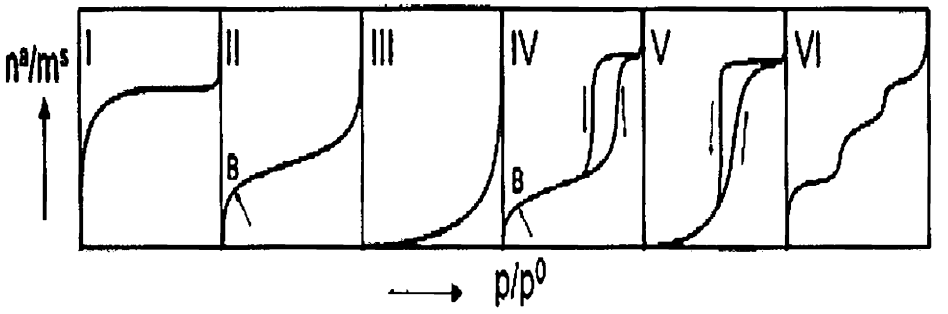


**Figure 2.1 Different Types of Adsorption-Desorption isotherms**

The reversible *Type I* isotherms are given by microporous solids having relatively small external surfaces. The reversible *Type II* isotherms is the normal form of isotherm obtained with a non-porous or macroporous adsorbent. It represents unrestricted monolayer-multilayer adsorption. The reversible *Type III* isotherms are not common, but there are a number of systems (e.g. nitrogen on polyethylene) which give isotherms with gradual curvature and an indistinct Point B. Characteristic features of the *Type IV* isotherm are its hysteresis loop, which is associated with capillary condensation taking place in mesopores. The *Type V* isotherm is uncommon, it is related to the Type III isotherm in that the adsorbent-

adsorbent interaction is weak, but is obtained with certain porous adsorbents. The *Type VI* isotherm, in which the sharpness of the steps depends on the system and the temperature, represents stepwise multiplayer adsorption on a uniform non-porous surface.

Normally, in the adsorption-desorption isotherms, the desorption isotherms do not retrace the adsorption ones but rather lie above them over a range of relative pressure, which form a hysteresis loop before eventually rejoining the adsorption isotherms. Hysteresis appearing in the multiplayer range of physisorption isotherms is usually associated with capillary condensation in mesopore structures. IUPAC has classified the various hysteresis loops that are observed experimentally as types H1, H2, H3 and H4 as shown in Figure 2-4.

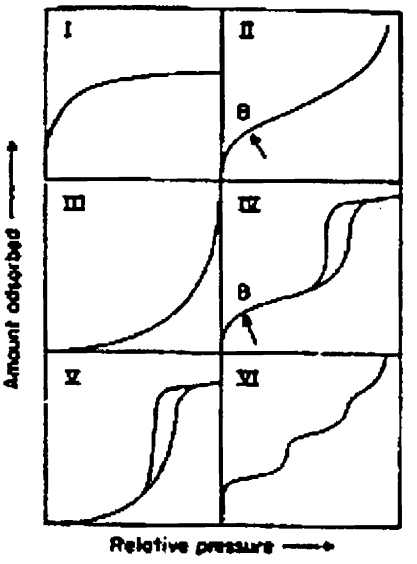


**Figure 2.1 Different Types of Hysteresis Loops**

Point B ,the beginning of the almost linear middle section of the isotherm ,is often taken to indicate the stage at which monolayer coverage

is complete and multiplayer adsorption about to begin[47].The observed hysteresis may be the result of two basic mechanisms, namely, "single pore mechanism" and "network mechanism"[48].

In "single pore mechanism", a metastable phase may persist beyond the vapor liquid coexistence pressure during the adsorption and desorption processes where a vapor phase may be present at pressure above the condensation pressure, and a liquid phase below the condensation pressure[49]. The second mechanism is related to the topology of the pore network. During the adsorption process, the vapors needed to fill the pore can be transported either through the liquid or through the vapor phases. However, during the desorption process, the desorbed vapors must be transported to outside only through the vapor phase. Vaporization therefore occurs only in pores connected to the bulk vapor phase, not in pores surrounded by other liquid filled pores. Once vaporization has occurred in some of the pores near the external surface, the adjacent pores now have contact with the vapor phases, and will vaporize when it is thermodynamically favorable. As a result, clusters of vapor-filled pores grow from the surface until enough pores are opened. $N_2$ Adsorption-Desorption measurements at 77K were made using a *Micromeritics Tristar 3000* surface area and Porosity analyzer. The samples were outgassed at 350°C for 4h under $N_2$ flow.

### 2.3.4 Thermogravimetric Analysis (TG).

Thermogravimetric analysis (TG) is used in catalyst characterization procedure as an important tool to provide valuable information regarding drying ranges, hydration, decomposition temperature, stability limits, etc. In thermogravimetry, the weight of a sample is recorded over a period of time while its temperature is being raised linearly. A thermogram is obtained by

plotting weight of a sample (on ordinate) against temperature (on abscissa). The horizontal region of the thermogram indicates the thermal stability of the sample, while weight loss is indicated by the curved portions. DTG is the first derivative plot of the TG curve from which a better understanding of the weight loss can be obtained from the dip in the curve. Thermogravimetric analysis of the samples were carried out using Perkin Elmer Pyris Diamond thermogravimetric /differential thermal analyzer by heating the samples at a rate of 20°C/min from room temperature to 1100°C in nitrogen atmosphere with samples mounted on an alumina sample holder.

### 2.3.5 Energy dispersive X-ray analysis (EDX).

The chemical compositions of catalysts were determined using energy dispersive X-ray analyzer. This technique (EDX) is used in conjunction with SEM. An electron beam strikes the surface of a conducting sample. The energy of the beam is typically in the range 10-20 K eV. This causes X-rays to be emitted from the point of the material. The energy of the X-rays emitted depends on the material under examination. The X-rays are generated in a region about 2 microns in depth. By moving the electron beam across the material an image of each element in the sample can be acquired. The detector used in EDX is the Lithium drifted Silicon detector. This detector must be operated at liquid nitrogen temperature. When an X-ray strikes the detector, it will generate a photoelectron within the body of the Si, as this photoelectron travels through the Si, it generates electron-hole pairs. The electrons and holes are attracted to the opposite ends of the detector with the aid of a strong electric field. The size of the current pulse generated depends on the number of electron-hole pairs created, which in turn depends on the energy of the

incoming X-ray. Thus, an X-ray spectrum can be acquired giving information on the elemental composition of the material under examination. The Si- Li detector is often protected by a Beryllium window. The absorption of the soft X-ray by Be precludes the detection of elements below an atomic number of 11 (Na). In windowless systems, element with atomic number as 4 (Be) have been detected, but the problems involved get progressively worse as the atomic number is reduced**[50]**. The chemical compositions of catalysts were obtained from Stereoscan 440 Cambridge, UK energy dispersive X-ray analyzer used in conjunction with SEM. Powdered sample is put on a double-sided carbon tape on a metal strip before analysis. EDX spectra of the samples were recorded in an EDX-JEM- instrument (JEOL Co. link system AN-1000-Si-Li detector). The atom/wt % of the metals loaded were obtained.

### 2.3.6 Scanning electron microscopy (SEM).

Scanning electron microscopy (SEM) is based on the strong interaction of electrons with matter and appreciable scattering by quite small atomic clusters. Electrons can be conveniently deflected and focused by electric or magnetic fields so that magnified real-space images can be formed in addition to simple diffraction patterns. This property of electron beam is used in SEM analysis. In SEM, the electron optics act before the specimen is reached to convert the beam into a fine probe, which can be as small as 100 Å in diameter at the specimen surface**[51]**. The technique is of high interest in catalysis because of its high resolution. However, a serious drawback is that the results need not be really representative of the whole sample. This can be overcome by making many analyses at different locations of the sample particles and for many catalyst particles.

SEM analysis of the sample was done using Stereoscan 440 Cambridge, U.K scanning electron microscope. Characteristic SEM images of two samples at 10μm magnification are presented. The images give a clear picture of the surface morphology of the catalysts.

### 2.3.7 Transmission Electron Microscopy(TEM)

Transmission electron microscopy (TEM) was used to study the particle morphologies and the pore ordering in the samples. This operates on the same basic principles as the light microscope but uses electrons instead of light whereby a beam of electrons is transmitted through an ultra thin specimen, interacting with the specimen as it passes through. An image is formed from the interaction of the electrons transmitted through the specimen; the image is magnified and focused onto an imaging device, such as a fluorescent screen, on a layer of photographic film, or to be detected by a sensor such as a CCD camera. TEMs are capable of imaging at a significantly higher resolution than light microscopes, owing to the small de Broglie wavelength of electrons. This enables the instrument to be able to examine fine detail-even as small as a single column of atoms, which is tens of thousands times smaller than the smallest resolvable object in a light microscope. TEM forms a major analysis method in a range of scientific fields, in both physical and biological sciences. At smaller magnifications TEM image contrast is due to absorption of electrons in the material, due to the thickness and composition of the material**[52].** At higher magnifications complex wave interactions modulate the intensity of the image, requiring expert analysis of observed images. Alternate modes of use allow for the TEM to observe modulations in chemical identity, crystal orientation, electronic structure and sample induced electron phase shift as well as the regular absorption based imaging. A high-resolution

transmission electron microscopy (HRTEM) investigation of the microstructure of $TiO_2$ is also carried out. The experimental observations reveal the structural features of the interface between the film and the substrate and three main types of crystal defects in the anatase $TiO_2$ film is revealed. Observation of the interface showed that the anatase was epitaxially grown on the substrates although defects, such as dislocations and distorted regions can be observed near the interface[53]. These methods were supported by X-ray diffraction and thermal analysis. The chemical and structural properties, as well as the size of grains, depend on the temperature of $TiO_2$ preparation. This technique, often called electron microscopy is to confirm the mesoporous nature of the materials prepared and is examined under the instrument transmission electron microscope TEM ( JEOL,JEM-2010).

### 2.3.8 X-ray photoelectron spectroscopy (XPS)

X-ray photoelectron spectroscopy (XPS) is one of the most widely used technique for surface analysis. In the technique, which has been applied by industry for more than 30 years, atom core electrons are excited by soft X-rays and the kinetic energy of the emitted electrons is measured. Peaks occur corresponding to the binding energy of the core electrons and their position gives therefore direct identification of atoms. Since the inelastic mean free path for electrons in the energy range studied (typically ~ 0.1 to 1.5 keV) is 0.5 – 3 *nm*, the peak intensity originates from electrons excited from atoms that are within a 2-5 *nm* thin surface layer[54]. The core electron binding energy varies slightly depending on the chemical environment of the atom, and this is used to get information on the chemical bonds. Scanning XPS has been increasingly more used in the past decade driven by substantial improvements in lateral resolution. The

interpretation of XPS has largely been based on simple peak intensity measurements and this strongly limits the quantitative accuracy of it. The depth resolution of XPS has usually been done by ion-etching the surface. In the past decade, significant advancements has however been done in the development of improved algorithms for quantitative XPS and non-destructive atom depth distribution analysis in the 0-10 *nm* depth range **[55]**. Formation of mixed oxide phase is an evidence of the well-known strong metal–support interaction (SMSI) effect occurring with the support **[56]**. The highest energy value is indicative of the highest oxidation state, whereas the lower binding energy is the evidence for an increased electron density of the supported metal. Such charge transfer is caused by the SMSI between metal and the support. This effect is more evident for small metal loadings corresponding to a better metal dispersion on the support **[57]**. At variance with previous study, the presence of strong shake up satellites are typical of the metal and could be consistent with the presence of surface dispersion **[58]**.For example about Co particles there was clear evidence of the oxide in the reports of A.M. Venezia et al**[59,60]**. The Cr(VI) species is likely to arise from the oxidation of the chromium precursors during the high temperature calcinations. Unlikely, the series of the other transition metals, the Fe $2p_{3/2}$ binding energy increased with increasing iron loading going from 709.9 eV of Fe/TiO2/0.3 to 711.0 eV of Fe/$TiO_{2.5}$ is observed. The samples loaded with molybdenum were characterized by well-resolved Mo $3d_{5/2}$ and Mo $3d_{3/2}$ doublets. The binding energy of the Mo $3d_{5/2}$ at 233.3 eV is indicative of Mo(VI) **[61]**. The vanadium doped samples were characterised by the binding energy V $2p_{3/2}$ equal to 517.3 eV typical of V(V) **[62]**. For the low loaded catalysts the exact position of the V $2p_{3/2}$ peak was difficult to ascertain due to the partial overlap with the strong O1s satellite. The W $4f_{7/2}$ binding energy of the powders containing

tungsten was found at 36.0 eV, typical of W(VI) [63]. For the fitting of the W 4f doublet, subtraction of the overlapping Ti 3p peak, according to the position and the relative intensity with respect to the Ti $2p_{3/2}$ peak as obtained from pure $TiO_2$, was performed. XPS spectra were recorded in an indigenously developed electron spectrometer equipped with Thermo VG Clamp-2 Analyser and a Mg Kα X-ray source (1253.6 eV, 30mA × 8 kV). A thin sample wafer of 12 mm in diameter was used in these studies. As an internal reference for the absolute binding energy of C 1s peak at 284.08 eV was used. The analyser operated in the constant analyser energy (CAE) mode. For the individual peak energy regions the pass energy of 20 eV set across the hemispheres was used. Survey spectra were measured at 50 eV pass energy. The sample powders were pelletised and then mounted on a double-sided adhesive tape. The pressure in the analysis chamber was in the range of $10^{-6}$ $Nm^{-2}$ during data collection. The constant charging of the samples was removed by referencing all the energies to the C 1s peak previously calibrated at 284.08 eV, arising from the adventitious carbon. The peaks were fitted by non-linear least-squares fitting program using properly weighted sum of Lorentzian and Gaussian component curves after background subtraction according to Shirley and Sherwood [64,65]. The binding energy (BE) values are quoted with a precision of ±0.15 eV. Atomic concentration ratios were obtained from peak area ratios and element sensitivity factors using the VG instrument software.

### 2.3.9 Diffuse Reflectance UV-Vis Spectroscopy (UV-Vis DRS)

The diffuse reflectance UV-Vis spectroscopy (UV-Vis DRS) is known to be a very sensitive probe for the identification and characterization of metal ion coordination. It is a non-invasive technique that uses the interaction of light, absorption and scattering, to produce a characteristic

reflectance spectrum, providing information about the structure and composition of the medium. It gives information regarding electronic transition between orbitals or bands in the case of atoms, ions and molecules in gaseous, liquid or solid state. Electronic transition of transition elements are of two types, namely, metal centered transitions [d-d or (n-1) d-ns] and charge transfer (CT) transitions. d-d transitions gives information about the oxidation state and the coordination environment of transition metal ion. (n-1) d-ns transitions are often too high in energy to be observed in the spectrum. The CT transitions are intense since they are Laporte allowed and are sensitive to the nature of donor and acceptor atoms[66,67]. The band gap can be calculated using KM equation[68].Diffuse reflectance UV-Vis spectra of the samples were recorded at room temperature between 200 and 800nm using Barium Sulphate as standard in *Labomed* instrument with a CCD detector. Absorbance measurements as well as onset absorption were taken in Spectrophotometer UV-Vis Double Beam UVD-3500, Labomed, Inc. Absorbance measurements of the UV irradiated methylene blue dye was taken at regular intervals. DRS studies of the prepared catalysts were carried out.

### 2.3.10 Temperature programmed desorption of ammonia (TPD)

Acid-base properties of the solid catalysts play decisive role in determining the catalytic activity and selectivity. Independent methods adopted for the thorough understanding of the acid-base properties of prepared catalysts by temperature programmed desorption of ammonia (TPD). The $NH_3$-TPD method is widely employed in characterizing the acidity of solid catalysts. This is an easy method used to find out the total acidity as well as acid strength distribution.

The pellets were prepared from the sample (about 0.5 g) using a pelletiser and activated at 500°C for 2 h. The accurately weighed pellets were placed in a home built stainless steel reactor of internal diameter 1 cm and length 15 cm kept in a cylindrical furnace. The temperature of the reactor is maintained using a temperature controller and the temperature was measured by an Al-Cr thermocouple kept inside the furnace. The sample was degassed at 300 °C using a flow of nitrogen for half an hour. It was then allowed to cool to room temperature and a definite amount of ammonia is injected into the reactor and allowed to adsorb uniformly over the catalyst surface. The physisorbed ammonia was flushed out using a flow of nitrogen gas. Under a controlled temperature programme, the amount of chemisorbed ammonia leached out -up to a temperature of 600 °C- was trapped into $H_2SO_4$ solution (0.025 N) and ammonia desorbed was determined by back titration with NaOH solution (0.025 N).

$$\text{Amount of ammonia desorbed} = \frac{\Delta V \times N_{NaOH} \times 5}{\text{Weight of the sample}}$$

Where $\Delta V$ is the difference in titre values of NaOH between blank $H_2SO_4$ and the ammonia trapped $H_2SO_4$ at each temperature. Ammonia TPD measurements were carried out in the range 100-600°C in a conventional flow type apparatus using a stainless steel reactor of 30 cm length and 1cm diameter kept in a cylindrical furnace. The catalyst is pelletized and put in the reactor under nitrogen flow at 300°C.The method is based on desorbing ammonia adsorbed on the solids by heating it at a programmed rate.

### 2.4.0 Catalytic activity studies

### 2.4.1 Photocatalytic activity

The photocatalytic activity of the prepared systems towards the degradation of dyes is intensively studied. The reactions were carried out in a Heber photoreactor (multilamp type, model HML-MP88) containing concentrically arranged eight numbers of 8W mercury lamps set in parallel and emitting 365nm wavelength. It has a reaction chamber with specially designed reflectors made of highly polished aluminium and built in cooling fan at the bottom. Open borosilicate glass tube of 50 ml capacity, 40 cm height and 20mm diameter with the total light exposure length of 330 nm was used as a reaction vessel. The solution with a photocatalyst and dye was taken in the borosilicate glass tube. The suspension was magnetically stirred for 30 min in dark for the attainment of adsorption equilibrium and then irradiated. After reaction, centrifuged to separate the catalyst and diluted if necessary and absorbance measurements of the dyes were taken at intervals.

Absorbance measurements as well as onset absorption were taken in a Spectrophotometer UV-Vis Double Beam UVD-3500, Labomed, Inc. The dyes under study were methylene blue, malachite green, Acid blue-25, Acid Red-1and Acid Orange7of $\lambda_{max}$ values - Methylene blue-660nm (MB), Malachite Green-614nm (MG), Acid Blue25-600nm (AB25) , Acid Red1-532nm (AR1) and Acid Orange7-483nm (AO7). DRS studies of the prepared catalysts were also carried out.

### 2.4.2 Chemical activity studies

The reaction studied for the present work were the liquid-phase reactions[69] such as epoxidation of cyclcohexene and hydroxylation of phenol.

**Materials**

The materials used for the catalytic activity measurement is as follows.

| | Materials | Suppliers |
|---|---|---|
| 1 | Benzyl Alcohol | Merck |
| 2 | Cyclohexane | Merck |
| 3 | TBHP | Merck |
| 4 | Phenol | Merck |
| 5 | Hydrogen peroxide | SD Fine-Chem Ltd |
| 6. | Acetonitrile | SD Fine-Chem Ltd |
| 7. | Ethanol | SD Fine-Chem Ltd |

**Methods**

A brief description of the experimental procedure for the different types of reactions studied is given below. The catalytic activity was expressed as the percentage conversion and the selectivity for a product is expressed as the amount of the particular product divided by the total amount of products multiplied by 100.

#### 2.4.2.1 Liquid Phase Reactions

Epoxidation of cyclohexene and hydroxylation of phenol were carried out in liquid phase. For the liquid-phase reactions, the reagents in the required molar ratio were taken in a 50 ml double-necked round bottom

flask fitted with water condenser and guard tube. The reactions were carried out in an oil bath using 0.1 g of the catalyst (activated at 300 °C for 2 h) and the temperature of the reaction was controlled using a dimmerstat. Using a magnetic stirrer, the uniform stirring of the reaction mixture was attained. The reaction mixture was analyzed by gas chromatography (Chemito 1000 GC, FID detector, $N_2$ carrier gas, SE30capillary column, OV17 column for phenol) and product identification was done by comparing the retention times with standards.

Microgravimetric measurements were carried out with a Sartorius AG,mod. TE6100 electro balance operating in controlled atmosphere.

## References


1. D. M.Antonelli, J. Y.Ying, *Angew. Chem., Int. Ed. Engl. 34*(1995) 2014.
2. D. M.Antonelli, *Microporous Mesoporous. Mater .30(*1999) 315.
3. M. Baltes, P. Van Der Voort, B. M .Weckhuysen, R. R. Rao, *Langmuir. 15(*1999) 8561.
4. C.J.Brinker,G.W.Scherer,Sol-Gel Science- The Physics and Chemistry of Sol-Gel Processing,Academic Press,New York.
5. Konstantin.I.Hadjiivanov,Dimiter.G.Klissurki,Chem.Soc.Review 61 (1996).
6. R.Debnath,J.Chaudhri,J.Mater.Sci.Lett 10 (1991)494.
7. N.Serpone,D.Lawless,R.Khairutdinov,J.Phy.Chem.99(1999)16646.
8. H.K.Park,V.T.Moon,C.H.Kin,J.Am.Ceram.Soc. 19(1996)2727.
9. M.Iwasaki,M.Hara,S.Ito.J.Mater.Sci.Lett.17(1998)1769.
10. A.Kato,Y.Tashita,Y.Katate. Mater.Res.Soc.Symp.Proc.155(1989)13.
11. Bargaretto,J.Kiwi,E.Pelizzetli,M.Visca,M.Geratzel,Nature289(1981)158.
12. B.E.Yoldas,J.Mater.Sci 21 (1986)1087.
13. N.Ulagappan,C.N.R.Rao,Chem.Commun (1996)1685.
14. L.Saadoun *et* al,Mater.Res.Bull 35(2000)193.
15. Mao-pingZheng *et* al,Master .Sci.Engg.B 87(2001)197.
16. B. O'Regan, M. Gratzel, Nature 353 (1991) 737.
17. S.T. Aruna, S. Tirosh, A. Zaban, J. Mater. Chem. 10 (2000) 2388.
18. H. Yin, Y. Wada, T. Kitamura, S. Murasawa, H. Mori, T. Sakata, S. Yanagida, J. Mater. Chem. 11 (2001) 1694.
19. H. Hayashi, K. Torii, J. Mater. Chem. 12 (2002) 3671
20. S.Y. Chae, M.K. Park, S.K. Lee, T.Y. Kim, S.K. Kim,W.I. Lee, Chem. Mater. 15 (2003) 3326.
21. A. Fujishima, T.N. Rao, D.A. Tryk, J. Photochem. Photobiol. C: Photochem. Rev. 1 (2001) 1.
22. M. Kondo, K. Shinozaki, R. Ooki, N. Mizutani, J. Ceram. Soc. Jpn. 102 (1994) 742.
23. A.I. Kontos, I.M. Arabatzis, D.S. Tsoukleris, A.G. Kontos, M.C. Bernard, D.E. Petrakis, P. Falaras, Catalysis Today. 101 (2005) 275–281

24. I. Kartini ,P. Meredith,J.C. Diniz da Costa , G.Q. Lu,J. Sol-Gel Science & Tech 31(2004)185–189.

25. P .Yang, D. Zhao, D I. Margolese, B. F. Chmelka, G. D .Stucky, *Nature396(*1998) 152.

26. D. Grosso, de A. A. Soler-Illia, G. J. Babonneau, F. C.Sanchez, P.-A.Albouy, A.Brunet-Bruneau, A. R. Balkenende, *Ad*V. *Mater. 13 (*2001) 1085.

27. Yolanda.segura *et* al *J. Phys. Chem. B 110* (2006) 948-955.

28. Evi Beyers, Pegie Cool, Etienne F. Vansant J.Phys .Chem.B109(2005)10081.

29. K.Cassiers, T.Linssen, M.Mathieu, Y.Q.Bai, H.Y.Zhu, P.cool, E.F.Vasant, *J. Phys. Chem* B108 (2004) 3713.

30. M.Baltes, P. Van Der Voort, B. M.Weckhuysen, R. R.Rao, G.Catana,R. A.Schoonheydt, E. F. Vansant, *Phys. Chem. Chem. Phys.2 (*2000)2673.

31. P. Van Der Voort, M. Baltes, E. F. Vansant, *J. Phys. Chem. B103 (*1999) 10102.

32. K.Schrijnemakers, E. F. Vansant, *J. Porous Mater.8 (* 2001)83.

33. Y.Segura, P.Cool, P.Van Der Voort, F.Mees, V.Meynen, E. F. Vansant, *J. Phys. Chem. B 180 (*2004)3794.

34. J. Matta, D. Courcot, E. Abi-Aad, A. Aboukais, Chem. Mater. 14 (2002) 4118.

35. E. Beyers, P. Cool, E.F. Vansant Microporous and Mesoporous Materials 30(2006) 60.

36. Tian B and Zhao D Nature Mater.,2(2003)159-163.

37. Tian B and Zhao D Chem.Commun(2002)1824-1825.

38. CrepaldeE.L.,Solar –Illia G.J.D.A.,grosso D.,Gagnol F.,Sanchez C.J.,Am.Chem.Soc.125(2003)9770-9786.

39. A.Howie; "Characterisation of Catalysts", (Eds., J.M.Thomas and R.M.Lambert), John Wiley, New York(1980)114.

40. C.Whiston, "X-ray methods", (Eds., F.E.Prichard), ACOL. Tmames Polytech., London(1991).

41. R.D.Waldron; Phy. Rev., 99 (1955) 1727.

42. W.B.White , B.A.DeAngelis, Spectrochemica Acta. 23A. (1967) 985.

43. C.N.Banwell and E.M.McCash; "Fundamentals of Molecular Spectroscopy", 4th Edn., Tata McGraw-Hill Publishing CompanyLtd., New Delhi, 1995.

44. Segura et al. *J. Phys. Chem. B,* 110 (2006 ) 950.

45. S.Braunauer, P.H.Emmett and E.Teller; J. *Am. Chem. Soc.*, 60 (1938) 309.

46. K. S. W.Sing, D. H.Everett, R. A. W.Haul, L. Moscou,; R. A. Pierotti, J.Rouquerol, T.Siemieniewska, *Pure & Appl. Chem.* **1985**, *57(4)*, 603.

47. Barrett, E. P.; Joyner, L.; Halenda, P. P. *J. Am. Chem. Soc.* (1951) *73.*

48. Lee, C. K.; Chiang, A. S. T.; Tsay, C. S. *Key Eng. Mater.* 21 (1996) *115*,

49. (a) S. A.Bagshaw, E.Prouzet, T. J. Pinnavaia, *Science 269 (*1995), 1242. (b) S.A.Bagshaw,T. J. Pinnavaia,*Angew.Chem.Int.Ed. Engl35*(1996)1102.

50. J.Matta, D.Courcot, E.Abi-Aad and A.Aboukais; Chem. Mater., 14 (2002) 411.

51. A. Howie, "In characterization of Catalysts", J. Thomas and R.M. Lambert Eds, John Wiley, New York (1980) 89.

52. M. Zhu, T. Chikyow, P. Ahmet, T. Naruke, M. Murakami, Y. Matsumoto, H. Koinuma, Material Science.441(2003)141-144.

53. A.M. Tonejc, M. Goti, B. Greta, S. Musić, S. Popovi, R. Trojko, A. Turkovi and I. MuŠevićMaterials Science and Engineering: B 40 (1996)177-184.

54. Sven Tougaard Microsc Microanal 11(2005) 2.

55. S. Tougaard Surf. Interf. Anal. 26 (1998) 249

56. S.J. Tauster, S.C. Fung, R.L. Garten, J. Am. Chem. Soc. 100 (1978)170.

57. B.A. Sexton, A.E. Hughes, K. Foger, J. Catal. 77 (1982) 301.

58. S.W. Ho, J.M. Cruz, M. Houalla, D.M. Hercules, J. Catal. 135 (1992)173.

59. A.M. Venezia, L. Palmisano, M. Schiavello, C. Mart´ın, I. Mart´ın, V.Rives, J. Catal. 147 (1994) 115.

60. R. Riva, H. Miessner, R. Vitali, G. Del Piero, Appl. Catal. A 196(2000) 111.

61. Y.V. Pluto, I.V. Babich, I.V. Plyuto, A.D. van Langeveld, J.A.Moulijn, Appl. Surf. Sci. 119 (1997) 11.

62. W.E. Slinkard, P.B. De Groot, J. Catal. 68 (1981) 423.

63. J.R. Regalbuto, T.H. Fleisch, E.E. Wolf, J. Catal. 107 (1987) 114.

64. D.A. Shirley, Phys. Rev. B 5 (1972) 4709.

65. P.M.A. Sherwood, in: D. Briggs, M.P. Seah (Eds.), Practical Surface Analysis, Wiley, New York(1990)181.

66. G.Ertl, H. Koninger, J. Weitkamp, "Handbook of Heterogeneous Catalysis" Vol.2, VCH, Weinheim (1997) p.646.

67. H.G. Hecht, "Modern aspects of Reflectance Spectroscopy" W.W. Wendlandt (Eds), plenum Press, New York (1968)

68. P.Kubelka , F.Munk ,Z. Tech. Phys., 12 (1931) 593.

69. L.F.Fiesser and M.Fiesser; "Reagents for Organic Synthesis", John Wiley, New York, (1967)125.

*Chapter* 3

# Physico- Chemical Characterization

## *Abstract*

This chapter deals with the characterization techniques. The physico chemical characterization of metal incorporated titania systems by the three routes namely Sol-gel, Hydrothermal and EISA route were done. A detailed investigation was performed by different techniques such as X-Ray diffraction analysis (XRD), Infra-Red spectroscopy (FTIR), Surface area and Pore volume measurements (BJH).Thermogravimetric analysis (TG/DTA), Energy dispersive X-Ray analysis(EDX), Scanning electron microscopy(SEM), Transmission electron microscopy(TEM),X-ray photoelectron spectroscopy (XPS) and UV-Vis diffuse reflectance spectroscopy (UV-vis.DRS). The evaluation of acid sites were done by the technique known as temperature programmed desorption of ammonia(TPD) and chemical catalytic activity studies such as liquid-phase reactions analyzed by gas chromatography (Chemitto 1000 GC, FID detector). Prior to the study of these techniques, the optimization of calcination temperature was done using X-Ray diffraction analysis(XRD), Surface area measurements (BET) and thermogravimetric analysis (TG)in sol-gel route.

### 3.1.0 Optimization of the calcination temperature

Catalyst characterization is a lively and relevant discipline in catalysis. In heterogeneous catalysis, the reaction occurs at the surface. Catalyst and catalytic surfaces need to be characterized with reference to their physical properties and by their actual performance as a catalyst [1].A thorough characterization of the prepared systems was undertaken using various spectroscopic as well as quantitative methods. The selection of calcination temperature is of critical importance in catalysis. The crystalline phase formation also depends on the calcination temperature. It has been reported that the transition of amorphous titania to crystalline titania takes place at 350°C for pure titania [2-4].An earlier study on the kinetics of the anatase to rutile transformation has shown that the transformation involves an overall contraction or shrinking of the oxygen structure and a co-operative movement of ions. The transformation needs to overcome both the strain energy for the oxygen ions to reach their new configuration and the energy necessary to break the Ti-O bonds as the titanium ions redistribute. A high activation energy is required for this purpose (over 420 KJ/mol) and so the phase transition takes place at a temperature around 500°C [5]. Also the phase transformation is generally accompanied with the crystal growth. In the present case, the titania samples calcined at 450°C contain the prominent characteristic peaks of anatase [6] than calcined at other temperatures in sol-gel route. Also the surface area seems to decrease as the calcination temperature is increased. A crystal size of about 10-11 nm is believed to be the optimum size for photocatalytic applications [7].Significant difference in crystallite size was observed for the crystallite size of the samples calcined at temperatures other than 450°C. TG graph also confirms the calcination temperature to be 450°C (723K). Comparing Fig. 3.1 and Table 3.2, the crystallinity of nanocrystals increased

(XRD became sharper, and FWHM decreased) as the calcination temperature is increased. At higher calcination temperatures, the crystallite sizes formed are larger in size (Table 3.2), which can be attributed to the thermally promoted crystallite growth. These results were in agreement with the previous results reported by Yu et al. **[8]**. So the calcination temperature was optimized to be 450°C.

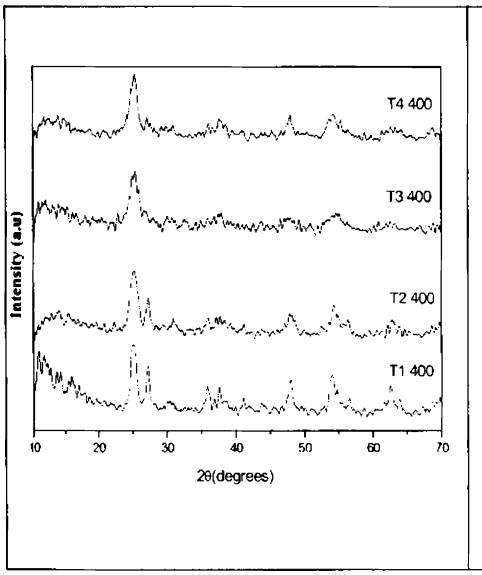


**Fig3.1 XRD of Titania catalysts at 400°C**

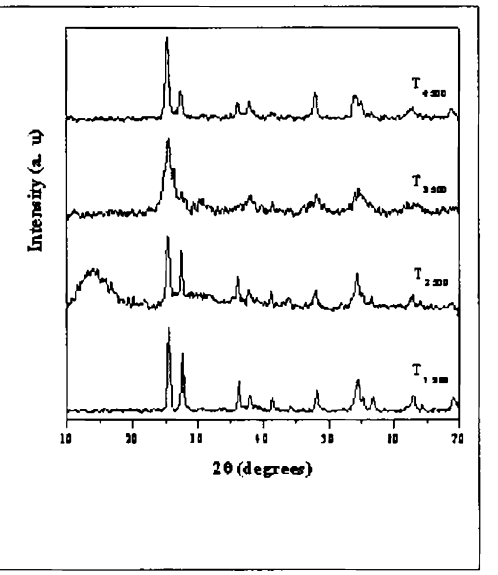


**Fig 3.2 XRD of Titania catalysts at 500°C**

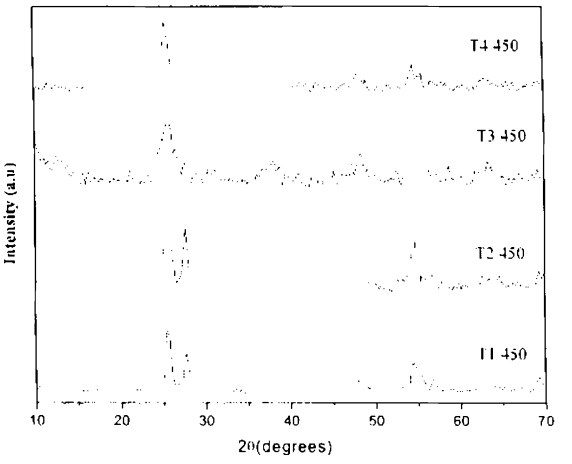


**Fig 3.3 XRD of Titania Catalysts by Sol-Gel route at 450°C**

| Catalyst | 400°C | 450°C | 500°C |
|---|---|---|---|
| T1 | 56 | 34 | 21 |
| T2 | 70 | 36 | 22 |
| T3 | 96 | 95 | 83 |
| T4 | 71 | 43 | 27 |

**Table 3.1 Surface area ($m^2/g$) of Titania Catalysts by Sol-Gel route**

| Catalyst | 400°C | 450°C | 500°C |
|---|---|---|---|
| T1 | 8.9 | 12.3 | 16.5 |
| T2 | 6.3 | 9.1 | 14.8 |
| T3 | 7.9 | 11.7 | 14.8 |
| T4 | 7.2 | 10.6 | 15.1 |

**Table 3.2 Crystallite size (nm) of Titania Catalysts by Sol-Gel route**

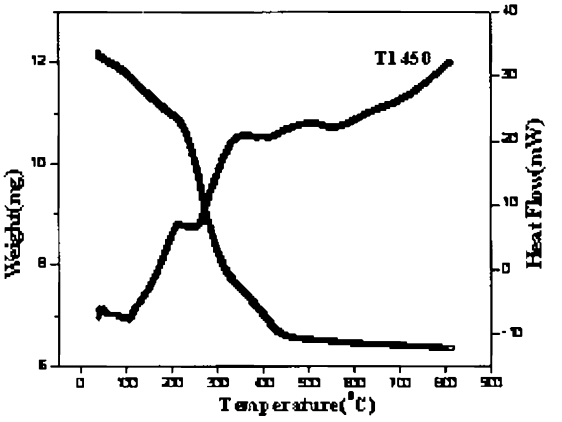


**Fig 3.4 TG/DTA graph of Titania Catalyst by Sol-Gel route at 450°C**

## 3.2.0 Characterization Techniques

A brief discussion of the characterization methods adopted was described below. The prepared systems were characterized by the following methods such as

1. Small and wide angle XRD
2. FT-IR
3. $N_2$ adsorption/ desorption analysis(BJH)
4. TG/DTA
5. EDX
6. SEM
7. TEM
8. XPS
9. TPD
10. UV-Vis.DRS
10. Liquid-phase reactions were analyzed by GC.

### 3.2.1 X-Ray Diffraction Analysis (XRD)

#### 3.2.1.1 Wide Angle XRD

X-ray diffraction (XRD) by crystals is the most widely employed method for determining the three dimensional structure of solid substances. Recording X-ray diffraction pattern of powdered polycrystalline samples by powder diffractometer method has many applications like qualitative phase analysis, quantitative phase analysis, determination of unit cell parameters, study of orientation and determination of particle size. The X-ray diffraction patterns of the catalysts were recorded using a Rigaku D-max C X-ray diffractometer using Ni filtered CuKα radiation source (λ=1.5406A°)in the range of 10-80° at a scan rate of 0.1°$sec^{-1}$using Bragg-Brantan configuration. The anatase peaks of the systems were confirmed by comparing with JCPDS data files. The percentage of phase formed was

determined from integrated peak at 2θ = 25.3 (101) for anatase and peak at 2θ = 27.4(110) for rutile.

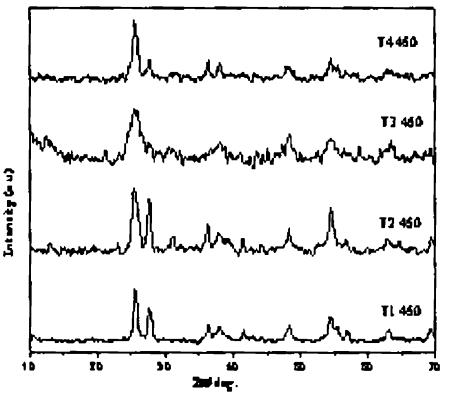


**Fig 3.5 XRD of Titania catalysts Sol-Gel route**

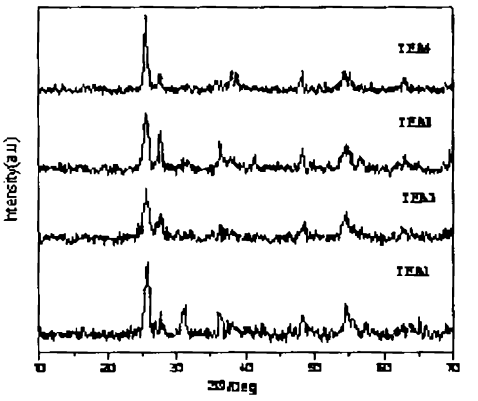


**Fig 3.6 XRD of Titania catalysts EISA route**

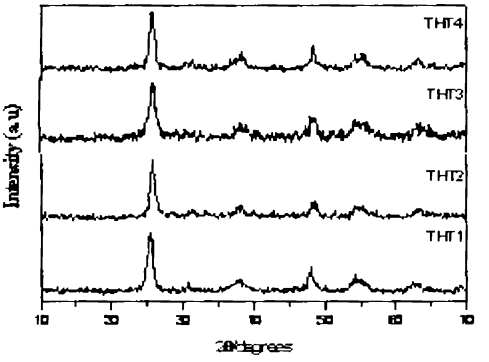


**Fig 3.7 XRD of Titania catalysts by Hydrothermal route**

The wide-angle XRD patterns showed increasing intensity of the(101) anatase peak alone with slight narrowing of the peak width in Hydrothermal route . Instead of controlling the pore formation, the presence of the block copolymer seems to retard an excessive anatase crystal growth. The XRD patterns of titania and metals incorporated titania (Ag, Ce and Cu) were given in Fig 3.8- 3.10. Anatase type structure is kept in all, indicating that the metals are merely placed on the surface of the crystals without being covalently anchored into the crystal. Pure titania

shows characteristics peaks at 2θ values 25.5, 37.4, 47.9 and 53.0 corresponding to the crystal planes (101), (004), (200), (105) and (211) according to JCPDS data. The small characteristic peaks of Ag were seen at 38.2,44.4.and 64.6 for the planes (111),(200), and (220) indicating that Ag metal exists on the $TiO_2$ surface as very fine metal particles and is supported by TEM images. JCPDS peaks for Ce is 29.8(020), 32.9(110), 34.4(021), 37.3(111) and for Cu 43.3(111), 50.4(200). Less intense diffraction peaks of metal particles of Ag at 34.2 and 44.4, Ce at 29.8and 32.9, Cu at 43.2and 50.4 suggesting that these are well dispersed on the $TiO_2$ surface. It may also be noted that the background of the X-ray pattern is flat indicating that $TiO_2$ is crystalline. Apparent full width at half maximum intensity (FWHM) was determined on (101)and (004) X-ray diffraction lines of anatase phase, as a measure of crystallinity. The crystallite size of the metals incorporated samples in different routes were estimated from line broadening of anatase (101) diffraction peak using Sherrer's equation is recorded in Table 3.3[9].

| Sol-Gel Route | | Hydrothermal Route | | EISA Route | |
|---|---|---|---|---|---|
| Catalyst | Crystallite Size(nm) | Catalyst | Crystallite Size(nm) | Catalyst | Crystallite Size(nm) |
| T1 | 12.3 | THT1 | 9.0 | TEA1 | 10.3 |
| T2 | 9.1 | THT2 | 11.6 | TEA2 | 10.5 |
| T3 | 11.7 | THT3 | 13.2 | TEA3 | 10.8 |
| T4 | 10.6 | THT4 | 12.1 | TEA4 | 18.4 |

**Table 3.3 Crystallite size (nm) of Titania Catalysts**

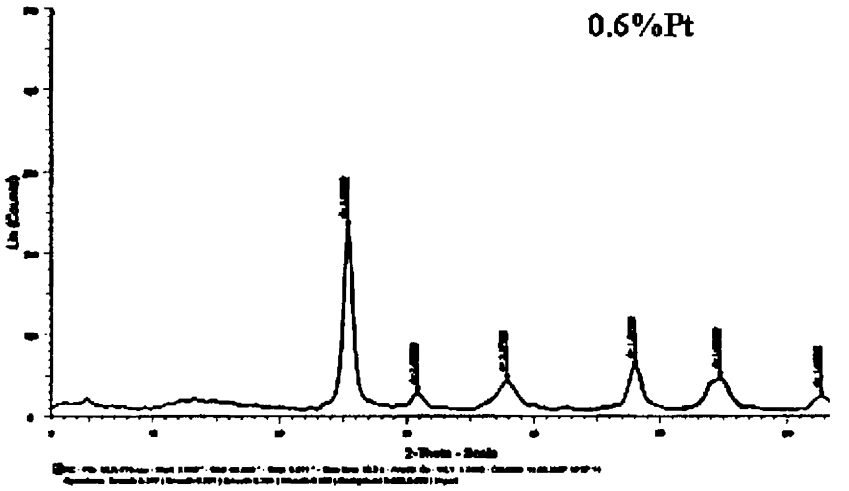


**Fig 3.8 XRD of $TiO_2$/0.6%Pt catalyst by Hydrothermal route**

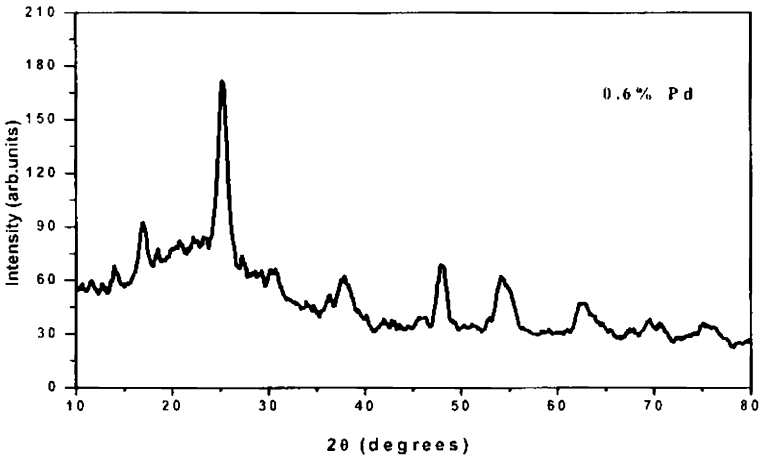


**Fig 3.9 XRD of $TiO_2$/0.6%Pd catalyst by Hydrothermal route**

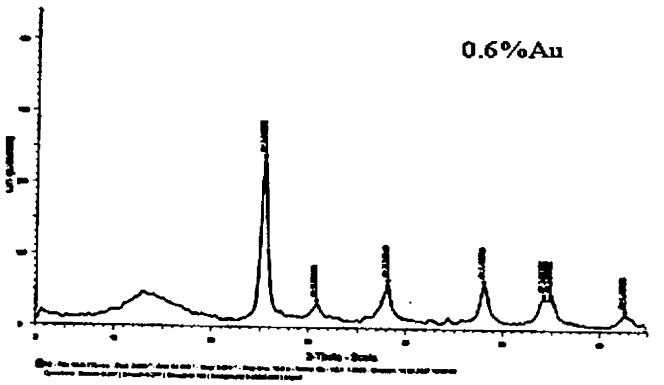


**Fig 3.10 XRD of 0.6%Au/$TiO_2$catalyst by Hydrothermal route**

All the prominent peaks at 2θ values 25.5 are assigned to anatase crystal phase. A weak broad peak at 39.8 for d value 2.26 A is that of Pt metal in Fig 3.8. The presence of Pt observed at 0.6% loading concentration at diffraction angle of 39.8°indexed to (111) plane, however the peak intensity is relatively weak, presumably due to the combination of its low content and small particle size. The crystallite size of the noble metals incorporated samples estimated from line broadening of anatase (101) diffraction peak using Sherrer equation is shown in Table 3.4. The Palladium shows a weak reflection at 40.13 having a d value of 2.25A.An intense peak at 38.18 of (111) plane is that of gold metal deposit over titania surface. The relatively wide width of the peaks indicates small crystallite size, which was estimated to be approximately between 11-13 nm using Scherrer's equation from the XRD peak broadening analysis at (101) **[10]**. It is worth to note that the crystallite size was in the range of 11-13 nm, which is known to be optimum for photocatalytic activity. This is because a very small crystallite size causes a blue shift in the light absorption spectrum and favors surface recombination of the photo-exited holes and electrons while a larger crystallite size exhibits lower surface area and thus a smaller number of catalytic active sites per unit mass of catalyst

[11,12]. It should also be noted that films made of nano size $TiO_2$ particles coated on substrates may exhibit resistance to abrasion and good mechanical stability [13]. So an optimum particle size as mentioned by Y.Q.Wang *et al* is required[7]. The UV–vis absorption band edge which is a strong function of the reactivity of the catalysts,reveals that the crystallite size of noble metals (0.2-1.0%) incorporated catalysts prepared by the hydrothermal method is about 11–13 nm while that of pure $TiO_2$ is 10 nm.

| Catalyst | 0.2% | 0.6% | 1.0% |
|---|---|---|---|
| $TiO_2$/Pt | 10.8 | 12.2 | 13.0 |
| $TiO_2$/Pd | 10.6 | 11.4 | 10.0 |
| $TiO_2$/Au | 12.1 | 13.0 | 13.2 |

**Table 3.4 Crystallite size (nm) of noble metals/ $TiO_2$ Catalysts**

### 3.2.1.2 Small Angle XRD

Figures below show the small-angle (SA) XRD patterns of the resultant titania after the assembly and subsequent calcination at 450°C.The patterns imply that the calcined powder has a long-range mesophase order .It should be noted that we could not determine the mesophase structure from this single peak. However, the $N_2$ adsorption-desorption analysis supports the conclusion that we have mesoporous order, as shown in Fig3.18-3.21 [14]. Mesoporous structure $TiO_2$ should be an even more effective catalyst because of its large surface area and porous frameworks [15-19]. Recently, Zhang et al. found that $TiO_2$ microspheres with porous structures have higher photocatalytic activity and are easy to be recovered and used repeatedly [20]. The breakthrough will open a novel pathway for the elevation of the photocatalysis of $TiO_2$ materials. The mesoporous materials have high surface area and high pore volume because of the large

dimensions of the pores and titania in a mesoporous state has high surface area in a continuous structure which makes the electron transfer easier, resulting in increased photocatalytic activity. However, the metal/$TiO_2$ catalysts show the same type of peak, characteristic of mesoporous materials which indicates that the deposition of metal oxides and the subsequent reduction in $H_2$ did not induce a collapse of the meso structure.

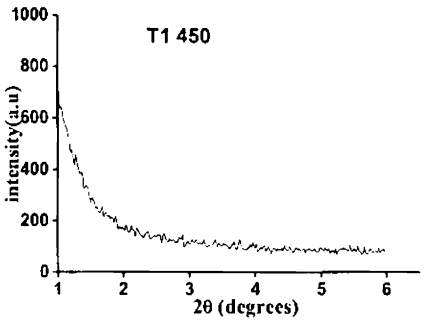


**Fig3.11 SAXRD of Titania Sol-Gel route**

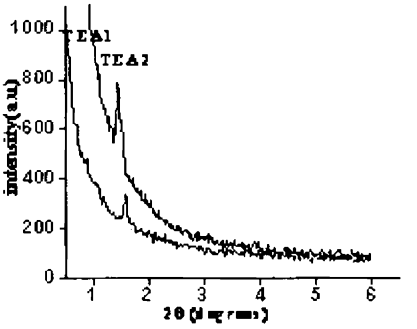


**Fig3.12 SAXRD of Titania EISA route**

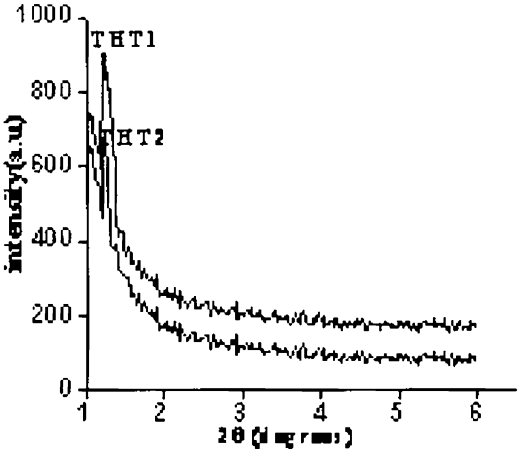


**Fig3.13 SAXRD of Titania in Hydrothermal route**

Except for the titania catalyst from sol-gel route, all patterns are similar and exhibit a single diffraction peak corresponding to d-spacings of

5.54, 5.48 and 5.25nm respectively. Small angle XRD gives peaks at 2θ values 1.5, 1.8 corresponding to the crystal plane (200) characterizing long-range meso order**[21]**. This single strong diffraction peak in the small-angle region indicates the presence of meso structure in samples. Meso-structures with more or less regular in diameter and packed at random(well ordered arrangement) often display a single peak in low-angle XRD. Although others have already demonstrated that similar single-reflection products still have short-range hexagonal symmetry **[22, 23]** those single strong diffraction peaks of the calcined samples may just indicate the presence of mesostructure. No obvious peak is observed on small–angle XRD patterns for the sample calcined at700°C **[24]** and 400°C for films by Stucky ***et al*** **[25]** suggesting the complete collapse of the mesoporous framework .

### 3.2.2 Fourier Transform Infra Red Spectroscopy (FTIR)

Infrared absorption spectroscopy is a rapid, economical and non-destructive physical method universally applicable for structural analysis. The technique is so versatile that it can be used both as a source of physical parameters of crystal lattice determinations and for eliciting purely qualitative relationship between samples. The number, position, bandwidth and intensity of adsorption bands may be correlated with the electronic and molecular structure. It also provides important information about the inter molecular forces acting between the atoms in a molecule, intermolecular forces in condensed phase and nature of chemical bond.

Infrared spectroscopy is a direct method for monitoring transitions between quantized vibrational levels induced by absorption of light in infrared region. A vibration that interacts with the electromagnetic field absorbs the radiation into the molecule, the interaction being provided by an oscillating dipole moment. The spectrum is generally recorded by passing a beam of polychromatic infrared light through a sample and monitoring the radiant power of transmitted light at each frequency of

source. The technique can be applied to solids as crystals or powder, liquids as solutions or melt, gases, films and adsorbed species.IR analysis can be used to almost any type of samples as long as the material is composed of compounds. Areas of application include catalysis, polymer chemistry, fast reaction dynamics, charge transfer complexes etc. Its utilization is spreading to other areas like layer thickness measurements, reflectivities and refractive index. The use of IR spectroscopy for samples is controlled by the constraints of overall symmetry of unit cell and local site symmetry of each atom within the unit cell.

FT-IR spectra was measured by the KBr technique over the wave number range 400-4000$cm^{-1}$ by using ABB BOMEM (MB Series) FT-IR spectrophotometer. Figures 3.14-3.16 show FTIR spectra of mesoporous titania catalyst as well as metal incorporated titania catalysts thermally treated at 450°C in air flow. FTIR spectra shows broad bands around 3500 $cm^{-1}$ are due to –OH strectching vibrations of free and hydrogen bonded surface hydroxyl groups in titania**[26-28]**. The adsorption bands at 1630 $cm^{-1}$ are arising from the bending vibrations of physisorbed water molecules in the catalysts**[29]**. After deposition of metals, a clear increase of the OH bands is observed. This surface hydroxylation is very advantageous for the photocatalytic activity of anatase because it provides higher capacity for oxygen adsorption**[30,31]**. Intensive and broad bands appearing at 565 $cm^{-1}$-660 $cm^{-1}$ is that of fundamental vibrations of $TiO_2$nano crystals ie.. stretching vibrations of Ti-O bonds**[32]**. It is obvious that –OH gps are more on the hydrothermally prepared catalysts which clearly indicates the adsorption capacity of the prepared catalysts and the result is enhanced photocatalytic activity. Figure 3.17 is FT-IR spectra of noble metals incorporated titania catalysts with the fundamental vibrations and peaks at 2362 $cm^{-1}$is due to asymmetric stretching of $CO_2$ adsorbed from the atmosphere.

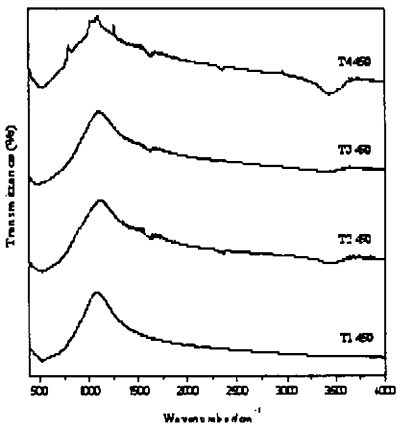

Fig3.14 FT-IR spectra of Titania catalysts by Sol- Gel route

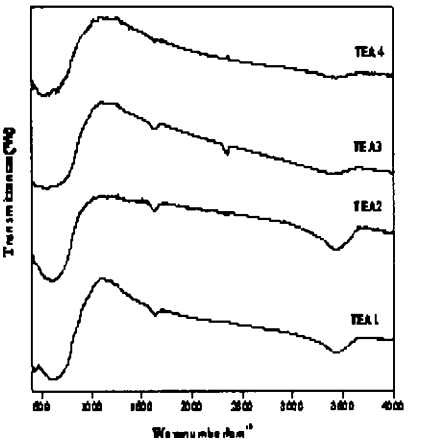

Fig3.15 FT-IR spectra of Titania catalysts by EISA route

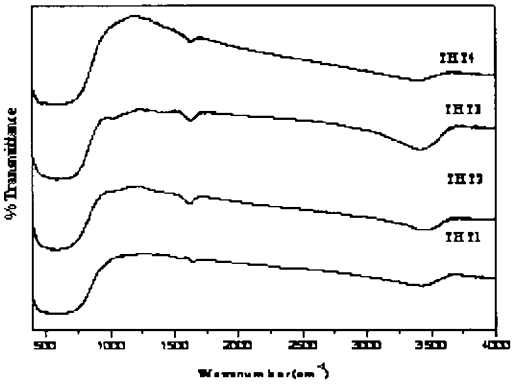


Fig3.16 FT-IR spectra of Titania catalysts by hydrothermal route

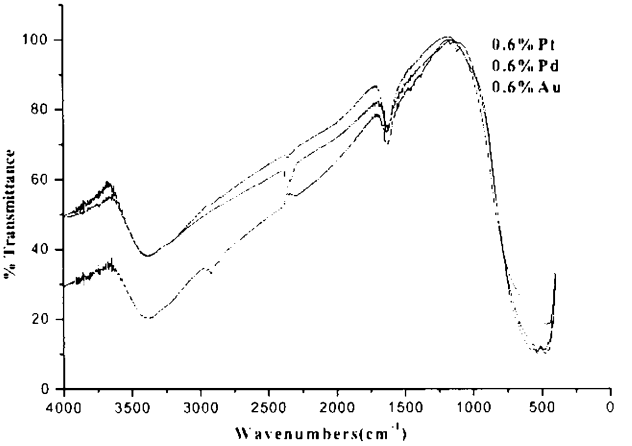


Fig3.17 FT-IR spectra of noble catalysts/$TiO_2$ by hydrothermal route

### 3.2.3 $N_2$ Adsorption-Desorption analysis (BJH)

#### 3.2.3.1 Surface area

The Brunauer, Emmett and Teller (BET) method has been adopted as standard procedure for surface area determination of powdered catalysts. Adsorption of nitrogen gas at its boiling point is generally used for surface area measurements using BET method. The BET theory of adsorption is an extension of Langmuir model to multi layer adsorption. The basic assumptions of BET model are

1. Heat of adsorption for adsorbate-adsorbant system does not change with surface coverage which means that all the adsorption sites on a given surface are energetically homogeneous.
2. Adsorption is multilayer and the heat of adsorption of second and subsequent layers are the same as heat of condensation of adsorbate
3. Dynamic equilibrium occurs within each layer

The **BET** equation is conveniently expressed in the form,

$$\mathbf{P/\,[V(P_0-P)\,] = [1/VmC\,]+[(C-1)/VmC\,]\,(P/P_0)}$$

where P-adsorption equilibrium pressure, $P_0$-standard vapour pressure of adsorbate ,V-volume occupied molecules adsorbed at equilibrium pressure, Vm-volume of adsorbate required for monolayer coverage and C-a constant related to heat of adsorption.

A plot of $P/\,V(P_0-P)$ against $P/P_0$ is a straight line with slope (C-1)/VmC and intercept 1/VmC. From the slope and intercept, Vm can be calculated and the specific surface area can be calculated using the relation,

$$\mathbf{A = VmN_0Am/\,W \times 22414}$$

Where$N_0$–the Avagadro number, Am –the molecular cross sectional area of adsorbate (for $N_2$ being $0.162nm^2$) and W-the weight of the sample.

The linearity of BET plot is severely restricted within the $P/P_0$ range of 0.005-0.30. Avery high or low C value will create considerable error in calculating the effective adsorbate surface area. High C values are likely to be associated with localized monolayer adsorption or with micropore filling. $N_2$ Adsorption-Desorption measurements at 77K were made using a *Micromeritics Tristar 3000* surface area & Porosity analyzer. This helps to determine structural characteristics of $TiO_2$ materials including Brunauer, Emmett, and Teller (BET) surface area, porosity, pore size and pore distribution in the mesoporous range, using nitrogen adsorption and desorption isotherms. The catalysts were purged with nitrogen gas for 4 h at $350^0$C using Flow reactor 060 (Micromeritics).

| Method | Catalyst | Crystal lite size (nm) | Surface area ($m^2/g$) | Pore volume ($cm^3/g$) | Pore diameter (nm) |
|---|---|---|---|---|---|
| Sol-gel Route | T1 | 12.3 | 34 | 0.074 | 6.4 |
| | T2 | 9.1 | 36 | 0.088 | 6.2 |
| | T3 | 11.7 | 95 | 0.133 | 6.0 |
| | T4 | 10.6 | 43 | 0.097 | 6.3 |
| Hydrothermal Route(HT) | THT1 | 9.0 | 110 | 0.369 | 9.9 |
| | THT2 | 11.6 | 92 | 0.343 | 11.4 |
| | THT3 | 13.2 | 132 | 0.453 | 9.4 |
| | THT4 | 12.1 | 125 | 0.389 | 8.8 |
| Evaporation Induced Self Assembly Route(EISA) | TEA1 | 10.3 | 63 | 0.287 | 13.0 |
| | TEA2 | 10.5 | 61 | 0.253 | 13.7 |
| | TEA3 | 10.8 | 88 | 0.329 | 12.6 |
| | TEA4 | 18.4 | 24 | 0.165 | 24.6 |

**Table3.5 Surface Properties**

In the publications of Song *et al*, the synthesis and characterization of $TiO_2$ nanoparticles with anatase mesostructure have been reported. His findings describe that this kind of materials which is a combination of the properties of nano scale powders and mesoporous materials contribute much to the photocatalytic and photoelectron chemical performances **[33,34].**

Crystallite size, calculated using scherrer equation from the (101) reflection of anatase is given in the Table3.5. Total Pore Volume is determined using adsorption branch at the single point of $P/P_0$ =0.989.Pore diameter, estimated using BJH model of the desorption branch **[35].** The physicochemical characterization data of the systems were given in the table 3.5-3.7. The specific surface area values of different systems observed to follow the general trend that, as the surface area increases the pore diameter decreases for all the catalysts prepared by different routes. The surface area, pore diameter and pore volume values suggests the mesoporous nature of the catalysts. The pores are formed by interstitial spaces between anatase particles. A crystal size of about 10-11 nm is reported to be the optimum size for photocatalytic application **[36].** Reported surface area in HT route for pure $TiO_2$ calcined at 400°C is 98 $m^2/g$, pore volume 0.24 $cm^3/g$ and pore diameter 8.01 nm **[37].** In this work, HT route prepared $TiO_2$ catalyst calcined at 450°C gives a specific surface area of 110$m^2/g$, pore volume 0.369$cm^3/g$ and pore diameter 9.9 nm higher than the reported value. Antonelli and Ying have used different surfactants such as alkyl phosphate anionic surfactants in EISA method and obtained 200$m^2/g$, 3.2nm, calcinedat 400°C) **[38].** Reported surface area in EISA route for ammonia modified $TiO_2$ catalyst is 340 $m^2/g$, pore volume is 0.28 $cm^3/g$ and pore diameter is 3.4nm as given in table 3.6 **[39].** But the surface area obtained in this work for non-treated EISA route catalysts

were 63 $m^2/g$, pore volume is 0.28 $cm^3/g$ and very large pore diameter is obtained which is about 13.0 nm[40-42]. As already stated above, the difference observed in surface area is due to the remarkably larger pore size of the catalyst. In the case of $TiO_2$ /Cu catalyst a pore size of about 24.6 nm is obtained. Kesong Liu *et al* reported that large pore size depends on the molar ratio of the precursor to the surfactant which is the structure-directing agent and the synthesis process [43]. In the investigated range of metal loading content, the surface area obtained from the different routes decreased in the following order: HT > EISA >SG. The surface areas and pore sizes of the obtained samples allow for comparison with the following results: [a] Stone and Davis ($300m^2/g$,2.4 nm, calcined at 400°C), [b] Blanchard et al.($350m^2/g$,2.1 nm, calcined at350°C). Surface area decreases with increase in calcination temperature and in this work all the systems were calcined at a temperature of 450°C. The mean pore diameter of the SG and HT photocatalysts remained almost identical to that of the $TiO_2$ support, while the total pore volume decreased in similar trend to the surface area which is optimum for the photocatalytic reactions. The pore diameter of the EISA photocatalysts remained almost different with low degradation in the reactions. Since ammonia modified $TiO_2$ metals catalysts given in table 3.6 showed less efficiency in the application reactions, these catalysts were not considered for further studies, may be due to the lower crystallite size and larger pore diameter. Also at temperatures of about 450°C, the conversion decreased due to oxidation of $NH_3$ by oxygen. [38,43,44].

| Method | Catalyst | Crystallite size (nm) | Surface area ($m^2/g$) | Pore volume ($cm^3/g$) | Pore diameter (nm) |
|---|---|---|---|---|---|
| Evaporation Induced Self – Assembly (EISA) Route | TEA1 $NH_3$ | 8.74 | 138.31 | 0.448 | 10.64 |
| | TEA2 $NH_3$ | 9.85 | 89.46 | 0.457 | 17.69 |
| | TEA3 $NH_3$ | 9.83 | 131.41 | 0.405 | 9.87 |
| | TEA4 $NH_3$ | 7.49 | 64.16 | 0.365 | 20.69 |

**Table3.6 Surface Properties of Ammonia modified$TiO_2$ metals catalysts**

| Method | Catalyst | Crystallite size (nm) | Surface area ($m^2/g$) | Pore volume ($cm^3/g$) | Pore diameter (nm) |
|---|---|---|---|---|---|
| Hydrothermal Route(HT) | $TiO_2$ | 10.0 | 97 | 0.257 | 9.80 |
| | $TiO_2$-0.2%Pt | 10.8 | 102 | 0.269 | 10.5 |
| | $TiO_2$-0.6%Pt | 12.2 | 101 | 0.230 | 9.1 |
| | $TiO_2$-1.0%Pt | 13.0 | 99 | 0.257 | 12.8 |
| | $TiO_2$-0.2%Pd | 10.6 | 104 | 0.265 | 10.2 |
| | $TiO_2$-0.6%Pd | 11.4 | 103 | 0.257 | 11.0 |
| | $TiO_2$-1.0%Pd | 10.0 | 100 | 0.261 | 9.9 |
| | $TiO_2$-0.2%Au | 12.1 | 94 | 0.210 | 11.0 |
| | $TiO_2$-0.6%Au | 13.0 | 91 | 0.245 | 11.2 |
| | $TiO_2$-1.0%Au | 13.2 | 88 | 0.215 | 10.1 |

**Table3.7 Surface Properties of noble metals/$TiO_2$catalysts**

In the case of noble metals/ $TiO_2$ catalysts prepared by hydrothermal route and calcined at 450°C possess optimum crystallite size and pore

diameter as in table 3.7, were efficient catalysts for the photocatalytic degradation reactions. Pd catalysts show the highest surface area[45-49]. In the investigated range of metal loading content, the surface area obtained from the HT method decreased in the following order: 0.2% > 0.6% > 1.0%. Pore volume shows the general trend.

### 3.2.3.2 Isotherm plots

Figure 3.18-3.19 shows the $N_2$ adsorption-desorption isotherms of pure mesoporous titania and metal incorporated mesoporous titania outgassed at 350°C for 4h under $N_2$ flow in the three routes. Except sol-gel route ,the isotherms of the calcined mesoporous titania and metal incorporated mesoporous titania by HT and EISA routes are type-IV according to IUPAC classification and exhibit a H2 hysteresis loop that is associated with plate like particles, which is typical for mesoporous materials[50]. In the $N_2$ adsorption-desorption isotherms these samples showed type-IV character with a characteristic inflexion around $P/P_0$ in the range 0.6-0.7 for each isotherm indicating capillary condensation in the mesopores. The high steepness of the hysteresis indicates, the high order of mesoporosity. The isotherm of the modified samples slightly decreases due to the metal present on the support (Figure 3.19) whereas the porosity of modified samples slightly increase compared to the blank support. However, the $TiO_2$/metals samples show the same type of hysteresis, which indicates that the deposition of metal oxides and the subsequent reduction in $H_2$ atmosphere did not induce a collapse of the mesostructure. Catalysts in HT route show narrow pore size distribution with a maximum pore diameter of 11.4nm and in the deposition of noble metals12.8nm. For large pore mesoporous materials by EISA type IV isotherm with a clear $H_2$ hystersis loop is reported [51,52]. It is reported that the non-treated catalysts prepared by EISA route, shows less photocatalytic activity although anatase

is present in the structure due to the loss of mesoporosity **[53].** The stabilizing effect of $NH_3$-treatment on mesoporous titania by EISA method is also reported**[54]**and is discussed above. However, it is surprisingly found in this work that the non-treated catalysts in EISA route were mesoporous in nature even after calcination and reduction. The photocatalytic activity was correlated to the formed mesoporous structures (results follows) and found to be less than the catalysts by HT method. So HT route is selected to be the best route for the incorporation of noble metals in $TiO_2$ catalysts.

In each isotherm three well-defined stages may be identified. First, a slow increase in $N_2$ uptake at low relative pressure corresponding to monolayer–multiplayer adsorption. Then, a sharp step at intermediate relative pressures indicative of capillary condensation within the mesopores. And a plateau with a slight inclination at high relative pressures associated with multilayer adsorption on the external surface. While, the end point of the hysteresis loop at around a relative pressure (P/Po) of 0.6 is indicative of the presence of a large pore mesostructure, which to our knowledge has not been reported for titania synthesised using this type of template [55–57].

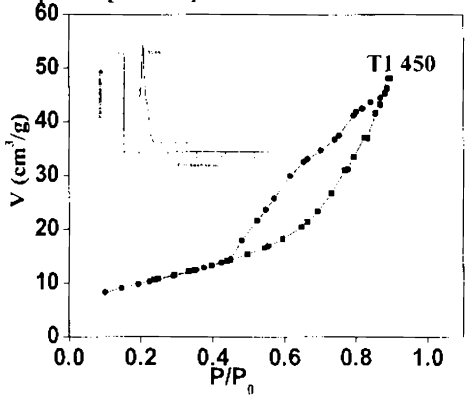


**Sol-Gel route**

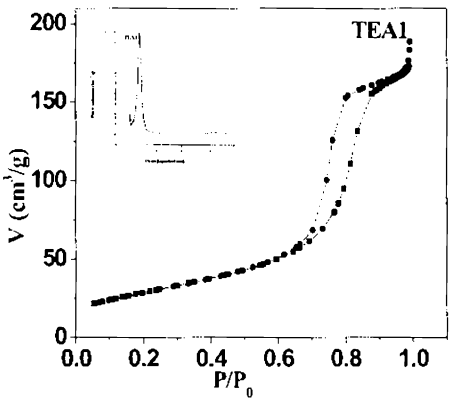


**EISA route**

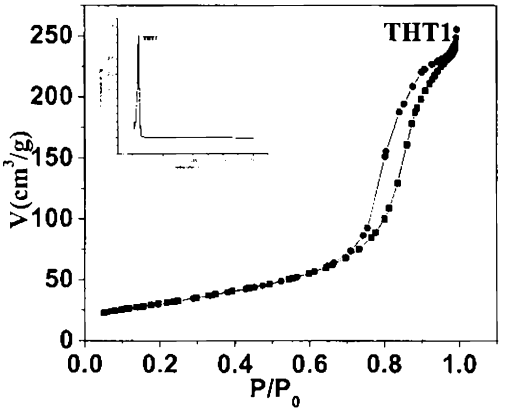


Hydrothermal route

**Fig.3.18 Isotherms of titania catalysts prepared by different routes**

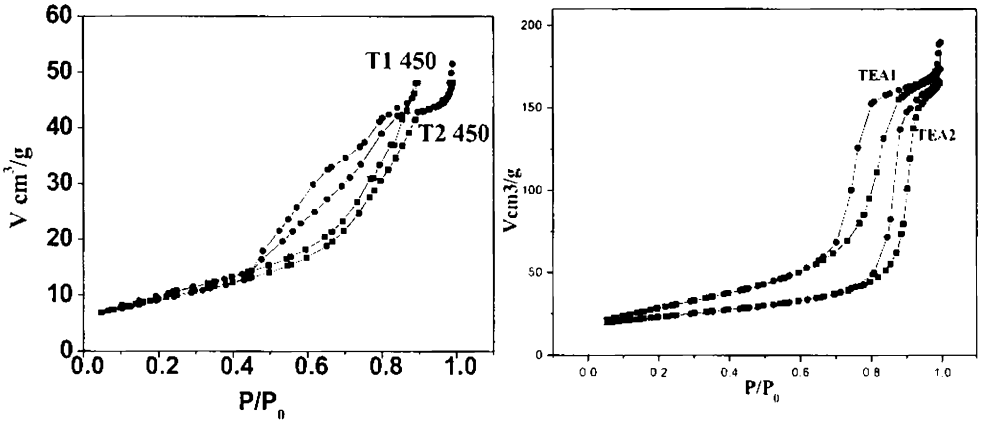


Sol-Gel route EISA route

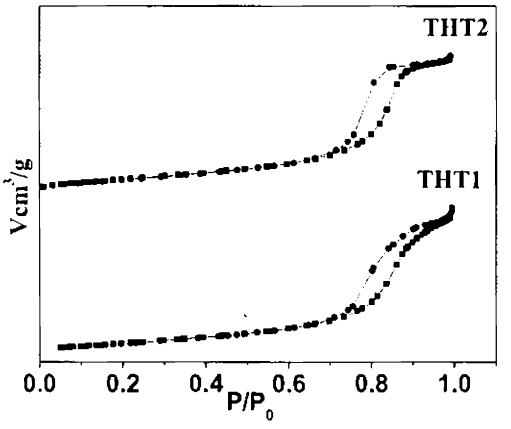


Hydrothermal route

**Fig.3.19 Isotherm plots of metal incorporated titania catalysts by different routes**

In the case of noble metals catalysts, the isotherms exhibit typical type IV pattern with hysteresis loop, characteristic of mesoporous materials according to the classification of IUPAC [58]discussed above. A steep hysteretic loop is observed, which is typical for mesoporous materials that exhibit capillary condensation and evaporation [59]. Higher loading blocks the pores, is evident from the curves as1% loading reduces the steepness from the other[60].Therefore an optimum loading of 0.6% metal,which gives the isotherm characteristic of mesoporous materials was taken for further studies.

It can be assumed that in this neutral hydrothermal route, the block-copolymer P123 works as a nanocrystallite segregating agent rather than a pore structure template as in the usual mesoporous materials synthesis. In this case, the titania particles were surrounded by block copolymers creating steric stabilisation which is attributed to the di-block hydrophilic characteristic of the Pluronic P123 [61]. The aggregation mechanism is driven by the surface charge potential. The subsequent removal of the block copolymer leads to interstitial pores structural arrangements resulting in the formation of uniform mesopores due to surface charge balanced interaction between coated composite particles. Therefore, the pore formation from interstitial spaces between particles is well controlled, and generates uniform mesopores. It is also observed that the length of the hydrothermal treatment has no significant effect, neither on the surface area nor the pore volume and pore size. But increasing the hydrothermal temperature generates a bigger pore size, thus decreasing the surface area as well as the pore volume [62]. This phenomenon can be related to densification due to the anatase crystal growth. The change in the hysteresis attributes to the presence of the incorporated metal particles on the surface of $TiO_2$ . The crystallite size ranges from 10-13 nm, which fairly covers the requirement

for the photocatalytic activity. The pore diameter is observed to be higher, in such cases the surface area seems to show a decrease and can be related to the densification due to the anatase crystal growth[63]. This affirms the mesoporous nature of the catalysts and in certain cases only, the pore volume is enhanced while the general pore size characteristics maintained.

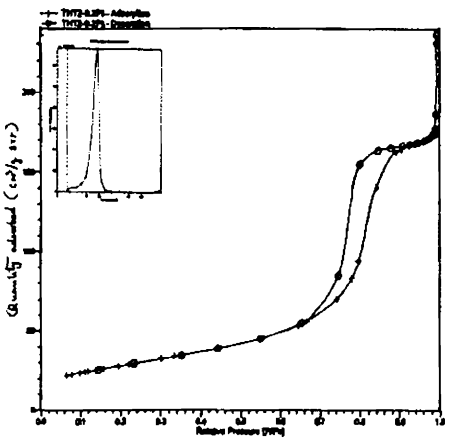

$TiO_2$/0.2wt% Pt

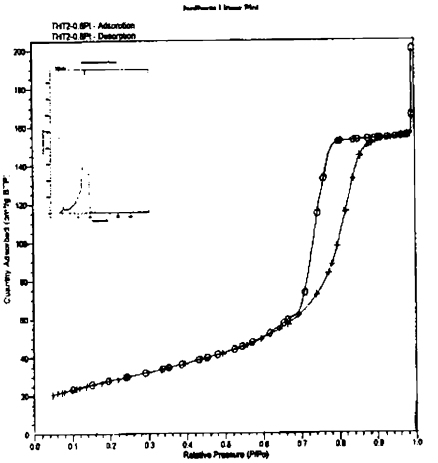

$TiO_2$/0.6wt% Pt

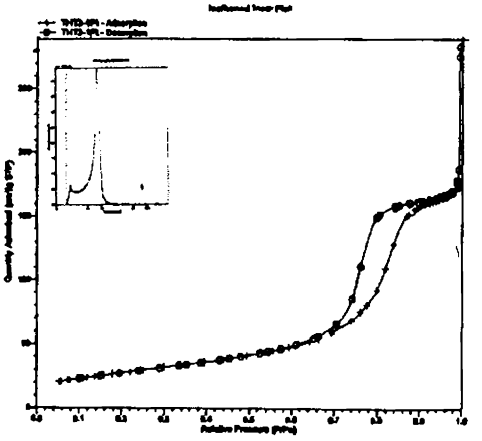

$TiO_2$/1.0wt% Pt

**Fig.3.20 Isotherm plots of different wt% Pt/$TiO_2$catalysts**

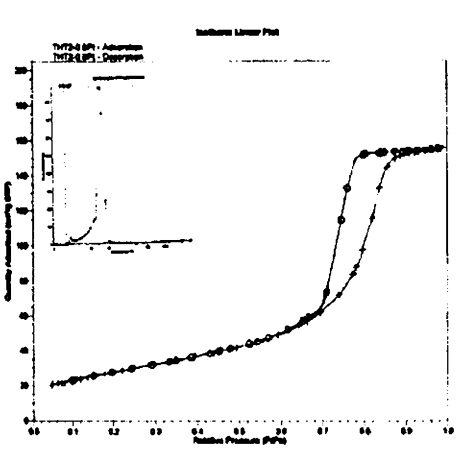

0.6wt%Pt

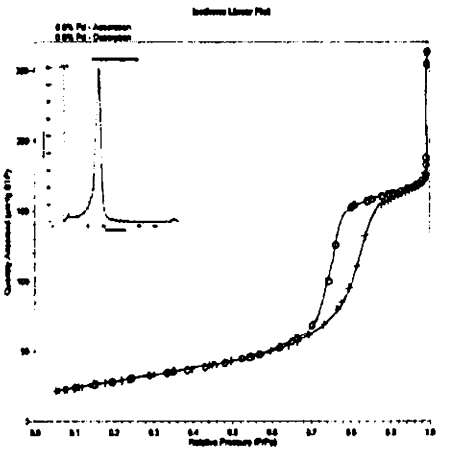

0.6wt% Pd

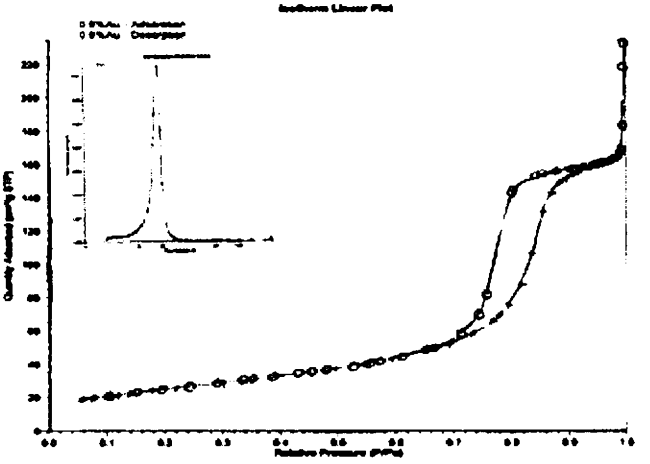

0.6wt% Au

**Fig.3.21Isotherm plots of noble metals/$TiO_2$catalysts**

### 3.2.3.3 Pore volume measurements

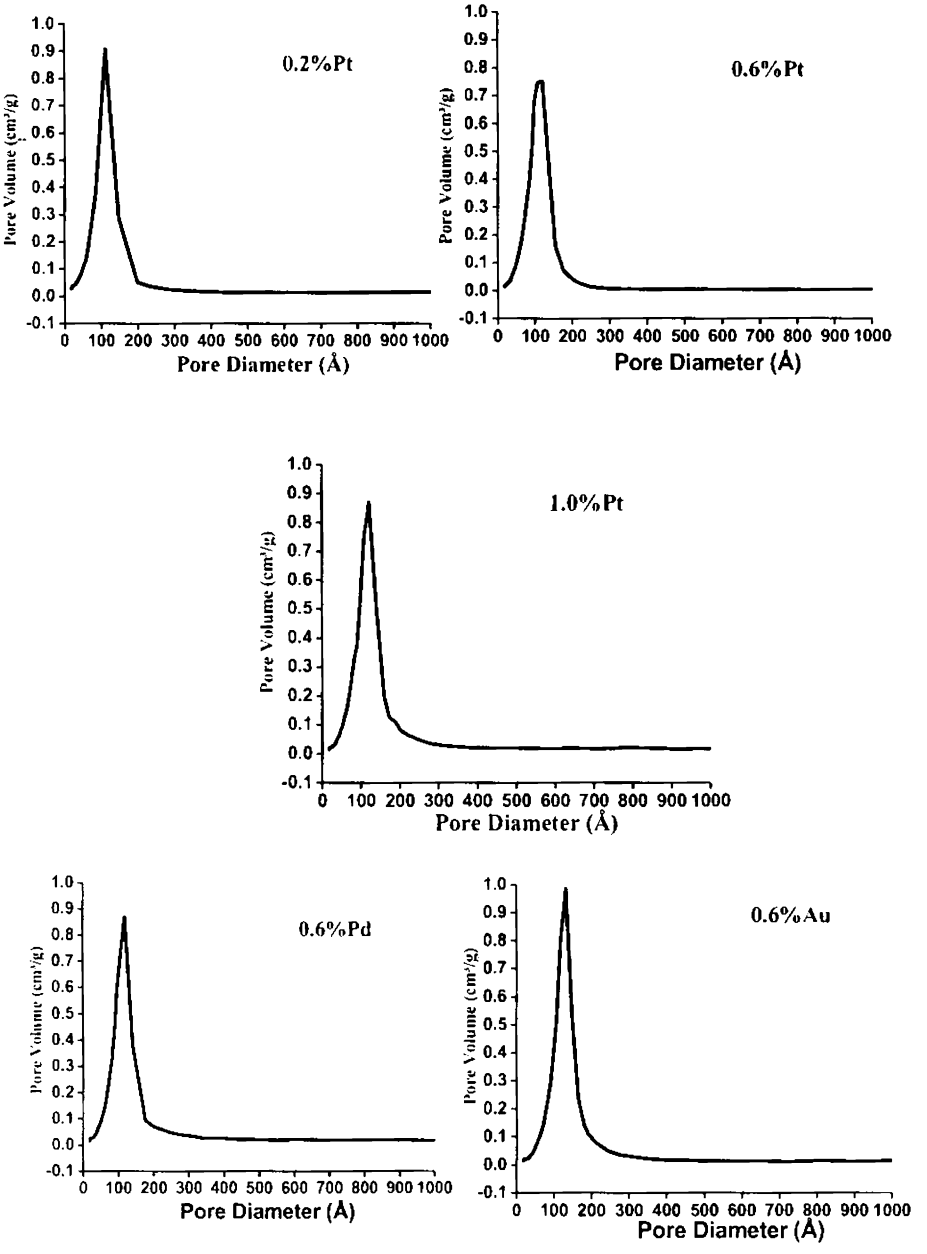


**Fig.3.22 Pore Volume Graphs of Pt, Pd, Au/ $TiO_2$catalysts**

Tuning the hydrothermal temperature in the self-assembly process controls the pore size. The maximum pore volume is contributed by 100 Å size pores. Mesopores are in the range of 20 to 200 Å size. This stemmed from the stabilization of capillary condensation, indicating the good homogeneity of the sample and fairly small pore size since the $P/P_0$ position of the inflection point is related to the pore size. The pore size distribution obtained with BJH method is noticeably narrow, confirming good quality of the sample. The textural properties of the photocatalysts prepared by the hydrothermal method is observed to be the best. The higher the loaded metal content, the larger the decrease in the BET surface area of all the samples **[64,65]**. The mean pore diameter of the photocatalysts remained almost identical to that of the $TiO_2$ support, while the total pore volume decreased in similar trend to the surface area. It may be concluded that such the small amount of loaded metal disturbed the mesopore volume by depositing at the outer and near the outer surface of the $TiO_2$ aggregates, while maintaining the general pore size characteristic.

### 3.2.4 ThermogravimetricAnalysis/Differential Thermal Analysis (TG/DTA)

Thermogravimetric analysis is a well established technique in catalysis for evaluating the thermal stability of the catalyst. It finds widest applications in the determination of different parameters on preparation of catalyst, nature and composition of active phase, effect of added promoters or presence of impurities on the catalyst, dispersion of active phase and active phase support interactions, nature and heterogeneity of active sites on catalyst surface, mechanistic aspects of the reaction under investigation, transient chemical changes that occur on the surface, catalyst deactivation and regeneration. This can also be used for quality control and catalyst

characterization through finger print spectra of different batches of the same catalyst. The technique involves the pursuit of weight of sample over a period of time while its temperature is raised linearly. Recording analytical data and the temperature curve with provision for controlled heating of sample is carried out. In a thermo gravimetric curve(TG), horizontal portions point out regions where there is no weight change, where as weight loss is indicated by curved portions. In derivative thermo gravimetric curve (DTG) plateaus correspond to zero weight change. Any decomposition of the sample is indicated by a dip in the curve and hence provide an idea about species lost during heating step. Differential thermal analysis curve (DTA) exhibits endothermal peak and exothermal peaks indicating changes in the catalyst.

TG/DTA were done on a Perkin Elmer Pyris Diamond thermogravimetric/differential thermal analyzer instrument under nitrogen atmosphere at heating rate of 20°C/ min from room temperature to 800°C with samples mounted on an alumina sample holder. TG- DTA profiles of some representative samples are given. Weight loss below 100°C, which is visible in the case of all the samples, is due to evaporation of hydrated water. An exotherm exhibited by $TiO_2$ can be proposed as being due to a phase transition from an amorphous into a crystalline form. It is clear from all the thermograms that there is no apparent weight loss after 400°C, which confirms the thermal stability. So the catalysts can be prepared at a lower temperature.

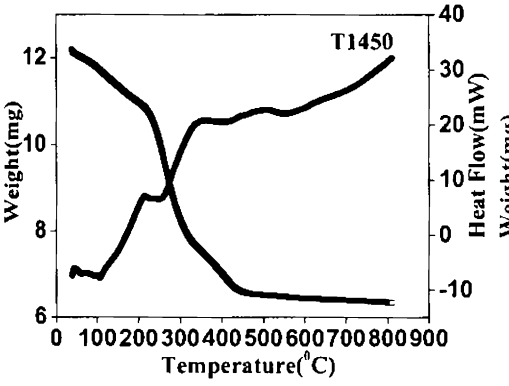


Sol-Gel route

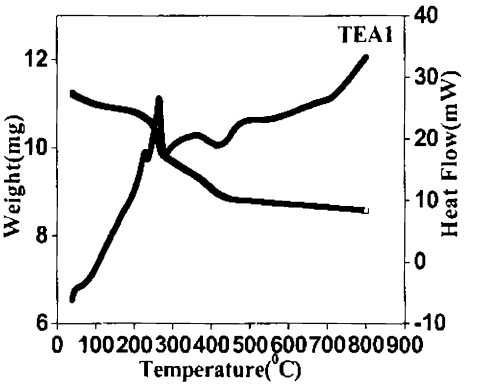


EISA route

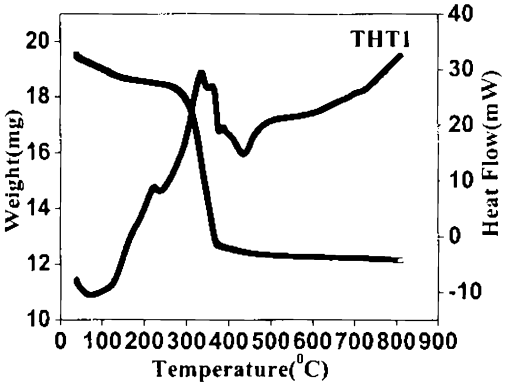


Hydrothermal route

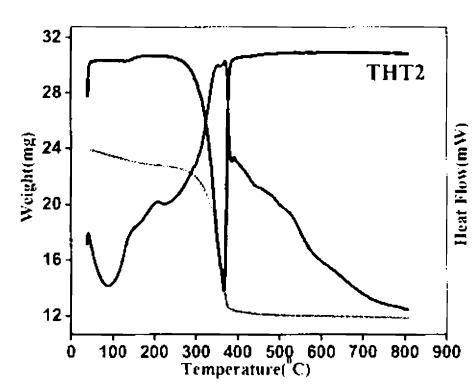


TG/DTG/DTA of $Ag/TiO_2$

**Fig.3.23 TG/DTA of $TiO_2$ catalysts by different routes**

Furthermore, DTA profiles exhibit an endothermal peak centered at around 115$^0$C and an exothermal peak in the range 400–425 $^0$C. The former is due to the loss of water adsorbed at the surface particle **[66]**, whereas the latter can be attributed to amorphous to anatase transformation **[67]**. In some cases a small exothermal peak at 290 $^0$C is observed which is usually

assigned to the loss of organic residue **[67,68].** In any case, crystallization seems to have been completed at 450 $^0$C which prompted to choose such a value as calcination temperature. TG/DTA of a representative sample in noble metal catalysts is given below.

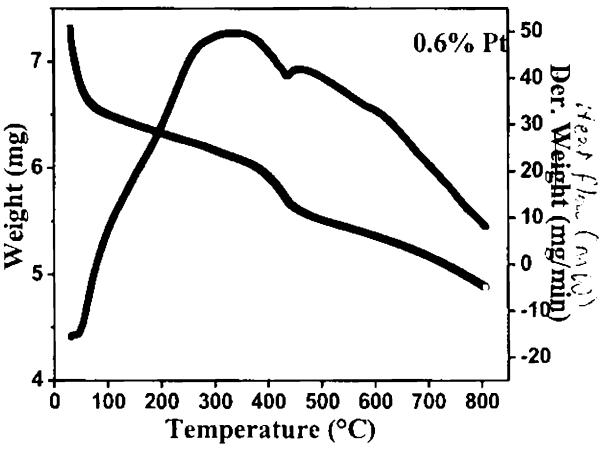


**Fig.3.24 TG/DTA of 0.6%Pt/$TiO_2$catalyst**

### 3.2.5 Energy Dispersive X-ray Analysis(EDX)

The stoichiometry of the compositions of the prepared catalysts were checked by EDX analysis and the results obtained are given in Table 3.8 and 3.9. As the first part of the research is to select a suitable route for the preparation, only 6.0 wt% of metals like Ag, Ce and Cu are incorporated to the $TiO_2$ matrix on a theoretical basis. It has been found that there is expected agreement between the experimentally obtained weight percentage of the elements and the theoretically calculated weight percentage. The EDX analysis performed on the catalysts clearly reveals the occurrence of various elements incorporated. Intensity of the spectra correlates to the amount of element (wt %) present in the catalysts. Data shows that effective promotion of Ag has been occurred on $TiO_2$ surface.

Composition (wt%) of noble metals incorporated in $TiO_2$ surface increases up to 0.6% in metal loading and then decreases .

| Route | $TiO_2$/Ag | | $TiO_2$/Ce | | $TiO_2$/Cu | |
|---|---|---|---|---|---|---|
| | TiO | Ag | TiO | Ce | TiO | Cu |
| Sol gel | 97.76 | 3.24 | 97.69 | 2.31 | 96.51 | 3.49 |
| Hydrothermal | 96.92 | 3.08 | 97.60 | 2.40 | 97.03 | 2.97 |
| EISA | 96.40 | 3.60 | 96.41 | 3.59 | 96.87 | 3.13 |

**Table3.8 EDX values (Wt %)**

| wt% of noble metals Incorporated | $TiO_2$/Pt | | $TiO_2$/Pd | | $TiO_2$/Au | |
|---|---|---|---|---|---|---|
| | TiO | Pt | TiO | Pd | TiO | Au |
| 0.2 | 99.90 | 0.10 | 99.89 | 0.11 | 99.85 | 0.15 |
| 0.6 | 99.58 | 0.42 | 99.55 | 0.45 | 99.48 | 0.52 |
| 1.0 | 99.30 | 0.70 | 99.35 | 0. 65 | 99.21 | 0.79 |

**Table3.9 EDX values (wt %)**

### 3.2.6 Scanning electron microscope analysis(SEM)

In addition to crystal structure (crystal phase and degree of crystallinity) of $TiO_2$, which is among the parameters determining its intrinsic catalytic properties, its structural properties are also important. This is because catalyst morphology can affect the transport of reactants and products to or from the catalytic active sites as well as the light absorbance for the photo-excitation of the catalyst and the generation of electron–holes pairs. The surface morphology of the catalysts were observed from the SEM images. It is to be noted that after the metal

incorporation, the surface morphology changes. This is attributed to the observed phenomenon to the poly layer behavior of $TiO_2$ particles with a wide size (and shape) distribution. Here the thickness of the cake vary in the range of 100-300 μm. It can be observed that the surface is uneven and the structure is very compact. The compactness of the $TiO_2$ cake could confirm the explanations by Xi and Geissen concerning the mechanism of cake build-up at low catalyst concentrations **[69].** The morphologies are noticeably dependent on the preparation procedure and the composition. The $TiO_2$/noble metals showed a highly porous and particulate surface.

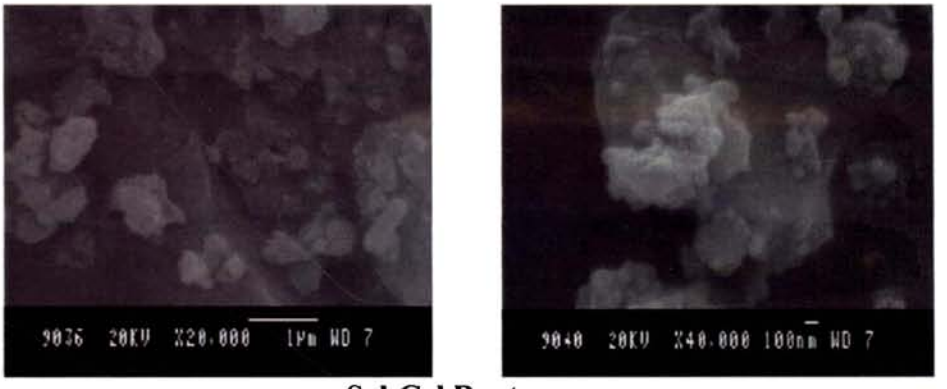


**Sol-Gel Route**

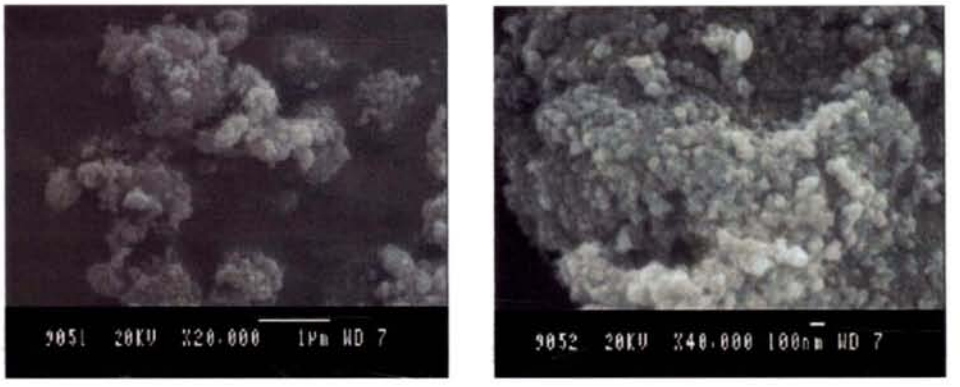


**Hydrothermal Route**

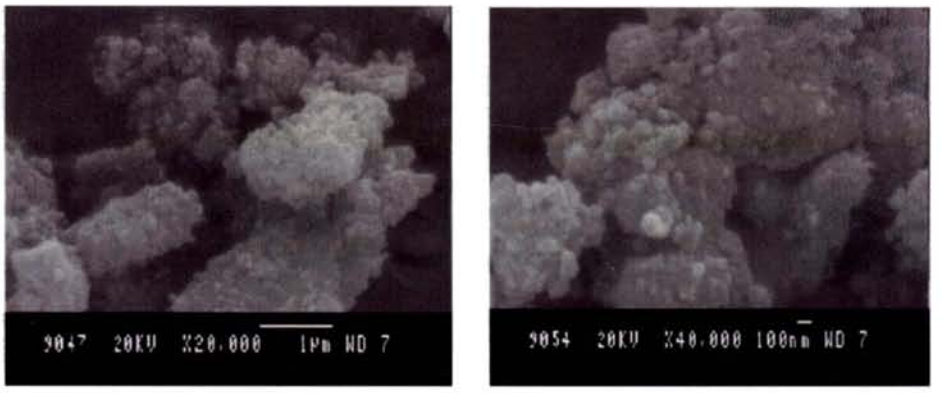


**EISA Route**

**Fig3.25 SEM images of $TiO_2$ and Ag /$TiO_2$catalysts by different routes**

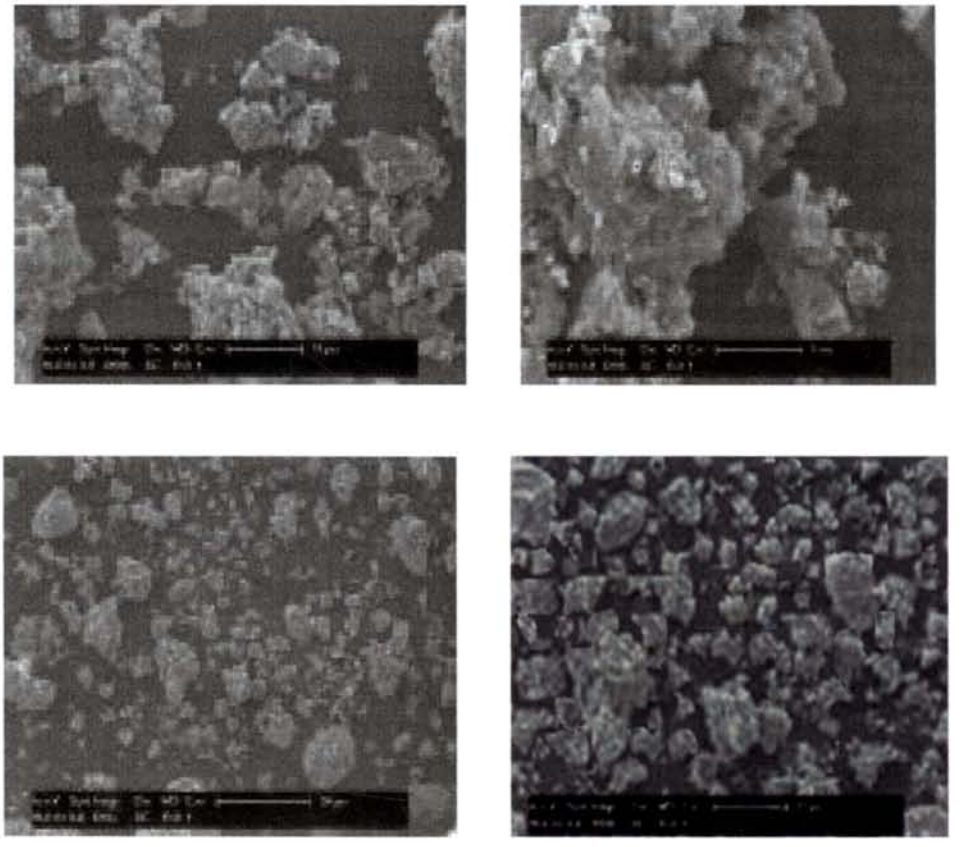

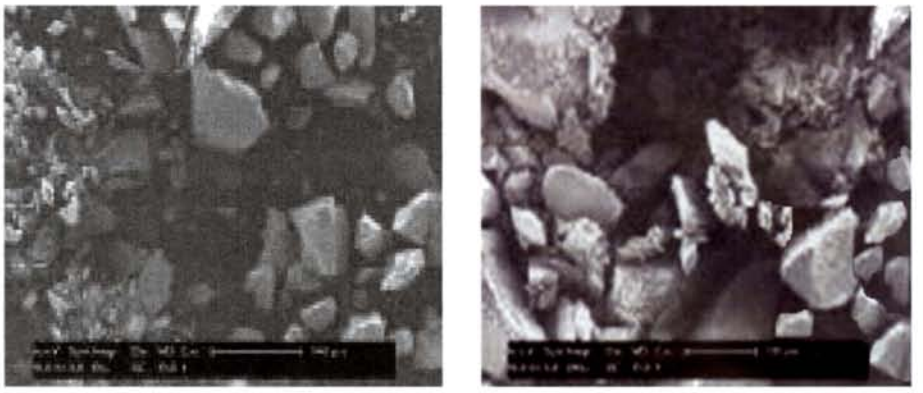

**Fig3.26 SEM images of Pt, Pd, Au loaded$TiO_2$ catalysts by Hydrothermal Route at different magnifications**

### 3.2.7 Transmission Electron Microscopy (TEM)

#### 3.2.7.1 TEM and HRTEM micrographs

Transmission electron microscopy (TEM) images shown below reveals the mesoporous nature of the titania catalyst in different routes. The images clearly indicate cubic ordered structure for titania catalysts prepared by Hydrothermal route, and regions of ordered structure prepared by EISA route, consistent with XRD data which showed broad, low intensity diffraction peaks for the mesoporous phase. The cubic structured mesoporous titania had higher stability than the hexagonal structure**[70]**and could be formed with a high content of nanocrystalline anatase with conservation of the meso- order. The high crystallite content was monitored by both X-ray diffraction together with dark field Transmission Electron Microscopy. From the images, it is clear that the incorporated metal was formed within the mesopores of titania. The XRD and TEM data are similar to those found by other researchers for porosity materials**[71-75].** TEM images show the mesoporous nature of the titania catalyst as well as it indicates cubic crystalline structure for metal loaded titania catalyst, consistent with XRD data. The dark spots are metal particles within titania..

The observed particle size of $TiO_2$ and Ag, Ce, and Cu incorporated $TiO_2$ catalysts were 10-13 nm is in good accordance with the crystallite size estimated from XRD. Results were given in tables 3.5 and 3.6. This crystal size is believed to be the optimum size for photocatalytic application **[76].**

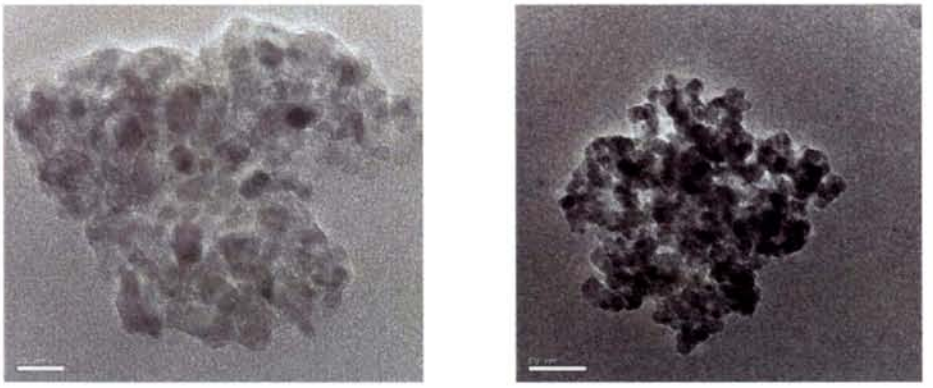

**(a) Hydrothermal Route**

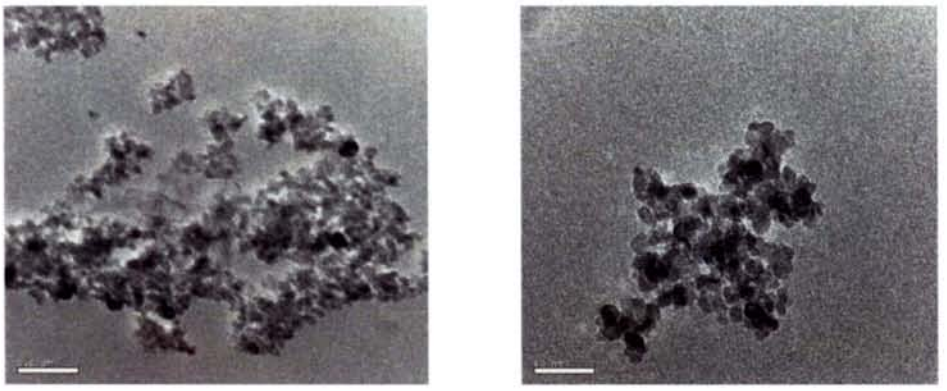

**(b) EISA Route**

**Fig3.27 TEM images of $TiO_2$ and Ag/$TiO_2$ catalysts prepared by different routes**

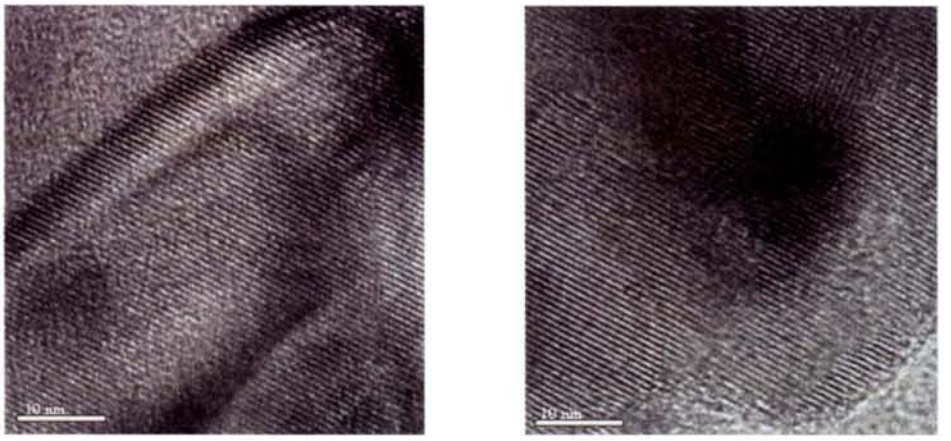

**(a) Hydrothermal Route**

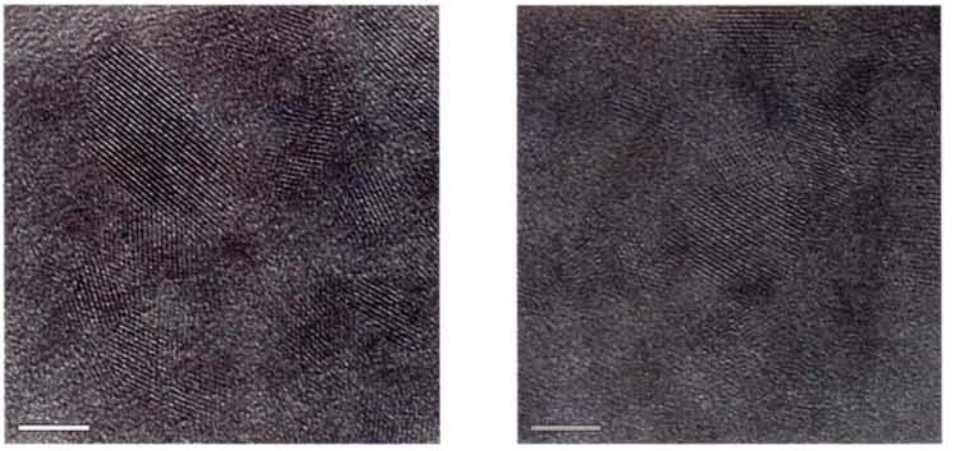

**(b) EISA Route**

**Fig3.28 HRTEM images of $TiO_2$ and $Ag/TiO_2$ catalysts prepared by different routes**

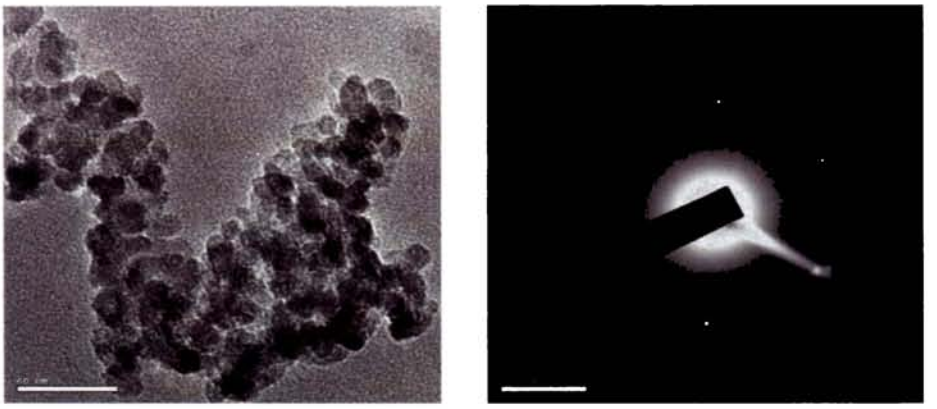

**Fig3.29 SA Electron Diffraction Pattern of Ag/$TiO_2$**

Figures 3.27 and 3.28 show TEM and HRTEM images of the $TiO_2$ powders prepared at a pH 6.6 slightly higher than the isoelectric point of titania (IEP) which is 5.8, respectively. It could be observed from Fig. 3.27(b) that the nano crystallite showed an agglomerated status, and mesoporous structures without a long-range order in EISA route catalysts. Fig.3.28 (b) shows the corresponding HRTEM image of the sample. It is clear that EISA route prepared catalysts indicate only regions of ordered cubic crystalline structure. But the Fig. 3.27(a) Fig.3.28 (a) show TEM and HRTEM images of the $TiO_2$ powders prepared at a pH 6.6 slightly higher than the iso electric point of titania (IEP) by Hydrothermal route . It could be observed that mesoporous structures with long-range order is there and it shows clear lattice fringes, which allowed for the identification of crystallographic spacing. The fringes of 0.35 nm is that of the (101) crystallographic plane of $TiO_2$ anatase. HRTEM micrographs show the ordered crystalline structure of titania as well as the mesoporous nature. Compared with the other $TiO_2$ preparations, these $TiO_2$ nanoparticles prepared from Hydrothermal route have several advantages, such as being in fully pure anatase crystalline form, having fine particle size with more uniform distribution and high-dispersion ability either in polar or non-polar

solvents, stronger interfacial adsorption and easy coating on different supporting material. The dark spots are the metal particles within titania. The white spots in Fig3.29 SA Electron Diffraction pattern are silver particles embedded within titania matrix.

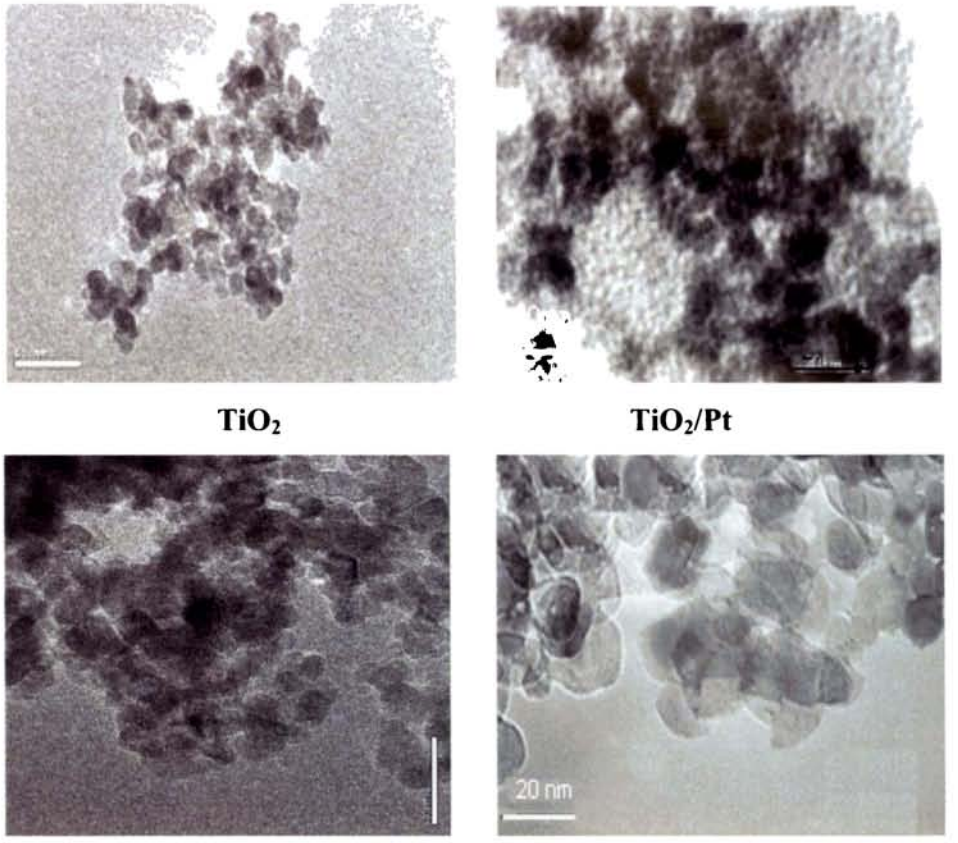


**$TiO_2$** **$TiO_2$/Pt**

**$TiO_2$/Pd** **$TiO_2$/Au**

**Fig3.30 TEM images$TiO_2$ and Pt, Pd, Au/$TiO_2$ catalysts**

The bright-field TEM images obtained in the case of noble metals on the same area of the $TiO_2$ sample shows the uniform, rounded rectangular shape of the anatase particles is clearly given in the histogram Fig3.29. Majority of $TiO_2$/Pt particles occupy a crystallite size of about 12.1nm, $TiO_2$/Pd of 11.6nm, $TiO_2$/Au of 13.0 nm whereas that of $TiO_2$ is

10.0 nm. ie.. size of the noble metals incorporated $TiO_2$ catalysts estimated from the TEM images was about 10-13nm, which was in good agreement with the values calculated from XRD pattern using the Scherrer equation(Refer Table 3.6). The image clearly shows that the pores are formed by interstitial spaces between anatase particles. The small crystallite anatase seed had experienced crystal growth during the second hydrothermal treatment and calcination processes, as demonstrated by the formation of larger crystal size (≈10–11nm) in the dark-field image. This crystal size is believed to be the optimum size for photocatalytic application **[76].**

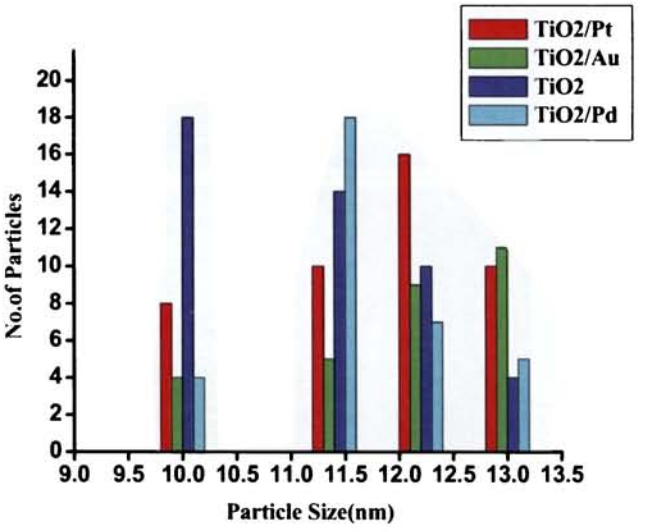


**Fig3.31 A histogram of particle size of $TiO_2$ and noble metals/$TiO_2$**

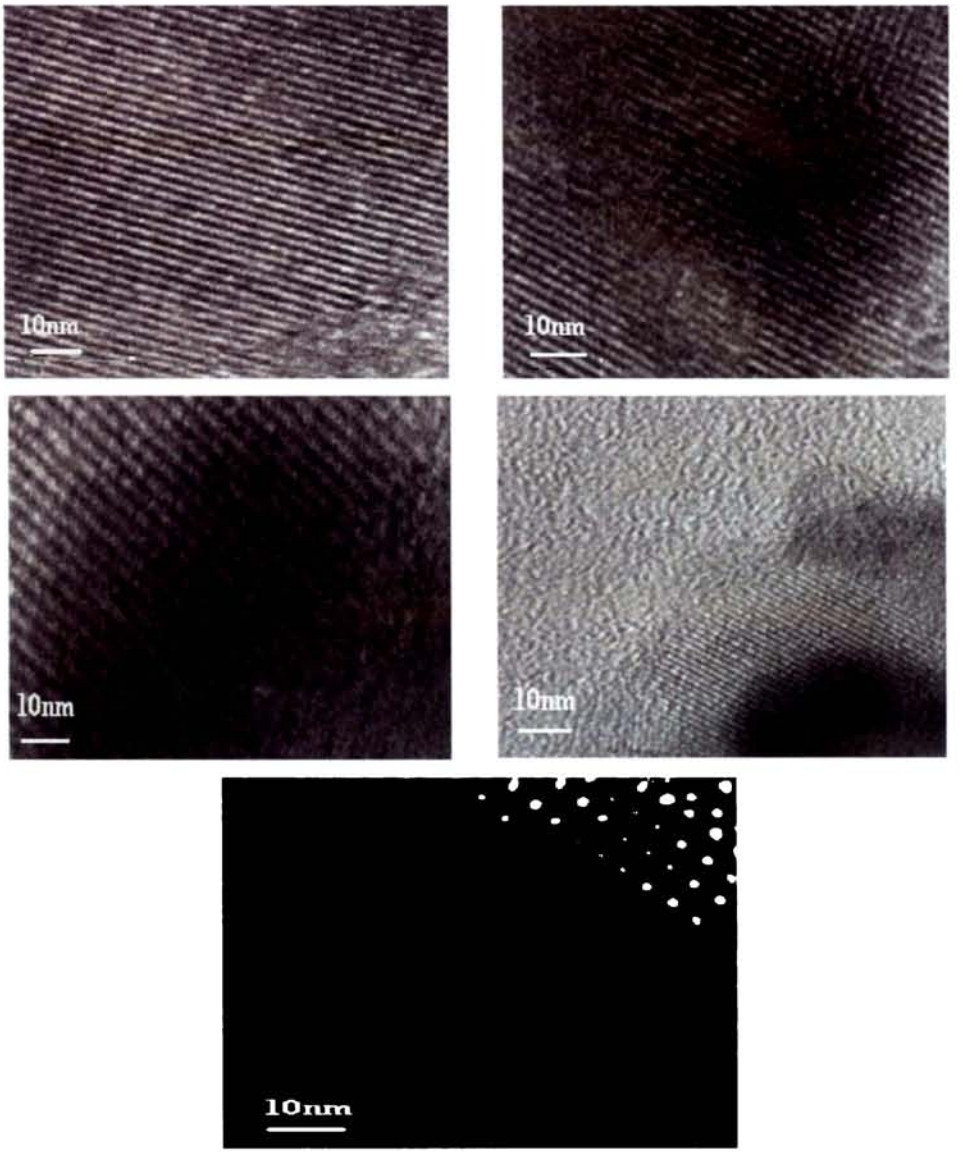


**Fig3.32 HRTEM micrographs of $TiO_2$ and Pt,Pd,Au/$TiO_2$**

Selected TEM images showing parallel (above) and perpendicular (below) views of the channels in location of the metal nano clusters. HRTEM micrographs show the ordered crystalline structure of titania as well as the mesoporous nature. The dark spots are the metal particles within titania.

### 3.2.8 X-ray photoelectron spectroscopy (XPS)

As far as XPS results are concerned, the binding energies of the most intense peaks of the various samples are listed in Table 4.0. The origin of the binding energy is the Fermi level. Only the values relative to the powders containing a definite amount of metal are given since, for most of the samples, the amount of different metal loadings did not affect the binding energies.

| Sample Name | Scan Details | Ti, $2p_{3/2}$, $2p_{1/2}$ eV | O, 1s eV (shoulder) | Metal |
|---|---|---|---|---|
| $Cu/TiO_2$ | Survey Scan | 464.93 | 534.51(sh) | 878.59 |
| | High resolution | 460.10 ($Ti^{4+}$) 465.89 | 531.58 | 931.79,951.78 |
| $Pt/TiO_2$ | Survey Scan | 466.26 | 528.31(sh) | 66.27 |
| | High resolution | 459.75 ($Ti^{4+}$) 465.54 | 531.04 | 73.38,76.38, 81.81,83.70 |
| $Pd/TiO_2$ | Survey Scan | 461.54 | 533.96(sh) | 338.23 |
| | High resolution | 459.94 ($Ti^{4+}$) 466.61 | 531.25 | 337.60,342.89 |
| $Au/TiO_2$ | Survey Scan | 459.87 | 533.52(sh) | 86.53 |
| | High resolution | 459.05($Ti^{4+}$) 464.94 | 532.40 | 83.96, 87.48 |

**Table 4.0 Binding energy values from the XPS scan spectra**

At some places, C 1s peak with binding energy value of 286.08 eV was referred to as the standard value for the surface adventitious carbon.

Thus if we include this correction the binding energy values observed in present study will be shifted to higher side by 0.02 eV. During the linear increase of the surface M/Ti ratio, a monolayer coverage of the surface by the dopant oxides is formed. Thereafter, the XPS signal increases very slowly because, due to the electron mean free path limitations, the probability of detecting electrons from a level below the monolayer decreases noticeably. The trend shown in, indicates similar dispersion among the different metal doped samples. In all cases, the monolayer coverage is reached in correspondence of the specific metal loading (6wt% in Cu and 0.6 wt% in noble metals). Above this loading, bigger oxide particles or thicker oxide layers are likely formed. Generally, the larger information depth, determined by the higher kinetic energy of 3d and 4f photoelectrons of the metal, may account for the different behaviour observed in the samples.

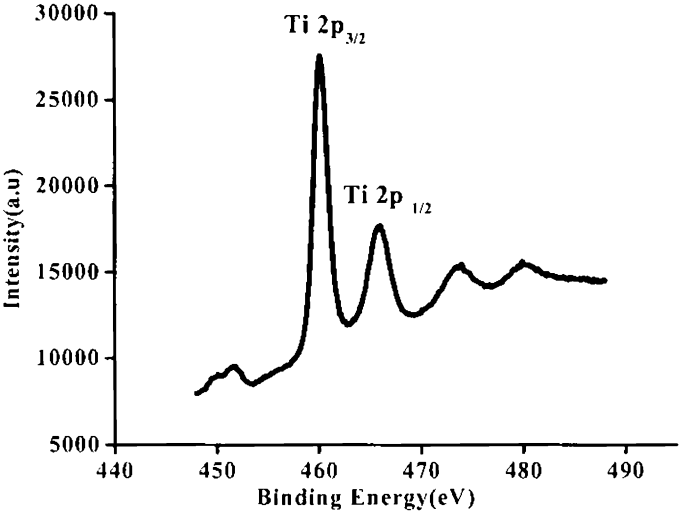


**Fig.3.33 XPS spectra of Ti in $Cu/TiO_2$.**

The Ti 2p XPS spectra showed two prominent peaks, one at 460.1 eV and other at 465.89 eV in the case Cu loaded titania. These were assigned to the Ti $2p_{3/2}$ and Ti $2p_{1/2}$ states. These doublet peaks were due to

the spin-orbit splitting of Ti 2p [77]. The above values corresponded to the 4+ oxidation state of Ti. Thus in the prepared samples titanium had 4+ oxidation state with stable Ti-O bond. Binding energies or Ti $2p_{3/2}$ peak clearly correspond to $Ti^{4+}$ in $TiO_2$ structure. The peak was characterized by a narrow width and it is indicative of Ti(IV) [78]. Subtraction of the normalized Ti 2p spectra did not allow to detect any reduced $Ti^{3+}$ ions in the samples. The binding energy shifts were smaller for the doped samples. These shifts of Ti core level signal, which were attributed to Ti 2p peaks of Cu-Ti-Cu or O-Ti-Cu suggested the successful incorporation of the metal into the titania matrix. For the pure titania these peaks were observed at 458.9 and 464.7 eV respectively (not shown), which were contributions from O-Ti-O in $TiO_2$ [79-81]. For the other samples such as Pt, Pd, Au the Ti $2p_{3/2}$ binding energy was found at 459.75 eV, 459.94 eV, 459.05 eV and Ti $2p_{1/2}$ states as 465.54 eV, 466.61 eV, 464.94 eV respectively. The XPS results indicated that the types of special peaks for Ti 2p in the metal-$TiO_2$ systems did not change much.

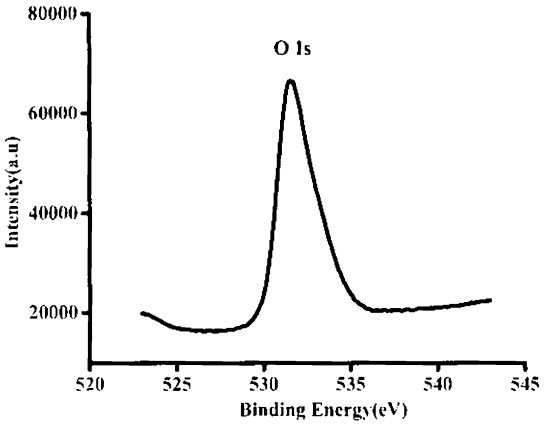


**Fig 3.34 XPS spectra of O in Cu/$TiO_2$.**

For oxygen, the 1s XPS spectra was de- convoluted using Gaussian multi- peak fitting programm gives a peak at a binding energy 531.58 eV for Cu loaded titania samples. Neither the amount nor the type of transition metal modifies the oxygen peaks typical of bare $TiO_2$. The valence band of

$TiO_2$ consisted mainly of the O 2p state, which is hybridised with the Ti 3d state **[82,83]**. Fitting of the oxygen region produced the O 1s peak at 531.58 eV for $Cu/TiO_2$ samples and the other at 531.04 eV, 531.25 eV, 532.40 eV. The shoulder at higher binding energy in the survey scan spectrum was associated with hydroxyl groups or adsorbed on the $TiO_2$ surface corresponding to $O^{2-}$ and to $OH^-$ respectively. Although the first O 1s peak (TiO) did not change in most of the samples, the shoulder observed in the survey scan of $Cu/TiO_2$ for O, being the second peak (TiOH) changed in various ways. Reports give that the larger the second peak, the greater the hydrophilic properties. Then it is clear from the spectra that, the hydrophilicity was greatest for $Pd\text{-}TiO_2$ **[84]**. Therefore, from the O/Ti ratio values, it is expected the existence of a certain number of oxygen vacancies. The presence of this oxygen deficient structure was already reported in $TiO_2$ samples impregnated with different inorganic acids **[85-89]**.

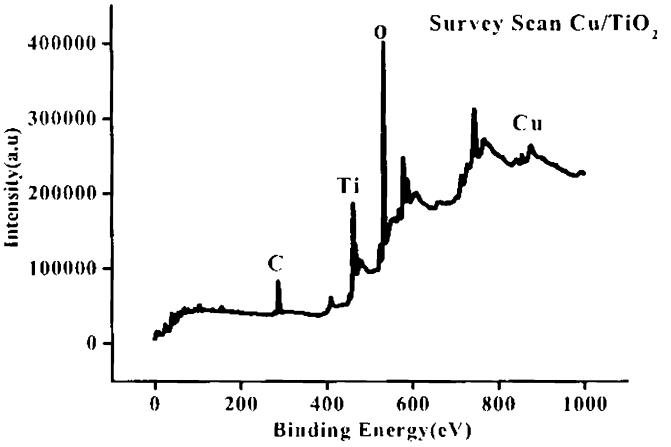


**Fig. 3.35 XPS Survey Scan spectra of $Cu/TiO_2$.**

XPS spectra corresponding to Cu loaded $TiO_2$ calcined at a temperature of 450°C shown in figure 3.35. The determination of the nature and oxidation state of Cu species ($Cu^0$, $Cu_2O$, CuO and $Cu(OH)_2$) is normally accomplished using XPS technique and in particular by means of

the Cu $2p_{3/2}$ peak study. The appearance of spin-orbit split Cu $2p_{3/2}$ and Cu $2p_{1/2}$ with their shake-up satellites which indicates that $Cu^{2+}$ species are formed on titania matrix. The Cu surface content and binding energy of Cu $2p_{3/2}$ peaks indicate the good dispersion of metal into $TiO_2$ matrix. The XPS peak intensity ratio of $I_{Cu2p}/ I_{Ti2p}$ is only 0.085 which is less than that of the threshold indicating highly dispersed CuO on $TiO_2$ surface [**90**].The modification of the electron properties of $TiO_2$ induced by the presence of $Cu^{2+}$ species appears to be not particularly beneficial for the photooxidation of organic substrates but could justify the photoefficiency of Cu-doped $TiO_2$ samples for $CO_2$ photoreduction **[91].**

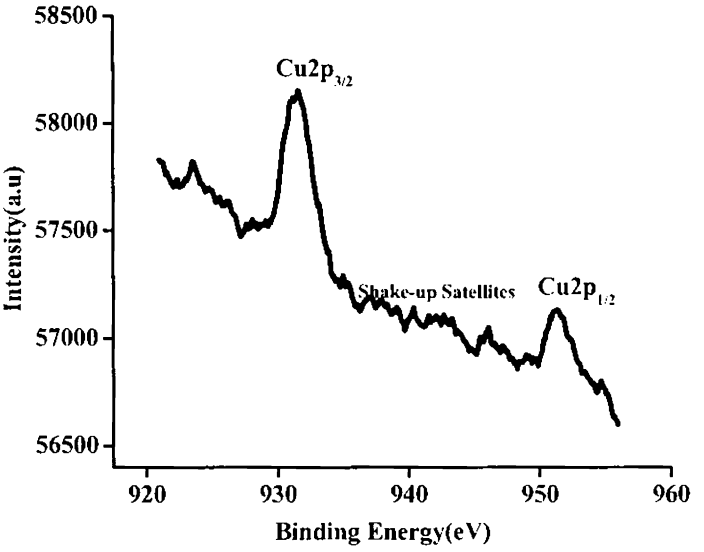


**Fig.3.36 High resolution XPS spectra of Cu in Cu/$TiO_2$.**

The main Cu $2p_{3/2}$ peak for CuO is shifted by 1.3±0.2 eV above that for the metal and $Cu_2O$, and by a further 1.2±0.15 eV for Cu(OH)2, allowing chemical differentiation **[92,93]**.The samples containing copper were characterized by a Cu $2p_{3/2}$ binding energy of 931.78eV. This value

and the presence of the satellite peak on the high binding energy side between 20 eV from the primary photoelectron are indicative of Cu(II) [94]. The presence of Cu(II) determines a broadening of all the features and an increase of the intensity of the low energy states. This perturbation may arise from a larger involvement of the copper d electrons in the molecular orbital, due to the large d occupancy of the Cu (II) species [95].

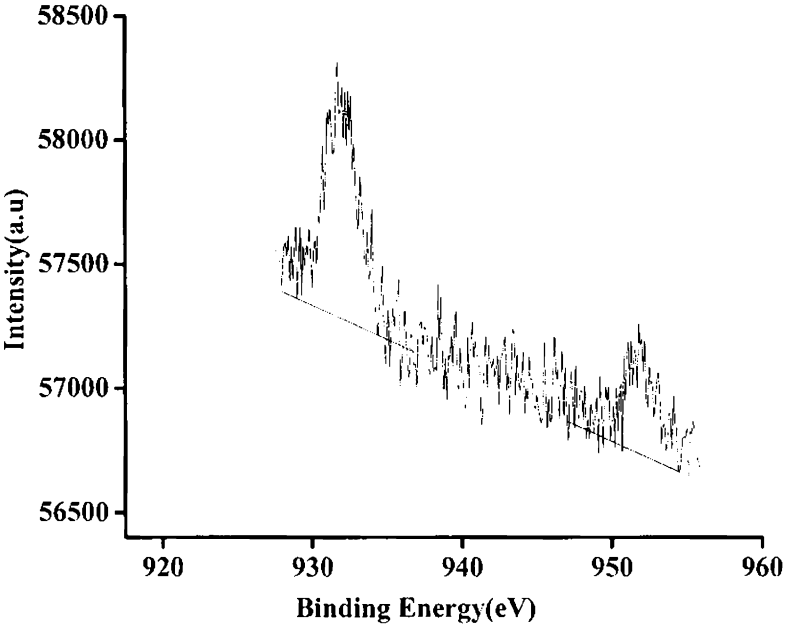


**Fig. 3.37 High resolution XPS spectra of Cu in $Cu/TiO_2$.**

The binding energy of the Cu $2p_{3/2}$ peak at around 931.78 eV together with the characteristic shake-up feature at a binding energy of 951.78 eV are indicative of $Cu^{2+}$ species [96] while slightly lower binding energy (932 eV) and the absence of shake-up peaks is characteristic of $Cu^{1+}$ [97].The shake-up peaks indicate a clear surface oxidation process for Cu during calcination. Large shake-up lines up to 20 eV apart from the main Cu $2p_{3/2}$ peak were observed, this phenomenon is quite similar to the results of Schon [98] and Novakov [99] who observed the satellite peaks and explained as a result of multiple excitation, but is different from that of Frost et al. [100] who observed that all cuprous compounds did not have any satellite peaks. Furthermore, a major difference between $Cu^{1+}$ and $Cu^{2+}$ species is the prominent satellite structure on the high binding energy side of the copper core lines for $Cu^{2+}$ species, with two strong shake-up peaks above the principal Cu 2p line. These satellites have been attributed to shake-up transitions by ligand-to-metal 3d charge transfer. This charge transfer cannot occur in $Cu^{1+}$ compounds and metallic Cu because of their completely filled 3d shells. The results point out that the copper species is present as $Cu^{2+}$ in $Cu/TiO_2$ though the existence of a small fraction of $Cu^{1+}$ cannot be discarded. In this case, the absence of shake-up peak appears in very low extent pointing out the presence of small amounts of $Cu^{1+}$ together with $Cu^{2+}$ species. Thus, a considerable stabilization of $Cu_2O$ species upon calcination is taking place for this system. Colon et al. in the reports observed a similar trend for $Cu/TiO_2$ showing an important effect of sulphuric acid in the initial precursor solution [101].

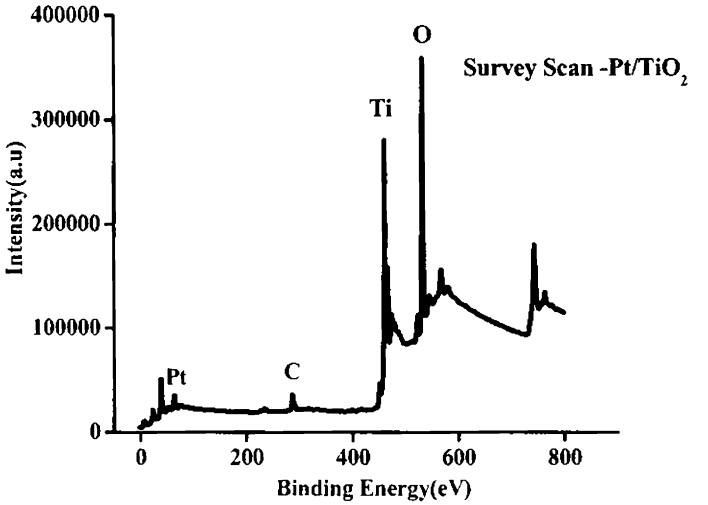


**Fig.3.38 XPS Survey Scan spectra of $Pt/TiO_2$.**

The XPS analysis on the Pt $4f_{5/2}$ and $4f_{7/2}$ regions deposited on $TiO_2$ is shown in Fig3.38. No noticeable difference was observed in the region of Ti 2p and O 1s between $Pt/TiO_2$ and other samples. The surface Pt concentration profile is closely correlated with that of photocatalytic activity in which the Pt loading rapidly increases the activity in initial deposition stage, and then starts to be saturated.

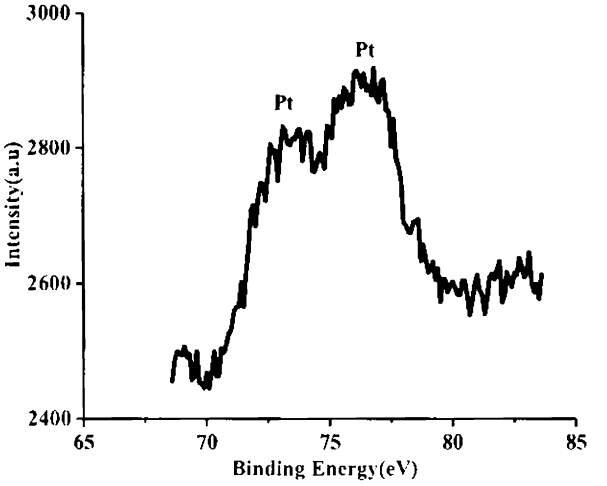


**Fig. 3.39 High resolution XPS spectra of Pt in $Pt/TiO_2$**

The de-convolution of the Pt spectra reveals that there exists the main Pt species as $Pt^0$. The Pt $4f_{5/2}$ and $4f_{7/2}$ binding energies for each species were assigned to 73.38 and 76.38eV for $Pt^0$ respectively. The normalized concentration profiles of $Pt^0$ species are almost identical. Whereas, a previous study **[102-104]** suggested that the photocatalytic activity increases with lowering Pt oxidation state. This is in contrast with the fact that most photocatalytic reactivities of $Pt/TiO_2$ are optimized at a few percent, here 0.6wt% of Pt concentration **[105,106].**

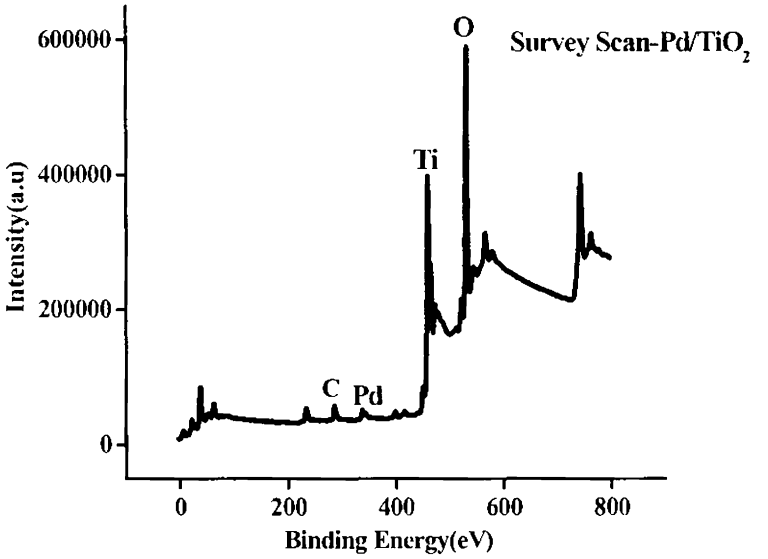


**Fig. 3.40 XPS Survey Scan spectra of $Pd/TiO_2$.**

This implies that the active oxidation state of the incorporated Pd as shown in Figure 3.40.

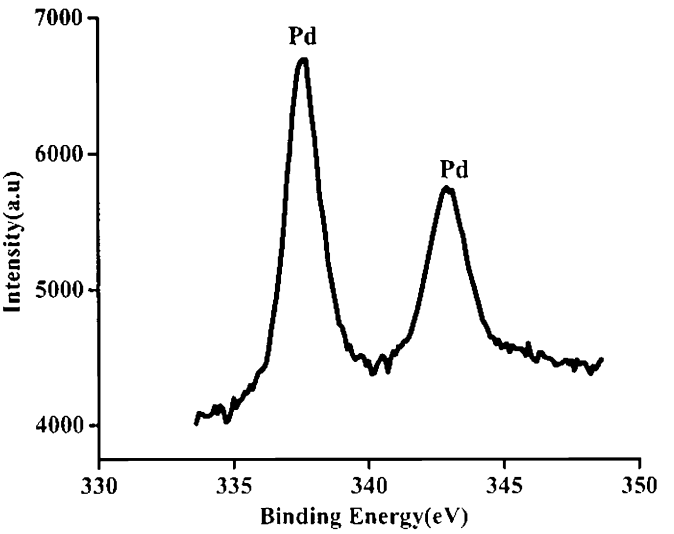


**Fig. 3.41 High resolution XPS spectra of Pd in $Pd/TiO_2$ .**

Two Pd states can be distinguished in these spectra: (*i*) Pd $3d_{5/2}$ of metallic Pd, which corresponds to the peak at 337.6eV (*ii*) the peak at 342.89 eV corresponds to the Pd $3d_{3/2}$ of metallic Pd. The XPS of Pd 3*d* spectrum with the binding energies of Pd $3d_{5/2}$ and Pd $3d_{3/2}$ lying at about 337.6 and 342.89 eV, respectively, suggest the presence of the $Pd^0$ species. This means that metallic state of Pd nanoparticles are stable in the catalyst and the presence of Pd nanoparticles enhances the photocatalytic activity, the reduction of it is worthy of remark in applying Pd nanoparticles to, as reported by Shouji et al. **[107]**.

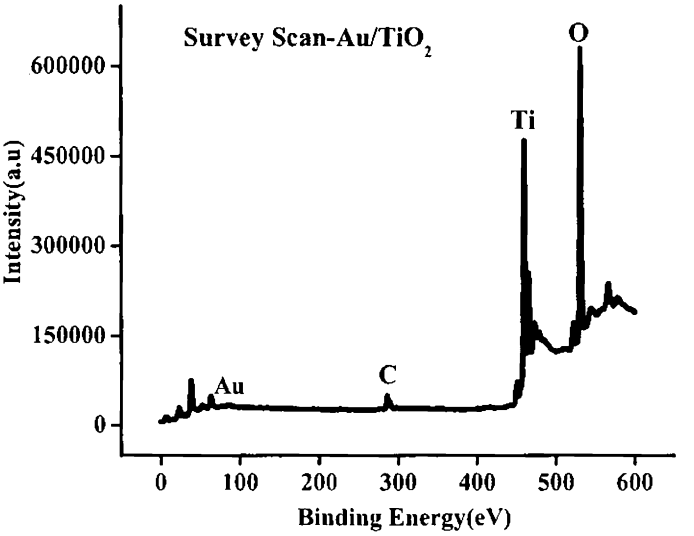


**Fig. 3.42 XPS Survey Scan spectra of $Au/TiO_2$.**

The Au 4-f emission from the figure reveals that the two sharp peaks 83.96 eV and 87.48 eV are consistent with the $Au^0$ state[108-110].

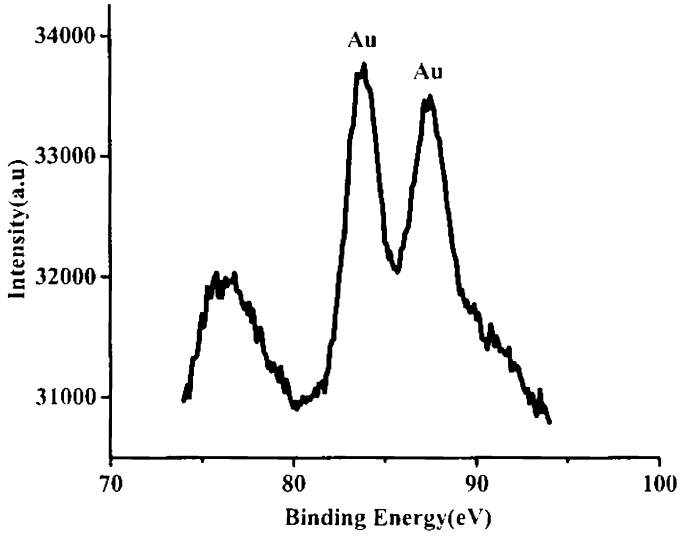


**Fig.3.43 High resolution XPS spectra of Au in $Au/TiO_2$.**

### 3.2.9 Ultraviolet Diffuse Reflectance Spectroscopy(UV-Vis DRS)

The measurement of radiation in the ultraviolet region reflected from a material surface constitutes the area of spectroscopy known as ultraviolet diffuse reflectance spectroscopy(UV-DRS).The technique is widely used for the study of solid or powdered solid samples although it can be used for the study of liquids or paste like materials also. Since only the surface of the sample is responsible for reflection and adsorption of incident radiation, it is used in the chemistry and physics of surfaces. The most appropriate theory treating diffuse reflections and transmission of light scattering layers is the general theory developed by Kubelka and Munk **[111,112]**. For an infinitely thick, opaque layer the Kubelka- Munk equation can be written as

$$F(R\alpha)=(1-R\alpha)^2/2R\alpha=k/s$$

where Rα- the diffuse reflectance of the layer relative to a non absorbing standard such as MgO, k is molar absorption coefficient of sample and s is the scattering coefficient.

In catalysis the information given by DRS mainly includes the active phase-support interactions, chemical changes during modification procedure leading to active phase and nature of active surface species. Metal centered (d-d) transitions and charge transfer (CT) transitions can be clearly differentiated by UV-DRS and assignment of these gives a picture about the oxidation state and coordination environment of the transition metals.

Absorbance measurements as well as band gap are taken in a Spectro UV-VIS Double Beam UVD-3500,Labomed, Inc. DRS studies of the catalysts prepared is carried out to calculate the band-gap . Absorbance measurements of the UV irradiated dye solution with the catalyst is also

taken in UV-vis Spectrophotometer. The UV–vis absorption band edge is a strong function of the crystallite size of nanosize $TiO_2$ catalyst. The band gap of semiconductor nano materials will increase with the decrease of particle size and this leads to the shift of the absorption edge to a higher energy; this is the so-called quantum size effect. Enough reports are there to support that the band gap between the valance band and the conduction band of semiconductor increases with decreasing particle size **[113]**. The band gap is a strong function of titania particle size for diameters less than 10nm because of the well known quantum size effect**[114]**. The interface interaction (matrix support effect) and changes in the coordination and ligand environment and the inter atomic distances of titania micro domains also results in the changes in the band gap absorption edge**[115-122]**.

TheUV–vis absorption spectrum of the catalysts prepared by different routes is shown in Fig 3.~~4~~3. The onset of absorption of wavelength (l) and the corresponding band gap energy (Eg) of $TiO_2$ material is well known to be l = 388 nm and Eg = 3.2 eV for anatase phase, respectively **[123]**. Charge-transfer from the valence band (mainly formed by 2p orbitals of the oxide anions) to the conduction band (mainly formed by 3d t2g orbitals of the $Ti^{4+}$ cations) occurs ($O^{2-} \rightarrow Ti^{4+}$)**[124]**. In the present work, characteristic band for the tetrahedrally co-ordinated titanium appear at about 390nm in all the routes. Extrapolating the spectral curve, the band gap energy of the $TiO_2$ catalyst prepared by Hydrothermal route was measured to be Eg = 3.1 eV corresponding to l = 390 nm which is in agreement with other research results **[125,126]**. The difference in Eg = 0.1 eV is the blue shift compared to bulk anatase $TiO_2$ particles indicated a size of $TiO_2$ crystallites smaller than 10 nm(Refer Table 3.5) due to so called quantum size effect **[127]**. However, the XRD and TEM data are similar to those found by UV–vis spectroscopy for pure $TiO_2$ prepared by

Hydrothermal route. Similar results were reported by other researchers also **[128-130]**.

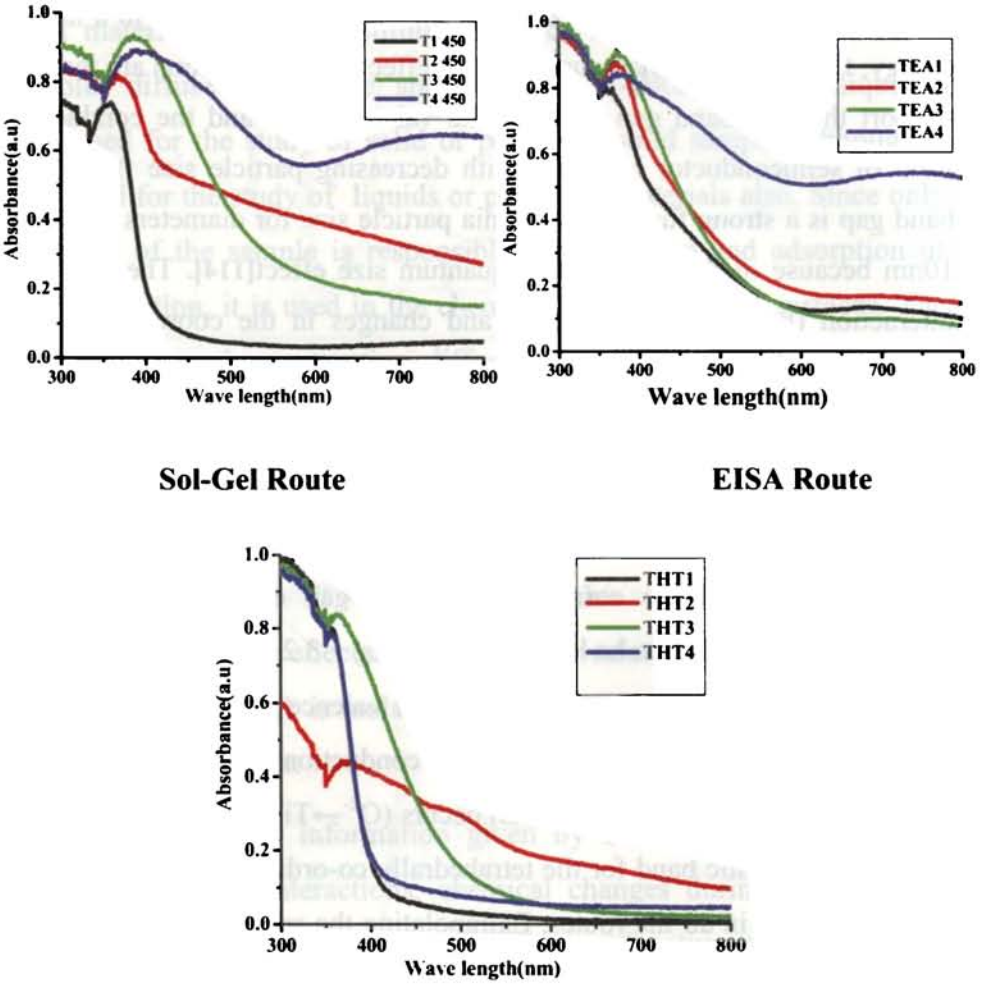


**Sol-Gel Route** **EISA Route**

**Hydrothermal Route**

**Fig 3.44 UV-vis DRS spectra of Titania Catalysts prepared by different routes**

### 3.2.9.1 Determination of Band gap of semiconductor

Modification of titania with other metal ions has a significant impact on the electronic properties of titania. And a direct relationship with the percentage of metal loaded and the band gap energy of titania is obtained in the present study.

Band gap of semiconductor can be estimated by

1. UV-vis.DRS spectra
2. Photocurrent measurement and
3. Cyclic voltammeter measurements

From UV-Vis.DRS, $E = h \times \nu$ , $= h \times c/\lambda$

B.G ( e V) = 1240/ Absorption onset (nm)

The measurements show that upon metal incorporation, the wavelength of catalysts were shifted to higher wavelength region.ie. a progressive shift in the wave length onset to the visible region is observed in the case of all the metal loaded catalysts in different routes. In Hydrothermal route, band-gap energy of $TiO_2$ is 3.1eV, $TiO_2$/Cu is 3.06 eV, TiO2/ Ce is 2.3 eV and $TiO_2$/ Ag is 2.1 eV according to KM equation corresponding to the wave lengths 390 nm,405 nm,539 nm and 590 nm. In Fig 3.44,observed that ceria and copper metal incorporated $TiO_2$ catalysts shifts entirely to the visible region with a band –gap around 2.3eVand 3.06 eV respectively and $TiO_2$/Cu catalyst shows an abnormal absorbance in the visible region like $TiO_2$/Au in figure 3.45. But the presence of ceria not only increased the surface area of mesoporous $TiO_2$ **[131]**nanoparticles, but also inhibited the mesopores collapse and the anatase-to-rutile phase transformation. This may be attributed to the presence of cerium oxide distributed on the $TiO_2$ matrix, which is in turn beneficial for effectively enhancing surface area of $TiO_2$ as reported in table 3.5**[132]**. The addition

of copper and gold ions and subsequent UV irradiation cause significant changes to the absorption spectrum of $TiO_2$ resulting in high absorbance from 400 nm to entire visible region which is characteristic of surface plasmon absorption(SPR)**[133,134]**. An absorption corresponding to the surface plasmon band of gold is observed. A band at 550 nm is characteristic of surface plasmon absorption of Au **[135]**. It is accounted with the presence of loosely bound conduction electron present or this absorption is ascribed to a collective oscillation of the free conduction band electrons of the gold and copper particles in response to optical excitation **[136,137]**. The band is strongly dependent on the shape and size of the gold clusters **[138,139]**.Such an absorption edge red shift for the gold modified titania materials depends directly on the Au load. This phenomenon is because, the surface electromagnetic waves that propagate in a direction parallel to the metal/dielectric (or metal/vacuum) interface(SPR). The actual SPR signal can be explained by the electromagnetic 'coupling' of the incident light with the surface plasmon of the copper or gold layer. This is the basis of many standard tools for measuring adsorption of material onto planar metal (typically gold and silver) surfaces or onto the surface of metal nanoparticles. About CuO, Larsson and Andersson also reported that the surface area of the $TiO_2$ support could also be stabilized by addition of CuO to the $TiO_2$ system**[140]**. Silver catalyst shows an absorbance of lower value and a high shift to the visible region. In noble metal incorporation, metallisation extends the light absorbtion to longer wave lengths. It shows that the lower energy transitions are possible. This is because the metal clusters give rise to localized energy levels in the band gap of $TiO_2$ into which valence band electrons of $TiO_2$ are excited at wavelengths longer than 390nm.It is clear from fig.3.36 and 3.37 that onset absorbance measurements that the wave length of all the catalysts shift entirely to the

visible region from 390 to 600nm. 0.6 wt.% Pd content shows the highest shift.

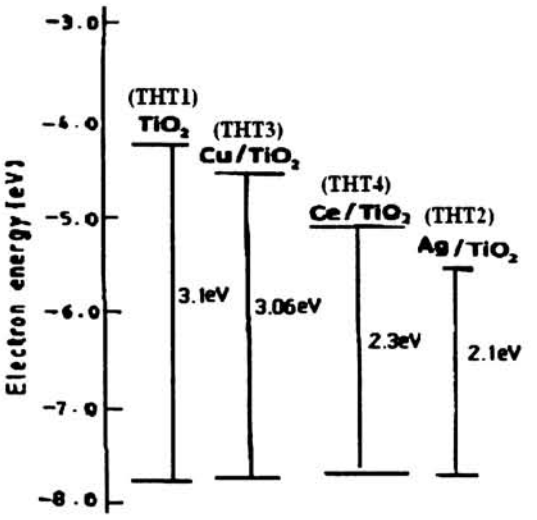


**Fig 3.45 Band gap of Catalysts in Hydrothermal Route**

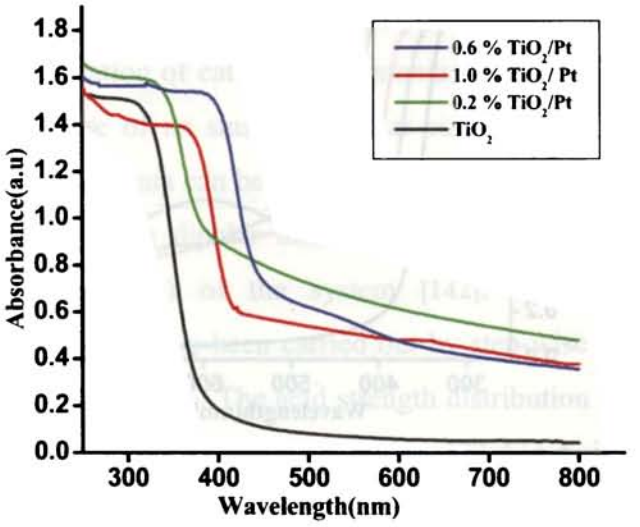


**Fig 3.46 UV-vis DRS (Abs) spectra of Pt/$TiO_2$Catalysts of different compositions**

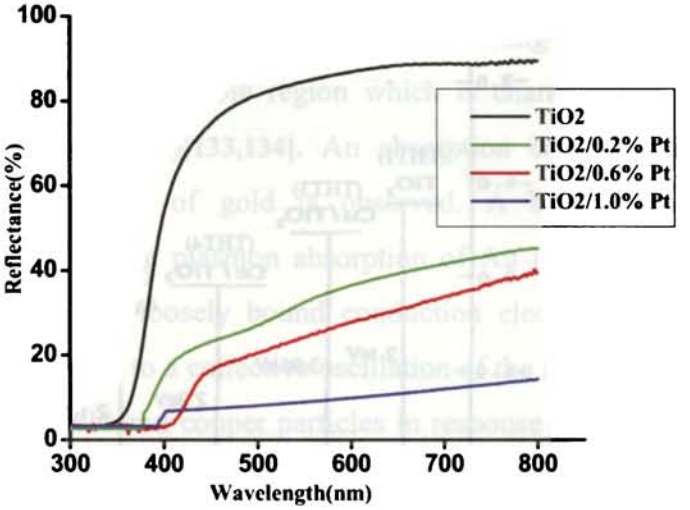


**Fig 3.47 UV-vis DRS(R%) spectra of $Pt/TiO_2$ Catalysts**

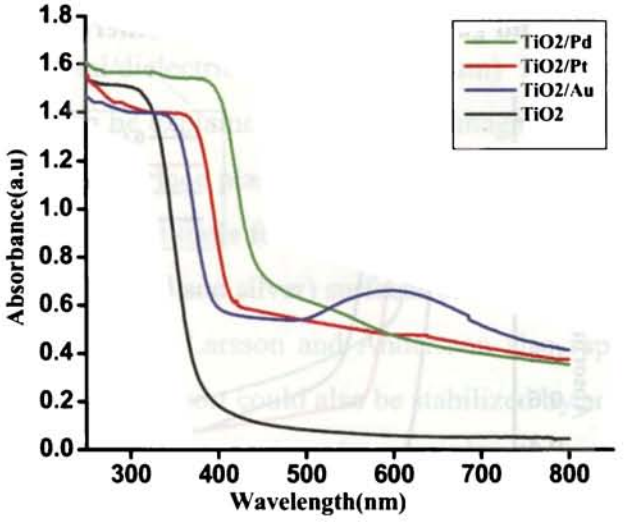


**Fig 3.48UV-vis DRS (Abs) spectra of noble metal/$TiO_2$Catalysts**

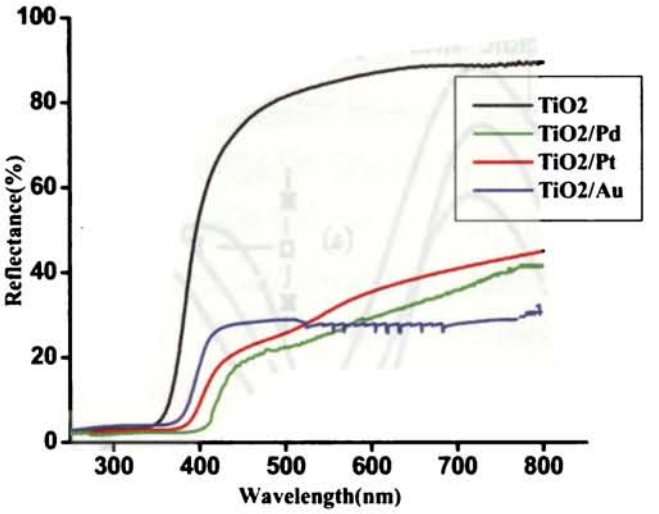


**Fig 3.49 UV-vis DRS (R%)spectra of noble metal/$TiO_2$Catalysts**

### 3.2.10 Study of Acid-base property

#### 3.2.10.1 Temperature programmed desorption of ammonia(TPD)

Temperature programmed desorption (TPD) has become a powerful tool for the characterization of catalysts. Ammonia is used frequently as a probe molecule because of its small molecular size, stability and strong basic strength**[141]**. Ammonia can be adsorbed on an oxide surface through hydrogen bonds or through dipolar interaction yielding the total acidity (Bronsted and Lewis type) of the system **[142]**. The total acidity measurements of catalysts have been carried out by step-wise temperature programmed desorption of $NH_3$. The acid strength distribution is classified depending on the desorption temperature; region 373-473 K is for weak, 474-673 K is due to medium, and 674-873 K is due to strong acid sites**[143]**. It is attempted to correlate the conversion with total acidity obtained from ammonia TPD measurements and got a very good correlation between activity of reactions such as Epoxidation of

cyclohexene and Hydroxylation of phenol carried out in liquid phase conditions over acidic sites supporting the suggested mechanism as in Figure3.50.

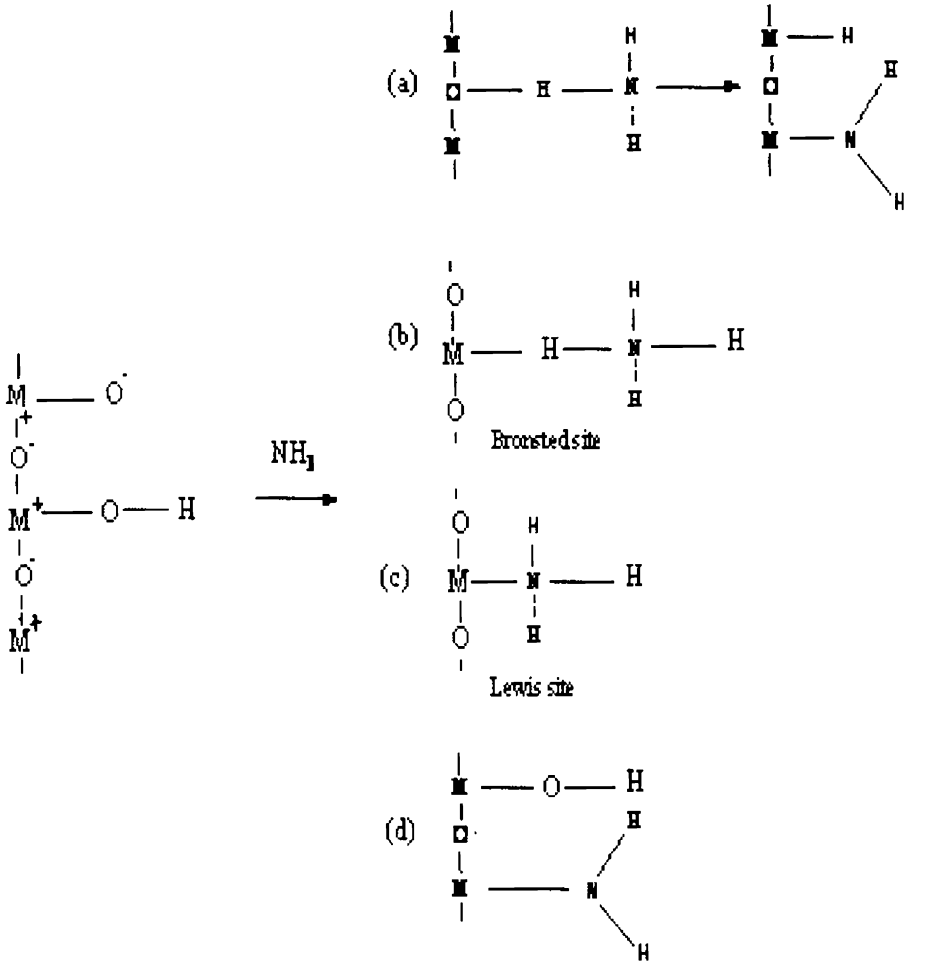


**Fig3.50 Mechanism of Temperature programmed desorption of ammonia**

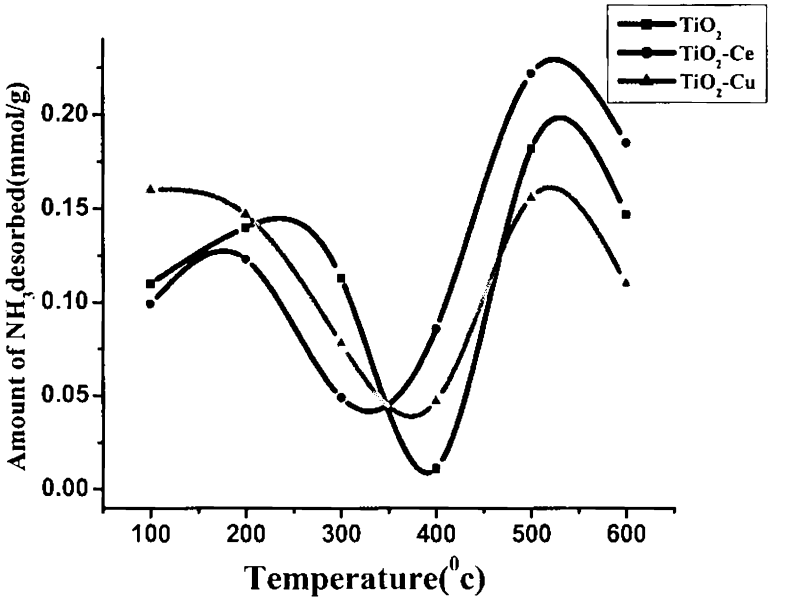


**Fig 3.51 Temperature programmed desorption (TPD) of ammonia**

Strong acidity is observed in the case of $TiO_2$-Ce catalyst than pure $TiO_2$ and $TiO_2$-Cu catalysts. Weak acidic sites are richer in $TiO_2$–Cu.The redox properties of Ceria and Copper enhance the oxidation reactions. In the case of $TiO_2$-Cu catalyst, the difference might be related to the stabilization of $Cu_2O$ species and the higher surface area with respect to pure $TiO_2$[144] .The results of the FTIR spectroscopic measurements of samples pretreated with ammonia presented by Busca et al.[145,146] showed that pure $TiO_2$-anatase exhibited only Lewis acidity. Since the Brønsted acid sites are absent on the surface of pure $TiO_2$ [147-149], it can be concluded that they originate from the incorporation of oxides of Ce and Cu. Ammonia molecules chemisorbed on Lewis acid centers are thermally more stable than ammonium ions[150]. The broad temperature range, in which ammonia desorbs from the surface of the pure mesoporous titania suggests the presence of Lewis centers that are characterized by various

acidic strength. The redox properties of Ceria and Copper enhances the oxidation reactions. This stabilization of $Cu_2O$ species in doped $TiO_2$ could be related to the presence of oxygen vacancies generated in the preparation procedure. However, incorporation of Cu significantly increases the surface area with respect to the former ones. This higher surface area values might be attributed to the effect of surfactant that thermally decompose during calcinations at a temperature lower than $450^0C$, increasing the porosity of surface and that the preparation route also improves the Cu loading effect of $TiO_2$. Reports on lewis acidity were given by Busch et al. and Davis et al. **[151,152].** The reaction parameters that influence both conversion and selectivity can be optimized in such a way to get maximum catalytic efficiency. Present systems show good conversion and selectivity when compared to the reported catalysts systems. All the experimental observations suggest that structural properties of the photocatalysts such as distribution of ions in the $TiO_2$ matrix and/or on the surface, aggregation/deaggregation and metal-assisted network formation as well as the dispersity of metal are important factors for the photocatalytic activity of these materials**[153].** The point of zero charge represents the pH value at which the coverage of $H^+$ equals the coverage of $OH^-$. The pzc is closely related to the surface acidity of a solid and its knowledge allows toevaluate the propensity of a surface to become either positively or negatively charged as a function of the pH. The pzc values of the powders containing Cr, Mo, V and W decrease significantly with increasing the metal content **[154]** indicating a surface enrichment of species with an acid behaviour as $CrO_3$, $MoO_3$, $V_2O_5$ and $WO_3$. For the samples containing Co, Cu and Fe the pzc moves to a value more basic than that of the support**[155].** A change in the surface acidity of oxides mixed with other oxides was already reported in the literature. In particular, Connell and Dumesic **[156,157]** studied the case of mixed oxides

in which an incorporation of the "guest" cation takes place onto the surface of the oxide support. The authors hypothesized that the formal charge on the supported cation is, in some case, not balanced by surface coordination of lattice oxide anions. In this way the coordinatively unsaturated cations are able to behave as surface Lewis acid centres, which strength depends on the electronegativity of the guest metal cation. The absence of Brønsted acidity in the powders containing chromium is at variance with the results of a previous study carried out following the adsorption of ammonia on Cr-loaded $TiO_2$ **[158]**. The difference can be due to the higher basicity and lower size of ammonia that allow to distinguish among different surface acid sites.

## References


1. A.V. Ramaswamy, "Catalysis Principles and Applications" Narora,New Delhi.
2. M. Gopal, W.J. Moberly Chan, L.C. De Jonghe, J. Mater. Sci. 32 (1997)6001.
3. J.C. Yu, J.G. Yu, W.K. Ho, L.Z. Zhang, Chem. Commun. (2001) 1942.
4. J.G. Yu, J.C. Yu, M.K.P. Leung, W.K. Ho, B. Cheng, X.J. Zhao, J.C. Zhao,J. Catal. 217 (2003) 69.
5. John. F. Porter, Yu-Guang Li and Chak K. Chan, J. Mat. Sci. 34 (1999) 1523.
6. R.D. Shannon and J.A. Pask, J. Amer. Ceram. Soc. 48 (8) (1965) 391.
7. Y.Q.Wang and J.Y.Ying,Chem.Mater. 11 (1999) 3113.
8. J.G. Yu, J.C. Yu,W. Ho, M.K.-P. Leung, B. Cheng, G. Zhang, X. Zhao, Appl. Catal. A: Gen. 255(2003) 309–320.
9. B.Cullity,Elements of X-ray Diffraction (1987)294.
10. S. Nakade, M. Matsuda, S. Kambe, Y. Saito, T. Kitamura, T. Sakata, Y.Wada, H. Mori, S. Yanagida, J. Phys. Chem. B 106 (2002) 10004.
11. Z. Zhang, C.-C.Wang, R. Zakaria, J.Y. Ying, J. Phys. Chem. B 102 (1998) 10871.
12. M. Anpo, T. Shima, S. Kodamo, Y. Kubokawa, J. Phys. Chem. 91 (1987) 4305.
13. A. Mills, S.L. Hunte, J. Photochem. Photobiol. A 108 (1997) 1.
14. K.S.W. Sing, D.H. Everett, R.A.W. Haul, L. Moscow, R.A. Pierotti, J.Rouquerol,T. Siemieniewska, Pure Appl. Chem.57(1985) 603–619.
15. Y.Wang, X. Tang, L.Yin, W. Huang, Y. R.Hacohen, A.Gedanken, *AdV. Mater.* 12(2000) 1183.
16. J. C.Yu, L. Zhang, J.Yu, *Chem. Mater. 14(*2002) 4647.
17. H.Luo, C.Wang, Y. Yan *Chem. Mater. 15(* 2003) 3841.
18. H. Yun, K.Miyazawa, H.Zhou, I.Honma, M.Kuwabara. *AdV.Mater.13 (* 2001) 1377.
19. P.Kluson, P.Kacer, T.Cajthaml, M.Kalaji. *J. Mater. Chem. 11 (*2001*)* 644.
20. B. L.Zhang, B. S.Chen, K. Y.Shi, S. J.He, X. D.Liu, Z.J. Du, K. L.Yang, Appl. Catal., B: Environ. 40*(*2003)253.

21. Sönke Haseloh, Sung Yeun Choi, Marc Mamak, Neil Coombs, Srebri Petrov, Naveen Chopra,Geoffrey A. Ozin. *C h e m . C o m m u n (* 2 0 0 4) 1 4 6 0.

22. Y.D. Wang, C.L. Ma, X.D. Sun, H.D. Li, Mater. Lett. 54 (2002)359.

23. T.Y.Peng, D Zhao, K.Dai,W.Shi,K..Hirao, J. Phys. Chem. B 109.(2005)4947.

24. Hao Chena, Ke Daia,b, Tianyou Peng ,Huanping Yang b, De Zhaob Materials Chemistry and Physics xxx (2005) xxx

25. Todd A.Ostomel ,Galen D. Stucky ,Chem. Commun.(2004)1016.

26. M. Primet, P.Pichat, M.Mathieu, *J. Phys. Chem.75* (1971)1216.

27. H.K. Park, D.K. Kim, C. Hee, J. Am. Ceram. Soc. 80 (1997) 743.

28. M. Zheng, M. Gu, Y. Jin, G. Jin, Mater. Sci. Eng. B 77 (2000) 55.

29. C. Deng, P.F. James, P.V. Wright, J. Mater. Chem. 8 (1998) 153.

30. B. Ohtani, Y.Ogawa, S. Nishimoto, *J. Phys. Chem. 101* (1997)3746.

31. C. Anderson, A. J.Bard. *J. Phys. Chem.99* (1995)9882.

32. Yunxia Zhang, Guanghai Li, Yucheng Wu, Yuanyuan Luo, Lide Zhang*J. Phys. Chem. B 109 (*2005) 5478-5481.

33. T.Y. Peng, D. Zhao, H.B. Song, C.H. Yan, J. Phys. Chem. B 109(2005) 4947–4952.

34. T.Y. Peng, D. Zhao, H.B. Song, C.H. Yan, J. Mol. Catal. A: Chem.238 (2005) 119–126.

35. E.P.Barret, L.G.Joyner and P.P.Halenda, J.Am.Chem.Soc. 73(1951)373.

36. Y.Q.WangandJ.Y.YingChemMater11(1999) 3113.

37. I. Kartini ,P. Meredith,J.C. Diniz da Costa , G.Q. Lu,J. Sol-Gel Science & Tech 31(2004)185–189.

38. D. M. Antonelli, J. Y. Ying, *Angew. Chem., Int. Ed. Engl* .34(1995) 2014.

39. Evi Beyers, Pegie Cool, Etienne F. Vansant *J. Phys. Chem. B. 109(*2005) 10081-10086.

40. C.J. Brinker, Y. Lu, A. Sellinger, H. Fan, Adv. Mater. 11 (1999) 579.

41. E.L. Crepaldi, G.J. de A.A. Soler-Illia, C. Sanchez, J. Am. Chem. Soc.125 (2003) 9770.

42. E.L. Crepaldi, G.J. de A.A. Soler-Illia, C. Sanchez, Chem. Commun.(2001) 1582.

43. Kesong Liu, Milin Zhang, Keying Shi, Honggang Fu .Materials Letters 59 (2005) 3308 – 3310.)

44. Y. Segura, L. Chmielarz, P. Kustrowski, P. Cool, R. Dziembaj, E. F. Vansant.*J. Phys. Chem. B 110 (*2006)948-955.

45. Lei Ge, Mingxia Xu, Haibo Fang. Applied Surface Science 253(2006) 2257–2263.

46. J. Arana, J.M. Dona-Rodrı´guez, O. Gonzalez-Dıaz, E. Tello Rendon, J.A.Herrera Melian, G. Colon, J.A.Navıo, J. Perez Pena, J. Mol. Catal. A 215(2004) 153.

47. N.Serpone,D.Lawless, J.Disdier, J.M.Herrmann, Langmuir 10 (1994) 643.

48. C.G. Wu, C.C. Chao, F.T. Kuo, Catal. Today 97 (2004) 103.

49. P. Pichat, J.M. Herrmann, J. Disdier, M.N. Mozzanega, H. Courbon, Stud.Surf. Sci. Catal. 19 (1984) 319.

50. K.S.W.Sing, D.H.Everett, R.A.W.Haul,L.Moscov,R.A.Pierotti,J. Rouquero, T. Siemieniewska, Pure Appl.Chem. 57(1985) 603.

51. M.KRUK, m.jaroniec ,Chem.Mater 13(2001)3169.

52. P. Yang, D. Zhao, D.I. Margolese, B.F. Chmelka, G.D. Stucky,Nature 396 (1998)152.

53. E. Beyers, P. Cool, E.F. Vansant Microporous and Mesoporous Materials xxx (2006) xxx–xxx.

54. K.Cassiers, T.Linssen, M.Mathieu, Y.Q.Bai,;Zhu,H.Y. P.cool, E.FVasant,hy B 2004,108,3713.

55. P.D. Yang, D.Y. Zhao, D.I. Margolese, B.F. Chmelka, G.D. Stucky, Chem. Mater. 11 (1999)2813.

56. H.S.Yun, K. Miyazawa, H.S. Zhou, I. Honma, andM.Kuwabara,Adv. Mater. 13(2001) 1377.

57. G. Soler-Illia, A. Louis, and C. Sanchez, Chem. Mater. 14(2002) 750.

58. F.Rouquerol,J. Rouquerol,K.Sing, Adsorption by Powders and PorousSolids: Principles, Methodology and Applications , Academic Press,1999,p467.

59. S.J. Gregg, K.S. Sing, Adsorption, Surface Area and Porosity, Academic Press, New York, 1982.

60. D. Margolese, J.A. Melero, S.C. Christiansen, B.F. Chmelka, G.D .Stucky,Chem. Mater. 12 (2000) 2448.

61. S. Eiden-Assmann, J. Widoniak, and G. Maret, Chem. Mater.16(2004) 6.

62. R.W.Cranston and F.A.Inkley, Advances in Catalysis. 9(1957)143.

63. C.Pierce, J.Phys.Chem. 57(1953)149.

64. G.Halsey, J.Chem.Phys. 16 (1948) 931.

65. C.G.Shull, J.Am.Chem.Soc. 70 (1948) 1405.

66. J. Livage, K. Doi, C. Maziieres, J. Phys. Chem, 93 (1989) 6769.

67. H. Xie, Q. Zhang, T. Xi, J.Wang, Y. Liu, Thermochim. Acta 381 (2002) 45.

68. L. Lei, H.P. Chu, X. Hu, P.L. Yue, Ind. Eng. Chem. Res. 38 (1999) 3381.

69. W. Xi and S.-U. Geissen, Water Res. 35 (2001)1256–1262.

70. P.C.A. Albertius, K.L. Frindell, R.C. Hayward, E. J ,Kramer, G.D. Stucky, B. F. Chmelka. *Chem. Mater.* 14(2002) *3284.*

71. A.M. Tonejc, M. Goti, B.Greta, S. Musić, S. Popovi, R. Trojko, A. Turkovi,I. MuŠević Materials Science and Engineering: B .40 (1996) 177-184.

72. M. Zhu, T. Chikyow, P. Ahmet, T. Naruke, M. Murakami, Y. Matsumoto, H. Koinuma, Material Science.441(2003)141-144.

73. Sebastian Polarz, Markus Antonietti. Chem. Commun.(2002) 2593–2604.

74. P.Prokesova,S.Mintova,J.Cejka,T.Bein.*MicroporousMesoporousMater.*64 (2003)165.

75. Y.Xia, R.Mokaya, *J .Mater Chem.* 14 (2004)863.

76. Y.Q. Wang and J.Y. Ying, Chem. Mater. 11(1999)3113.

77. C.Di Valentin, G. Pacchioni, A. Selloni, S. Livraghi, E. Giamello., J.Phys. Chem. B 109 (2005) 11414.

78. A.M. Venezia, L. Palmisano, M. Schiavello, C. Martın, I. Martın, V.Rives, J. Catal. 147 (1994) 115.

79. M. Sathish, B.Viswanathan, R.P. Viswanath, C.S. Gopinath., Chem. Mater. 17, (2005), 6349. 21.

80. Horst Kisch, Shanmugasundaram Sakthivel, Marcin Janczarek , Dariuz Mitoraj., J. Phys. Chem. C 111 (2007) 11445.

81. H. X. Li. J. X. Li, Y. I. Huo., J. Phys. Chem. B 110 (2006) 1559.

82. Y. Tezuka, S. Shin, A. Agui, M. Fujisawa, T. Ishii, A. Yagishita, J.Elect. Spectrosc. Relat. Phenom. 79 (1996) 195.

83. H. Onishi, T. Aruga, C. Egawa, Y. Iwasawa, Surf. Sci. 199 (1988) 54.

84. Misook Kang*J.* Ind. Eng. Chem,13(2007)143.

85. G. Colon, M.C. Hidalgo, G. Munuera, I. Ferino, M.G. Cutrufello, J.A.Navio, Appl. Catal. B: Environ.63(2006) 45.

86. E.P. Barret, L.G. Joyner, P.P. Halenda, J. Am. Chem. Soc. 73 (1951) 37.

87. R.A. Spurr, H. Myers, Anal. Chim. 29 (1957) 760.

88. G. Colon, M.C. Hidalgo, J.A. Navio, Appl. Catal. B: Environ. 45 (2003)39.

89. G. Colon, J.M. Sanchez-Espana, M.C. Hidalgo, J.A. Navio, J. Photochem.Photobiol. A: Chem. 179 (2006) 20.

90. J.Bandara,C.P.K.Udawatta,C.S.K.Rajapaske Photochem. Photobiol. Sci.4 (2005)857.

91. H. Yamashita, H. Nishiguchi, N. Kamada, M. Anpo, Y. Teraoka, H.Hatano, S. Ehara, K. Kikui, L. Palmisano, A. Sclafani, M. Schiavello, M.A. Fox, Res. Chem. Intermed. 20 (1994) 815.

92. N.S. McIntyre, M.G. Cook, Anal. Chem. 47 (1975) 2208.

93. M.P.Seah, in:D. Briggs, M.P. Seah (Eds.), Practical Surface Analysis, John Wiley and Sons(1990).

94. G. Moretti, S. De Rossi, G. Ferraris, Appl. Surf.Sci. 45(1990) 341.

95. Agatino Di Paola a, Elisa Garcia-Lopez, Giuseppe Marci, Cristina Martin, Leonardo Palmisano, Vicente Rives, Anna Maria Venezia Applied Catalysis B: Environmental 48 (2004) 223.

96. R. Bechara, A. Aboukais, J.P. Bonnelle, J. Chem. Soc. Faraday Trans. 89(1993) 1257.

97. D. Briggs, M.P. Seah (Eds.), Practical Surface Analysis by Auger and XPS, Wiley, New York, 1983.

98. G. Schon, Surf. Sci. 35 (1973) 96.

99. T. Novakov, Phys. Rev. B 3 (1971) 2693.

100. D.C. Frost, A. Ishitani, C.A. Mcdowell, Mol. Phys. 24 (1972) 861.

101. G. Colon, M. Maicu, M.C. Hidalgo, J.A. Navio Applied Catalysis B: Environmental 67 (2006) 41.

102. A.V. Vorontsov, E.N. Savinov, J. Zhensheng, J. Photochem. Photobiol. A 125 (1999) 113.

103. J. Lee, H. Park, W. Choi, Environ. Sci. Technol. 36 (2002) 5462.

104. G.R. Bamwenda, S. Tsubota, T. Nakamura, M. Haruta, Catal. Lett. 44 (1997) 83.

105. E. Bae, W. Choi, Environ. Sci. Technol. 37 (2003) 147.

.06. W. Choi, J. Lee, S. Kim, S. Hwang, M.C. Lee, T.K. Lee, J. Ind. Eng. Chem. 9 (2003) 96.

.07. E. Shouji, D. A. Buttry, J. Phys. Chem. B 102 (1998)1444.

108. M.Brust,M.Walker,D.Bethell,D.J.Schiffrin,R.Whymann,J.Chem.Soc, Chem. Commun .7(1994)801.

109. H.G.Boyen,G.Kastle,Science.297(2002)1533.

110. T.Jeramillo,S.H.Baeck,B.R.Cuenya,E.W.McFarland,J.Am.Chem.Soc.125(20 03) 7149.

111. S. Sakthivel, H. Kisch, Angew, Chem.Int.Ed 42(2003)4908.

112. J. E. Herrera, D. E, Resasco. J. Phys. Chem.B.107(2003)3738.

113. Yunxia Zhang, Guanghai Li, Yucheng Wu, Yuanyuan Luo, and Lide Zhang *J. Phys. Chem. B 109(* 2005) 5478.

114. V.F. Stone, Jr, R.J. Davis, Chem. Mater, 10 (1998) 1468.

115. C. Beck, T. Mallat, T. Burgi and A. Baiker, J. Catal,204 (2001) 428.

116. R. J. Davis, Z.F. Liu, Chem. Mater, 9 (1997) 2311.

117. X. Gao and I.E. wachs, Catal. Today, 51 (1999) 233.

118. A. Fernandez, J. Leyrer, A.R. Gonzales-Elipe, G. Munuera and H. Knozinger, J. Catal, 112(1988) 489.

119. G. Lassaletta, A. Fernandez, J.P. Espinos and A.R. Gonzales-Elipe, J.Phys. Chem, 99 (1995) 1484.

120. C.K. Gorgenson, "Modern Aspects of Ligand Field Theory", North Holland, Amsterdam, 1971.

121. M.R. Boccutti, K.M. Rao, A. Zecchina, G. Leofanti and G. Petrini, Stud. Surf. Sci. Catal, 48 (1989) 133.

122. S. Klein, B.M. Weekhuysen, J.A. Martens, W.F. Maier and P.A. Jacobs, J. Catal, 163 (1996) 489.

123. C. Kormann, D.W. Bahnemann, M.R. Hoffmann, J. Phys. Chem. 92 (1988) 5196.

124. H. Gerischer, A. Heller, J. Phys. Chem. 95 (1991) 5261.

125. S.-Y. Kwak, S.H. Kim, S.S. Kim, Environ. Sci. Technol. 35 (2001) 2388

126. Y. Li, T.J. White, S.H. Lim, J. Solid State Chem. 177 (2004) 1372.

127. A. Henglein, Ber. Bunsen-Ges. J. Phys. Chem. 86 (1982) 241.

128. S.V. Gaponenko, Optical Properties of Semiconductor Nanocrystals, Cambridge University Press, Cambridge, 1998.

129. P.C.A. Alberius, K.L. Frindell, R.C. Hayward, E.J. Kramer, G.D. Stucky B.F. Chmellka, *Chem.Mater*14(2002)3284.

130. L.E. Brus, J. Chem. Phys. 80 (1984) 4403.

131. Nikolaos Dimitratos, Alberto Villa, Claudia L. Bianchi,Laura Prati, Michiel Makkee Applied Catalysis A: General 311 (2006) 185–192.

132. C.P. Sibu, S. Rajesh Kumar, P. Mukundan, K.G.K. Warrier, Chem.Mater. 14 (2002) 2876–2881.

133. J.M. Herrmann, H. Tahiri, Y. Ait-Ichou, G. Lassaletta, A.R.G. Elipe A.Fernandez, Appl. Catal. B 13 (1997) 219.

134. E. Stathatos, P. Lianos, P. Falaras, A. Siokou, Langmuir 16 (2000) 2398.

135. I.M.Arabatzis,T.Stergiopoulos,D.Andreeva,S.Kitova,S.G.Neophytide, P.Falaras.J.Catal 220(2003)127-135.

136. P.V.Kamat. J. Phys. Chem.B 106(2002)7729.

137. M.M.Alvarez,J.T.Khoury,T.G.Schaaff,M.N.Shafigullin,I.Vezmar,R.L. Whetten.J. Phys. Chem.B 101(1997)3706.

138. U.Kreibig, M.Gartz, A.Hilger, H.Hovel, in:E.Pelizetti (Ed). Fine Particles Sci. & Tech. Kluwer (1996)499-515.

139. U.Kreibig, M.Vollmer.Springer,Berlin(1995).

140. P.O. Larsson, A. Andersson, J. Catal. 179 (1998) 72–89.

141. H. A. Benesi, J. Am. Chem. Soc. 78 (1956) 5490.

142. S. Sugunan, N.K. Renuka, Bull. Chem. Soc. Jpn. 75 (2002) 463.

143. S. Sugunan, N.K. Renuka, A.R. Koshy, S.M. Varghese, C.G Ramankutty, React. Kinet. Catal. Lett. 67 2 (1997) 267.

144. G. Colo´n,M. Maicu,M.C. Hidalgo,J.A.Navı´o Applied Catalysis B: Environmental 67 (2006) 41–51.

145. G.Busca, H.Saussey, O. Saur, J. C.Lavalley, V.Lorenzelli, *Appl. Catal. 14* (1985) 245.

146. G. Ramis, G. Busca, V. P.Lorenzelli, P.Forzatti. *Appl. Catal. 64* (1990)243.

147. G. Busca, H. Saussey, O. Saur, J.C. Lavalley, V. Lorenzelli, Appl. Catal.14 (1985) 245.

148. G. Ramis, G. Busca, V. Lorenzelli, P. Forzatti, Appl. Catal. 64 (1990) 259.

149. H. Miyata, Y. Nakagawa, T. Ono, Y.J. Kubokawa, J. Chem. Soc., Faraday Trans. 179 (1983) 2343.

150. R. A.Rajadhayaksha, H.Knozinger. *Appl. Catal.64* (1990)243.

151. O.M. Busch, W. Brijoux, S. Thomson, F. Schuth, J. Catal. 222 (2004)174.

152. B.H. Davis, R.A. Keogh, S. Alerasool, D.J. Zalewski, D.E. Day, P.K.Doolin, J. Catal. 183 (1999) 45.

153. Chuan-yiWang, Ronald Pagel, Jürgen K. Dohrmann, Detlef W. Bahnemann. C. R. Chimie 9 (2006) 761–773 .

154. A. Di Paola, G. Marci, L. Palmisano, M. Schiavello, K. Uosaki, S. Ikeda, B. Othani, J. Phys. Chem. B 106(2002)637.

155. Agatino Di Paola, Elisa Garcia-Lopez, Giuseppe Marc, Cristina Martin, Leonardo Palmisano, Vicente Rives, Anna Maria Venezia. Applied Catalysis B: Environmental 48 (2004) 223.

156. G. Connell, J.A. Dumesic, J. Catal. 102 (1986) 103.

157. G. Connell, J.A. Dumesic, J. Catal. 102 (1986) 216.

158. A.M. Venezia, L. Palmisano, M. Schiavello, C. Martin, I. Martin, V. Rives, J. Catal. 147 (1994) 115.

# Chapter 4

# Photocatalysis of Ag,Ce and Cu loaded titania

## *Abstract*

Semiconductor photocatalysis has become an increasing, promising technology in environmental remediation. Of various types of photocatalysts, titanium dioxide and the modified $TiO_2$ catalysts were the suitable candidates in this field. In the previous chapters, the three different routes by which the catalysts were synthesized, modified by incorporating metals like Ag, Ce, and Cu in$TiO_2$ matrix, and physio-chemical characterization were discussed. This chapter deals with the selection of a best route by which $TiO_2$ catalysts were prepared, based on the application of the catalyst on the degradation of Methylene Blue (MB), a common organic dye, by varying all possible parameters. A brief account of the advantages of modification of $TiO_2$, dyes in advanced oxidation process (AOP) and photocatalytic degradation were also discussed.

## 4.1.0 Introduction

Research interests based on $TiO_2$ material is ever increasing and it will be a material of central attraction in photocatalysis for varied challenging applications as semiconductor photocatalysis is an emerging technique relevant to water and air purification. Semiconductors have played the most promising role in several areas, addressing problems of both fundamental and applied nature. One of the major applications of this technology is the degradation of organic pollutants in water and air streams which is considered as one of the so-called advance oxidation processes (AOP). The most studied compounds are oxidation of dyes, organic waste, phenol derivatives, etc., $TiO_2$ has been identified as the most effective and useful photocatalyst because of its outstanding beneficial physical and chemical properties and wide range of applications in antimicrobial, deodorization, air purification and wastewater treatment **[1–3]**. However, it has been also known that this type of photo oxidation has two typical defects: firstly,$TiO_2$ is active only under ultraviolet (UV) light with wavelength shorter than 388 nm because of it wider band gap (Eg = 3.2 eV), only about 10%of the solar spectrum falls in this UV range. This practically rules out the use of sunlight as an energy source for the photoreaction in $TiO_2$. Secondly, a low rate of electron transfer to oxygen and a high recombination of photogenerated electron–hole pairs results low photo quantum efficiency **[4–6]**.

To improve the response of $TiO_2$ to visible light and enhance the separation of electron–hole pairs, numerous methods including transition metal **[7–10]** or nonmetal **[11–15]** modified $TiO_2$ and dye or metal complex sensitized $TiO_2$ **[16-18]** have been developed. Co-doped **[19]** $TiO_2$ is also effective for enhancing the photocatalytic activity by Li et al **[20]**. Metal

ions can also serve as charge trapping sites and thus reduce electron–hole recombination rate **[21,22]**.The effect of incorporation of metals (doping or loading) on the activity of $TiO_2$, depends on many factors, e.g. the method of doping , the type and the concentration of dopant etc. **[23]**. Both detrimental and beneficial effects of transition metal ion doping have been reported. The comparison between the reported results is difficult since in addition to different preparation methods of the doped samples, the experimental conditions for the determination of photo reactivity were also different **[24]**.

In this study, the $TiO_2$ samples were synthesized by three different methods namely Sol-Gel, Hydrothermal and EISA method at a calcination temperature of 450°C. The $TiO_2$ catalysts in the three routes were modified by loading with metals like Ag, Ce ,Cu and the catalysts were reduced in a current of $H_2$, the metal atoms form individual phases attached to $TiO_2$ though the concentration is very less. Investigations were carried out to demonstrate the effect of metal incorporation in preventing the recombination rate of electron–hole pair in the semiconductor and the band-gap decrease of $TiO_2$.Also to explain the photocatalytic activity of mesoporous nanocrystalline $TiO_2$ for degradation of dyes in aqueous medium under ultraviolet light irradiation .The mechanism in terms of work function is reported by Tayade *et al* **[25]**.Similarly, modification of $TiO_2$ by doping of transition metal ions on the titania can also significantly enhance the quantum efficiency, either by expanding the light absorption range or by improving the redox potential of the photogenerated radicals**[26-30]**.The mechanism as well as the reports**[31]** clearly stress that efficient photocatalysis is due to the presence of the metal in catalysts. Characteristic band for the tetrahedrally co-ordinated titanium appear at about 388nm.The

light absorbtion capacity is an important parameter which influences the efficiency of any photocatalytic reaction. The absorption is associated with the $O^{2-}$ to $Ti^{4+}$ charge transfer corresponding to electronic excitation from the valence band to the conduction band. The key mechanism of photocatalysis [32] is as follows:

$$O_2 + e^-_{CB} \rightarrow O_2^{-\bullet}$$

$$O_2^{-\bullet} + H^+ \rightarrow HO_2^{\bullet}$$

$$2\,HO_2^{\bullet} \rightarrow H_2O_2 + O_2$$

$$H_2O_2 \rightarrow 2HO^{\bullet}$$

$$HO^- + h^+_{VB} \rightarrow HO^{\bullet}$$

The valence electrons of $TiO_2$ catalyst are excited to the conduction band by UV light and after various other events, electrons on the $TiO_2$ particle surface are scavenged by the molecular oxygen to produce reactive oxygen radicals, whereas the valence hole become trapped as the surface-bound $OH^{\bullet}$ radicals on oxidation of either the surface OH group and/or the surface $H_2O$ molecules. These hydroxyl radicals ($HO^{\bullet}$) have very high oxidation potential of 2.80V according to Legrini *et al,* hence named advanced oxidation process(AOP) oxidizes the pollutants[33].Actually metal nanoparticles deposited on $TiO_2$ act as electron traps, enhancing the electron–hole separation and the subsequent transfer of the trapped electron to the adsorbed $O_2$ acting as an electron acceptor. The superoxide anion ($O_2^{-\bullet}$) thus formed is the active species which enhances the photocatalytic reactions [34–37]. Therefore, the charge separation on $TiO_2$ is a crucial factor in affecting the efficiency of the photodegradation under UV irradiation. The intermediate $HO_2^{\bullet}$ are hydroperoxy radicals.

### 4.2.0 Photocatalysis on metal/$TiO_2$ interface

Photocatalysis on Ag/$TiO_2$ interface is schematically given by T.Sakata,*et al* [38]. Electrons are transferred to metal surface, reduction of $H^+$ ions takes place at the metal surface, the holes move into the other side of semiconductor while oxidation takes place at the semiconductor surface.

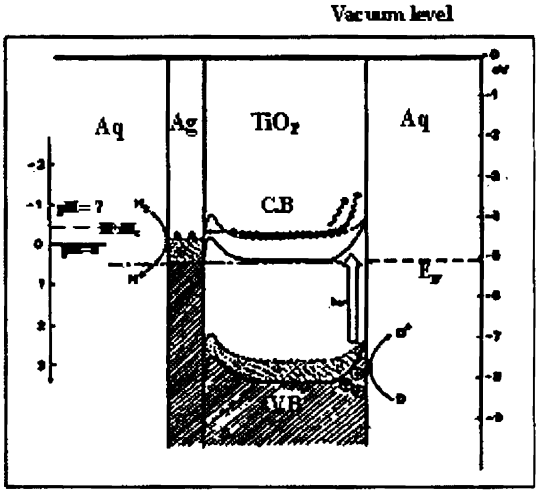


T.Sakata, *et al Chem. Phys. Lett. 88 (1982) 50*

**Fig.4.1 Photocatalysis on Ag/$TiO_2$ interface**

$CeO_2$ is frequently incorporated to catalysts due to its considerable performance for the catalytic combustion of hydrocarbons [39]. It has been reported that $CeO_2$ has the property of stabilizing the active phase and inhibiting the thermal loss of the catalyst surface area and the catalytic activity [40,41]. However, there are only a few reports on the photocatalytic activity of cerium-doped materials [42-44]. Herein, cerium-doped $TiO_2$ nanoparticles with anatase mesostructures were fabricated via hydrothermal process by using P123 ($EO_{20}PO_{20}EO_{20}$) which acts as a pore -directing and forming agent. The effect of cerium doping on the phase transformation

and photocatalytic activity of $TiO_2$ was reported **[45].** Liu *et al* studied the effect of an n-type impurity band, interpreted as the existence due to the substitution of $Ti^{4+}$ for $Ce^{3+/4+}$ at the interface between the two oxides, in the gap of $TiO_2$**[46].**Cu-doped $TiO_2$ systems with improved photocatalytic activity is discussed by G. Colon et al **[47].**This improvement might be related to the stabilization of $Cu_2O$ species in doped $TiO_2$ prepared in the presence of acid and it could be related to the presence of oxygen vacancies generated in the preparation procedure. Copper doped $TiO_2$ has been traditionally used for the $CO_2$ photocatalytic reduction processes **[48–50].** On the other hand, the use of copper doped $TiO_2$ for photo-oxidation process is scarce **[51,52].** The reported photocatalytic behaviour is poor by A. Di Paola et al and in any case, no information about the oxidation state of Cu is reported **[53,54].** Huaming Yang et al in their paper discussed about Electrochemical synthesis and photocatalytic property of cuprous oxide nanoparticles under UVirradiation and observed that $Cu_2O$ nanoparticles were kept its cubic crystal phase, but fractionally oxidized to be CuO after the photocatalysis**[55].**

### 4.3.0 Dyes in advanced oxidation process (AOP)

Dye molecules consist of a chromagen and there are about 12 classes of chromagenic groups, the most common of which is the azo type that makes up to 60–70% of all textile dye stuffs produced. Another classification of dyes is based on their mode of application to textiles and distinguishes acidic, reactive, metal complex, disperse, direct, vat, mordant, basic and sulfur dyes. Research is focused on reactive dyes because they represent an increasing market share, a large fraction of the applied reactive dye is wasted due to dye hydrolysis in the alkaline dye bath, and finally, conventional wastewater treatment plants have low removal efficiency for

reactive and other anionic soluble dyes [56,57]. The release of azo dyes into the environment is of great concern due to the coloration of natural waters, the toxicity, the mutagenicity, and carcinogenicity [58-60]. The consequence of this release in the eco-system is a dramatic source of aesthetic pollution, eutrophication and perturbation in aquatic systems [61,62]. Up to the present, dye removal methods include chemical, oxidative or most commonly active sludge biochemical processes. Adsorption and chemical coagulation do not result in dye degradation and create an ongoing waste disposal problem. The chemical oxidation treatments are usually effective towards the destruction of chromophoric structures of dyes. In this way the water coloration is removed, but often a complete mineralization is not achieved. Chlorination and ozonisation cause decolorization by means of chemical reactions. The by-products of chlorination are chlorinated organics that may be more toxic than the dye itself [63-65]. Problems with using ozone include its instability and its hazardous nature due to strong and non-selective oxidizing power. Therefore, a post treatment destruction unit must be used to prevent unreacted ozone from escaping into the atmosphere.

Heterogeneous photocatalysis is an advanced oxidation process (AOP), which can be successfully used to oxidize many organic pollutants present in aqueous systems. AOP's are all characterized by the same chemical feature: production of radicals ($OH^{\bullet}$) through a multistep process given above, although different reaction systems, different source of illuminations were used. According to other researchers, UV-mechanism is prevalent and its contribution to the dye degradation is much more important than the visible light initiated mechanism [66,67]. These radicals show little selectivity of attack and are able to oxidize various organic

pollutants due to their high oxidative capacity (reduction potential of $HO^{\bullet}$ $E_o$ = 2.8 V) **[68]**. Experimental observations indicate almost complete oxidation of most of the organic compounds to $CO_2$, $H_2O$ and inorganic anions, can be achieved through photocatalytic processes. The use of titanium dioxide ($TiO_2$) as a catalyst for the photo-oxidation of organic compounds has received much interest because $TiO_2$ is plentiful, inexpensive, powerful and environmentally friendly. The photocatalytic activity of titania towards the degradation of various anionic dyes such as Alizarin S, Azo methyl red, Congo red, Orange G and cationic dyes like methylene blue and malachite green was reported in literature**[69-72]**. Nitrogen doped $TiO_2$ in the photocatalytic degradation of three azodyes like Acid orange 7, Procion red MX-5B and Reactive Black were some among them **[60]**. Illuminated titania is also capable of degrading dyes like Acid blue 9, X-GL, active Brilliant red Dye X-3B **[73-75]**. The photocatalytic oxidation of dyes is generally monitored by measuring the decolorization rate, the organic content reduction and the by-products obtained at the different photocatalytic stages. However, the qualitative and quantitative analysis of all individual by-products is very often incomplete, due to technical or financial limitations. Additionally, the generation of by-products that may be more toxic than the parent compounds and phenomena, such as bioavailability, synergistic or antagonistic effects, make toxicity testing of the photocatalytic process essential **[76,77]**. The Microtox test is amongst the most widely used bioassays for an integrated evaluation of the effectiveness of the photocatalytic process in terms of pollutant decomposition **[78,79]**. Doped titania also shows an excellent photoactivity as evaluated by the extent of decomposition of methylene blue when exposed to UV light**[80]**.In the present work, the photocatalytic degradation of a commercial textile dye in aqueous solutions using $TiO_2$

catalysts prepared by three different routes has been examined. The main objectives of the study were (i) to estimate the kinetics of the dye disappearance (ii) to examine the influence of various parameters, such as the type and mass of the catalyst, the initial concentration of the dye, initial pH etc., (iii) to evaluate the degree of mineralization of the products etc..

### 4.4.0 Photocatalytic reactions on the dye methylene blue

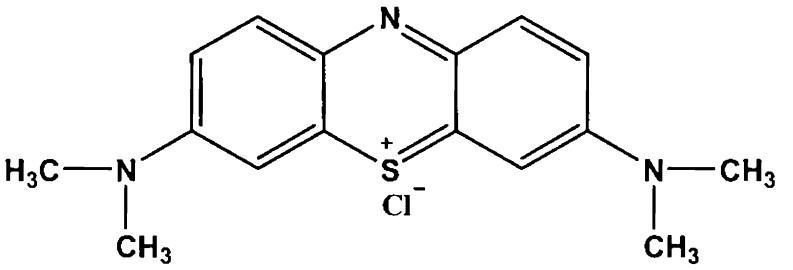


**Fig.4.2.0 Methylene Blue (MB-660nm)**

Methylene Blue (MB) is a cationic dye that is used extensively in a variety of industrial applications as well as in photocatalysis. It is chosen to be a model pollutant as the absorbance of MB is at a wavelength 660nm. Dyes are commonly used as model pollutants, partly because their concentration can be easily monitored using a spectrometer. The photocatalytic degradation intermediates of MB solution was determined by House et al., Torres *et* al and M.Gattrell *et al* **|81-83|**. The photocatalytic reactions were carried out in a Heber photoreactor (multilamp type, model HML-MP88) containing concentrically arranged eight numbers of 8W mercury lamps set in parallel and emitting 365nm wavelength. It has a reaction chamber with cooling fan at the bottom. Open borosilicate glass tube of 50 ml capacity was used as a reaction vessel. The solution with the dye and the photocatalyst were taken in the borosilicate glass tube. The

suspension was magnetically stirred for 30 min in dark for the attainment of adsorption equilibrium and then irradiated. The practice of taking out the solution at regular time intervals was not followed in this work. Instead, after optimization,20 ml of the dye and 0.1gm of the catalyst were used for irradiation in each lot and centrifuged twice to remove $TiO_2$ particles or the catalyst and diluted. Absorbance measurements of the dyes were taken. Experiments were conducted by varying the concentration of the dye ($10^{-3}$, $10^{-4}$ and $10^{-5}$ M), the pH of the dye in aqueous medium(4-10), the amount of the catalyst(0.05,0.1 and 0.15 g) and varying the lamp intensity. A general mechanism of degradation of dye is given in figure 4.2.1

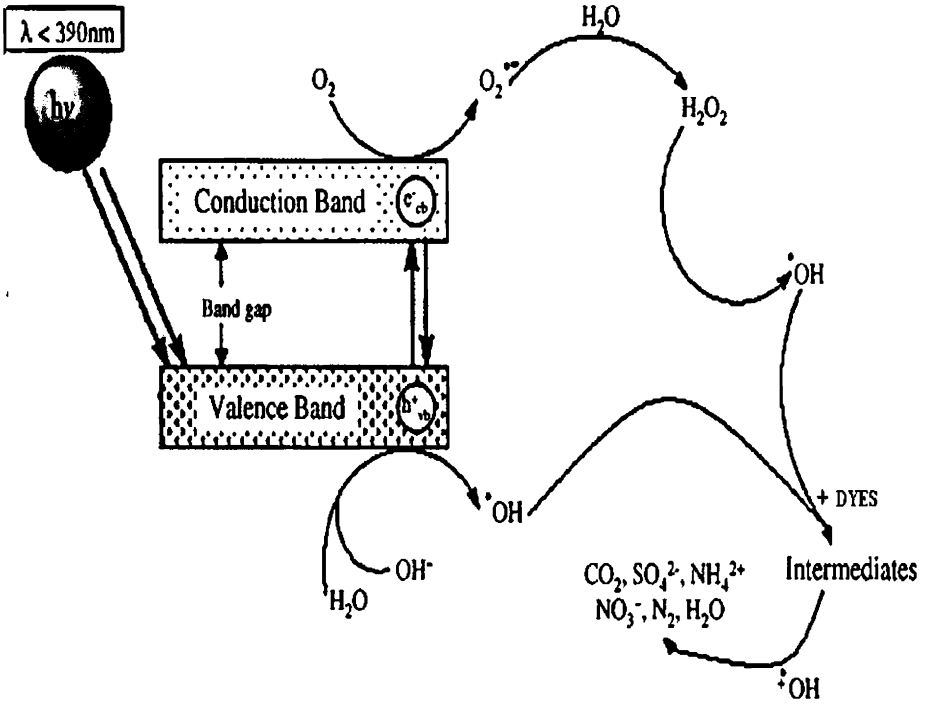


**Fig.4.2.1 A General mechanism of Dye Degradation [84]**

### 4.4.1 Mechanism of degradation on methylene blue

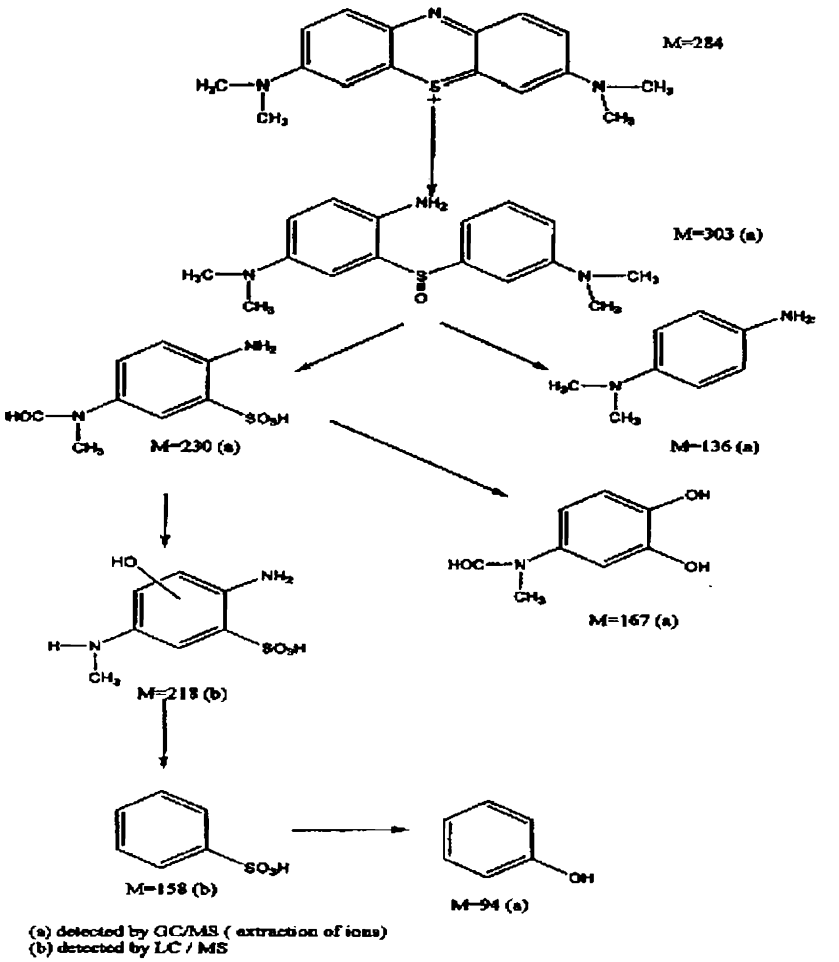


A. Houas et al. Applied Catalysis B: Environmental 31 (2001)145 [81]

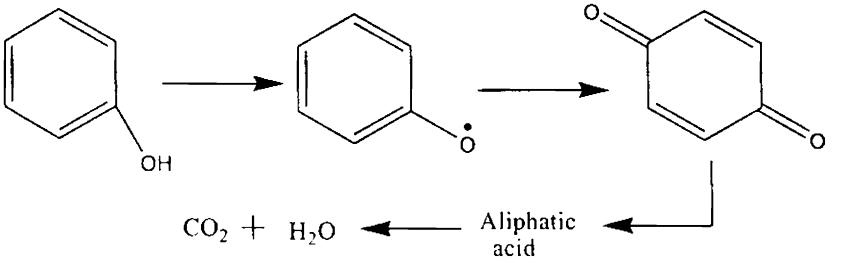


Torres *et* al., *Chemosphere* (2003) [82,83]

**Fig.4.2.2 Mechanism of methylene blue Degradation**

### 4.4.2 Reaction studies on methylene blue

#### 4.4.2.1 Activity of the catalysts in different routes

A $10^{-4}$ molar concentration of the dye, methylene blue of pH= 9.8, is used for the purpose. About 20 ml of the dye is taken and 0.1gm of the catalyst is added. Prior to irradiation, the system was magnetically stirred during 30 min to establish an adsorption–desorption equilibrium, between the catalytic surface and the dye. Then the system is subjected to UV irradiation in the photoreactor. Absorbance measurements were taken at half an hour interval time up to 3 hours (½, 1, 1½, 2, 2½ and 3). All the systems except a few got decolourised completely after three hours.

**Reaction Conditions**

| | |
|---|---|
| Dye Conc. | - 20 ml $10^{-4}$M |
| Catalyst amount | - 0.1g |
| Lamp power | - 48 watts |
| Irradiation time | - 60 min |

| Catalyst | %Degradation in 60 min | | |
|---|---|---|---|
| | Sol-Gel Route | Hydrothermal Route | EISA Route |
| $TiO_2$ | 48.1 | 90.0 | 75.0 |
| $Ag/TiO_2$ | 67.1 | 100.0 | 80.3 |
| $Ce/TiO_2$ | 37.4 | 60.0 | 41.7 |
| $Cu/TiO_2$ | 40.0 | 75.0 | 69.8 |

**Table4.1 % Degradation w.r.t Time in different routes**

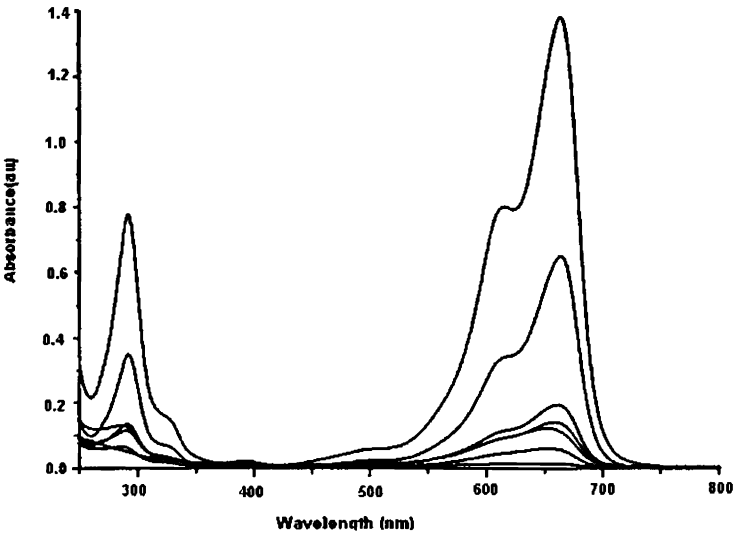


**Fig.4.2.3 Scan Spectrum of Degradation of Methylene blue at pH =9.8**

The photocatalytic bleaching of Methylene blue(MB) in presence of $TiO_2$ at different time intervals was observed at $\lambda_{max}$ 660 nm indicating that the dye is degraded on irradiation .The absorbance at 290nm indicate the degradation of aromatic part of the dye. Catalysts prepared by Hydrothermal route (HT) were observed to show higher activity over catalysts in other routes in terms of degradation of MB. It can be inferred that the surface hydroxyl groups were higher for the catalysts prepared by this route and were in a highly ordered mesoporous state which is favourable for photocatalytic activity. It is observed that mesoporous materials of larger surface can present more active sites to adsorb water, hydroxyl groups and dye molecules leading to high photocatalytic reaction rate [85-87]. The distribution and reactivity of these –OH groups strongly depend on the preparation procedure and is responsible for the adsorption of the dyes that leads to degradation. The catalysts prepared by this route possess the optimum crystallite size for photocatalytic applications. The interfacial charge transfer process depends mainly on the surface

characteristics of $TiO_2$ particles, on the charge carrier mobilities and life-times[88] .

### 4.4.2.2 Activity of catalysts w.r.t. time in HT route

**Reaction conditions**

Dye con. – 20ml $10^{-4}$M

Catalyst amount – 0.1g

Lamp power – 48 watts

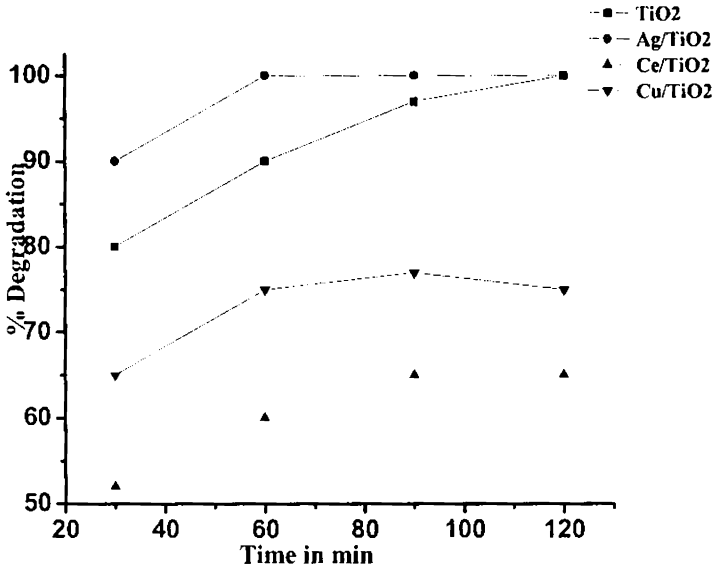


**Fig.4.3 % Degradation w.r.t Time in HT route**

The results show that silver loaded titania catalysts exihibit appreciable activity among all the other systems. The greater activity of the Ag-loaded $TiO_2$ presented in the Table 4.1 could be explained by assuming that the loaded metal decreases the semiconductor band gap of $TiO_2$, favouring electron transfer from the valence band to the conduction band. This may therefore lead to an increase in the rate of formation of oxidative species such as hydroxyl radicals under the same conditions[89]. It is also known that loading of semiconductors with transition metal ions leads to

drastic retardation of the electron-hole recombination rate [90]. Kondo and Jardim [89] revealed that the X-ray data of neat and Ag loaded $TiO_2$ did not show any change in the crystalline structure of the anatase form and occurs as typical surface process. The experimental results also indicated the lower photocatalytic activities of cerium-doped samples than undoped one. The detrimental effect of ceria loaded catalyst is because the catalyst cannot be reduced as the reduction potential of $Ce^{+4}$ to $Ce^{0}$ is highly negative. Therefore a higher temperature than 450°C is required for the reduction of the catalyst to the metal. And therefore loading of cerium partially blocks the surface sites of $TiO_2$, available for the photodegradation or to be photoactive. This can be explained as follows. It is known that the photogenerated $OH^{\cdot}$ radicals drive degradation reactions, which can eventually lead to the decomposition of organic pollutants. The $Ti^{4+}$–$OH^{\cdot}$ entities are formed by a surface hydroxyl trapping a hole. However, Coronade et al. [91] have found that some of the photoproduced holes are stabilized as $Ti^{4+}$–$O^{-}$ radicals in the $CeO_2/TiO_2$ catalyst. The $CeO_2/TiO_2$ catalyst displays a reduced concentration of $Ti^{4+}$–$O^{-}$ radicals, which is apparently less prone to trap photogenerated holes than the undoped $TiO_2$. In addition, the coverage of the $TiO_2$ surface by ceria entities removes $OH^{\cdot}$ groups, which will lead to decrease not only the active $OH^{\cdot}$ radicals but also the adsorption sites for organic pollutants [92] Therefore, that the lower photocatalytic rate of $Ce^{+4}/TiO_2$ is very likely due to the partial blockage by ceria on the semiconductor surface sites, which may further lead to decrease the trapping efficiency of the holes and the adsorption of the organic. Lin et al [93,94] reported that the mixtures of titania with $Y_2O_3$ or $La_2O_3$ were shown to have higher photocatalytic activities than pure $TiO_2$,

while the mixture of $TiO_2$ with $CeO_2$ have lower photoactivity than pure $TiO_2$. They ascribed the lower photocatalytic activities of the mixture of $TiO_2$ and $CeO_2$ to the change in the amount of surface hydroxyl groups resulting from the interaction between the rare-earth oxides and $TiO_2$. The number of surface hydroxyl groups was less due to the blockage of cerium on the titania, but the amount of adsorption of the dye on cerium-doped $TiO_2$ surface was higher because doped titania has higher surface area **[95]**. But the presence of ceria not only increased the surface area of mesoporous $TiO_2$ nanoparticles, but also inhibited the mesopores collapse and the anatase-to-rutile phase transformation. This may be attributed to the presence of cerium oxide distributed on the $TiO_2$ matrix, which is in turn beneficial for effectively enhancing surface area of $TiO_2$ as reported **[96]**. $Ce^{4+}$ did not enter into the crystal lattices of $TiO_2$ and was uniformly dispersed into $TiO_2$ as the form of $CeO_2$ with small size, which possibly made Ce dopant have a great inhibition on $TiO_2$ phase change. Cu does not adsorb hydrogen at room temperature to a significant extent**[97]**. Deactivation might be due to the possible segregation/formation of CuO species at the surface, as it may not be completely reduced to metallic copper. Owing to the trapping of conduction band electrons by the $Cu^{2+}$ions, the reduction of $O_2$ becomes difficult and blocks the formation of reactive $O_2^{\cdot-}$species**[98]**. Cu species at the surface could be identified as $Cu^{2+}$ from XPS results. These $Cu^{2+}$ species would easily uptake one photogenerated electrons from the $TiO_2$ conduction band leading to $Cu^{1+}$and avoiding the diffusion of electrons to the surface and the formation of $OH^{\cdot}$radical from this route. A rapid $Cu^{2+}$ reduction toward $Cu^{1+}$ ( $Cu^{2+}$/ $Cu^{1+}$ redox potential 0.154 V versus NHE) is probably taking place once $TiO_2$ is photoexcited. Since no stabilization of $Cu^{1+}$ ion might be considered, a subsequence reoxidation would occur by a hole trapping and

$Cu^{2+}$ would be formed. Therefore, the existence of $Cu^{2+}$ sites would be considered as recombination centre[99].It is also known that $Cu^{2+}$ions adsorbed on the surface were difficult to reduce to Cu metal [100,101].

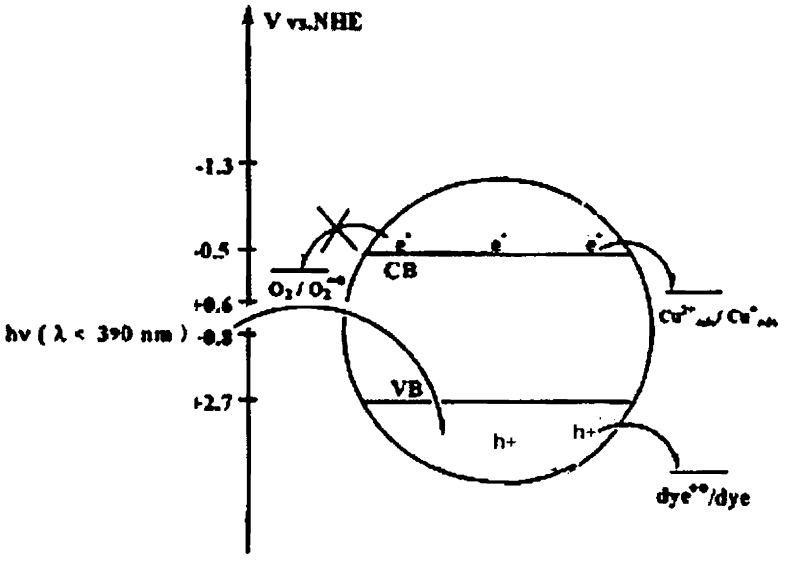


**Fig.4.4 Electron Transfer Pathway on Addition of $Cu^{2+}$ in $TiO_2$ Aqueous Dispersions**

### 4.4.2.3 Activity of catalysts w.r.t. dye concentration in HT route

**Reaction conditions**

| | |
|---|---|
| Catalyst amount | – 0.1g |
| Dye conc. | –20ml$10^{-3}$,$10^{-4}$,$10^{-5}$M |
| Lamp power | – 48 watts |
| Irradiation time | – 60 min |

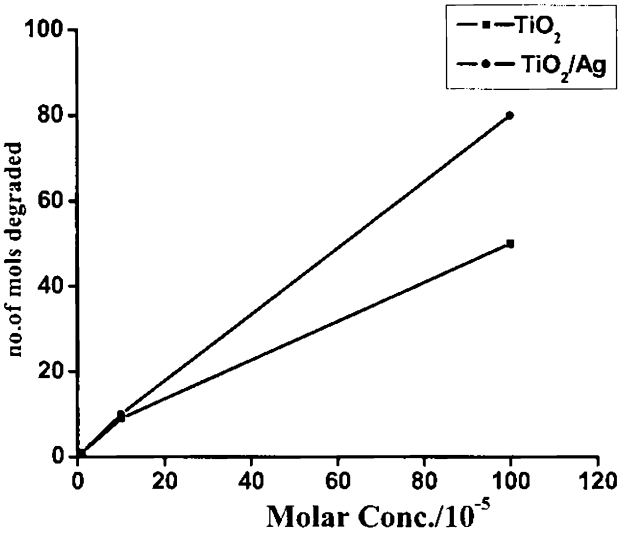


**Fig.4.5 No. of moles degraded w.r.t. dye concentration**

Significant changes in the degradation with respect to different concentrations of methylene blue were observed in the figure 4.5. The initial concentrations of methylene blue like $10^{-3}$, $10^{-4}$and $10^{-5}$M were prepared to evaluate the influence of the concentration of the dye on the efficiency of the reaction with otherwise identical reaction conditions. It can be seen that the concentration has a remarkable effect on the degradation rates. The rate of photocatalytic dye molecules even available for excitation and energy transfer is greater and hence an increase in the rate was observed. But in this work, it is observed that as the concentration of methylene blue increases, there is a decrease in the number of moles degraded. The decrease with increase in concentration of the dye is because the dye will start as a filter for the incident light and will not permit the desired light intensity to reach the semiconductor particles. This behaviour is expected

since the ratio of methylene blue molecules/active sites of $TiO_2$ is lower leading to a retardation of the overall disappearance of the compound.

### 4.4.2.4 Activity of catalysts w.r.t. initial pH in HT route

The influence of the initial pH of the dye solution was studied as pH could be considered as one of the most important parameters that can affect the photo-oxidation process. Increase in one unit of pH shifts the valence and conduction band potential towards the cathodic direction by 59mV as shown $E_{VB}$ = 3.15 – 0.059 pH, $E_{CB}$ = -0.05 – 0.059 pH **[102]** ; So pH control is very important.

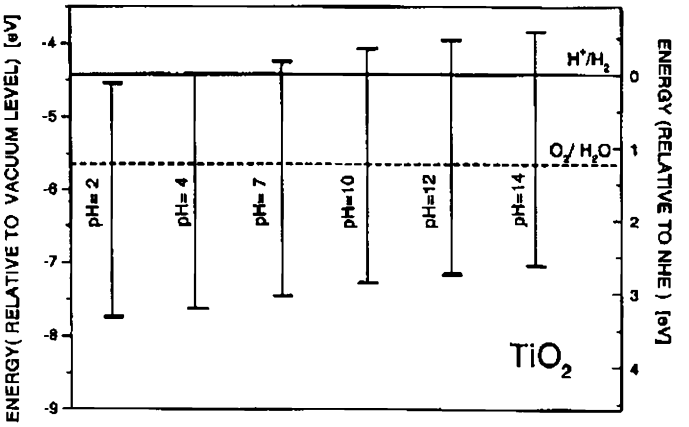


**Fig.4.6 Effect of pH on energy of $TiO_2$**

**Reaction conditions**

| | |
|---|---|
| Dye conc. | – 20ml $10^{-4}$M |
| Catalyst amount | – 0.1g |
| Lamp power | – 48 watts |
| Irradiation time | – 60min |

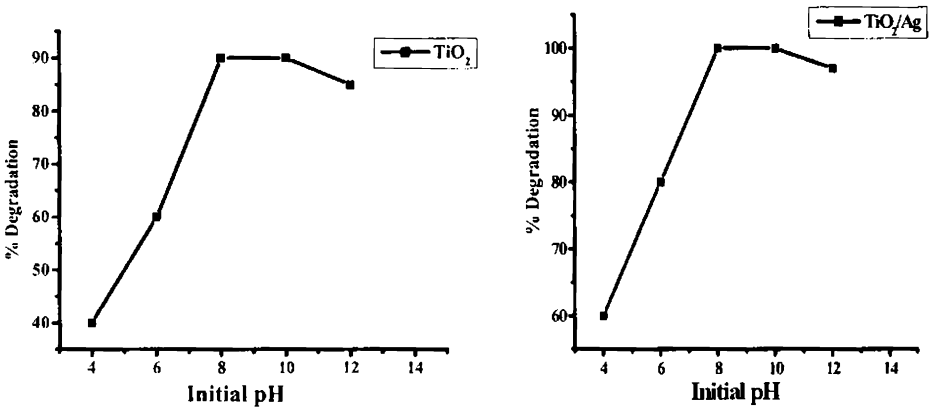


**Fig.4.7 %Degradation of $TiO_2$and Ag/$TiO_2$ catalysts w.r.t pH of MB solution**

The activity of $TiO_2$and Ag /$TiO_2$ catalysts changes w.r.t pH of MB dye, in three different pH values (acidic, neutral and alkaline) is presented. For altering pH in the acidic and in alkaline area, HCl 2M and NaOH 2M solutions respectively, have been used. The effect of the solution pH on the degradation rate can be explained mainly by the availability of $OH^-$ ions in solution. Since MB is a cationic dye it is conceivable that at high pH's, its adsorption is favored on a negatively charged surface. Increase is due to more availability of $OH^-$ ions at higher pH values. Decrease may be due to the fact that the dye does not remain in its structural form due to greater con. of $OH^-$ ions. Also can be explained by the modification of the electrical double layer of the solid–electrolyte interface, which consequently affects the sorption-desorption processes and the separation of the photogenerated electron–hole pairs in the surface of the semiconductor particles. In basic suspensions, the adsorption of the dye on the $TiO_2$ particles was significantly increased comparing to the extent of adsorption in neutral or acidic suspensions. This is attributed to the fact that $TiO_2$ shows an amphoteric character so that either a positive or a negative charge can be

developed on its surface. The point of zero charge represents the pH value at which the coverage of $H^+$ equals the coverage of $OH^-$.The point of zero charge known for $TiO_2$ is 6.8 (Degussa p-25), so below this value the surface of the particles is positively charged and above it is negatively charged. Because adsorption is favored in high pH (the extent of adsorption gives 20%increase for the dye compared to the one at neutral pH value), it can be assumed that molecules of dye were positively charged so an electrostatic attraction is developed [103].

$$pH > pzc : Ti\text{-}OH + OH^- \rightarrow TiO^- + H_2O$$

$$pH < pzc : Ti\text{-}OH + H^+ \rightarrow TiOH_2^+$$

### 4.4.2.5 Activity of catalysts w.r.t. catalyst amount in HT route

**Reaction conditions**

Dye conc. – 20ml 10 $^{-4}$M soln

Irradiation time – 60 min

Lamp power – 48 watts

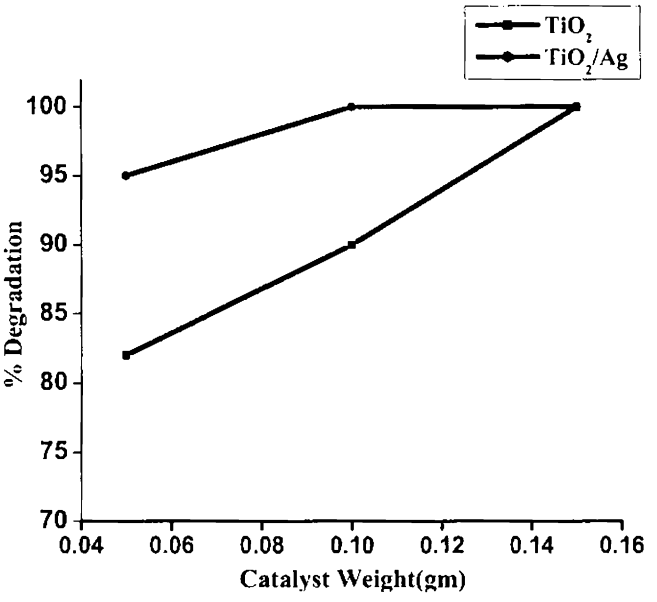


**Fig.4.8 % Degradation w.r.t catalyst amount in HT route**

The influence of the catalyst amount on the decolorization kinetics of the dye solution has been investigated using different concentrations of $TiO_2$ varying from 0.05 to 0.15 g/L and the results are presented in Fig.4.8. By increasing the amount of the catalyst the degradation becomes faster. Silver doped titania catalysts show immediate decolourisation in all the cases. Initially, the exposed surface area increases and reaches a saturation point. It is obvious that the rate increases with an increase of the concentration of catalyst up to a limit above which no improvement is obtained and the curves formed are reminiscent of a Langmuir type adsorption isotherm. A similar observation has been made by other authors, as well**[104-108].** Further addition increases only the thickness of the layer at the bottom of the vessel. The increased degradation rate that follows the increase in the catalyst loading can be attributed to the fact that a larger amount of photons are, thus, adsorbed accelerating the process. The plateau, which is recorded after a certain amount of catalyst is added, may be a consequence of the fact that the reaction takes place on dye molecules adsorbed at the $TiO_2$surface. When all the dye molecules are adsorbed on $TiO_2$ ,no improvement is achieved by adding more catalyst. The decrease in efficiency may be due to an increasing opacity of the suspension and to an enhancement of the light reflectance, because of the excess of $TiO_2$ particles **[109, 110].** Moreover, particle–particle interaction becomes significant as the amount of particles in solution increases, thus, reducing the site density for surface holes and electrons, because the rate of deactivation of activated molecules by collision with ground state titanium dioxide increases **[62,111].**

### 4.4.2.6 Activity of catalysts w.r.t. light intensity in HT route

**Reaction conditions**

Dye conc. – 20ml $10^{-4}$M

Catalyst amount – 0.1g

Irradiation time – 60 min

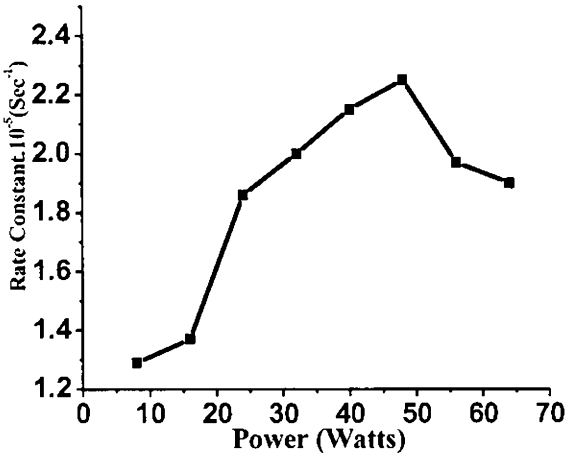


**Fig.4.9 Variation in rate w.r.t. power supplied**

The intensity of radiation falling on the catalyst surface plays an important role in any photocatalytic process. Here, the degradation of methylene blue, having a concentration of 20ml $10^{-4}$M is monitored using 0.1g of titania for 60 minutes with varying intensities of radiation. The reaction was carried out with two, four, six and eight lamps on, the angles sustained by the adjacent lamps at the samples are 45,90and 180° respectively. Figure4.9 clearly illustrates the dependence of light intensity in the rate of the reaction of the dye. The degradation of the dyes follows a pseudo-first-order kinetics according to the Langmuir–Hinshelwood model. Generally, the logarithmic plot of concentration data gives a straight line,

which its slope helps to predict the rate constant of reaction. That is $\ln(C_0/C) = kt$ **[112-114],** where $C$ is the dye concentration (mg/l) at instant $t$ (sec), $C_0$ the dye concentration (mg/l) at $t = 0$ (sec), and $k$ is the reaction rate constant ($sec^{-1}$).The reaction doesn't occur actually in the dark. Investigation of the photocatalysis using 16 watts power and 48 watts power in the microreactor under identical conditions revealed that high energy radiation is more effective in bringing out the photocatalysis**[115].** As the intensity of light was increased, the bleaching action was accelerated because the no. of photons /unit area increase**[116,117].** However, a decrease may be due to some side reactions or thermal effects. The catalyst does not loose its activity on illumination. Reuse of the catalyst indicate the photocatalytic efficiency **[118].** Also the percentage degradation of methylene blue rises steeply with intensity upto 48 Watts and hereafter it declines. So an optimum of 48W is chosen for the comparison of all the catalyst systems.

#### 4.4.2.7 Reusability of the catalysts

Photocatalytic nano-$TiO_2$ surfaces were repetitively used to degrade the MB solution under UV-light. Used catalysts were employed to degrade a fresh MB solution under the same conditions. The process was repeated several times under UV light. Before using repeatedly, the catalysts were stored in the dark at room temperature **[119].**

**Reaction conditions**

| | |
|---|---|
| Dye conc. | – 20ml $10^{-4}$M |
| Catalyst amount | – 0.1g |
| Irradiation time | – 60 min |
| Lamp power | – 48watts |

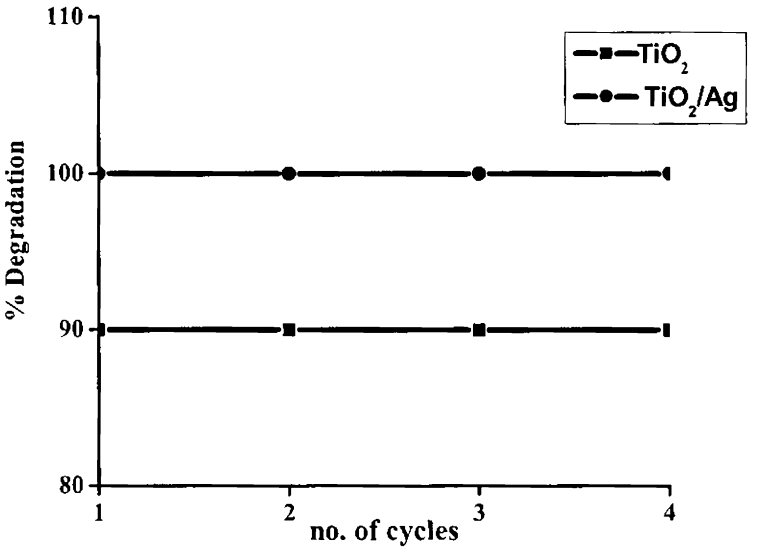


**Fig.5.0 Effect of deactivation of the catalysts**

## References


1. C. Galindo, P. Jacques, A. Kalt, J Photochem.Photobiol. A: Chem. 130 (2000) 35– 47.
2. I. Arslan, I.A. Balcioglu, T. Tuhkanen, Environ.Tech.20 (9) (1999) 921–931.
3. K. Konitou, S. Maeda, S. Hongyou, K. Mishima, Can. J. Chem. Eng. 80 (2002)208.
4. T. Sauer, G.C. Neto, H.J. Jos´e, R.F.P.M. Moreira, J. Photochem.Photobiol. A: Chem. 149 (2002) 147–157.
5. N. Daneshvar, D. Salari, A.R. Khataee, Photochem. Photobiol. A: Chem. 157 (2003) 111–121.
6. K.R. Ramakrishna, T. Viraraghavan, Water Sci. Technol. 36 (2) (1997) 189–196.
7. R. Asahi, T. Morikawa, T. Ohwaki, K. Aoki, Y. Taga, Science 293 (5528) (1995)269–271.
8. X. Fu, W.A. Zeltner, M.A. Anderson, Abst. Paper Am.Chem. Soc. 210 (1995), 163-Coll Part 1.
9. K. Tennakone, I.R.M.Kottegoda, J. Photochem. Photobiol. A: Chem. 96 (1996) 79–81.
10. G. Colon, M.C. Hidalgo, J.A. Navio, J. Photochem. Photobiol. A: Chem. 138 (2001) 79–85.
11. H.X. Fu, G. Lu, S.B. Li, J. Photochem. Photobiol. A: Chem. 114 (1998) 81–88.
12. Y. Zhu, L. Zhang, W. Yao, L. Cao, Appl. Surf. Sci. 158 (2000) 32.
13. Y. Zhu, L. Zhang, L. Wang, Y. Fu, L. Cao, J. Mater. Chem. 11 (2001) 1864.
14. S.K. Zheng, T.M. Wang, W.C. Hao, R. Shen, Vacuum 65 (2002)155.
15. A. Fujishima, T.N. Rao, D.A. Tryk, J. Photochem. Photobiol. C 1 (2000) 1.
16. T.Watanabe, A. Nakajima, R.Wang, M. Minabe, S.Koizumi, A. Fujishima,
17. K. Hashimoto, Thin Solid Films 352 (1999)260.
18. L. Zhang, Y. Zhu, Y. He, W. Li, H. Sun, Appl.Catal. B: Environ. 40 (2003) 287.
19. Y. Cao,W.Yang,W. Zhang, G. Liu, P.Yue, New. J. Chem. 28 (2004) 218.
20. G. Colon, M.C. Hidalgo, J.A. Navio, Catal. Today 76 (2002) 91.

20. X.M. Wu, L. Wang, Z.C. Tan, G.H. Li, S.S. Qu, J. Solid State Chem. 156 (2001) 220.

21. M. Gratzel, R.F. Howe, J. Phys. Chem. 94 (1990) 2566.

22. X. Li, P.L. Yue, C. Kutal, New J. Chem. 8 (2003) 1264.

23. M. Anpo, M. Takeuchi, J. Catal. 216 (2003) 505.

24. O. Carp, C.L. Huisman, A. Rellr, Prog. Solid State Chem. 32 (2004) 33.

25. R. J.Tayade, R. G. Kulkarni, R. V. Jasra Ind. Eng. Chem. Res. 45 (2006) 5231-5238

26. M.R.Hoffmann,S.T.Martin,W. Choi, D.W.Bahnemann,Chem. Rev. 95 (1995) 69–96.

27. A. Linsebigler, G. Lu, J.T. Yates, Chem. Rev. 95 (1995) 735–758.

28. J. Lin, J.C. Yu, D. Lo, S.K. Lam, J. Catal. 183 (1999) 368–372.

29. M. Anpo, Stud. Surf. Sci. Catal. 130 (2000) 157–163.

30. G. Soler-Illia, A. Louis, C. Sanchez, Chem. Mater. 14 (2002).

31. Nikolaos Dimitratos, Alberto Villa, Claudia L. Bianchi,Laura Prati, Michiel Makkee Applied Catalysis A: General 311 (2006) 185–192.

32. C.D. Jaeger, A.J. Bard, J. Phys. Chem. 83 (1979) 3146.

33. O.Legrini,E.Oliveros,A.M.Braun Chem.Rev. 93 (1993)671.

34. J. Herrmann, J. Disdier, P. Pichat, J. Phys. Chem. 90 (1986) 6028.

35. A. Henglein, J. Phys. Chem. 83 (1979) 2209.

36. J.M. Herrmann, in: R.T.K. Baker, S.J. Tauster, J.A. Dumesic (Eds.), ACS Symposium Series. 298( 1986)200.

37. J. Disdier, J.M. Herrmann, P. Pichat, J. Chem. Soc. Faraday Trans. I 77 (1981) 2815.

38. T.Sakata, et al Chem. Phys.Lett. 88 (1982) 50

39. A. Trovarelli, Catal. Rev. Sci. Eng. 38 (1996) 439–520.

40. P.O. Larsson, A. Andersson, J. Catal. 179 (1998) 72–89.

41. M.S.P. Francisco, V.R. Mastelaro, Chem. Mater. 14 (2002) 2514–2518.

42. J. Lin, J.C. Yu, J. Photochem. Photobiol. A: Chem. 116 (1998)63–67.

43. J.M. Coronado, A.J. Maira, A. Martinez-Arias, J.C. Conesa,J. Soria, J. Photochem. Photobiol. 150 (2002) 213–221.

45. A.W. Xu, Y. Gao, H.Q. Liu, J. Catal. 207 (2002) 151–157.

46. C.P. Sibu,S.Rajesh Kumar, P. Mukundan, K.G.K. Warrier, Chem.Mater.14 (2002) 2876–2881.

47. Liu, Guo Zhaolin, Hong Bing, Jiang Liang, Huixin Journal of Physics andChemistry of Solids, 66(2005)161-167.

48. G. Colon, M. Maicu, M.C. Hidalgo, J.A. Navıo Applied Catalysis B: Environmental .67 (2006) 41–51.

49. H. Yamashita, H. Nishiguchi, N. Kamada,M. Anpo, Res. Chem. Intermed.20 (1994) 815.

50. I.H. Tseng, J.C.S. Wu, Catal. Today 97 (2004) 113.

51. Slamet, H.W. Nasution, E. Purnama, S. Kosela, J. Gunlazuardi, Catal.Commun. 6 (2005) 313.

52. J. Arana, C. Garriga i Cabo, J.M. Dona Rodrıguez, O. Gonzalez Dıaz, J.A.Herrera Melıan, J. Perez Pena, Appl. Surf. Sci. 239 (2004) 60.

53. J. Arana, C. Fernandez Rodrıguez, O. Gonzalez Dıaz, J.A. Herrera Melıan,J. Perez Pena, Catal. Today 101 (2005) 261.

54. A. Di Paola, E. Garcıa Lopez, S. Ikeda, G. Marcı, B. Ohtani, L. Palmisano, Catal. Today 75 (2002) 87.

55. A. Di Paola, E. Garcıa Lopez, G. Marcı, C. Martın, L. Palmisano, V. Rives, A.M. Venezia, Appl. Catal. B: Environ. 48 (2004) 233.

56. Huaming Yang, Jing Ouyang, Aidong Tang, Yu Xiao, Xianwei Li, Xiaodan Dong, Yongmei Yu Materials Research Bulletin 41 (2006) 1310.

57. P.C. Vandevivere, R. Bianchi, W. Verstraete. J. Chem. Technol. Biotechnol. 72 (1998) 289–302.

58. V. Augugliaro, C. Baiocchi, A. Bianco Prevot, E. Garcia-Lopez, V. Loddo, S. Malato, G. Marci, L. Palmisano, M. Pazzi, E. Pramauro.Chempsphere 49 (2002) 1223–1230.

59. J. Li, P.L. Bishop, Wat. Sci. Technol. 46 (1–2) (2002) 207.

60. J. Li, P.L. Bishop, Wat. Sci. Technol. 49 (11–12) (2004) 237.

61. Y. Liu, X. Che, J. Li, C. Burda, Chemosphere 61 (2005) 11.

62. C. Burda, Y. Lou, X. Chen, A.C.S. Samia, J. Stout, J.L. Gole, NanoLetters 3 (2003) 1049.

63. F. Nerud, P. Baldrian, J. Gabriel, D. Ogbeifun, Chemosphere 44 (2001) 957.

64. K. Sopajaree. Proceedings of the 6th Intrnetional Conference on Environmental Science and Technology, Pythagorion, Samos,Greece, 30/8–2/9/1999.

65. J. Sarasa, M.P. Roche, M.P. Ormad, E. Gimeno, A. Puig, J.L. Ovelleiro. Water Res. 32 (1998) 2721–2727.

66. C. Hu, Y. Wang. Chemosphere 39 (1999)2107–2115.

67. C.Galindo, P.Jacques,A.Kalt,J. Chem.Technol.Biotechnol. 130 (2000)35–47.

68. F. Zhang, J. Zhao, T. Shen, H. Hidaka, E. Pelizzetti, N. Serpone. Appl. Catal. B:Environ. 15 (1998) 147–156.

69. S. Espulgas, J. Gimenez, S. Contreras, E. Pascual, M. Rogriguez. Water Res. 36 (2002) 1034–1042.

60. Chantal Guillard, Hinda Lachheb, Ammar Houas, Mohamed Kisbi, Elimame Elaloui and Jean Marie Herrmann, J Photochem Photobio A: Chemistry, 158 (2003) 27.

70. Jincai Zhao, Kaiqun Wu, Taixing Wu, Hisao Hidaka and Nick Serpone, J. Chem. Soc, Faraday Trans, 94 (5) (1998) 673.

71. Wenjie Wang, Mingyuan Gu and Yanping Jin, Mat. Lett, 57 (2003) 3276.

72. Lili Zhao, Yun Yu, Lixin Song, Xingfang Hu, Andre Larbot, Applied Surface Science 239 (2005) 285.

73. Kazuhiro Doushita, Tetsuro Kawahara, J. of Sol-Gel Science and Technology 22 (2001) 91.

74. Qiaorong Sheng, Shuai Yuan, Jinlong Zhang , Feng Chen, Microporous and Mesoporous Materials 87 (2005) 177.

75. Yibing Xie, Chunwei Yuan, Xiangzhong Li, Colloids and Surfaces A: Physicochem. Eng. Aspects 252 (2005)

76. I.K. Konstantinou, T.A. Albanis.A review, Appl. Catal. 49 (2004) 1–14.

77. A. Kungolos, P. Samaras, A.M. Kipopoulou, A. Zoumboulis, G.P. Sakellaropoulos.Water Sci. Technol. 40 (1) (1999) 357.

78. K. Chiang, T.M. Lim, L. Tsen, C.C. Lee. Appl.Catal. A: Gen. 261 (2004) 225–237.

79. A.R. Fernandez-Alba, D. Hernando, A. Aguera, J. Caceres, 109(2000)361.

80. K.G.KWarrier,W.Wunderlich,MaterialsChem&Phy,90(2005)123-127.

81. A. Houas et al. Applied Catalysis B: Environmental 31 (2001)145.

83. R.A.Torres,W.Peringer,C.Pulgarin .Chemosphere.50(2003)97-104.

84. M.Gattrell,D.W.Kirk.Canadian J.Engg. 68 (1990)997-1003.

85. M.A.Behnajady,N.Modirshahla,R.Hamzavi.J.HazardousMater.B 133(2006) 226-232.

86. D.R. Rolison, Science 299 (2003) 1698

87. T.R. Pauly, Y. Liu, T.J. Pinnavaia, S.J.R. Billinge, T.P. Rieker, J. Am.Chem. Soc. 121 (1999) 8835.

88. J.C. Yu, X. Wang, X. Fu, Chem. Mater. 16 (2004) 1523.

89. A.Hagfieldt, ,M.Gratzel, Chem.Rev .95(1995) 49.

90. M. Kondo, W. Jardim. Water Res. 25(1991)823.

91. P. V. Kamat. Chemical Rev. 93(1993)267.

92. J.M. Coronado, A.J. Maira, A. Martinez-Arias, J.C. Conesa, J. Soria, J. Photochem. Photobiol. 150 (2002) 213.

93. A.J. Maira, J.M. Coronado, V. Augugliario, K.L. Yeung,J.C. Conesa, J. Soria, J.Catal. 202 (2001) 413.

94. J. Lin, J.C. Yu, D. Lo, S.K. Lam, J. Catal. 183 (1999) 368.

95. J. Lin, J.C. Yu, J. Photochem. Photobiol. A: Chem. 116 (1998) 63.

96. Jiangrong Xiaoa, Tianyou Penga,_, Ran Lia, Zhenghe Penga, Chunhua Yanb Journal of Solid State Chemistry 179 (2006) 1161.

97. C.P. Sibu, S. Rajesh Kumar, P. Mukundan, K.G.K. Warrier, Chem.Mater. 14 (2002) 2876.

98. I.A.-Ichou,M.Formenti,B.Pommier,S.J.Teichner,J.Catal.,91,(1985)293.

99. Chuencheng Chen,Xiangzhong Li,Wanhong Ma,Jincai Zhao,Hisao Hidaka Nick Serpone J. Phys. Chem. B 106 (2002) 318.

100. G. Colon, M. Maicu, M.C. Hidalgo, J.A. Navio Applied Catalysis B:Environmental 67 (2006) 41.

101. L.Zang,C.Liu,X.Ren,J.Chem.Soc.,Faraday.Trans91(1995)917.

102. K.Okamoto,Y.Yamamoto,H.Tanaka, M.Tanaka A.Itaya. Bull. Chem. Soc. Jpn.58(1985)2015.

103. T. Bak. et al. Int. J. Hydrogen Energy 27 (2002) 991.

104. Hinda Lachheb, Eric Puzenat, Ammar Houas, Mohamed Ksibi,Elimame Elaloui, Chantal Guillard, Jean-Marie Herrmann. Applied Catalysis B: Environmental 39(2002) 75–90.

105. I. Poulios, I. Aetopoulou. J. Chem. Technol. Biotechnol. 74 (1999) 349–357.

106. M.S.T. Goncalves, A.M.F. Oliveira-Campos, E.M.M.S. Pinto, P.M.S. Plasencia, M.J.M.S.Queiroz. Chemosphere 39 (1999) 781–786.

107. B. Neppolian, H.C. Choi, S. Sakthivel B.Arabindoo, V. Murugesan, Chemosphere (2002) 1173–1181.

108. L.-C. Chen, T.-C. Chou. J. Mol. Catal. 85 (1993)201–214.

109. I. Poulios, A. Avranas, E. Rekliti, A. Zouboulis. J. Chem. Technol. Biotechnol. 75(2000) 205–212.

110. Y. Ma, J.-N. Yao.J. Chem. Technol. Biotechnol. 116 (1998) 167–170.

111. F. Chen, Y. Xie, J. Zhao, G. Lu .Chemosphere 44 (2000) 1159–1168.

112. W.Z. Tang, H. An, UV/TiO2 .Chemosphere 31 (1995) 4157–4170.

113. V.A. Sakkas, I.M. Arabatzis, I.K.Konstantinou, A.D. Dimou, T.A. Albanis, P. Falaras App. Catal. B: Environ. 49 (2004) 195–205.

114. A.I. Kontos, I.M. Arabatzis, D.S. Tsoukleris, A.G. Kontos, M.C. Bernard, D.E.Petrakis, P. Falaras, Catal. Today 101 (2005) 275–281.

115. F. Sayılkan, M. Asilturk, P. Tatar, N. Kiraz, E. Arpac, H. Sayılkan. J. Hazardous Materials xxx (2006) xxx–xxx

116. C.Karunakaran,S.Senthilvelan,S.Karuthapandian J Photochem Photobio A: Chemistry, 172 (2005) 207-213.

117. I.K.Konstantinou,T.A.Albanis.Appl.Catal.B.49(2004)1-14.

118. N. Daneshvar, M. Rabbani, N. Modirshahla, M.A. Behnajady, J Photochem Photobio A 168(2004)39-45.

119. L.B. Reutergardh, M. Iangphasuk, Chemosphere 35 (1997) 585–596.

120. 1. Poulios, I. Tsachpinis.J. Chem. Technol.Biotechnol. 74 (1999) 349–357.

# Chapter 5

# Photocatalysis of Pt, Pd, Au loaded titania


## *Abstract*

$TiO_2$ photocatalysis has attracted considerable scientific and practical interest during the last three decades. One major current direction in this research area is the design and preparation of novel $TiO_2$-based photocatalysts possessing high photocatalytic activity to satisfy the requirements for practical applications. For the development of successful strategies to achieve this goal it is, however, of utmost importance to improve the mechanistic understanding of the basic principles of photocatalysis that was dealt in the previous chapters of this thesis. Even a review is given on the photocatalytic properties of metal-loaded $TiO_2$ in the introduction. This chapter discusses about AOP's, an outline of preparation procedure, modification of titania with noble metals ,and the catalysts application on different dyes.

## 5.1.0 Introduction

Semiconductor photocatalysis has found growing interest due to its widespread applications in many fields, especially in solar energy conversion and environmental remediation. Research interests based on $TiO_2$ material is ever increasing and it will be a material of central attraction in photocatalysis for varied challenging applications. In recent years, a new class of techniques devoted to pollutant remediation, broadly referred to as advanced oxidation processes (AOPs) [1,2] has emerged. One of the major applications of this technology is degradation of organic pollutants in water and air streams. The most studied compounds are oxidation of dyes, organic waste, phenol derivatives, etc. AOP methods are characterized by a common chemical action, which basically relies on the primary reactivity of $OH^{\cdot}$ radicals in driving oxidation processes, ultimately resulting in the mineralization of a variety of pollutants. Within AOPs, photocatalyst-based degradation methods represent a very interesting branch of research in continuous development. Since then, basic principles of semiconductor photocatalysis have been well documented in the literature [1-4].Band-gap photo-excitation of semiconductors generates [5-7] electron–hole pairs capable to attack the organic matter either directly or indirectly by means of highly reactive species deriving from their reaction with the solvent and/or additives. In the case of $TiO_2$, generally recognized as one of the most efficient, non-toxic, and inexpensive photocatalyst, most extensive studies have been carried out by using the oxide powder suspended in aqueous solution containing the target molecules [8,9]. More recently, $TiO_2$ based catalysts deposited on to suitable substrates have become an attractive alternative to circumvent the technological difficulty as well as the high costs related to the catalyst recovery. Unfortunately, the potential

of this approach has been limited by the inevitable reduction of the overall surface active area associated to catalyst immobilization, leading to significant loss of performances. In the present work, the photocatalytic degradation of several commercial textile dyes in aqueous solutions using Pt,Pd, Au/$TiO_2$ catalysts prepared by hydrothermal route had been examined. The main objectives of the study were

1. to estimate the percentage of the dye disappearance
2. to examine the influence of various parameters, such as the mass of the catalyst, the initial concentration of the dye, pH etc.,
3. to evaluate the degree of mineralization of the products.

**5.2.0 Hydrothermal synthesis**

The chemical and physical properties of titania photocatalysts depend also on the procedures and conditions of preparation. A few methods, such as hydrolysis (chemical precipitation) **[10]**, reverse micelles (microemulsion) **[11,12]**, sol–gel **[13,14]**, and liquid phase deposition **[15]**, have been used to prepare $TiO_2$ nanocrystalline photocatalyst. However, various mesoporous materials have been synthesized via conventional approaches using surfactants as templates based on a liquid crystal template mechanism **[16-18]**. These methods often require a long time and multiple-step procedures. Comparing with these methods, the hydrothermal method has been studied to be the most effective route, discussed in the previous chapters, with many advantages **[13,14]**:

1. Crystallization temperature for anatase phase is below200° C.
2. By tuning hydrothermal conditions (such as temperature, time, reactant concentration, additives, etc.), various crystalline products with different composition, structure and morphology could be

obtained.

3. Low energy consumption and environmentally friendly process.
4. The equipment and processing required are simpler, and the control of reaction conditions is easier, etc.

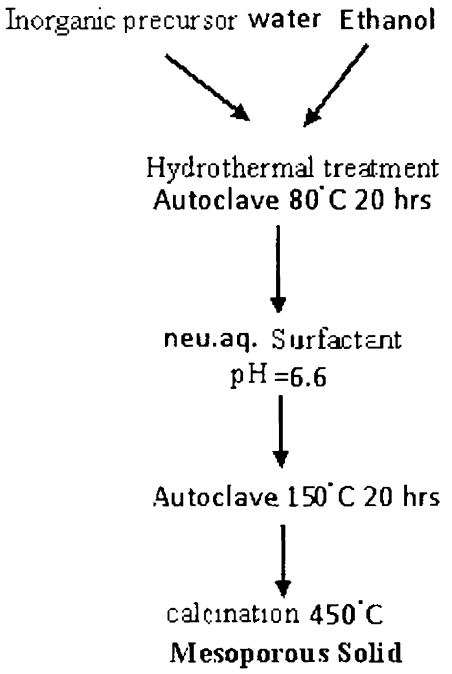


**Fig.5.1 Preparation of Meso-porous Solids.**

Hence this hydrothermal synthesis is an effective method for the preparation of semiconductor photocatalyst. In this work, highly photoactive mesoporous nanocrystalline $TiO_2$ powder photocatalyst was prepared by a two-step hydrothermal method in an autoclave at stages of 80°C and 150°C for 20h each at pH 6.6 slightly higher than the iso electric point of titania (IEP).The effects of initial pH values on the microstructures and photocatalytic activity of mesoporous titania powders were important. A

key characteristic of a catalyst is its high surface area, which allows the rate of reaction to increase, as the efficiency of a photocatalyst is proportional to its surface area. Despite the positive attributes of $TiO_2$ as an ideal photocatalyst, there are some drawbacks associated with its use;

1. charge carrier recombination occurs within nanoseconds, and
2. the band edge absorption's threshold of $TiO_2$ is < 400nm[19].

### 5.3.0 Photocatalysis on $TiO_2$ Surfaces

To circumvent these two limitations, a number of strategies have been proposed to improve the light absorption features and lengthen the carrier lifetime characteristics of $TiO_2$.To improve the photoefficiency of $TiO_2$ photocatalysis, the $e^-$-$h^+$ recombination rate must be reduced. In addition, $TiO_2$ is a solid-state material, thus its photocatalytic activity is unavoidably influenced by many factors such as particle size and distribution, surface area, crystal and surface structure etc. Hence, the strategy to design and prepare $TiO_2$-based photocatalysts with high photoefficiency has become a major topic leading to intensive research in this field.

### 5.3.1 Noble metals modified $TiO_2$

In photocatalysis, the addition of noble metals to a semiconductor can change the photocatalytic process by changing the semiconductor surface properties. It has been shown that the photocatalytic electron transfer processes at the semiconductor interface can be greatly enhanced by depositing a noble metal on the semiconductor particle[20-24]. Also it can enhance the yield of a particular product or the rate of the photocatalytic reaction. The enhancement in reactivity was first observed for the photoconversion of $H_2O$ to $H_2$ and $O_2$ using the $Pt/TiO_2$ system

[25].The addition of a metal to a semiconductor surface can also change the reaction products. The deposition of a noble metal on semiconductor nanoparticles is an essential factor for maximizing the efficiency of photocatalytic reactions[26,27]. Fundamental understanding of the photoinduced interactions between a semiconductor and metal as well as the interfacial charge-transfer process in nanoparticles is important to elucidate the role of noble metals in semiconductor assisted photocatalysis. The incorporation of metals like silver, platinum, palladium, gold etc., to the photocatalysts, result in a decrease of recombination rate and increase of the degradation efficiencies most probably because of the stabilization of the photogenerated charge carriers [28]. Similarly, doping of transition metal ions in titania can also significantly enhance the quantum efficiency, either by expanding the light absorption range or by improving the redox potential of the photogenerated radicals [4,92,29-31]. The textural properties of the photocatalysts prepared by this method observed that, the higher the metal content loaded, the larger the decrease in the BET surface area of the samples. Wold summarized the early work which used $TiO_2$ powders and thin films of treated metals such as silver and platinum [32]. A critical amount of metal was required for maximum photocatalysis and he concluded that the metal increased the rate of transfer of photoelectrons to the surface adsorbed oxygen. That is, there is an optimum loading of metal in $TiO_2$ for efficient photocatalysis.

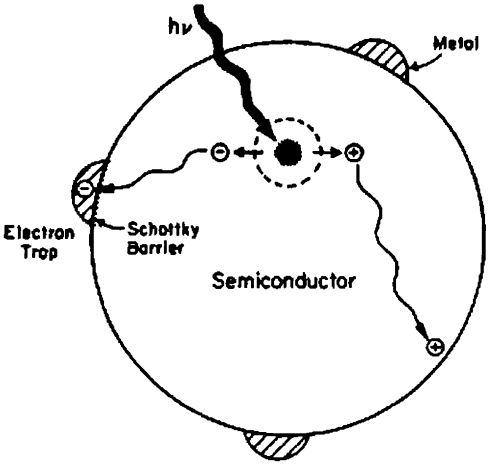


**Fig. 5.2 Metal-modified Semiconductor Photocatalyst Particle [89].**

In this context, this work has been focused on the improvement of $TiO_2$ photocatalyst nanoparticles by loading noble metals like Pt, Pd and Au respectively, which are typical approaches employed to inhibit the fast recombination of photoexcited electrons and holes. It is generally accepted that metal centers form shallow charge trapping sites within the $TiO_2$ matrix as well as on the particle surface through the replacement of Ti(IV) by metal [33]. Based on their favorable energy levels, metal centers may act either as electron or as hole traps leading to a temporarily more efficient separation of the photogenerated charge carriers. In particular, noble metal-modified semiconductor nanoparticles become of current importance for maximising the efficiency of photocatalytic reactions. Most studies of noble metal-modified $TiO_2$ photocatalysts have focused that during photocatalytic process, the illumination of a semiconductor photocatalyst with ultraviolet radiation activates the catalyst, establishing a redox environment in the aqueous solution[34]. The noble metal which acts as a sink for photoinduced charge carriers, promotes interfacial charge-transfer processes. A direct correlation between the work function of the metal and the photocatalytic activity is well known. When metals are deposited onto

the surface of $TiO_2$, a Schottky junction at the metal–$TiO_2$ interface develops resulting in the movement of electrons from the conduction band of $TiO_2$ to the metal, consequently trapping electrons at the metal surface [35]. Trapping these electrons inhibits electron/hole recombination, providing more efficient charge separation [36].

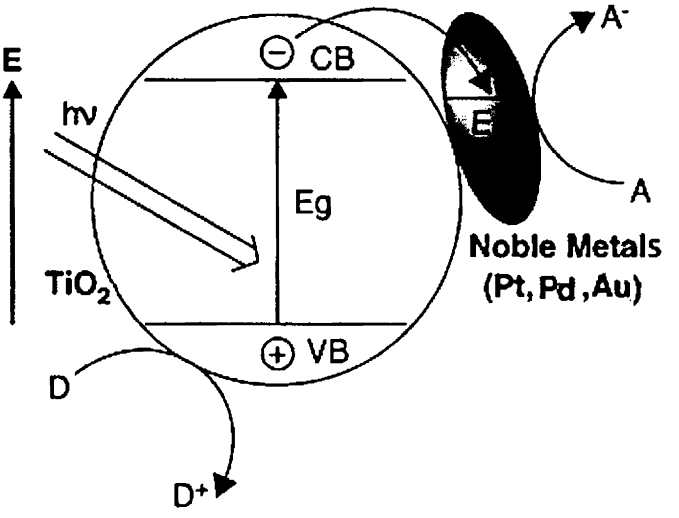


**Fig.5.3 Promotion effect by noble metals on $TiO_2$ photocatalysis[37].**

The $Pt/TiO_2$ system is the metal-semiconductor system most commonly studied. The interest in platinum-loaded titania ($Pt/TiO_2$), has rapidly increased due to their high activity in a multitude of important reactions [38-41]. Among them, photocatalytic $H_2$ generation from water splitting has recently been attracting rapidly growing interest due to clean, storable, and renewable energy development, aiming to replace exhausting fossil fuels by use of solar energy ever since Fujishima and Honda's report on the photoelectrochemical water splitting by $TiO_2$ electrode[42]. The photocatalytic activity and especially the stability of platinum strongly depends on both the state and structure of the support and the specific

interaction between platinum and support. The type of the support is of crucial importance to obtain highly dispersed platinum particles with good performances [43]. It has been suggested a good possibility to apply the mesoporous $TiO_2$ for the first time as a support for platinum towards the photocatalytic reaction of $H_2$ evolution. Pt,Pd and Au were of particular interest as it displays a high work potential, allowing it to trap a large number of electrons [44]. Reports reveal that metals belonging to VIII group, as for instance Pd and Pt,have been deposited onto the surface of the semiconductors to improve the separation of photo produced electron–hole pairs [45-50]. The presence of platinum as an electron sink has long been known to enhance the separation of photogenerated electron-hole pairs [51] and hence to improve the photocatalytic efficiency in general [52-54]. The noble metals such as Pt [55,56] and Au [57,58] deposited or doped on $TiO_2$ have the high Schottky barriers among the metals and thus act as electron traps, facilitating electron–hole separation and promotes the interfacial electron transfer process [59-62]. Pt deposited on $TiO_2$ [63-76] has been reported to improve [63,64, 67-74],be detrimental [65,77] or have negligible effects [66] on photocatalysis. Vorontsov and Dubovitskaya [72] reported up to a two times increase in the rate of ethanol photo oxidation at various Pt loadings and He et al. [74] reported a 4.2 times rate increase when photocatalytically degrading formic acid using photodeposited Pt (0.64 at.% loading) on a sol–gel coated $TiO_2$ thin film. Chen et al.observed a 2.5 times decrease in the chloroform degradation rate and a 12 times decrease in the degradation of trichloroethylene for 1 at% Pt on Degussa P25 $TiO_2$[76]. Coleman et al. found 2 at.% platinised Degussa P25 exhibited no effects when degrading selected endocrine disrupting chemicals although the low concentrations of organics required to mimic environmental levels meant the conditions were in the mass transfer limited

domain [66]. Lee and Choi found the effects of $TiO_2$ platinisation depend on the oxidation state of Pt and type of substrate being degraded [75]. They reported $Pt^0$ as the most active oxidation state of the Pt deposits for the organic substrates they considered where the oxidation states of the noble metals are clearly described in the XPS results. Metijevic and co-workers have shown that a variety of surface coatings can be produced on cores of very different compositions of Au/$TiO_2$Particles [77-79].They have shown that the formation of coatings on particles dispersed in liquids need not depend on specific interfacial reactions. Averitt et al have deposited a gold nanoshell onto silica nanoparticles by mixing amine-functionalized silica particles with a solution of gold nanoparticles for directly attaching it to the silica surface [80].

Metal/semiconductor nanocomposites have been synthesized by the reduction of [$AuCl_4$] on the surface of preformed $TiO_2$ nanoparticles. The concentration of the $TiO_2$ core directly influences the particle size and the stability of these composite nanoparticles[81]. Arana et al. studied gasphase photocatalytic oxidation of ethanol on Pd system and indicated that Pd(0) is more active[82].

The activity of palladium was studied by C.G.Wu et al and concluded that Pd-doped systems are efficient catalysts which are currently in progress[83]. When doped with the noble metal Pd, the surface morphology of the catalyst was observed to have a uniform distribution of particles of about 11.6 nm than with Pt and Au loadings which satisfies the requirement in photocatalysis. In this work, a considerably high photocatalytic performance of palladium supported on mesoporous $TiO_2$ via hydrothermal route was observed.

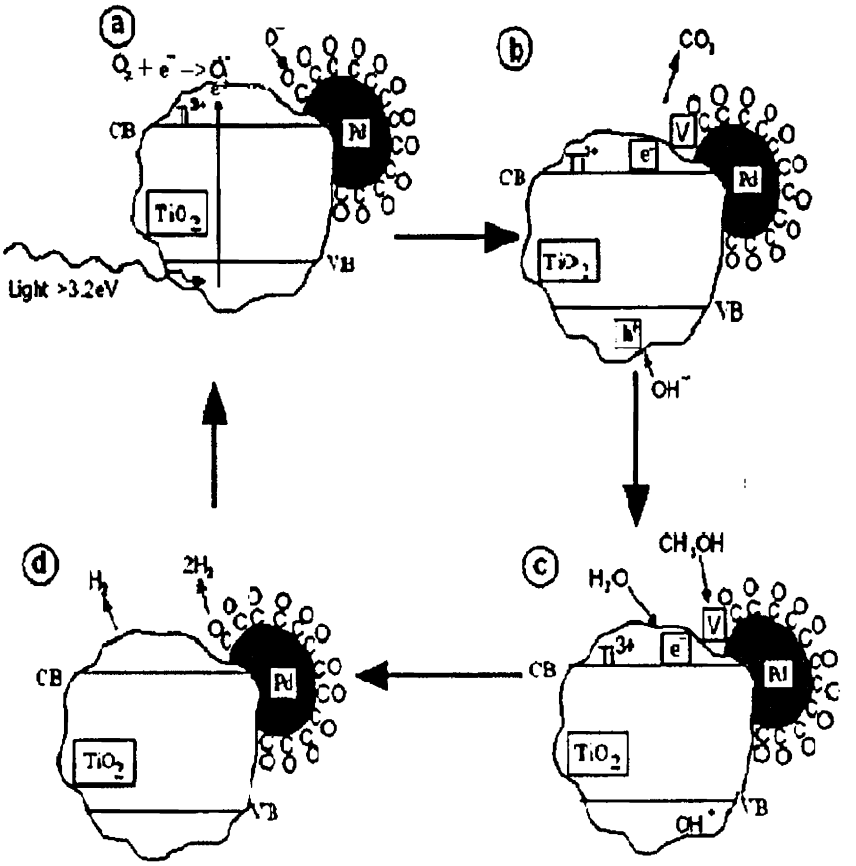


**Fig 5.4 Mechanism of Pd metal on$TiO_2$**

### 5.4.0 Dyes used for photocatalytic degradation studies

Heterogeneous photocatalysis appears as an emerging and interesting technology for the degradation of organic pollutants such as dyes as it can utilize sunlight as a source of energy, which is free and inexhaustible [84-91]. Dying processes represent an intense activity in textile industries, could treat efficiently and at low cost, wastewater contaminated by dyes since sunlight is very abundant. However, in the present work, it was attempted to determine the feasibility of the total degradation by a UV/$TiO_2$ treatment of some dyes in aqueous solution

despite the low percentage of UV light absorbable by $TiO_2$, it is possible to perform solar detoxification of wastewater contaminated by dyes as metal incorporation reduced the band-gap of $TiO_2$ to a considerable extent so as to perform enhanced activity in the visible region. Nevertheless, an increase in visible absorption, in principle, does not guarantee visible-light induced activity; since photocatalytic reactions proceed through redox reactions by photogenerated positive holes and photoexcited electrons. No activity may be observed if, for example, all of these species recombine. Various activity evaluation systems with different probe materials or indicators have been reported **[92]**. However, as dyes also absorb light, especially in the visible range, the influence of this photoabsorption by dyes should be excluded for evaluation of the real photocatalytic activity of photocatalysts. In this work UV illumination of 365nm was used.

The dyes used were having different chemical structures, such as hetero-polyaromatic Methylene Blue (MB-660nm), Malachite Green (MG-614nm),anthraquinonic dye Acid Blue 25(AB25),azo dyes like Acid Red1(AR1-532nm) and Acid Orange 7 (AO7-483nm) were investigated.

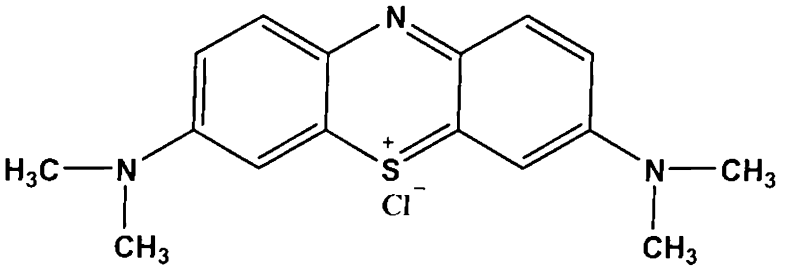


**Methylene Blue (MB-660nm)**

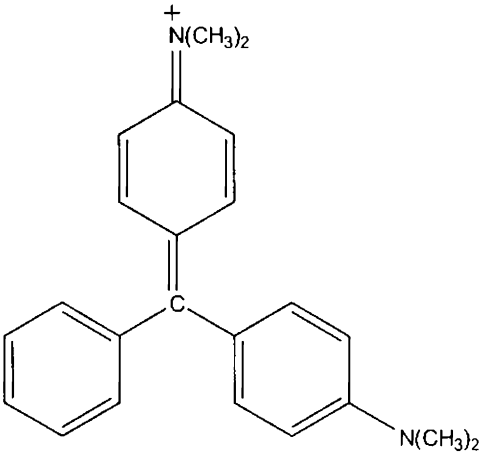


**Malachite Green (MG-614nm)**

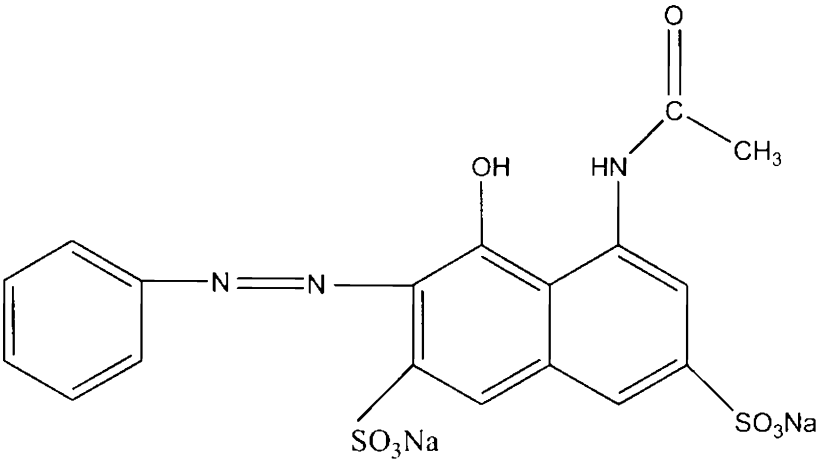


**Acid Red1(AR1-532nm)**

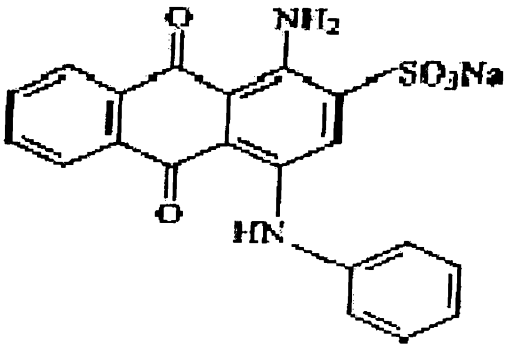


**Acid Blue25(AB25-600nm)**

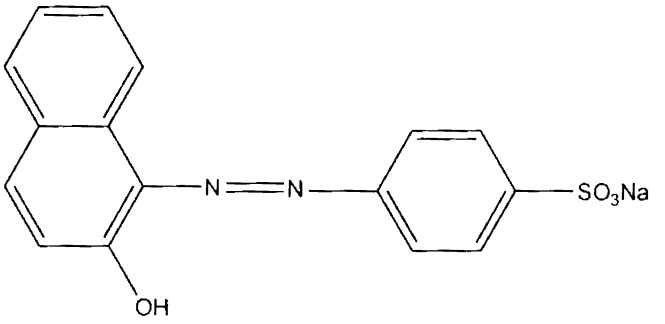


**Acid Orange 7 (AO7-483nm)**

**Fig 5.5 Name and Structure of the dyes ( λ max)**

### 5.5.0 Degradation Reactions of the Catalysts with the dyes

To optimize the kinetics of the degradation process, several parameters such as dye concentrations, catalyst amount, pH were studied. Prior to irradiation all the systems were stirred for half an hour in the dark to maintain an adsorption-desorption equilibrium between the catalyst and the dye.

### 5.5.1 Activity of Pt Catalysts w.r.t. time on Different dyes

**Optimized Reaction Conditions**

Dye conc. -20ml $10^{-4}$M

Catalyst amount - 0.1g

Lamp power - 48 Watts

| Dye | pH | Time(min) for 100%Degradation | | | |
|---|---|---|---|---|---|
| | | $TiO_2$ | 0.2%Pt | 0.6%Pt | 1.0%Pt |
| MB | 9.8 | 105 | 60 | 45 | 50 |
| MG | 9.4 | 150 | 90 | 75 | 80 |
| AR1 | 6.2 | 90 | 45 | 30 | 30 |
| AB25 | 6.4 | 60 | 30 | 15 | 25 |
| AO7 | 6.0 | 45 | 15 | 10 | 10 |

**Table 5.1 %Degradation of catalysts on different dyes**

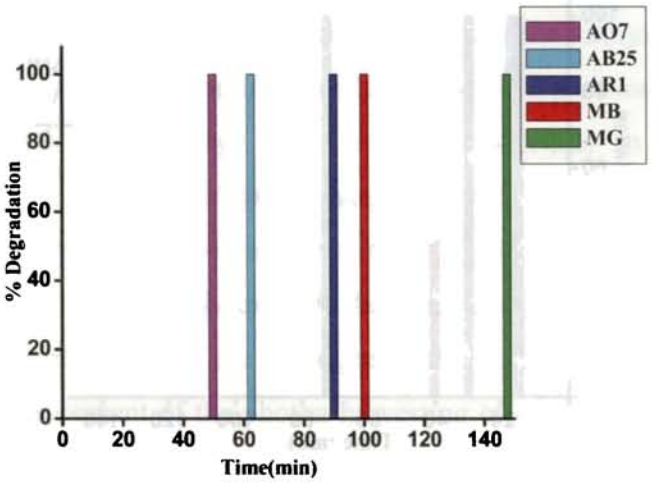


**Fig.5.6 · %Degradation of $TiO_2$ catalyst on different dyes**

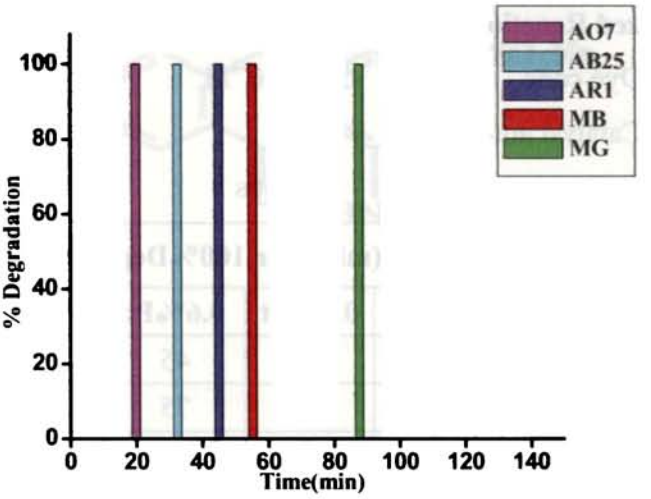


**Fig.5.7 %Degradation of 0.2%Pt/$TiO_2$ catalyst on different dyes**

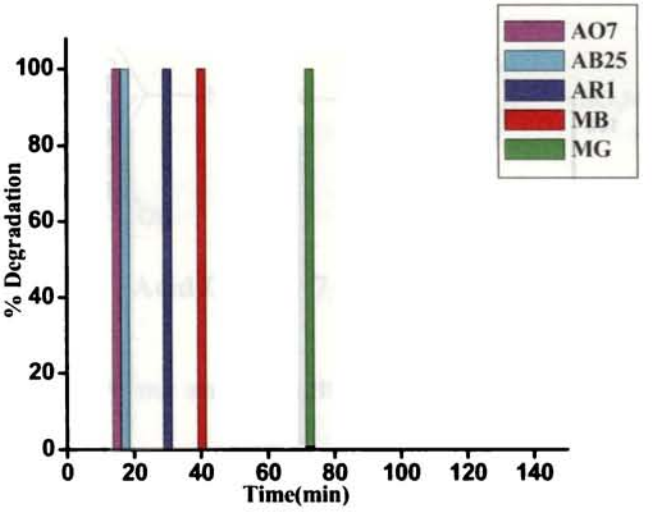


**Fig.5.8 %Degradation of 0.6%Pt/$TiO_2$ catalyst on different dyes**

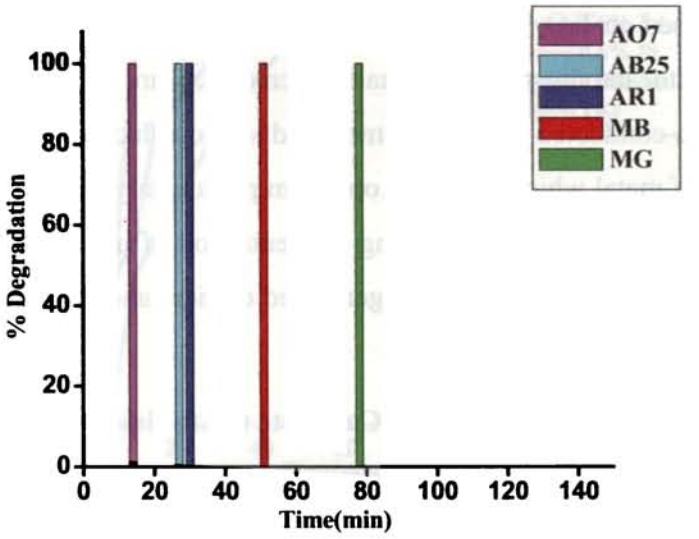


**Fig.5.9 %Degradation of 1.0%Pt/$TiO_2$ catalyst on different dyes**

Different loadings of Pt metal on $TiO_2$ (0.2,0.6,1.0)reveals that at higher metal loadings ,space charge region narrows (SCR),the cluster size will increase and the efficiency of charge seperation is reduced which results in the higher absorption and lower activities of the catalyst. Pleskov [93] reported that there is an optimal concentration of dopant ions to make the thickness of space charge layer substantially equal to the light penetration depth, because the space charge region becomes very narrow when the concentration of doping ions is too high, and the penetration depth of light into $TiO_2$ greatly exceeds the space charge layer, which will result in the recombination of the photogenerated carriers becoming easier. Finally, the enhancement of the photon harvesting efficiency derived from the red shift of the electronic absorption of noble metal-doped $TiO_2$ is not significant under these conditions, because the energy of most of the photons emitted by the UV source (maximum emission at 365 nm) is larger than the band gap interval of the studied materials. Further studies are necessary to clarify the effects of the surface area, doping, microstructure,

and crystalline composition of $TiO_2$ on the photocatalytic activity and the dye adsorbed on $TiO_2$ [94] .Above the optimum metal content the efficiency of the photocatalytic process actually decreases. Care must be taken when studies are conducted on a metal-modified semiconductor to work with the quantity of metal which gives the optimum photocatalytic efficiency[95].To sum up, there is an optimal doping concentration of metal in $TiO_2$ for the most efficient separation of photogenerated carriers and thus photocatalytic activity.

### 5.5.2 Activity of 0.6%Pt, Pd, Au Catalysts w.r.to time on Different dyes

| Dye | pH | Time(min) for 100%Degradation | | | |
|---|---|---|---|---|---|
| | | $TiO_2$ | 0.6%Pt | 0.6%Pd | 0.6%Au |
| MB | 9.8 | 105 | 45 | 30 | 60 |
| MG | 9.4 | 150 | 75 | 60 | 90 |
| AR1 | 6.2 | 90 | 30 | 20 | 45 |
| AB25 | 6.4 | 60 | 15 | 15 | 35 |
| AO7 | 6.0 | 45 | 10 | 10 | 30 |

**Table 5.2 %Degradation of $TiO_2$ and 0.6%Pt, Pd, Au/ $TiO_2$catalysts**

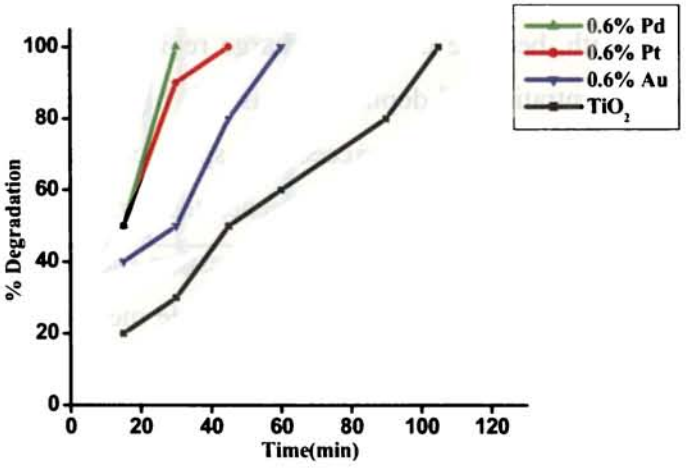


**Fig.5.10 %Degradation of 0.6%Pt, Pd, Au /$TiO_2$ catalysts on MB dye**

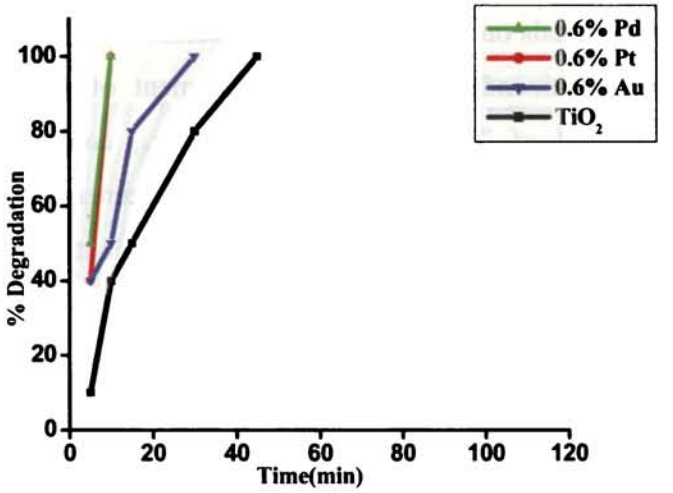


**Fig.5.11 %Degradation of 0.6%Pt, Pd, Au /$TiO_2$ catalysts on AO7dye**

The features in the figures 5.10 and 5.11 clearly explains that, the addition of Pd, Pt and Au, improved the catalytic performance of bare-$TiO_2$. A little more enhancement is observed in the case of 0.6%of Pd/$TiO_2$.The reactions on a noble metal surface can be related to the electron affinity, redox potential and work function of the metal atom **[96,97].** Hydrogen evolution increases linearly with increase in the redox potential of the noble metal. The more positive the redox potential of a metal, it facilitates faster reduction of $H^+$ ion. The work function of the metal is another factor that influences the electron release, if it is high, the reduction rate increases. ~~Electron affinities~~ work function and reduction potentials of metal ions/metal redox couples of noble metals like Pt ,Pd and Au are given below:

$Pt^{2+} + 2e^- \text{----}\rightarrow Pt$ $E^0$ (v) =1.118, work function of the metal Pt = 5.65eV

$Pd^{2+} + 2e^- \text{----}\rightarrow Pd$ $E^0$ (v) = 0.951, work function of the metal Pd =5.12eV

$Au^+ + e^- \text{----}\rightarrow Au$ $E^0$ (v) =1.760, work function of the metal Au =5.42eV

As the electron affinity of the metal Pt and Au are greater, dispersion of metals on $TiO_2$, results in the formation of a Schottky barrier at the metal/semiconductor interface, movement of electrons from the conduction band of $TiO_2$ to the metal occurs, consequently trapping electrons at the metal surface which leads to decrease in electron–hole recombination rate, as well as to a more efficient charge separation **[98-100].** But Sakata et al suggests that if a barrier is formed, the more suppressed is the electron transfer of photoinduced electrons from the semiconductor to the metal and limits the reaction **[101].** Also reports suggest that, recombination of photogenerated $H_2$ and $O_2$ to the production of $H_2O$ is efficiently catalysed by Pt, accounts for the loss of its activity. The cluster formation in the case of the $Au/TiO_2$ resulted in SPR diminishes the activity of the catalyst. Thus the increased activity of Pd accounts for the optimum redox potential, work function and electron affinity of the metal atom.

### 5.5.3 Activity of $TiO_2$and 0.6 wt.% $Pd/TiO_2$ catalyst w.r.to time on different dyes

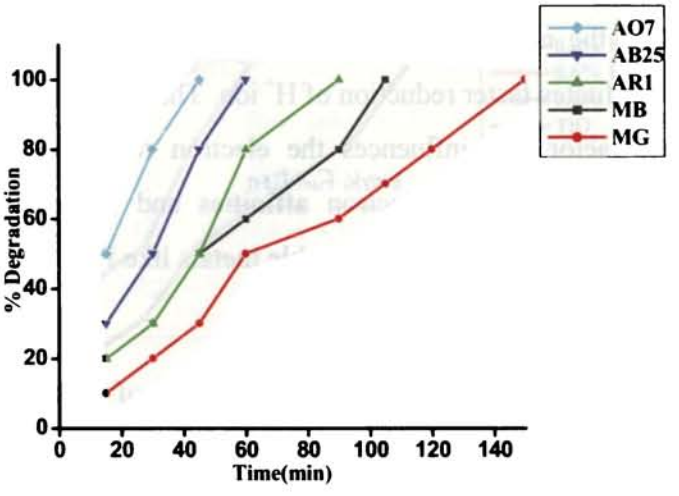


**Fig.5.12 %Degradation of $TiO_2$ catalyst on different dyes**

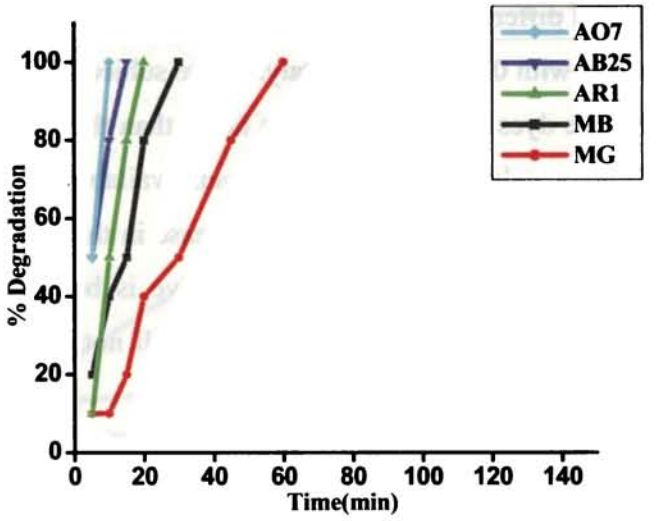


**Fig.5.13 %Degradation of 0.6%Pd/$TiO_2$ catalyst on different dyes**

The photocatalytic experiments demonstrate that Pd doping can effectively enhance the photocatalytic activities of the catalyst in decomposition of aqueous dyes under UV light irradiation. The experiment exhibit that 0.6 wt% Pd content is optimum to achieve the highest efficiency, shows marked increase in photocatalytic decoloration of different dyes within short period. The anionic dye AO7,which gives an absorbance at 483nm shows100% degradation within 10 minutes while the cationic dye methylene blue of absorbance at 660 nm degrades within a period of 30 minutes. Malachite green is a cationic dye for which the interaction with both the metal ions and the surface of the photocatalyst is considerably weaker**[102].** The existence of the dye in the dimeric state may be the reason for it to take about an hour to degrade completely.

### 5.5.4 Effect of dye Concentration on 0.6 wt.% Pd/$TiO_2$ Catalyst

20 ml of different concentrations of the dye like $10^{-3}$M, $10^{-4}$M and $10^{-5}$M solutions with 0.1gm of the catalyst were subjected to the study. It is observed that the dyes of $10^{-4}$M degrades faster than the other. It is because the rate of photocatalytic dye molecules even available for excitation and energy transfer is greater and hence an increase in the rate was observed. The decrease with increase in con. of the dye is because the dye will function as a filter for the incident light and will not permit the desired light intensity to reach the semiconductor particles.

**Reaction Conditions**

| | |
|---|---|
| Dye conc. | -20ml$10^{-3}$M,$10^{-4}$M,$10^{-5}$M |
| catalyst amount | -0.1g |
| Lamp power | -48 Watts |
| Irradiation time | -10 min |

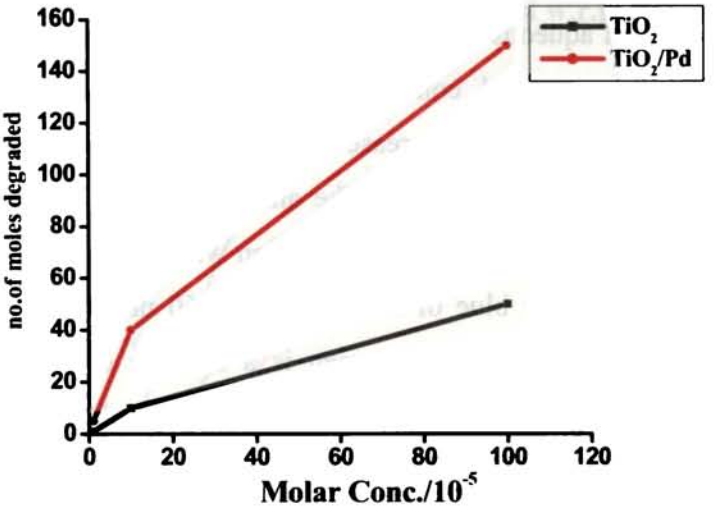


**Fig.5.14 No. of moles degraded w.r.t. concentration of the dye, MB.**

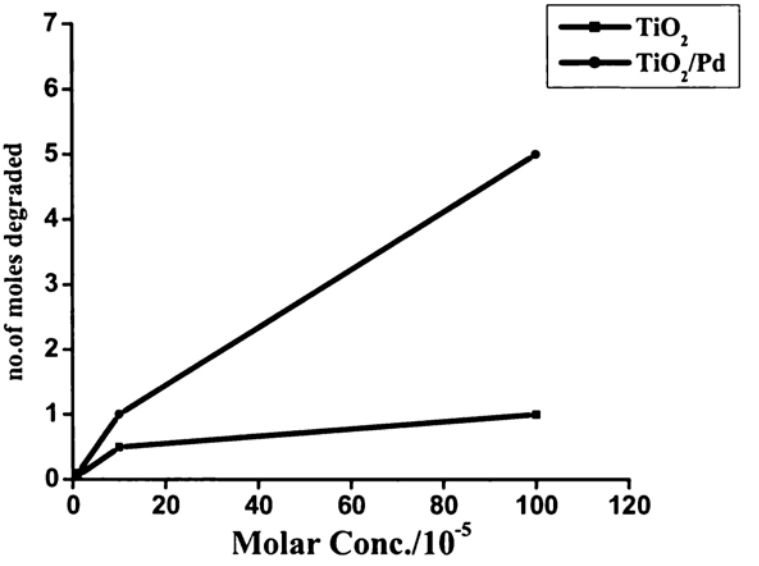


**Fig. 5.15 No. of moles degraded w.r.t. concentration of the dye, MG.**

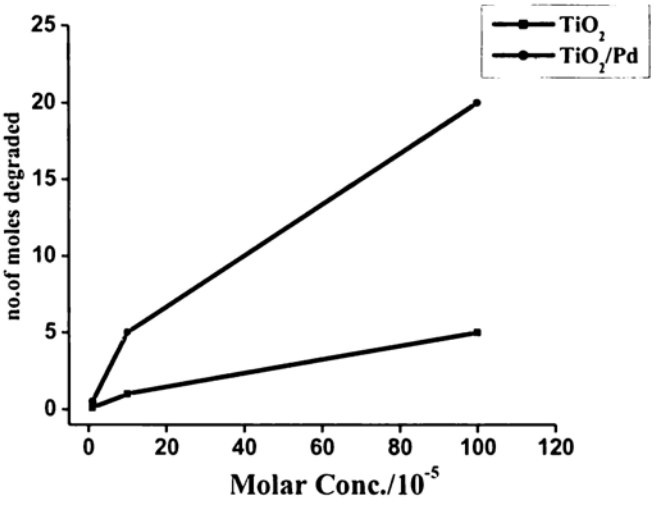


**Fig. 5.16 No. of moles degraded w.r.t. concentration of the dye, AR1.**

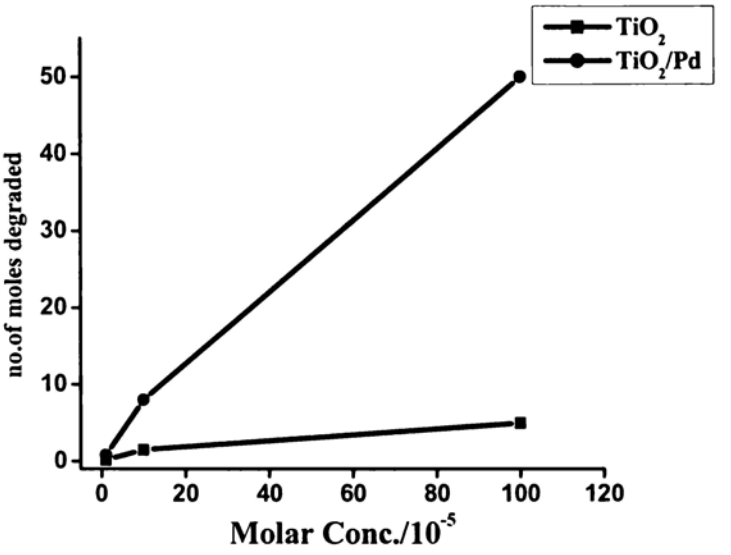


**Fig. 5.17 No. of moles degraded w.r.t. concentrationof the dye, AB25.**

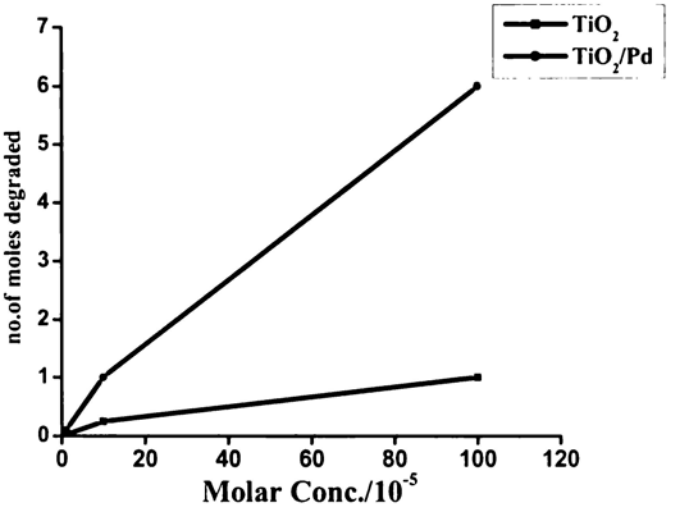


**Fig. 5.18 No. of moles degraded w.r.t. concentrationof the dye, AO7.**

### 5.5.5 Effect of Different Amounts of 0.6 wt.% $Pd/TiO_2$ Catalyst on dyes

**Reaction Conditions**

Dye conc. -20 ml $10^{-4}$M

Lamp power -48 Watts

Irradiation time -30 min

| Catalyst amount(gms) | % Degradation | | | | |
|---|---|---|---|---|---|
| | MB | MG | AR1 | AB25 | AO7 |
| 0.05 | 65 | 30 | 70 | 75 | 80 |
| 0.1 | 100 | 50 | 100 | 100 | 100 |
| 0.15 | 90 | 55 | 93 | 95 | 98 |
| 0.2 | 88 | 52 | 90 | 91 | 95 |

**Table 5.3 %Degradation of the dyes w.r.t amount of catalyst**

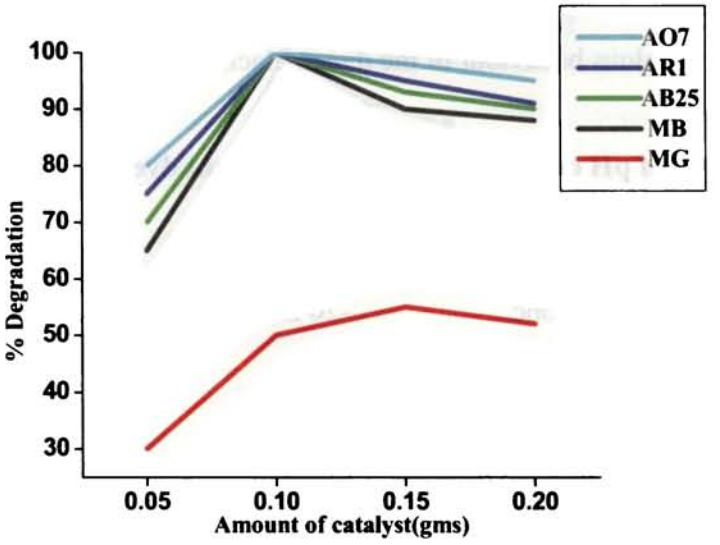


**Fig5.19 %Degradation of the dyes w.r.t amountof 0.6%$Pd/TiO_2$catalyst**

Percentage degradation increases proportionally to the concentration of the catalyst and levels off for values close to $5gl^{-1}$. Above this value, the degradation becomes independent of the concentration. Such a value which depends on the nature of the compounds and on the photoreactorgeometry is in full agreement with the other ones reported in literature for $TiO_2$ Degussa-P25, which range from 0.1 to 5.0 $gl^{-1}$ **[103-107].** This phenomenon may be explained both by a screening effect of excess particles which masks part of the photosensitive surface and by the scattering of the light which reduces the amount of photons which have fallen on the catalyst.

Malachite green is a cationic dye for which the interaction with both the metal ions and the surface of the photocatalyst is considerably weaker. Further research in adsorption of the substrate to semiconductor and electronic properties of metal and semiconductor will give the explanation for the anomalous behaviour of the dye, malachite green.

### 5.5.6 Effect of pH on %degradation of Different dyes

**Reaction Conditions**

| | |
|---|---|
| Dye conc. | -20 ml $10^{-4}$M |
| $TiO_2$/Pd Catalyst | - 0.1g |
| Lamp power | -48 Watts |
| Irradiation time | -30 min |

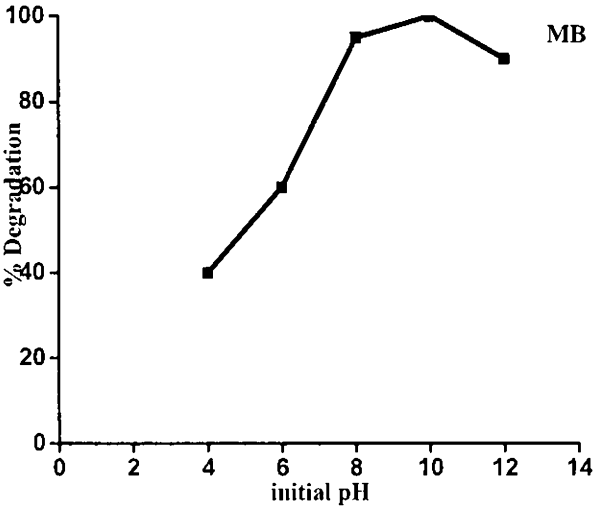


**Fig.5.20 %Degradation of 0.6%Pd/$TiO_2$ catalyst on MB dye**

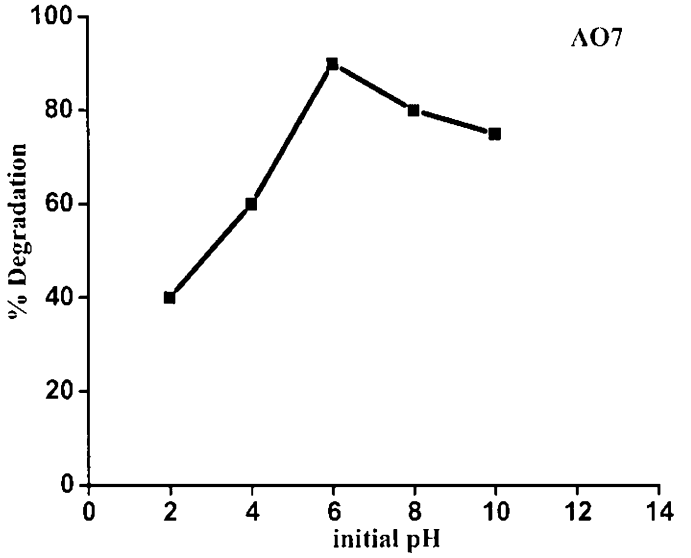


**Fig.5.21%Degradation of 0.6%Pd/$TiO_2$ catalyst on AO7dye**

pH variation w.r.t the cationic dye, methylene blue was discussed in chapter 4 in detail. It is shown that when the pH increases, a decrease of the amount of dye adsorbed on $TiO_2$ occurs w.r.t the anionic dye, AO7. Such a result can be better understood taking into account both the surface state of titania and the ionization state of the dye. The point of zero charge (pHpzc) of $TiO_2$ is known to be close to pH 6.8 for Degussa P-25 $TiO_2$**[108]**, pH chosen is near to pHpzc, which means that for pH's higher than 6.8, the surface becomes negatively charged according to the electrochemical equilibrium:

$$TiOH + OH^- \rightleftarrows H_2O + TiO^- \quad (1)$$

And at pH < pHpzc, the surface of titania is positively charged according to

$$TiOH + H^+ \rightleftarrows Ti\text{-}OH_2^+ \quad (2)$$

On the other hand, AO7 is an anionic dye bearing an anionic sulfonate function. In this context, it is conceivable that at high pH values, an electrostatic repulsion between $TiO_2$ and the dye occurs which leads to a decrease in the amount of dye adsorbed on $TiO_2$and hence a pH close to 6.0 was used. Whatever be the pH chosen, a decrease of the amount of dye adsorbed is observed when temperature increases. Moreover, for pH lesser than the pHpzc, similar values are obtained whereas, for pH higher than pHpzc, values become more important since molecules have to overcome electrostatic repulsion between $TiO_2$ and the dye to be adsorbed. These findings are in agreement with those concerning the photocatalytic degradation of anionic dyes, where the persistence of various aromatic compounds was reported after long-term irradiation **[109,110]**. The result confirms the favorable degradation of AO7 at acidic pH's as already observed for AB25, another anionic dye **[111]** and is mainly concerned by

the attack of the dye molecule by $OH^{\bullet}$ radicals formed by the following reactions:

$$TiO_2 + hv \rightarrow e^- + h^+ \quad (1)$$

$$(H_2O \rightarrow H^+ + OH^-) + h^+ \rightarrow H^+ + OH^{\bullet} \quad (2)$$

$$OH^{\bullet} + Dye \rightarrow H_2O + I_1. \rightarrow \cdots \quad (3)$$

where $I_1$. is the first radical intermediate.

### 5.5.7 Reusability of the Catalysts.

One of the main advantages of heterogeneous catalysts over homogeneous one's lies in its reusability **[112-114]**. As mentioned in the previous chapter, the catalysts can be used several times in photocatalysis.

**Reaction Conditions**

| | |
|---|---|
| Dye conc. | - AO7 20ml $10^{-4}$M |
| catalyst amount | -0.1g |
| Lamp power | -48 Watts |
| Irradiation time | -10 min |

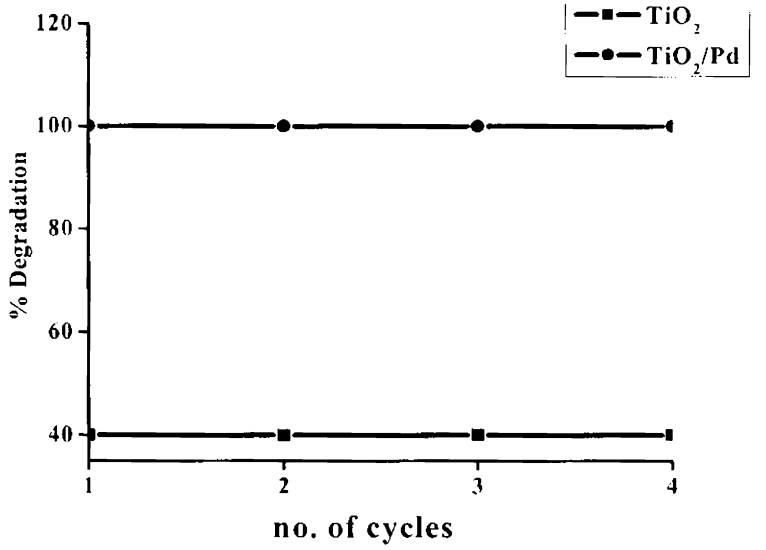


**Fig.5.22 Effect of deactivation of the catalysts**

## References


1. A. Fujishima, K. Hashimoto, T. Watanabe, $TiO_2$ Photocatalysis: Fundamentals and Applications, BKC, Tokyo,Japan, 1999.
2. D.F. Ollis, E. Pelizzetti, N. Serpone, Environ. Sci. Technol. 25(1991) 1522.
3. J.M. Herrmann, C. Guillard, P. Pichat, Catal. Today 17 (1993)7.
4. M.R. Hoffmann, S.T. Martin, W.Y. Choi, D.W. Bahnemann,Chem. Rev. 95 (1995) 69.
5. J.Y. Ying, C.P. Mehnert, M.S. Wong, Angew. Chem. Int. Ed.Engl. 38 (1999) 56.
6. W.Yu-de, M. Chun-lai, S. Xiao-dan, L. Heng-de, Appl. Catal.A 246 (2003)161.
7. S. Velu, M.P. Kapoor, S. Inagaki, K. Suzuki, Appl. Catal. A245 (2003)317.
8. D. Trong On, D. Desplantier-Giscard, C. Danumah,S. Kaliaguine, Appl.Catal. A 222 (2001) 299.
9. A. Sayari, P. Lui, Micropor. Mater. 12 (1997) 149.
10. C.C. Wang, J.Y. Ying, Chem. Mater. 11 (1999) 3113.
11. Y.T. Qian, Q.W. Chen, Z.Y. Chen, C.G. Fan, G.E. Zhou, J. Mater. Chem.3(1993) 203.
12. H.M. Cheng, J.M. Ma, Z.G. Zhao, L.M. Qi, Chem. Mater. 7 (1995) 663.
13. J.G. Yu, X.J. Zhao, Q.N. Zhao, Thin Solid Films 379 (2000) 7.
14. F.B. Li, X.Z. Li, Appl. Catal. A 228 (2002) 15.
15. J.G. Yu, H.G. Yu, B. Cheng, X.J. Zhao, J.C. Yu, W.K. Ho, J. Phys. Chem.B. 107 (2003) 13871.
16. N.Perkas,O.Palchik,I.Brukental,I.Nowik,Y.Gofer,Y.Koltin,A.Gedanken.J.Phys.Chem.107(2003)8772-8778.
17. J.G.Yu,J.C.Yu,W.K.Ho,M.K.P.Leung,B.Cheng,G.K.Zhang,X.J.Zhao.Applied Catalysis A:General 255(2003)309.
18. Z.Qingmin,L.Yan,H.Fuzhi,G.Zhennan.J.MaterialScienceLetters.20 (2001)1233.
19. B.Viswanathan, S.Sivasanker and A.V.Ramaswamy, Catalysis-Principles and applications, Narosa Publishing house,New Delhi.

20. N. R.de Tacconi, J.Carmona, K.Rajeshwar, J. Phys. Chem. B 101(1997)10151.

21. A. Heller, Pure Appl. Chem. 58(1986)1189.

22. Y. Nosaka, Y.Ishizuka, H.Miyama, Ber. Bunsen-Ges. Phys. Chem. 90(1986)1199.

23. Y.Chen,; Z.Wei, Y.Chen, H.Lin, Z.Hong, H.Liu, Y.Dong, C.Yu, W.Li, J. Mol. Catal21(1983)275.

24. Y.Nakato,H.Tsubomura,Isr. J. Chem. 22 (1982) 180.

25. Sato, S.; White, J. M. Chem. Phys. Lett. 72(1980)83.

26. A. J. Bard, J. Phys. Chem.86 (1982)172.

27. A. J. Bard, M. A. Fox, Acc. Chem. Res.28 (1995)141.

28. X. Fu, W.A. Zeltner, M. Anderson, Appl. Catal. B 6 (1995) 209–224.

29. J. Lin, J.C. Yu, D. Lo, S.K. Lam, J. Catal. 183 (1999) 368–372.

30. M. Anpo, Stud. Surf. Sci. Catal. 130 (2000) 157.

31. G. Soler-Illia, A. Louis, C. Sanchez, Chem. Mater. 14 (2002).

32. Wold A. Chem Mater 1993;5:280.

33. M.I. Litter, J.A. Navio, J. Photochem. Photobiol. A-Chem. 98 (1996) 171.

34. Y.Zhang, J.C.Crittenden, D.W.Hand, Chemistry and Industry, (1994) 714.

35. R. Memming, Semiconductor Electrochemistry, Wiley–VCH, Germany, (2001)24.

36. A.V. Vorontsov, V.P. Dubovitskaya, J. Catal. 221(2004)102.

37. Chuan-yiWang, Ronald Pagel, Jürgen K. Dohrmann, Detlef W. Bahnemann C. R. Chimie 9 (2006) 761.

38. G. Cocco, R. Campostrini, M.A. Cabras, G. Carturan, J. Mol.Catal. 94 (1994) 299.

39. J.C. Yang, Y.C. Kim, Y.G. Shul, C.H. Shin, T.K. Lee, Appl.Surf. Sci.121–122 (1997) 525.

40. J.L. Falconer, K.A. Magrini-Bair, J. Catal. 179 (1998) 171.

41. Y. Li, G. Lu, S. Li, Appl. Catal. A 214 (2001) 179.

42. A. Fujishima, K. Honda, Nature 238 (1972) 37.

43. D.G. Duff, T. Mallat, M. Schneider, A. Baiker, Appl. Catal. A133 (1995) 133.

44. K. Kalyanasundaram, in: M. Gratzel .Academic Press Inc., London (1983)217.

45. L. Palmisano, A. Sclafani, in: M. Schiavello (Ed.), Heterogeneous Photocatalysis, Wiley Series in Photoscience and Photoengineering, 3 (1997) 109.

46. R. Memming, in: M. Schiavello (Ed.), Photoelectrochemistry, Reidel, Dordrecht(1985)107.

47. P.C. Lee, D. Meisel, J. Catal. 70 (1981) 160.

48. C.M. Wang, A. Heller, H. Gerischer, J. Am. Chem. Soc. 114 (1992) 5230.

49. A. Sclafani, L. Palmisano, G. Marc`ı, A.M. Venezia, Solar Energy & Solar Cells 51 (1998) 203.

50. S. Ikeda, N. Sugiyama, B. Pal, G. Marc`ı, L. Palmisano, H. Noguchi, K. Uosaki, B. Ohtani, Phys. Chem. Chem. Phys. 3 (2001) 267.

51. Sangman Hwang, Myung Churl Lee, Wonyong Choi.Applied Catalysis B: Environmental 46 (2003) 49.

52. W. Mu, J.M. Herrmann, P. Pichat, Catal. Lett. 3 (1989) 73.

53. K. Chiang, R. Amal, T. Tran, Adv. Environ. Res. 6 (2002) 471.

54. Y. Liu, C. Liu, Q. Rong, Z. Zhang, Appl. Surf. Sci. 220 (2003) 7.

55. A. Sclafani, J.M. Herrmann, J. Photochem. Photobiol. A Chem.113(1998) 181.

56. A. Wold, Chem. Mater. 5 (1993) 280.

57. V. Subramanian, E. Wolf, P. Kamat, J. Phys. Chem. B 105 (2001) 11439.

58. C.Y. Wang, C.Y. Liu, X. Zheng, J. Chen, T. Shen, Colloid Surf. A 131(1998) 271.

59. J. Herrmann, J. Disdier, P. Pichat, J. Phys. Chem. 90 (1986) 6028.

60. A. Henglein, J. Phys. Chem. 83 (1979) 2209.

61. J.M. Herrmann, in: R.T.K. Baker, S.J. Tauster, J.A. Dumesic, ACS Symposium Series, 298(1986)200.

62. J. Disdier, J.M. Herrmann, P. Pichat, J. Chem. Soc. Faraday Trans. 1 77(1981) 2815.

63. K. Chiang, T.M. Lim, L. Tsen, C.C. Lee, Appl. Catal. A 261 (2003) 225.

64. M. Linder, J. Theurich,D.W. Bahnemann,Water Sci. Technol. 35 (4) (1997)79.

65. J.C. Crittenden, J. Liu, D.W. Hand, D.L. Perram,Water Res. 31 (3) (1997)429.

66. H.M. Coleman, K. Chiang, R. Amal, Chem. Eng. J. 113 (2005) 65.

67. W. Zhao, C. Chen, X. Li, J. Zhao, H. Hidaka, N. Serpone, J. Phys. Chem.B 106 (2002) 5022.

68. D. Hufschmidt, D. Bahnemann, J.J. Testa, C.A. Emilio, M.I. Litter, J. Photochem.Photobiol. A 148 (2002) 223.

69. U. Siemon, D. Bahnemann, J.J. Testa, D. Rodr´ıguez, M.I. Litter, N. Bruno,J. Photochem. Photobiol. A 148 (2002)47.

70. K. Kalyanasundaram, in: M. Gr¨atzel (Ed.), Energy Resources Through Photochemistry and Catalysis, Academic Press Inc., London, 1983,pp.217.

71. R. Memming, Semiconductor Electrochemistry, Wiley–VCH, Germany,(2001)24.

72. A.V. Vorontsov, V.P. Dubovitskaya, J. Catal. 221 (2004) 102.

73. W.Y. Teoh, L. M¨adler, D. Beydoun, S.E. Pratsinis, R. Amal, Chem. Eng.Sci. 60 (2005) 5852.

74. C. He, Y. Xiong, X. Zhu, X. Li, Appl. Catal. A 275 (2004) 55.

75. J. Lee, W. Choi, J. Phys. Chem. B 109 (2005) 7399.

76. J. Chen, D.F. Ollis, W.H. Rulkens, H. Bruning, Water Res. 33 (1999)3.

77. V.Hardikar, E.Matijevic.J. Colloid Interface Sci 221(2000)133.

78. M. Ocana, W. P. Hsu, E.Matijevic. Langmuir 7(1991)2911.

79. H.Giesche, E.Matijevic J. Mater. Res. 9(1994)436.

80. R. D.Averitt, S. L.Westcott, S. J.Oldenburg, T. R.Lee, N. J Halas, Langmuir 14(1998)5396.

81. Amy Dawson, Prashant V. Kamat J. Phys. Chem. B 105 (2001)960-966.

82. J. Arana, J.M. Dona-Rodrıguez, O. Gonzalez-Dıaz, E. Tello Rendon, J.A.errera Melian, G. Colon, J.A. Navıo, J. Perez Pena, J. Mol. Catal. A 215(2004) 153.

83. C.G.Wu,C.C.Chao,F.T.Kuo,Catal Today.97(2004) 103.

84. M. Schiavello (Ed.), NATO ASI Series C, Kluwer Academic Publishers, London 238(1987).

85. D.F. Ollis, H. Al-Ekabi (Eds.), Elsevier, Amsterdam(1993).

86. O. Legrini, E. Oliveros, A. Braun, Chem. Rev. 93 (1993) 671.

87. D. Bahnemann, J. Cunningham, M.A. Fox, E. Pelliziti, P. Pichat, N. Serpone, in: G.R. Zepp, D.G. Crosby (Eds.), Aquatic and Surface Photochemistry, Lewis, Boca Raton, FL,(1994).

88. D.M. Blake, NREL/TP-430-22197,National Renewable Energy Laboratory, Golden Co., (1997, 1999).

89. J.M. Herrmann, Catal. Today 53 (1999) 115.

90. J.M. Herrmann, in: F. Jansen, R.A. van Santen (Eds.), Catalysis Science Series, vol. 1, Imperial College Press,London.9(1999)171.

91. E. Pelizzetti, E. Minero, C. Pramauro, in: H.I. Lasa, G. Dogu, A. Ravella (Eds.), Kluwer Academic Publishers, The Netherlands, (1993)77.

92. Xiaoli Yan , Teruhisa Ohno, Kazumoto Nishijima, Ryu Abe, Bunsho Ohtani .Chemical Physics Letters 429(2006) 606–610.

93. Y.V. Pleskov, Sov. Electrochem. 17 (1981) 1.

94. Jiangrong Xiaoa, Tianyou Penga,_, Ran Lia, Zhenghe Penga, Chunhua Yanb J.Solid State Chemistry 179 (2006) 1161–1170.

95. Amy L. Linsebigler, Guangquan Lu, ,John T. Yates Jr. Chem Rev. 95(1995)735.

96. M.Milazzo ,S. Caroli, "Tables of standard eletrode potentials".A Wiley Interscience Publication,NY.(1978).

97. K.T.Ranjit,T.K.Varadarajan, B.Viswanathan, J. Photochem. Photobiol. A: Chem.96(1996)181.

98. A.L. Linsebigler, G. Lu, J.T. Yates Jr., Chem. Rev. 95 (1995) 735.

99. R. Memming, Semiconductor Electrochemistry, Wiley–VCH, Germany,(2001)24.

100. A.V. Vorontsov, V.P. Dubovitskaya, J. Catal. 221 (2004) 102.

101. T. Sakata, T.Kawai,and K.Hashimoto, Chem. Phys. Lett. 88 (1982) 50.

102. F. Sayılkan,M. Asilturk, P. Tatar, N. Kiraz, E. Arpac, H. Sayılkan J. Hazardous Materials xxx (2006) xxx–xxx

103. D. Chen, Q.A.K. Ray, Appl. Catal. B: Environ. 23 (1999) 143.

104. G. Al-Sayyed, J.C. D'Oliveira, P. Pichat, J. Photochem. Photobiol. A: Chem. 58 (1991) 99.

105. J.P. Percherancier, R. Chapelon, B. Pouyet, J. Photochem. Photobiol. A: Chem. 87 (1995) 261.

106. J. Gimenez, D. Curco, M.A. Queral, Catal. Today 54 (1999) 229.

107. S. Parra, J. Olivero, C. Pulgarin, Appl. Catal. B: Environ. 36 (2002) 75.

108. T.Ohno,K.Sarukawa, K. Tokieda, M.Matsumura, J.Catal. 203 (2001) 82.

109. (109) J. Theurich, D.W. Bahnemann, R. Vogel, F.E. Ehamed, G. Alhakimi, I. Rajab, Res. Chem. Intermed. 23 (1997) 247.

110. A.B. Prevot, C. Baiocchi, M.C. Brussino, E. Pramauro, P. Savarino, V. Augugliaro, G. Marci, L. Palmisano, Environ. Sci. Technol. 35 (2001) 971.

111. I. Bouzaida, C. Ferronato, J.M. Chovelon, M.E. Rammah, J.M. Herrmann J.Photochemistry and Photobiology A: Chemistry 168 (2004) 23.

112. G.M.Colonna,T.Caronna,B.Marcandalli,Dyes Pigments41(1999)211.

113. C.S.Poon,Q.Huang,P.C.Fung, Chemosphere 38 (1999) 1005.

114. M.Neamtu, I.Siminiceanu, A.Yediler, A.Kettrup, Dyes Pigments 53 (2002)93.

# Chapter 6

# Summary and Conclusions

### 6.1.0 Summary

Semiconductor photocatalysis is the reaction assisted by photons in the presence of a catalyst.The catalyst absorbs light and transfers energy and the result is the simultaneous oxidation and reduction reactions of the electron–hole pair. The mechanism of this photocatalysis is the electron migration from the semi-conductor valence band to the conduction band leaving a hole behind and the redox reactions due to electrons and holes. One of the major applications of this technology is the degradation of organic pollutants in water and air streams which is considered as one of the so-called advance oxidation processes(AOP). AOP methods are characterized by a common chemical action, which basically relies on the primary reactivity of $OH^{\cdot}$ radicals in driving oxidation processes, ultimately resulting in the mineralization of a variety of pollutants. This research work is on the degradation of dyes because they represent an increasing market share and a large fraction of the applied reactive dye is wasted due to dye hydrolysis in the alkaline dye bath, and finally, conventional wastewater treatment plants have low removal efficiency for reactive and other anionic soluble dyes[1].

Factors considered in photocatalysis are band gap and band positions, redox level of the substrate, surface area, solution pH etc. Titania is a suitable semiconductor as its band gap is 3.2 eV,inert to most chemicals and is resistant to photocorrosion.Titania exists as three different crystalline structures namely anatase, rutile and brookite. But it is well known that the anatase phase exhibits better photocatalytic activity than rutile and of a wider band gap(3.2 eV) than rutile(3.02eV)[2]. Despite the positive attributes of $TiO_2$ as an ideal photocatalyst, there are some drawbacks associated with its use;

1. Charge carrier recombination occurs within nanoseconds, and
2. The band edge absorption's threshold of $TiO_2$ is < 400nm[3].

To circumvent these two limitations, a number of strategies have been proposed to improve the light absorption features and lengthen the carrier lifetime characteristics of $TiO_2$. The addition of a metal to a semiconductor surface can alter the condition. The deposition of a noble metal on semiconductor nanoparticles is an essential factor for maximizing efficiency of the photocatalytic reactions[4,5].

This research work describes the photocatalysis of titania supported noble metals catalysts prepared by a selected route, in the degradation of dyes .The different steps involved in the work of photocatalysis were

A. Selection of a route by loading metals like Ag, Ce, Cu.
B. Incorporation of noble metals in the selected route.
C. Degradation studies of different dyes.

In this work, mesoporous titania is synthesized with anatase in its structure by sol-gel route, hydrothermal route and evaporation induced self assembly (EISA) method. A mesopore-directing surfactant template and

the precursor titanium tetra isopropoxide were used in the preparation of the catalysts. Catalysts of surface area 132 $m^2/g$ and a pore size of 11 nm is achieved by hydrothermal route higher than the reported value [6]. About 6wt%of metals like Ag, Ce and Cu were loaded into this mesoporous network by wet impregnation method [7] to enhance the photocatalytic activity. When a metal is loaded into the semiconductor, the improvement is that the loaded metal acts as a sink for electrons and suppresses the electron-hole recombination of the semiconductor[8] and the catalyst absorbance shifts to the visible region. The catalysts were characterized by low and wide angle XRD,FT-IR,BJH($N_2$-adsorption/desorption isotherms) , TG/DTA, SEM, TEM, TPD, UV-Vis.DRS.

Photocatalytic studies were carried out by the degradation of the dye, methylene blue. A route is selected by comparing catalysts prepared in the three different routes mentioned, for the incorporation of noble metals like platinum ,palladium and gold contents (0.2 – 1.0 wt%). It is supported on the synthesized mesoporous $TiO_2$ prepared from hydrothermal method .These noble metals catalysts were also characterized by low and wide angle XRD, FT-IR,BJH( $N_2$-adsorption/desorption isotherms), TG/DTA,SEM, TEM,UV-Vis .DRS. The degradation of the textile dyes like Acid Orange7(AO7), Acid red1 (AR1), Acid blue25(AB25), methylene blue and malachite green were carried out by the prepared noble metal incorporated titania catalysts. Reactions were carried out by changing the parameters like amount of the catalyst, concentration of the dye, pH of the solution, power of the lamp etc..Immediate decolourisation of the dyes also proposes a great prospect to the development of highly active photocatalysts. The utilization of these noble metals doped $TiO_2$ photocatalyst investigated towards the photocatalytic degradation of dyes

gives an eco-friendly technique as well as the broadest photocatalytic activity window.

### 6.2.0 Conclusions

#### Chapter1

As the introduction of this thesis, chapter1 deals with a brief account of the history of catalysis, photocatalysis, semiconductor photocatalysis, $TiO_2$, its applications and the literature survey. Also deals with the various structural aspects of titania on metal incorporation as well as different methods of preparation and mechanisms of photocatalysis. An outline of the research work that is followed can be understood from this chapter.

#### Chapter2

This chapter gives a detailed description of the catalyst preparation and pretreatment conditions, materials used, the techniques used to characterize the catalysts, the experimental set up and measures used for the catalytic activity study. It also discusses methods adopted for the present investigation in detail with flow-charts. From the methodology discussed, one is able to understand the instrumental techniques and chemistry behind each analysis that is carried out in the present research.

#### Chapter3

Surface characterization was done by BET surface area and analysis of pore characteristics by BJH, crystal phase nature by X-ray diffraction and chemical composition from energy dispersive X-ray analysis. Thermal stability was confirmed by TGA/DTA analysis. The oxidation state of the metal incorporated was confirmed by the XPS analysis. Surface morphology was collected on scanning electron microscope and also TEM

to know about the ordered mesoporous nature. Information regarding the band-gap of the catalysts was obtained from UV-vis DRS. Surface acidic properties of the catalysts were done by TPD of ammonia .The physico chemical characterization of metal incorporated titania systems by the three routes namely Sol-Gel(SG), Hydrothermal(HT) and EISA route were described. The two-step HT process produces a material with a fully anatase crystalline domain at a low temperature and further confirms that the catalysts prepared via HT route gives higher amount of surface hydroxyl groups than in other synthesized $TiO_2$ catalysts and expect this particular synthesis route described here could be widely adopted. Evidently, modification by metals not only increased the surface properties, but also induced a tremendous change in the band-gap of the catalysts than reported.The crystallite size of the mesoporous anatase catalysts ranges from 10-11 nm, which fairly covers the requirement for the photocatalytic activity [9] was found to exhibit a good correlation between the XRD values and that calculated from TEM. In conclusion, by tuning the hydrothermal temperature we can successfully prepare mesoporous titania and suggests that the material may be useful for the development of improved performances of photocatalytic applications.

**Chapter4**

Focuses on the selection of the best route by which $TiO_2$ catalysts were prepared, based on the application of the catalyst on the degradation of Methylene Blue (MB), a common organic dye, by varying all possible parameters. It is inferred that the photochemical degradation of methylene blue occurred effectively over the prepared catalysts. The percentage degradation of the dye for various systems could be correlated with the large surface area, crystallite size, mesoporous nature and the band gap

energy. Titania in a mesoporous state has high surface area in a continuous structure which makes the electron transfer easier, resulting in high activity. From the data it is clear that the catalysts prepared by hydrothermal route are more efficient and the silver catalysts showed enhanced photocatalytic activity. A detrimental effect of ceria catalysts due to its existence in the ionic state as the reduction of $Ce^{+4}$ to $Ce^{0}$ requires a much higher temperature than450 $^{0}$C **[10].** Cu does not adsorb hydrogen at room temperature to a significant extent **[11].** Deactivation might be due to the possible segregation/formation of CuO species at the surface, as it may not completely reduced to metallic copper which was easily confirmed by the XPS analysis. The present piece of research is also aimed at exploring the effect of the presence of different metals on the structure and photocatalytic activity of titania-based catalysts.

**Chapter5**

This chapter discusses about AOP's, an outline of preparation procedure, modification of titania with noble metals, and the catalysts application on different dyes. Among the noble metals incorporated, Pd catalysts showed higher photocatalytic activity than Pt and Au. Dye solns were successfully decolorized using the noble metal catalysts within avery short period of time than reported and the AO7 dye is easily degraded by the $TiO_2$-Pd catalysts. Thus the application of the $TiO_2$ photocatalytic method is proved to be efficient in mineralization and sterilization of waste water. An interpretation of reactivity order in noble metal incorporation is difficult, since it is probably the result of many factors: surface area, crystallinity, crystal size, band-gap energy. Moreover, the addition of metals could be either beneficial or detrimental depending on whether such metals decrease the electron/hole recombination rate or on the contrary

behave as electron/hole recombination centers [12]. Furthermore, photoactivity is dependent on the nature of the organic photoozidised [13]. The conjunction of all those features made that the addition of Pd, Pt and Au improved the catalytic performance of bare-$TiO_2$ (a positive effect which is generally accepted in the literature [14,15]), The specific surface areas of $TiO_2$ and Pt/$TiO_2$ were determined as 96(±1) m2/g and 101(±1) m2/g, respectively, indicating platinisation provided significant change in surface area [16]. Among the noble metal catalysts ,Pd incorporated catalyst shows high activity due to its optimum electron affinity and redox potential to give an ohmic contact than the schottkey barrier of $TiO_2$ -Pt and $TiO_2$ -Au catalysts[17]. Immediate decolourisation of AO7 dye of $\lambda$ max 483 nm than all other dyes is of great interest and reveals that the shift of band gap to the visible region by the incorporation of suitable metals is an innovative path in dye industry for pollution abatement.

### 6.3.0 Future Outlook

Photocatalysis is a mature field with extensive practical applications in the society. There is a large body of literature, including a number of reviews, describing $TiO_2$ catalysed photochemistry [18-20]. Noteworthy are the 1995 contribution of Hoffmann et al. which includes 441 references [21] and the excellent review paper by Hashimoto et al. [22] This study confirms that photocatalysis is suitable not only for decolorizing colored aqueous effluents but also fortunately degrading the dyes and its degradation intermediates to innocuous mineral products ($CO_2$, $H_2O$, $SO_4^{2-}$etc). With good photocatalytic activity under UV irradiation and the ability to be readily separated from the reaction system, this novel kind of catalyst exhibited the potential to be effective in the treatment of organic pollutants in aqueous systems.

Recently, many opportunities have been evolved. Deposition techniques have been considerably perfected and hence can be exploited in various other applications like thin film technology especially for various devices and sensory applications. The knowledge of the defect chemistry has been considerably improved and developed. Optical collectors, mirrors and all optical analysis capability have increased which can be exploited in many other future optical devices. The understanding of the electronic structure of materials has been advanced and this has helped to our background in materials chemistry. Many electrodes have been developed, which can be a useful for all other kinds of electrochemical devices.

Further aim in this field is to make improvements in the efficiency by identifying and designing new semiconductor materials with considerable conversion efficiency and stability. Constructing multilayer systems or using sensitizing dyes that can increase absorption of solar radiation, formulating multi-junction systems or coupled systems so that one can optimize and utilize the possible regions of solar radiation, developing nanosize systems that can efficiently dissociate water. Deeper understanding the roles of the different components in synthesis process is important for a rational design and reproducible construction of mesoporous materials. Also suggest that a better understanding of adsorption can lead to better models and more successful systems.

## References


1. P.C. Vandevivere, R. Bianchi, W. Verstraete, Journal of Chemical Technology and Biotechnology 72 (1998) 289–302.
2. M.I.Litter, Applied CatalysisB:Enviornmental 23 ( 1999) 89 .
3. B.Viswanathan, S.Sivasanker and A.V.Ramaswamy, Catalysis-Principles and applications, Narosa Publishing house,New Delhi.
4. A. J. Bard, J. Phys. Chem.86 (1982)172.
5. A. J. Bard, M. A. Fox, Acc. Chem. Res.28 (1995)141.
6. Kartini, P.Meredith, J.C.Diniz Da Costa ,G.Q.Lu,. Journal of Sol-Gel Science and Technology 31 (2004) 185-189.
7. W. Zou, R.D.Gonzalez,Catalysis Letters 12 (1992)73.
8. Zhang ,H.; Banfield,J.F. J.Phys.Chem.B 104 (2000)3481.
9. Y.Q.Wang, J.Y.Ying,. Chem.Mater. 11 (1999) 3113.
10. C.P. Sibu, S. Rajesh Kumar, P. Mukundan, K.G.K. Warrier, Chem.Mater.14 (2002)2876–2881.
11. I.A.-Ichou,M.Formenti,B.Pommierand S.J. Teichner, J. Catal., 91, (1985) 293.
12. E.Piera, M.I. Tejedor-Tejedor, M.E. Zorn, M.A. Anderson, Appl. Catal. B 46 (2003) 671.
13. V. Vamathevan, R. Amal, D. Beydoun, G. Low, S. McEvoy, Chem. Eng.J.98 (2004) 127.
14. A. Sclafani, M.N. Mozzanega, P. Pichat, J. Photochem. Photobiol. A 59 (1991) 181.
15. C. Hu, Y. Tang, Z. Jiang, Z. Hao, H. Tang, P.K.Wong, Appl. Catal. A 253
16. Frans Denny, Jason Scott, Ken Chiang, Wey Yang Teoh, RoseAmal.J. Mol. CatalA: Chemical 263 (2006) 93–102.
17. T. Sakata, T.Kawai,and K.Hashimoto, Chem. Phys. Lett. 88 (1982)
18. Wold A. Chem Mater 5(1993)280.
19. M.R. Hoffmann, S.T.Martin, W. Choi, DW .Bahnemann. Chem Rev.95(1995)69–96.
20. U .Diebold. Surf Sci Rep.48(2003)53–229.
21. A.L. Linsebigler, G. Lu, JT. Yates Jr. Chem Rev .95(1995)735–58.
22. K .Hashimoto, H. Irie, Fujishima A. Jpn J Appl Phys Part 1.44(2005)8269–85.

# Chapter 7

# Chemical Catalysis


## *Abstract*

Oxidation is a fundamental transformation in organic synthesis, and numerous chemical reactions are reported in the literature. It is a core technology for converting petroleum based materials to useful chemicals of a higher oxidation state. Catalytic oxidation offers the advantage that volatile organic compounds can be removed from aerial effluents to very low levels. In industrial chemistry, heterogeneous catalyst systems are preferred over homogeneous system due to easy recyclability and separability of the catalyst. Due to the increasing environmental concerns, oxidation using environmental friendly catalysts as well as oxidants such as molecular oxygen and hydrogen peroxide are more desirable these days. This chapter discusses about the catalytic oxidation techniques, mechanisms, volatile organic compounds (VOC), $TiO_2$ based catalysts etc.

## 7.1.0 Introduction

Catalytic oxidation is the largest class of organic reactions in the petrochemical industry. Since hydrocarbon derivatives containing oxygen and other heteroatom are intermediate to practically all important plastics, synthetic rubber, chemical fibers, products of household industry etc.[1]. Heterogeneous catalytic oxidation, both in the liquid and vapour phase, is an important technological area in the field of processes for the production of bulk organic chemicals, the production of fine chemicals and for pollution abatement [2]. These oxidation processes can be divided into two groups, namely selective oxidation and total oxidation reaction. In the selective oxidation reactions like ammoxidation and oxychlorination, the desired reaction product is not the most thermodynamically stable one and in the other type, the desired reaction products are thermodynamically the most stable. In general, the former type of reaction is for the production of bulk organic chemicals whereas the latter is for energy conservation and pollution abatement[3].There is a growing interest in the oxidation of saturated hydrocarbons especially under mild conditions due to the wide ranging utility of the ensuing functionalized compounds as raw materials and intermediates in industrial and pharmaceutical industry[4-6]. The oxidation products of cyclohexane, viz., cyclohexanol and cyclohexanone, are key intermediates in the production of caprolactam (a monomer in the manufacture of nylon-6) and adipic acid (a building block of polyamides viz. nylon-66 and polyurethane resins) [7-9]. While the oxidation of olefin into α,β-unsaturated ketone has been utilized in the synthesis and transformations of several natural products. The oxidation products of cyclohexene and ethylbenzene are widely employed as intermediates in organic, steroid, and resin synthesis. For example cyclohexene epoxide could replace cyclohexenone as an intermediate in the synthesis of adipic

acid, the precursor for Nylon 66. Cyclohexene epoxidation could be used as an important step of a greener synthesis of adipic acid [10]. The direct epoxidation of alkenes has been the main process for preparing the epoxides. Industrial olefin epoxidation has been carried out in the presence of alkaline earth metal chlorides promoted by chlorine containing substances. This method has several disadvantages, one of which is the use of chlorine containing reagents. Chiker et al. synthesized new mesoporous catalysts by grafting titanium on mesoporous silica (SBA15) by means of titanium tetrachloride in gas phase and tested for green epoxidation of cyclohexene [11]. The organic effluents containing phenolic compounds from pharmaceutical, fine chemical and petrochemical industries, on account of their poor biodegradability, form a major threat to the ecological balance. Mineral acids[12-14], simple metal ions [15,16] and metal complexes[17] are the traditional catalysts for this reaction, but these homogeneous catalysts are difficult to be separated and recovered from the reaction mixture, which prevents their practical utilization in phenol hydroxylation. Therefore, heterogeneous catalysis over various metal oxides and complexes, such as metal oxides or supported ones [18-20], metal complex oxides [21,22], zeolite encapsulated metal complexes[23] and hydrotalcite like compounds [24,25] have been of great interest to many researchers for a long time. The performance of the catalytic systems points to its potential in the degradation of phenolic wastes. The selective oxidation of phenol to industrially useful diphenols forms a convenient route to the efficient disposal of phenolic compounds. Hence, the development of catalytic methods involving clean oxidants for the selective oxidation of hydrocarbons is of great practical interest [26].

Nowadays, large scale industrial chemical processes, which generally involve several steps afflicted with the generation of by products

and waste are subject to continuously increasing environmental concerns and suffer from severe regulations. Commonly used oxidants are molecular oxygen, hydrogen peroxide and alkyl hydro peroxide. Molecular oxygen is obviously an ideal oxidant, but aerobic oxidation is often difficult to control and sometimes results in combustion and the reaction is performed with a low conversion to avoid over-oxidation. In the last decade, $N_2O$ has also attracted growing attention as a selective oxygen donor for oxidation reactions [27-30]. In addition, for environmental constraints, classical stoichiometric oxidants, such as dichromate or permanganate, should be replaced by new environment friendly catalytic processes using clean oxidants like molecular oxygen or hydrogen peroxide[31,32]. Metal-containing aluminophosphate molecular sieves and rare earth exchanged zeolite Y offers tremendous potential as catalysts in the oxidation reactions to transform hydrocarbons into valuable products [33, 34]. Corma et al. reported that properly coupling catalyst design and reaction conditions could give very high turnover numbers for Baeyer-Villiger oxidation using Sn-Beta/$H_2O_2$ and Al-Beta/$H_2O_2$ as catalysts in acetonitrile solvent [35]. Titanium containing catalysts and their modification is of great importance in the liquid phase oxidations of heterogeneous catalysis.$TiO_2$ containing xerogels are active catalysts for a variety of oxidation reactions with $H_2O_2$, including epoxidation of alkenes, oxidation of secondary alcohol and hydroxylation of phenol [36-39]. According to Guin et al. who have studied styrene oxidation, the oxygen vacancies present in the catalysts will facilitate the adsorption of hydrogen peroxide to form molecular oxygen for the oxidation reaction [40]. Benzyl alcohol oxidation has been studied using hydrogen peroxide as oxidizing agent. According to V.R. Choudhary et al.on hydrotalcite like materials, the formation of benzladehyde and benzoic acid occurs through the involvement of molecular oxygen [41].

Wada et al. have studied the Benzyl alcohol oxidation reaction over palladium oxide nanoparticles and reported the involvement of molecular oxygen for the oxidation process [42]. The molecular oxygen liberated by the adsorption of hydrogen peroxide over the catalyst surface may be utilized for the oxidation of benzyl alcohol to benzaldehyde [34].In short, eco-friendly method of conducting organic reactions with environmentally benign catalysts and oxidants were discussed in this chapter.

### 7.2.0 Mechanism

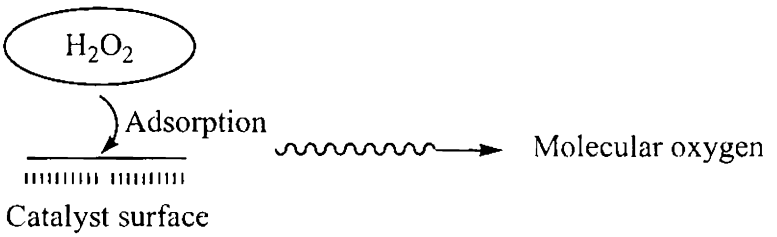


**Scheme 7.1 Action of $H_2O_2$ on Catalyst Surface**

Heterogeneous oxidations are commonly described by certain kinetic rate laws like Mars-van Krevelen mechanism, Eley-Rideal mechanism and the Langmuir-Hinshelwood mechanism[43,44].An important part of the Mars and van Krevelen mechanism is that the lattice oxygen is replenished by gas phase oxygen in a reoxidation process. This mechanism has come to be the most widely applied in heterogeneous oxidation catalysis. It is stated that contact oxidation is performed by a redox cycle of metal oxide catalysts and, as a result, the oxidation activity is dependent on the redox action, that is, a pair of reducibility and reoxidizability. The rate-determining step in this mechanism is the diffusion of oxygen in the catalyst bulk. The mechanism proposed was that the hydrocarbon extracts lattice oxygen from the surface layer of the catalyst, thereby generating a reduced catalyst.

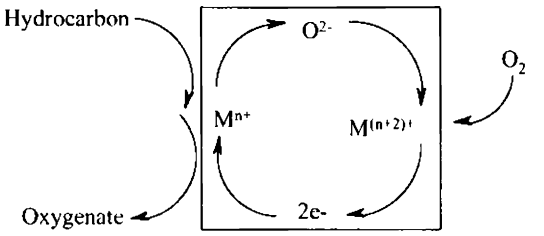


**Scheme 7.2 Mechanism of heterogeneous oxidation catalysis**

In general, the Mars-van Krevelen mechanism is assumed to be operative for selective oxidation reactions. First, the reactant to be oxidized is adsorbed on the surface of the catalyst resulting in the formation of an adsorbed complex. Subsequently a reaction takes place between the adsorbate and oxygen from the lattice of the catalyst, resulting in the formation of a partially oxidized product, which after desorption leaves an oxygen vacancy at the surface. Re-oxidation of this vacancy takes place via gas phase oxygen, as represented in scheme 7.2. The lattice oxygen is inserted in the hydrocarbon molecule while the reduced solid is reoxidized by gaseous oxygen. The insertion of lattice oxygen in the hydrocarbon and the incorporation of gaseous oxygen as lattice oxygen commonly take place at different cation sites. Then, the catalyst should allow electrons, lattice oxygen $O^{2-}$ and anion vacancies to move between those sites**[45]**. The mechanism can best be defined as a mechanism in which one of the products leaves the surface, containing one of the constituents of the lattice. With this mechanism oxidation, reduction, de-oxygenation and oxidative dehydrogenation can be described. If diffusion of lattice oxygen is sufficiently fast, the $O^{2-}$ surface species will migrate into the lattice. This process can continuously take place as long as reactants are present to reduce the catalyst and oxygen to re-oxidize the surface. The presence of metal ions of which the lower oxidation state is relatively stable is a

prerequisite for the development of this mechanism. The surface of a metal oxide catalyst is likely to contain an amount of metal ions of a lower oxidation state. Up to a certain concentration, these metal sites can be considered as defects in the metal oxide matrix. However, when the oxygen vacancy concentration becomes too high, a new solid phase can form. Formation of a new solid phase generally calls for a nucleation step, which usually proceeds too slowly to give rise to a marked catalytic activity. If the redox mechanism is to be operative, it is undesirable that the catalyst becomes crystalline. Catalysts exhibiting the Mars-van Krevelen mechanism therefore should be able to contain a certain amount of lattice defects without recrystallizing into a metal suboxide**[46]**.

### 7.3.0 Volatile Organic Compounds (VOC)

A great deal of the early work into semiconductor photocatalysis focused on the removal of organic pollutants from water. However, of probably greater interest in recent years, has been its use in the removal of organic pollutants in the gas phase. Since volatile organic compounds, (VOCs) are often responsible for malodorous air, it is common for the use of semiconductor photocatalysis in the removal of VOC to be also referred to as photodeodorisation **[47-51]**.

The volatile organic compounds are the polluting agents. Any compound based on carbon and hydrogen with the vapour pressure greater than2mm Hg at 25°c is called a volatile organic compound. It may contain oxygen, nitrogen and other elements. Examples are Hexane, Benzene, Toulene, Dichloro ethane, Methanol, Ethyl Acetate etc. Exceptions are CO, $CO_2$, $H_2CO_3$, $CH_4$, metal carbides and metal carbonates. Thus industrial wastes or exhausts, combustion of fuels, petro chemical complexes and storage and usage of organic solvents release voluminous polluting agents.

Textile finishing mills discharge waste water containing a great variety of organic contaminants in a wide range of concentration. The release of this colored waste waters poses a major problem for the industry as well as threat to the environment.[52-53]. Also common treatment processes, e.g. adsorption on activated carbon, floccculation and electrocoagulation[54] are not efficient methods because they appear in solid wastes ,thus creating another environmental problem requiring further treatments. Health effects caused due to this are skin cancer and eye irritation, central nervous system gets affected, loss of memory, immunological disorders, respiratory problems, and the damage of lung tissues. It can be eliminated by thermal oxidation with flame (natural gas or propane) or flameless heat exchanging bed, membrane separation by liquefying VOC, regenerative thermal oxidation (RTO) using adsorbent materials, catalytic oxidation etc.. The application of a suitable catalyst in reactions so as to minimize the pollution is an eco-friendly method.

### 7.4.0 Selective oxidation of hydrocarbons

The objective of the selective oxidation is to oxidize the organic molecule while keeping its skeleton. The catalysts used are solids, most often mixed oxides with elements with different oxidation states, which present redox properties. They can be continuously reduced by hydrocarbons and oxidized by the oxygen present in the reaction mixture. Processes involving the oxidation of hydrocarbons in the liquid phase, using air or oxygen, are of great importance to industrialized economics because of its role in converting petroleum hydrocarbon feedstocks such as alkanes, olefins, and aromatics into industrial organic chemicals, important in the polymer and petro-chemical industries. Because oxidation of hydrocarbons ultimately gives carbon dioxide and water, it is clear that, the

partial oxidations are of greatest interest to the industry, and the success of an industrial oxidation process depends on proper control of the reaction to yield the desired intermediates with reasonable selectivities [55]. The complex chemistry of hydrocarbon oxidations leads to a multiplicity of products even at fairly early stages in the conversion. In modern heterogeneous catalysis, in-situ characterization and catalytic design have not only added to our understanding of catalytic phenomena, but also have led to new solid catalysts capable of remarkably selective oxidation of hydrocarbons [56]. The selective catalytic oxidation of organic molecules continues to be a very important method for the preparation of primary and specialty chemicals in the chemical industry world wide [57].

An increasing attention is being given recently to phase transfer oxidation catalysts in the presence of tungsten and molybdenum compounds, which are efficient catalysts for oxidation with hydrogen peroxide solutions of various organic substrates, viz., olefins, alcohols and aromatic hydrocarbons [58]. Titania and metal modified titanium catalysts are highly promising catalysts in the liquid phase oxidations in organic chemistry. Titania-silica mixed oxides are active and selective epoxidation catalysts, offering an efficient alternative to conventional titania on silica and titanium substituted zeolites[59-70]. The unmodified as well as the methyl- and phenyl- groups modified titania-silica aerogels were active and selective in the epoxidation of cyclohexene with tert- butyl hydroperoxide [71]. Novel mesoporous TS-1 catalyst is shown to be active in epoxidation of oct-1-ene and significantly more active in epoxidation of cyclohexene than conventional TS-1[72]. The epoxidation of alkenes using titanium silicate (TS-1) as a solid catalyst and aqueous hydrogen peroxide as oxidant has been studied extensively.

The redox property of small metal particles differs from their bulk value and depends on the size and structure of the modified particle. The redox properties of ceria and copper and the high lability of its lattice oxygen are among the most important factors that contribute to the catalytic reactivity of $CeO_2$and CuO in oxidation reactions [73,74] .Generally, the oxidation rate is limited by the oxygen transfer from the liquid phase to the metal active sites, while $CeO_2$, able to enhance this oxygen transfer to efficiently catalyze oxidations[75]. The promotional oxidation activity of ceria-containing catalysts clearly assigned to role of ceria in creating $Ce^{3+}/Ce^{4+}$ redox couple[76-78] like $Cu^{1+}/Cu^{2+}$. The $Ce^{3+}/Ce^{4+}$ and $Cu^{1+}/Cu^{2+}$ redox couples present in catalysts is known to be responsible for the intrinsic property because it acts as an oxygen buffer by storing and releasing oxygen under controlled conditions[79-81]. Variable valency of the ions $Ce^{3+/4+}$ and $Cu^{1+/2+}$ usually lead to nonstoichiometric $MO_{2-x}$. This aspect and the defect structure on the catalysts were due to oxygen vacancies and metal interstitial to maintain electrical neutrality. Variable-valence cerium ions can favour the formation of oxygen active sites $O^-_{(sur)}$, which are stabilized near cation vacancies through the reaction shown in scheme 7.3 and this additional dioxygen activation pathway lead to an increase in the activity of the catalyst [82-84].

$$O_{2\,(gas)} + 2Ce^{3+} \rightleftharpoons O^{2-}_{2\,(ads)} + 2Ce^{4+}$$

$$\rightleftharpoons 2\,O^-_{(sur)} + 2Ce^{4+}$$

**Scheme 7.3 Equation of the redox couple**

The main objective of this research is to promote titania based catalysts like $CeO_2/TiO_2$ and $CuO/TiO_2$in liquid phase reactions. The structural evidence is that the stabilization of anatase phase of titania at this

temperature is effected by this redox couple. The experimental results show that cerium-doped titania samples stabilizes the anatase phase until 800°C, whereas copper-doped samples calcined at the same temp. upto 600°C. So, $CeO_2$ is a better stabilizer for anatase phase than CuO. But in this work all the reactions were carried out at a low temperature. According to De Farias et al, $CeO_2$ and CuO are better stabilizers for anatase phase than $SnO_2$[85]. A study about the stabilization of anatase phase at high temperature carried out in liquid phase reactions offers the introduction of more and more fresh reagents into the catalyst system without any work up. A catalyst's efficiency is found to be high when deactivation on continuous run is low. There is a decrease in conversion due to blocking of active sites where selectivity remains constant. The results indicate the efficiency and $CeO_2/TiO_2$ as the more efficient one in catalysis. The increased activity and decreased deactivation are clearly understood from the reusability pattern. The use of noble metal containing catalyst like platinum over alumina generates lesser build up. However, due to its weaker reactivity, longer reaction times and higher oxidation temperatures are required [86]. Liquid phase oxidation of Pt,Pd,Au were reported by D.I. Enache *et al* with less selectivity [87] .Hamoudi *et al* also investigated the catalytic oxidation of phenol in aqueous solution in presence of Pt and Ag promoted $MnO_2/CeO_2$[88]. Hocewar *et al,* investigating on the catalytic wet peroxide oxidation of copper containing catalysts observed that $Ce_{1-x}Cu_xO_{2-\delta}$ system was insoluble in hot acidic solutions[89]. The same system when prepared in the form of highly dispersed copper oxide phases on $CeO_2$ support by sol gel route was catalytically active under mild conditions. Jun Wang *et al* reported $Cu^{2+}$ exchanged zeolites as efficient catalysts for phenol hydroxylation with hydrogen peroxide as the oxidant [90].

### 7.5.0 Catalytic activity measurements

Titania, being a well known photocatalyst, the influence of it and the metal modified systems were applied for chemical activity studies also, in detail. Liquid phase reactions like epoxidation of cylcohexene and hydroxylation of phenol were carried out using $CeO_2/TiO_2$ and $CuO/TiO_2$ catalysts denoted in this work as $TiO_2$-Ce as $TiO_2$-Cu respectively . Also different wt% of metal incorporated titania catalysts like 3, 6, 9 wt% $CeO_2/TiO_2$ and $CuO/TiO_2$were subjected to the present study. Therefore, In order to test the catalytic activity of the prepared systems, the experimental conditions were optimized using 6wt. % loaded $CeO_2/TiO_2$ catalyst, denoted as $TiO_2$-Ce 6. Oxidation of aromatics to give various industrially important products can be successfully carried out in liquid phase over the prepared catalytic systems. The role of a catalyst in bringing about a chemical reaction is a stimulating one.

In the present case, epoxidation of cyclohexene and hydroxylation of phenol were carried out in the liquid phase. Both the reactions were carried out in liquid phase following a standard procedure. The reactants in the required molar ratio with the oxidant and a definite amount of the catalyst were taken in a 50ml round bottom flask fitted with a water condenser. The whole set up is placed in an oil bath, placed on the top of a magnetic stirrer. The temperature of the oil bath can be adjusted according to the requirement for a particular reaction and kept constant with the help of a dimmerstat. The product analysis was done using gas chromatograph *(Chemito)* equipped with Flame ionization detector (FID) and a capillary column SE-30 for the epoxidation reaction and an OV-17 column used for the phenol hydroxylation reaction. The catalytic activity was expressed as the percentage conversion and the selectivity for a product is expressed as the amount of the particular product divided by the total amount of products multiplied by 100.

## References


1. J.R. Kosak, T.A. Johnson, Catalysis of Organic Reactions, Marcel Dekker Inc, New York (1994).
2. P. Brandao, A. Valente, A. Ferreira, V.S. Amaral, J. Rocha, Microp.Mesop. Mater. 69 (2004) 209.
3. A. Sakthivel, P. Selvam. J. Catal. 211 (2002) 13438.
4. V. Kesavan, D. Dhar, Y. Koltypin, N. Perkas, O. Palchik, A. Gedanken, S. Chandrasekaran, Pure Appl. Chem. 73 1 (2001) 85.
5. U.R. Pillai, E.S. Demessie, New J. Chem. 27 (2003) 525.
6. M. Hayashi, K. Yamada, S. Nakayama, H. Hayashi, S. Yamazaki, Green Chem. 2 (2000) 257.
7. I. Belkhir, A. Germain, F. Fajula, E. Fache, J. Chem. Soc., Faraday Trans. 94 12 (1998) 1761.
8. C.M. Ho, T.C. Lau, New J. Chem. 24 (2000) 587.
9. U.R. Pillai, Endalkachew, Chem. Commun. 18 (2002) 2142.
10. Lu, Xiaolin Guo, WeilinWang, Xikui GeneralReview CA Section: 49 (Industrial Inorganic Chemicals) 18(2004) 35-38
11. K. Sato, M. Aoki, R. Noyori , Science, 281 (1998) 1646.
12. F.Bourdin,M .Costantini,M.Jouffret,G.Latignan,Ger.Patent. 2, 064, 497 (1971).
13. Skepalik. C, Ger. Patent., 2,138,735 (1973).
14. J. Varagnat, Ind. Eng. Chem. Prod. Res. Dev., 15 (1976) 212.
15. G.A.Hamilton, J.W.Hamfin, J.P.Friedman, J. Am.Chem.Soc., 88(22), (1966) 5269.
16. M.A.Brook, L.Gatle,I.R.Lindsay, J.Chem.Soc,PerkinTrans 2(1982) 687.
17. D.R.C.Hytbrechts, I. Vaesen, H.X.Li, P.A.Jacobs, Catal. Lett., 8(1),(1991), 237.
18. Ai. M, J.Catal., 54(2)(1978), 223
19. N. Al-Hayck., Water res, 19(1985)657.
20. S. Goldstein, G.Czapski, J.Robani., J.Phys.Chem.,98(26)(1994) 6586.

21. R.Yu, F.Xiao, D.Wang, J.Sun, Y.Liu, G.Pang, S.Feng, S.Qiu, R.Xu, C.Fang, Catal Today., 51(1)(1999),39.

22. J.Sun, X.Meng, Y.Shi, R.Wang, S.Feng, D.Jiang, R.Xu, F.Xiao, J.catal.,193(2)(2000) 199.

23. M.R.Maurya, S.J.J.Titinchi, S.Chand,I.M.Mishra, J.Mol. Catal.A. Chem., 180(2002) 201.

24. K.Zhu, C.Liu, X.Ye, Y.Wu, Appl. Catal.A,Gen.,168(2) (1998),365.

25. A.Dubey, V.Rives, S.Kannan , J.Mol.Catal.A,Chem., 181(2002), 151.

26. S.E. Dapurkar, A. Sakthivel, P. Selvam, New J. Chem. 27 (2003) 1184.

27. V.I. Avdeev, S.P. Ruzankin, G.M. Zhidomirov, Chem. Commun. (2003) 42.

28. E. Selli, A. Isernia, L. Forni, Phys. Chem. Chem. Phys. 2 (2000) 3301.

29. E.J.M. Hensen, Q. Zhu, R.A. van Santen, J. Catal. 233 (2005) 136.

30. J. Jia, K.S. Pillai, W.M.H. Sachtler, J. Catal. 221 (2004) 119.

31. F. Gao, R. Hua, Appl. Catal. A: Gen. 270 (2003) 223.

32. H.H. Monfared, Z. Amouei, J. Mol. Catal. 217 1-2 (2004) 161.

33. E.L. Pires, M. Wallau, U. Schuchardt, J. Mol. Catal. A: Chem. 144 1 (1999) 91.

34. J. Chisem, I.C. Chisem, J.S. Rafelt, D.J. Macquarrie, J.H. Clark, Chem. Commun.(1997) 2203.

35. A. Corma, V. Fornes, S. Iborra, M. Mifsud, M. Renz, J. Catal. 221 (2004) 67.

36. J. Zhang, Y. Tang, G. Li, C. Hu, Appl. Catal. A: Gen. 278 (2005) 251.

37. K. Nomiya, K. Yagishita, Y. Nemoto, T.A.K. Mataki, J. Mol. Catal. A: Chem.126 (1997) 43.

38. C.W. Lee, W.J. Lee, Y.K. Park, S.E. Park, Catal. Today 61 (2003) 137.

39. R.S. da Cruz, J.M. de Silva, U. Arnold, M.S. Sercheli, U. Schuchardt, J. Braz.Chem. Soc. 13 2 (2002) 170.

40. D.Guin, B.Barawati and S.V.Manorama; J. Mol. Catal. A. Chem. 242 (2005) 26.

41. V.R.Choudhari, P.A.Choudhari and V.S.Narkhede; Catal. Commun., 4(2003) 171.

42. K.Wada, K.Yano, T.Kondo and Take-aki Mitsudo; Catal. Today, 117 (1-3) (2006) 242.

43. B.K Hodnett, Heterogeneous Catalytic Oxidation: Fundamental and Technological Aspects of the selective and Total Oxidation of Organic Compounds, John Wiley, New York (2000).

44. J. Hagen, Industrial Catalysis: A Practical Approach, New York, Wiley-VCH, (1999).

45. S. Larrondo, B. Irigoyen, G. Baronetti, N. Amadeo, Appl. Catal. A: Gen. 250 (2003) 279.

46. K.V.R Chary, K.R. Reddy, T. Bhaskar, G.V. Sagar, Green Chem. 4 (2002) 206.

47. A. Mills, S. L. Hunte, J. Photochem. Photobiol. A: Chem. 108 (1997) 1.

48. Prashant V. Kamat, Dan Meisel ,C. R. Chimie. 6 (2003) 999–1007.

49. Martin. S. T., Herrmann. H., Choi. W., Hoffmann. M. R. Trans. FaradaySoc. 90 (1994) 3315-3323.

50. D.Hufschmidt , L.Liu ,V.Seizer,D.Behnemann,Water Sci Technol.49(2004)135.

51. J. Peral, X. Domenech, D. F. Ollis, J. Chem. Technol. Biotechnol. 70 (1997) 117.

52. G.M.Colonna,T.Caronna,B.Marcandalli,Dyes Pigments.41(1999)211-220.

53. C.S.Poon,Q.Huang,P.C.Fung,Chemosphere .38 (1999) 1005-1014.

54. N.Daneshvar,H.Ashassi-Sorkhabi,A.Tizpar,Sep.Purif.Technol.31( 2003)153-162.

55. A.K. Suresh, M.M. Sharma, T. Sridhar, Ind. Eng. Chem. Res. 39 (2000) 3958.

56. S. Mohebbi, D.M. Boghaei, A.H. Sarvestani, A. Salimi, Appl. Catal. A: Gen. 278 (2005) 263.

57. S.I. Murahashi, N. Komiya, Y. Hayashi, T. Kumano, Pure Appl. Chem. 73 2 (2001) 311.

58. M.N. Timofeeva, Z.P. Pai, A.G. Tolstikov, G.N. Kustova, N.V. Selivanova, P.V. Berdnikova, K.P. Brylyakov, A.B. Shangina and V.A. Utkin, Russian chemical Bulletin, Int. Edn, 52 (2003) 480.

59. S. Imamura, T. Nakai, H. Kanai and T. Ito, Catal. Lett, 28 (1994) 277.

60. R. Hutter, T. Mallat and A. Baiker, J. Catal, 153 (1995) 177.

61. S. Imamura, T. Nakai, H. Kanai and T. Ito, J. Chem. Soc – Faraday Trans,91 (1995) 1261.

62. Z. Liu, G.M. Crumbaugh and R.J. Davis, J. Catal, 159 (1996) 83.

63. D.T. On, M.P. Kapoor and S. Kaliaguine, Chem. Commun, 1161 (1996).

64. D.C.M. Dutoit, M. Schneider, R. Hutter and A. Baiker, J. Catal, 161 (1996) 651.

65. S. Klein, S. Thorimbert and W.F. Maier, J. Catal, 163 (1996) 476.

66. R.J. Davis and Z.F. Liu, Chem. Mater, 9 (1997) 2311.

67. M. Dusi, T. Mallat and A. Baiker, J. Catal, 173 (1998) 423.

68. C.A. Muller, A. Gisler, M. Schneider, T. Mallat and A. Baiker, Catal. Lett, 64 (2000) 9.

69. T. Mallat and A. Baiker, Appl. Catal. A 200 (2000) 3.

70. C. Beck, T. Mallat, T. Burgi and A. Baiker, J. Catal, 204 (2001) 428.

71. C.A. Muller, R. Deck, T.Mallat and A. Baiker, Topics Catal, 11 (2000)

72. Iver Schmdt, Anne Krogh, Katrine Wienberg, Anna Carlsson, Michael Brorson and Claus J. H. Jacobsen, Chem. Commun, (2000) 2157.

73. A. Piras, S. Colussi, A. Trovarelli, V. Sergo, J. Llorca, R. Psaro, L. Sordelli, J.Phys. Chem. B 109 (2005) 11110.

74. G. Colon, M. Maicu, M.C. Hidalgo, J.A. Navıo Applied Catalysis B: Environmental 67 (2006) 41–51.

75. B.Renard, J.Barbier Jr,D.Duprez, S.Durecu, Appl.Catal. B:Environ. 55 (2005)1.

76. M.M. Mohamed, S.M.A. Katib, Appl. Catal. A: Gen. 287 (2005) 236.

77. R. Niewa, Z. Hu, C. Grazioli, U. Robler, M. S Golden, M. Knupfer, J. Fink, H. Giefers, G. Wortmann, F.M.F. de Groot, F.J.D. Salvo, J. Alloys Comp. 346 (2002) 129.

78. F. Zhang, S.W. Chan, J.E. Spanier, E. Apak, Q. Jin, Appl. Phy. Lett. 80 1 7(2002) 127.

79. E.Abi-Aad,R.Bechara,J.Grimblot,A.Aboukais,Chem.Mater.5(1993) 793.

80. B.M. Reddy, A. Khan, Y. Yamada, T. Kobayashi, S. Loridant, J.C. Volta,J. Phys. Chem. B. 106 (2002) 10964.

81. J.Matta,D.Courcot,E.Abi-Aad,A.Aboukais,Chem.Mater.14(2002) 4118.

82. A.B.Lopez,K.Krishna,M.Makke,J.A.Moulijn,J.Catal.230 1(2005) 237.

83. A.G. Dedov, A.S. Loktev, V.A. Menshchikov, M.N. Kartasheva, K.V. Parkhomenko, Academician I.I. Moiseev, Doklady Chem. 380 4-6 (2001).

84. D.M. Lyons, K.M. Ryan, M.A. Morris, J. Mater. Chem. 12 (2002) 1207.

85. De Farias, F. Robson, Airoldi, Claudio,Journal of Non-Crystalline Solids.351(2005)84-88.

86. S.Hamoudi, F.Larachi, A.Sayari, J. Catal.., 177 (1998) 247.

87. S.Hocevar, U.O.Krasovec, B.Orel, A.S.Arico, H.Kim, Appl. Catal. B: Environ., 28 (2000) 113.

88. A.Alejandre, F.Medina, P.Salagre, A.Fabregat, J.E.Sueiras, Appl. Catal. B:Environ., 18(1998) 307.

89. D.I. Enache, J.K. Edwards, P. Landon, B. Solsona-Espriu, A.F. Carley,A.A.Herzing, M. Watanabe, C.J. Kiely, D.W. Knight, G.J. Hutchings,Science 311(2006) 362.

90. Jun Wang, Jung-Nam Park, HaCheol Jeong, Kwang-Sik Choi, Xian-Yong Wei, Suk-In Hong and Chul Wee Lee, Energy and fuels., 18(2004)470.

# Chapter 8

# Epoxidation of Cylcohexene


## *Abstract*

Epoxides are important intermediates in organic synthesis of fine chemicals and pharmaceuticals. Therefore the synthesis of an epoxide by an easier method and a low cost route is of great interest to researchers working in this field. Titanium containing catalysts showed an increased activity and epoxide selectivity. The $Ce^{3+}/Ce^{4+}$ and $Cu^{1+}/Cu^{2+}$redox couple present in $TiO_2$-containing catalysts is known to be responsible for the intrinsic property because it acts as an oxygen buffer by storing and releasing oxygen under controlled conditions. The present chapter illustrates an exhaustive investigation on the liquid phase epoxidation of cyclohexene over the prepared catalytic systems. The influence of various reaction parameters like time, temperature, mole ratio of the reactant:oxidant, amount of the catalyst and nature of the solvent were investigated thoroughly.

## 8.1.0 Introduction

In recent years, several heterogeneous and homogeneous catalysts have been shown to be effective in the selective oxidation of olefins[1-5]. Heterogenization of alkene epoxidation catalysts was done recently to produce an appropriate material, which would allow the obtention of epoxides with high selectivity under industrial conditions[6]. Framework Ti- substituted and Ti- grafted MCM-41 mesoporous materials have been tested as catalysts for cyclohexene oxidation[7]. The mesoporous structure of the catalyst plays an important role in the oxidation of cyclohexene, especially when bulky TBHP was used as the oxidant. The mesoporous materials with different compositions, new pore systems, and novel properties have attracted considerable attention because of their remarkably large surface areas and narrow pore size distributions, which make them ideal candidates for catalysis [8]. Recently, much attention has been directed to the synthesis of nanostructured mesoporous oxides using surfactant templating method. It has been developed for the synthesis of materials with a narrow mesopore size distribution and controlled pore structure [9–11]. It is generally anticipated that the use of a high surface area mesoporous oxide support, rather than a commercial, low surface area support, for noble metals or transition metals has some beneficial effects on the catalytic performance [12]. The mesoporous support would give rise to well dispersed and stable metal particles on the surface upon thermal treatments and as a consequence would also show an improved catalytic efficiency.

Cyclohexene epoxide is of great technical importance as it is applied in the modification of epoxy resin properties and the synthesis of new polymers, copolymers and solvents. Another very interesting

application is the preparation of cyclohexanol and pyrocatechins **[13]**. Special attention was paid to cyclohexene because cyclohexene epoxide could replace cyclohexenone as an intermediate in the synthesis of adipic acid, the precursor for Nylon- 66**[14]**. The current production of adipic acid amounts to 2 million tones/year worldwide. It involves cyclohexenone oxidation by nitric acid and those reduction products include $N_2O$. Nitrous oxide is a strong green house gas, 200 times more potent than $CO_2$, and is partly involved in ozone layer damage. Also the epoxide materials are largely used for the synthesis of several perfume materials, epoxy resins, plasticizers, drugs, sweeteners, etc.

Titanium containing carbon-silica composite catalysts showed an increased activity and epoxide selectivity **[15]**. This may be attributed to the hydrophobic nature of the carbon surface and the local environment of active titanium centers on the silica support. Peng Wu *et al* studied the liquid phase alkene epoxidation activity over a novel titanosilicate with the MWW topology**[16]**. Interaction of titanosilicates (TS-1, TiMCM-41 and Pd $_{(n)}$-TS-1) with $H_2O_2$, urea- $H_2O_2$, and ($H_2$ + $O_2$) generates reactive Ti(IV)-superoxo and hydroperoxo/peroxo species**[17]**. The selectivity for epoxidation over these catalysts can be enhanced by controlling the type of Ti-oxo species. The organic modification of titania - silica catalysts by mono and bidendate functional groups enhanced the rate of epoxidation of cyclohexene remarkably**[18]**. A high and stable activity for ceria/tiania catalyts has been established for the water-gas shift reaction. The relationship between metal loading and catalytic activity was studied over a wide temperature range for the epoxidation. It was shown that tiania plays the role of an active support capable of producing oxygen. The high and

stable activity of ceria / titania catalysts could arise from the high and stable dispersion ceria present during the catalytic operation[19, 20]. .

Many efforts have been made to develop new catalysts to oxidize cyclohexene under mild conditions with high selectivity for the target products using different oxidizing agents. A noteworthy development in this regard was the results by K.U.Ingold et al[21].The concepts and informations given by Sheldon et al were of much importance in the field of catalytic oxidations[22-24]. The activity of these catalysts in liquid phase oxidation was generally been correlated with the redox properties of the catalysts. In this work, titania based catalysts like $CeO_2/TiO_2$ and $CuO/TiO_2$were used. Variable valency of the ions $Ce^{3+/4+}$ and $Cu^{1+/2+}$ usually lead to the efficient catalytic activity of the reaction. There are a variety of experimental systems capable of carrying out an oxygen transfer to an alkene double bond to produce an epoxide. The oxygen vacancies present in the catalysts will facilitate the adsorption of hydrogen peroxide to form molecular oxygen for the oxidation reaction [25].In a number of them, the oxygen added to the olefin comes from a peroxo group, either in the form of an organic peroxide or coordinated to a transition metal. The use of cleaner oxidants than usual hazardous and costly organic peroxides for epoxidation allows the development of greener reaction. Hydrogen peroxide ($H_2O_2$) and tert-butyl hydroperoxide (TBHP) are more suitable from environmental point of view of green chemistry because their reduction products, water or alcohol can be easily recycled [26]. The profitability of epoxidation with hydroperoxides depends on the possible utilization of co-products, namely tert-butyl alcohol in the case of TBHP [27].

The general reaction pathway is represented in scheme 8.1. The nature of the products demonstrates that cyclohexene can suffer either epoxidation yielding epoxy cyclohexane (cyclohexene epoxide) and glycol (cyclohexane diol) or an allylic attack forming cyclohex-2-ene-1-ol (cyclohexenol) and cyclohex-2-ene-1-one (cyclohexenone). All the catalytic systems showed considerable activity towards the reaction with high selectivity towards cyclohexene epoxide.

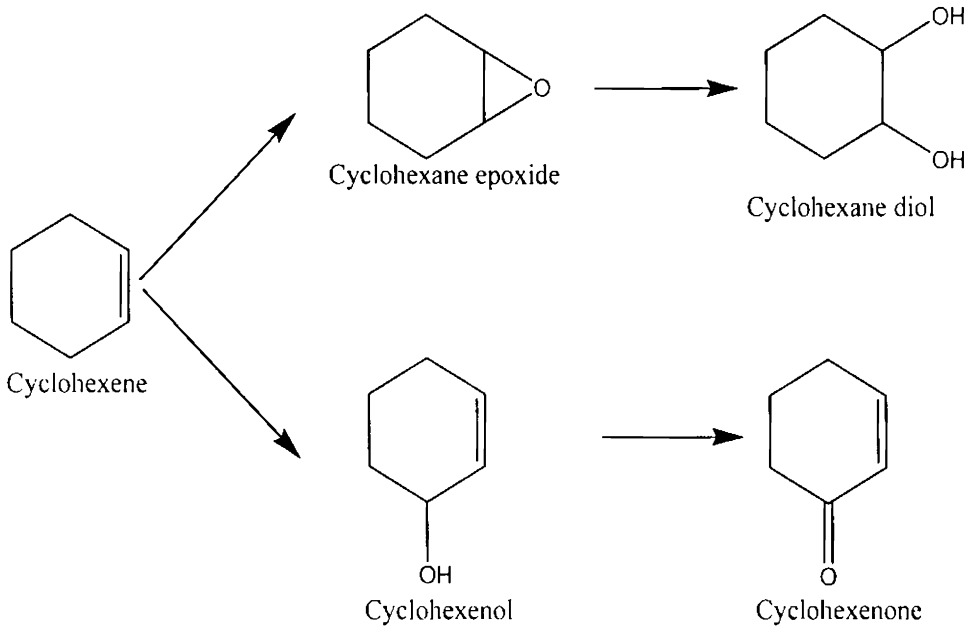


**Scheme 8.1 Reaction Pathway of cyclohexene epoxidation**

### 8.2.0 Mechanism of the Reaction

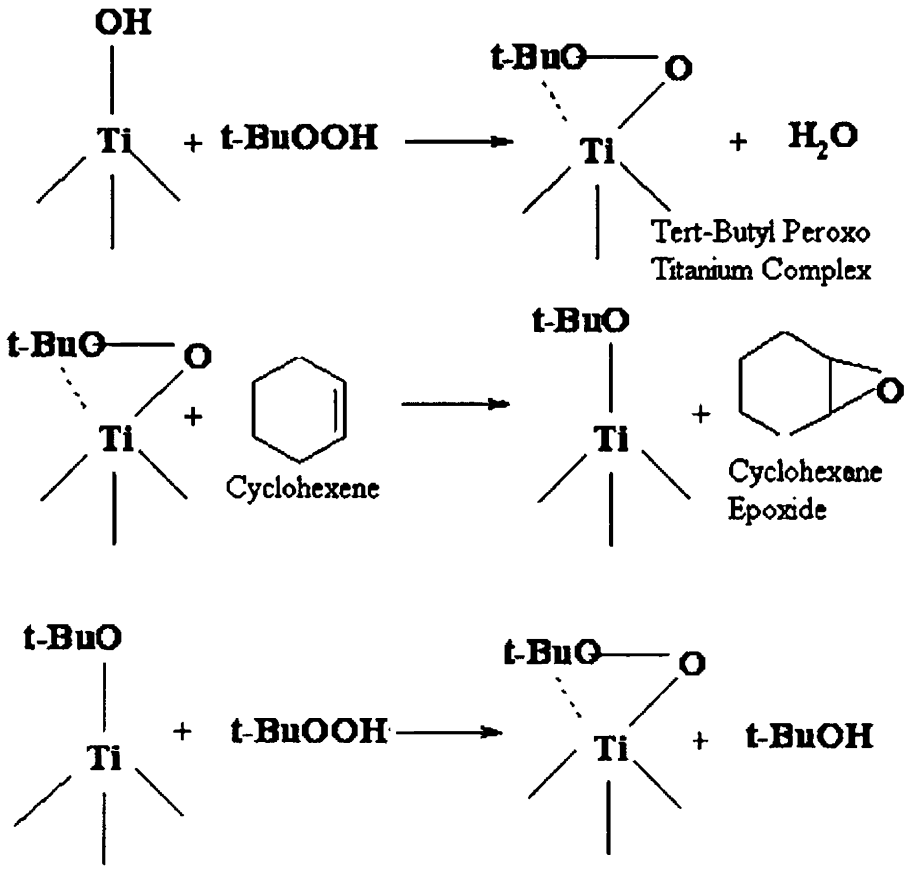


**Scheme 8.2 Proposed pathway for the epoxidation of cyclohexene**

In the epoxidation of cyclohexene, the oxidant (TBHP) interacts with titanium centers and transfers oxygen to cyclohexene. The cyclohexene epoxidation proceeds via free alkoxyl radical chemistry (ie, O-O bond homolysis of TBHP). Upon the exposure of $TiO_2$ surface with this TBHP, *tert-* butyl peroxo titanium complex is formed. The peroxo titanium complex formed by the direct reaction between the prepared catalysts of titania and TBHP should have been considered as another candidate for an active species. This suggests that the Ti–OO-*t*-Bu is a plausible active

species .The cyclohexene epoxidation is then proceeded by oxygen transfer from the *tert-* butyl peroxo titanium complex to the cyclohexene double bond. The consumed complex is finally regenerated by *tert-* butyl hydro peroxide. The enhanced cyclohexene conversion in the case of metal modified titania systems may be attributed to the assistance of the added metal oxide to form the corresponding *tetra.-* butyl peroxo titanium complex. The additional possibility of the added metal to form the corresponding *tetra.-* butyl peroxo complex due to the ability of the metal to form a variety of high valent oxocomplex cannot be ignored. A schematic representation of the reaction mechanism is also given :-

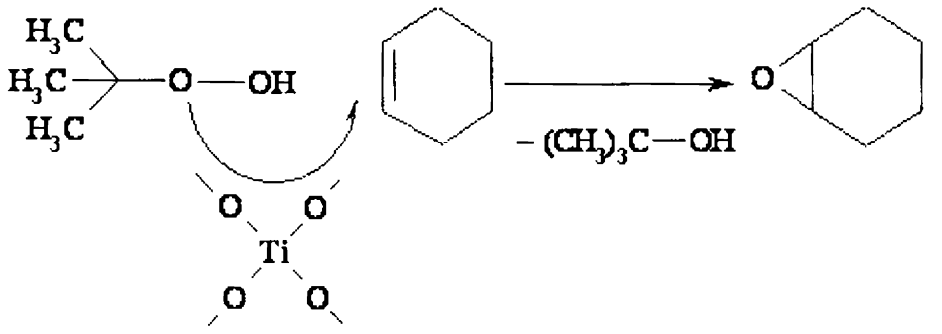


**Scheme 8.3 Schematic representation of the reaction mechanism**

### 8.3.0 Procedure of the Reaction

The epoxidation of cyclohexene with tert-butyl hydroperoxide was carried out in a 50 ml round bottomed flask having a side tube equipped with a reflux condenser and a thermometer. The reactor and oil bath were continuously stirred to ensure that the system was well mixed and isothermal. In a standard procedure 0.1g of the catalyst,$TiO_2$-Ce 6 and

reactant cyclohexene and oxidant TBHP, in the mole ratio 1:2 were added into 10ml of the solvent, acetonitrile. The mixture was heated to 313K under stirring. All the reagents were used as such without further purification. The samples were withdrawn at different reaction time and the products were separated by filtration .Then the products were analyzed by gas chromatography using a capillary column (Chemitto GC 1000, FID, SE 30 column-12m length, 0.25mm Dia,$N_2$ carrier gas). Product identification was done by comparing the retention times with standards. Two other systems were also performed keeping the temperature at 323K and 333K respectively.

When the reaction is conducted in the absence of a catalyst (blank run) and in the presence of the catalyst (0.1g $TiO_2$.Ce6),it is observed that in the blank run, even after 3h, the percentage conversion is only 2wt % and the number of detectable side products remained very low. When conducted in presence of 0.1g of $CeO_2/TiO_2$ catalyst under the same reaction conditions, the yield is 89 wt % with prominent selectivity for all the products formed. From this it can be concluded that in presence of the catalyst, the reaction proceeded through a different path with lower activation energy. Hence the percentage conversion is higher in the catalyzed reaction.

**8.4.0 Influence of reaction conditions**

The reaction is conducted by varying the reaction parameters like the time of the reaction, temperature, mole ratio of reactant and oxidant, amount of the catalyst, different solvents and compared the activity of these systems under the same reaction condition to get an favourable optimized state. This is discussed below.

### 8.4.1 Effect of Time

The epoxidation of cyclohexene, was carried out continuously for 6h at 323K using TBHP as the oxidant in presence of acetonitrile as solvent over the prepared catalyst systems in order to study the effect of time on the reaction. Figures 8.1,8.2 and 8.3 show the time courses for the epoxidation of cyclohexene over $TiO_2$, $TiO_2$-Ce6, and $TiO_2$-Cu6 respectively. It is observed that a common trend is followed in the activity as well as in the epoxide selectivity. During the initial stages of the reaction the percentage conversion increased and approached an almost steady value within 3h. But the selectivity towards the corresponding epoxide increased till to 3h of the reaction and thereafter it drops suddenly. This may be due to the possible side reactions. These reactions afford mostly allylic oxidation products and oligomers, and thus limit the epoxidation selectivity.

**Reaction Conditions**

| | |
|---|---|
| Catalyst chosen | -0.1g $TiO_2$, $TiO_2$-Ce6, $TiO_2$-Cu6 |
| Cyclohexene : TBHP | -1:2 |
| Solvent | -10ml Acetonitrile |
| Temperature | -323K |

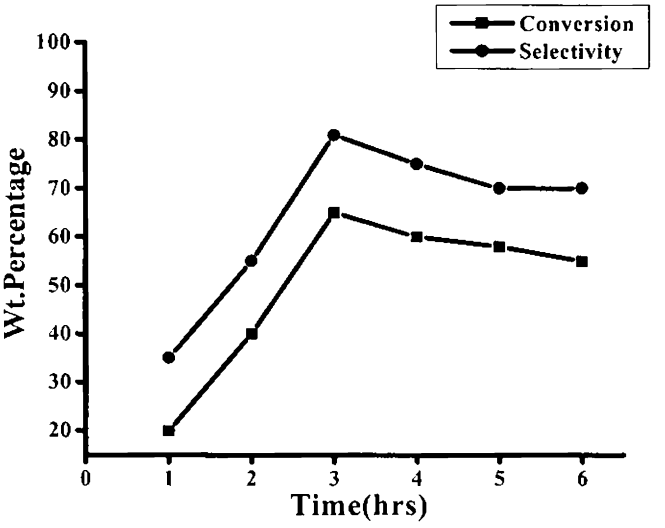


**Fig8.1 Effect of time on the reaction by $TiO_2$**

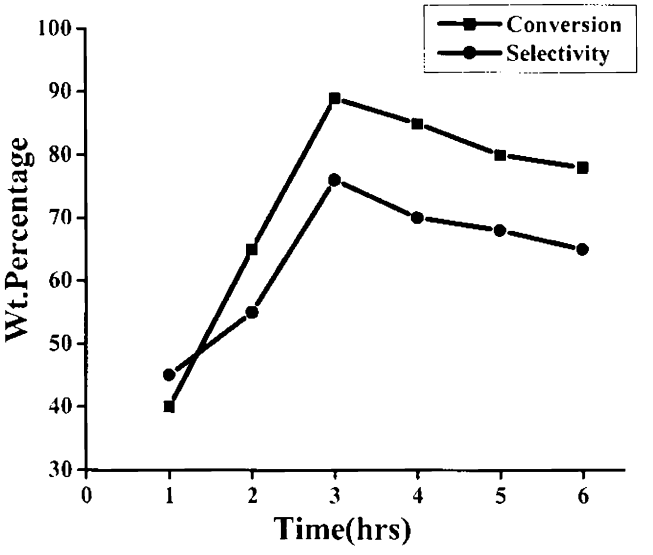


**Fig8.2 Effect of time on the reaction by $TiO_2$-Ce6**

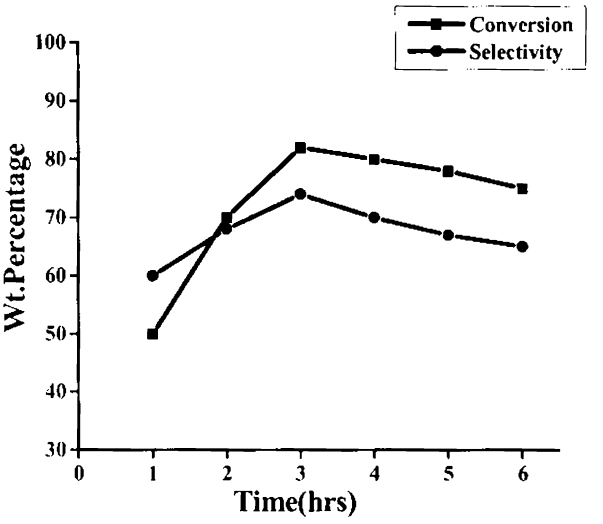


**Fig8.3 Effect of time on the reaction by $TiO_2$-Cu6**

### 8.4.2 Effect of Temperature

The epoxidation of cyclohexene depends greatly on the reaction temperature. The reaction was carried out with the oxidant TBHP at different reaction temperatures as 313,323 and 333K respectively and the results were given in figure 8.4. Interstingly, the product distribution varied depending on reaction temperature. The percentage conversion was 60% when conducted at a temperature of 333K. The cyclohexene conversion reached about 89% when the temperature reaches 323K with a epoxide selectivity of 76%. But as the temperature is increased, the amount of allylic oxidation products increases leading to a lower selectivity of epoxide. The percentage cyclohexene conversion decreases with temperature beyond 323K. From the results it can be concluded that the epoxidation of cyclohexene proceeds with high activity and selectivity under gentle reaction temperature. The high conversion is not accompanied

by the highest selectivity of transformation to epoxide with regard to TBHP consumed. This is due to the decomposition of TBHP to alcohol and oxygen at higher temperature. $(H_3C)_3C\text{-}OOH \rightarrow (H_3C)_3C\text{-}OH + 0.5\ O_2$

**Reaction Conditions**

Catalyst chosen - 0.1g$TiO_2$.Ce6

Cyclohexene : TBHP -1:2

Solvent -10ml Acetonitrile

Duration -3hrs

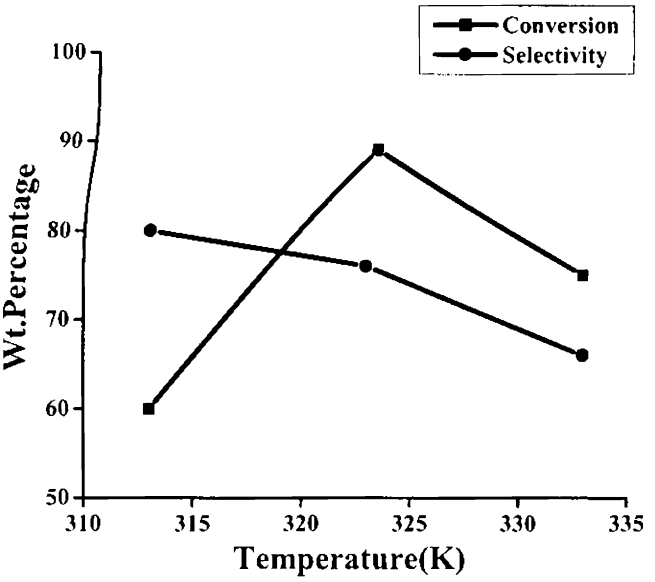


**Fig8.4 Effect of temperature on the reaction by $TiO_2$-Ce6**

### 8.4.3 Effect of Mole Ratio of Reactant:Oxidant

The epoxidation reaction was carried out using oxidants like hydrogen peroxide and tert-butyl hydroperoxide. A blank run was made by conducting the reaction without the addition of an oxidant and that yields negligible conversion with a poor selectivity of cyclohexene epoxide. At

333K,the corresponding epoxides are obtained with 50% selectivity though the percentage cyclohexene conversion is only 40 wt.%. Here the colour of the catalyst changed to brown. This can be due to the possible formation of hydroperoxy complexes with titanium. When the epoxidation is carried out with TBHP as oxidant, the conversion was very much higher with a percentage epoxide selectivity of 76 %. Despite its outstanding interest in green chemistry, hydrogen peroxide gives poorer results and so TBHP is preferred in the epoxidation of cyclohexene. Here only the TBHP graph is shown. To investigate the effect of concentration of TBHP on the rate of cyclohexene epoxidation, a series of reactions were performed with varying concentration of the reactant:the oxidant TBHP from1:1to 1:3. From the figure 8.5, it is evident that an optimum mole ratio of cyclohexene : TBHP is needed for maximum activity as well as selectivity of the products. As the concentration increases, the rate of epoxidation of cyclohexene increases with a good selectivity of cyclohexene epoxide. The rate reaches a maximum value for 1:2 mole ratio and thereafter goes on decreasing. From the observation of XPS values it can be noticed that hydroxylation degree of systems prepared in the presence of TBHP appears slightly higher. This could indicate that the presence of metal could enhance the acidic properties of the surface and hence the strength of hydroxyl groups at the surface **[28].**

**Reaction Conditions**

| | |
|---|---|
| Catalyst chosen | -0.1g $TiO_2$.Ce6 |
| Solvent | -10ml Acetonitrile |
| Temperature | -323K |
| Duration | -3hrs |

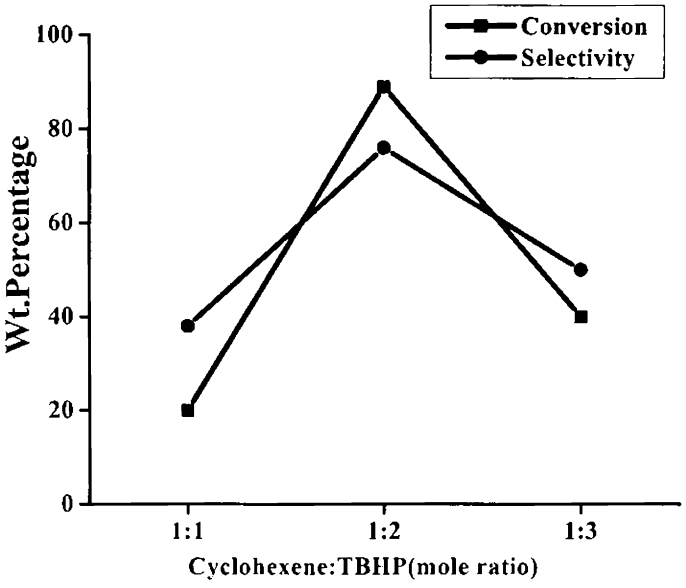


**Fig8.5 Effect of mole ratio on the reaction by $TiO_2$-Ce6**

### 8.4.4 Effect of catalyst amount

In heterogeneous catalysis, the amount of the catalyst plays an important role in determining the rate of the reaction. To study this, the catalyst weight is varied by taking different amounts of $CeO_2/TiO_2$ catalyst under otherwise identical reaction conditions. Figure 8.6 shows the influence of amount of catalyst weight on the catalytic activity and selectivity. In the absence of a catalyst, the conversion is negligible. Addition of 0.05g catalyst changes the percentage conversion from 65 to 78 in the epoxidation of cyclohexene. An initial sharp rise in the percentage conversion is observed when the catalyst amount is increased to 0.1g. After that the percentage conversion remains almost the same even though the catalyst amount is changed to 0.15g. But the percentage conversion decreases with further increase in catalyst weight. The effect of catalyst weight is more substantial when considering the epoxidation activity, but

no clear correlation of catalyst weight with the percentage conversion can be established. A gradual change in the epoxide selectivity is also noticed with the change in catalyst weight. An optimum catalyst weight of 0.1g is chosen for the present reaction, considering the percentage conversion as well as epoxide selectivity.

**Reaction Conditions**

| | |
|---|---|
| Catalyst chosen | -$TiO_2$-Ce 6 |
| Cyclohexene : TBHP | -1:2 |
| Solvent | -10ml Acetonitrile |
| Duration | -3hrs |
| Temperature | -323K |

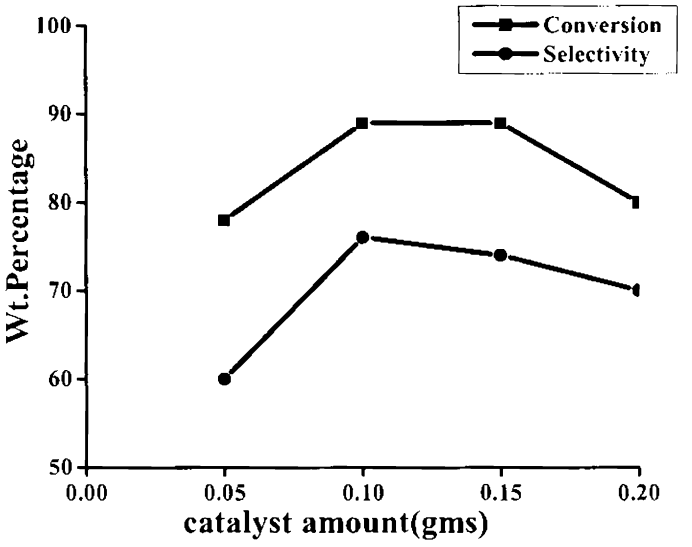


**Fig8.6 Effect of catalyst amount on the reaction by $TiO_2$-Ce6**

### 8.4.5 Effect of Solvent

Catalytic activity depends largely on the nature of solvent used. So it is necessary to find out an ideal solvent for the epoxidation of cyclohexene using TBHP as the oxidant. K.U.Ingold *et al* reported in his work that the solvent suitable for olefin epoxidation is one, which is not a hydrogen bond donor (HBD) and is also only a relatively poor hydrogen bond acceptor (HBA)**[29]**. If the solvent is a strong HBA, it would be expected to deactivate the catalyst (via any surface hydroxyl groups) and also deactivate the hydroperoxide (via ROOH....HBA hydrogen bonding).

When water is used as a solvent for epoxidation, the catalyst systems showed the least activity as well as selectivity of the epoxide. Another change noticed was the formation of a product like cyclohexene-3-(t-butyl) peroxide in appreciable amount other than this epoxide, cyclohexane diol, cyclohexenol and cyclohexenone. It has been reported that when water was added to the reaction mixture, significant amounts of cyclohexene-3- (t-butyl) peroxide was produced **[30]**. A nice balance between these various solvent requirements is achieved for TiCe6 catalyst by using acetonitrile, which may well be the optimum solvent for these epoxidation reactions.

**Reaction Conditions**

| | |
|---|---|
| Catalyst chosen | -0.1g$TiO_2$.Ce 6 |
| Cyclohexene : TBHP | -1:2 |
| Solvent volume | -10ml |
| Duration | -3hrs |
| Temperature | -323K |

| Solvent | Conversion (wt %) | Selectivity (%) | | |
|---|---|---|---|---|
| | | Epoxide | Diol | 1-ene + 1-ol |
| Water | 10 | 10 | 48 | 42 |
| Acetonitrile | 89 | 76 | 18 | 6 |
| Isopropanol | 15 | 20 | 52 | 28 |

**Table8.1 Effect of solvent on the reaction by $TiO_2$-Ce6**

## 8.5.0 Catalytic activity of different systems in the reaction

**Optimized Reaction Conditions**

Catalyst amount -0.1g

Cyclohexene: TBHP -1:2

Solvent -10mlAcetonitrile

Temperature -323K

Duration -3hrs

| Catalyst | Conversion (wt %) | Selectivity (%) | | |
|---|---|---|---|---|
| | | Epoxide | Diol | enol + enone |
| $TiO_2$ | 65 | 81 | 17 | 2 |
| $TiO_2$ -Ce 3 | 82 | 65 | 35 | - |
| $TiO_2$ -Ce 6 | 89 | 76 | 18 | 6 |
| TiO2 -Ce 9 | 85 | 80 | 12 | 8 |
| TiO2 -Cu 3 | 79 | 52 | 48 | - |
| TiO2 -Cu 6 | 82 | 74 | 16 | 10 |
| TiO2 -Cu 9 | 78 | 75 | 13 | 12 |

**Table 8.2 Effect of the catalysts in the reaction**

A comparative account of the catalytic activity of various metal modified titania systems in the epoxidation of cyclohexene is given in the Table 8.2. All the prepared systems were tested for activity over a reaction time of 6h under the optimized reaction conditions, temperature of 323K using 10 ml acetonitrile solvent and the reactant: oxidant mole ratio as cyclohexene : TBHP is 1:2. The results of epoxidation of cyclohexene over metal modified titania systems were presented in the table 8.2. Titania catalyts like 3,6 and 9 wt % metal incorporated systems were subjected to the study of this particular reaction.The different catalytic systems were represented- for 3wt%of the metal loaded catalyst of ceria and copper as $TiO_2$-Ce 3,$TiO_2$-Cu 3 , for 6wt%of the metal loaded catalyst of ceria and copper as$TiO_2$ -Ce6 ,TiO2 -Cu 6 and TiO2 -Ce 9 TiO2 -Cu 9 for 9 wt %of the metal loaded catalyst of ceria and copper. Pure titania exhibited poor activity towards the epoxidation of cyclohexene. The interesting point to be noted is that in spite of its poor activity, pure titania shows a very good selectivity towards cyclohexene epoxide. Whatever be the nature of the metal incorporated, all the catalytic systems give cyclohexene epoxide as the major product. Higher conversion of cyclohexene is observed in the case of $TiO_2$ -Ce 6 and TiO2 -Cu 6 catalysts. Remarkable conversion was shown by $TiO_2$-Ce 6 catalyst among all the other systems. But the selectivity to cyclohexene epoxide is higher in the case of 9wt% incorporated metals of Ceria and Copper modified titania catalytic systems. An attempt to investigate the influence of the metal loading on catalytic activity is quite reasonable. As expected, variation in metal loading had a significant impact on the catalytic cativity. As the percentage of metal loading is increased from 3 to 6wt.%, the conversion is also increased and thereafter it decreases but the selectivity increased gradually. Reports

provide access to highly dispersed Lewis acidic sites, which can effectively activate the alkyl hydroperoxide oxidant[31-32].It is concluded that Lewis acidic sites are electron acceptors and $Ce^{4+}$ state accepts electron and gets changed to $Ce^{3+}$state.The good epoxidation activity and selectivity of modified titania systems is attributed to the presence of highly dispersed Lewis acidic titanium sites which is evident from the $NH_3$-TPD graph.

**8.6.0 Reusability of the catalysts**

Regeneration and stability studies of the catalysts were tested for various cycles by introducing the same catalyst in the reaction mixture and observed that the recovered catalysts are less effective as expected in comparison to fresh ones. Though pure titania exhibited poor activity towards the epoxidation of cyclohexene it can be recycled. But owing to leaching of cerium ions under the same reaction conditions the activity of the $TiO_2$-Ce 6 catalyst systems seems to diminish. This is generally observed with all liquid-phase reactions more predominantly with peroxide catalyzed reaction in acetonitrile solvent [33]. Generally, use of 30% peroxide and acetonitrile as solvent results considerable leaching[34]. But it has been found that even after four regeneration cycles the activity, i.e. both conversion as well as selectivity of $TiO_2$-Cu6 catalyst remains same as in the initial cycle, showing the efficiency of the catalysts.

## References


1. M.G. Clerici, Topics Catal, 13 (2000) 373.
2. N.N. Trukhan, V.N. Romannikov, A.N. Shamkov, M.P. Vanina, E.A. Paukshtis, V.I. Bukhtiyarov, V.V. Kriventsov, I. Yu. Danilov and O.A. Kholdeeva, Micropor. Mat. 59 (2003) 73.
3. A. Tuel and L.G. Hubert – Pfalzgraf, J. Catal. 217 (2003) 343.
4. P.T. Tanev, M. Chibwe and T. Pinnavaia, Nature, 368 (1994) 321.
5. L.Y. Chen, G.K. Chuah and S. Jaenicke, Catal. Lett, 50 (1998) 107.
6. Regina Buffon and Ulf Schuchardt, J. Braz. Chem. Soc, 14 (2003) 347.
7. L.Y. Chen, G.K. Chuah and S. Jaenicke, Catal. Lett, 50 (1998) 107.
8. D. Trong On, D. Desplantier-Giscard, C. Danumah,S. Kaliaguine, Appl.Catal. A 222 (2001) 299.
9. A. Sayari, P. Lui, Micropor. Mater. 12 (1997) 149.
10. J.Y. Ying, C.P. Mehnert, M.S. Wong, Angew. Chem. Int. Ed.Engl. 38 (1999) 56.
11. W.Yu-de, M. Chun-lai, S. Xiao-dan, L. Heng-de, Appl. Catal.A 246 (2003)161.
12. S. Velu, M.P. Kapoor, S. Inagaki, K. Suzuki, Appl. Catal. A245 (2003)317.
13. G. Tolstikov, Reactions of Hydroperoxide Oxidation, Nauka, Moscow, U.S.S.R (1976).
14. Lu, Xiaolin Guo, WeilinWang, Xikui GeneralReview CA Section: 49(Industrial Inorganic Chemicals) 18(2004) 35-38
15. Hee-Seok Cheong, Kyoung-Ku Kang and Hyun-Ku Rhee, Catal. Lett, 86 (2003) 145.
16. Peng Wu and Takashi Tatsumi, Catal. Surveys from Asia, 8 (2004) 137.
17. Vasudev N. Shetti, P. Manikandan, D. Srinivas and P. Ratnasamy, J. Catal,216 (2003) 461.
18. A. Gisler, C.A. Muller, M. Schneider, T. Mallat and A. Baiker, Topics Catal, 15 (2001) 247.
19. Epoxidation of olefins using molecular oxygen Patent Application WO 200158887, BayerAG(2001).
20. Catalyst for the production of epoxide comprises carrier containing oxide of titanium etc.Patent Application US2001020105, Nippon Shokubai (2001).

21. K.U. Ingold, Darren W. Snelgrove, Philip A. MacFaul, Richard D. Oldroyd and John Meurig Thomas, Catal. Lett, 48 (1997) 21.

22. R.A. Sheldon and J. Dakka, Catal. Today, 19 (1994) 215.

23. R.A. Sheldon and J.K. Kochi, Metal catalyzed oxidations of organic compounds, (Academic Press, New York, 1981).

24. R.A. Sheldon, Chemtech (1991) 566.

25. D.Guin, B.Barawati and S.V.Manorama; J. Mol. Catal. A. Chem. 242 (2005) 26.

26. F. Chiker, F. Launay, J.P. Nogier and J.L. Bonardet, Environ Chem Lett, 1 (2003) 117.

27. Grzegorz Lewandowski and Eugeniusz Milchert, Ind. Eng. Chem. Res, 40 (2001) 2402.

28. G. Colon, M.C. Hidalgo, G. Munuera, I. Ferino, M.G. Cutrufello, J.A.Navio, Appl. Catal. B: Environ.63(2006) 45.

29. Matt C. Rogers, Bamidele Adisa and David A. Bruce, Catal. Lett, 98 (2004) 29.

30. R. Hutter, T. Mallat and A. Baiker, J. Catal, 157 (1995) 665.

31. R. Hutter, T. Mallat, D. Dutoit and A. Baiker, Topics Catal, 3 (1996) 421.

32. K. Kosuge and P.S. Singh, J. Phys. Chem. B, 103 (1999) 3563.

33. Deng, C. Lettmann, W.F. Maier, Appl. Catal. A: Gen. 214 (2001) 31.

34. J.D. Chen, R.A. Sheldon, J. Catal. 153 (1995) 1.

Chapter 9

# Hydroxylation of Phenol


## *Abstract*

Hydroxylation of phenol is an industrially important reaction as the products, namely catechol and hydroquinone finds diverse applications. The catalytic efficiency of the prepared titania systems in the hydroxylation of phenol was carried out in liquid phase. In the present study, the catalytic activity of pure titania as well as metal modified titania systems towards phenol hydroxylation is analysed in detail. Phenol Hydroxylation reaction seems to proceed along a complex pathway involving a series of consecutive reactions. The influence of reaction variables such as reaction time, temperature of the reaction, phenol to hydrogen peroxide ratio, catalyst weight and the effect of solvent were studied so as to optimize the reaction conditions.

## 9.1.0 Introduction

A variety of heterogeneous catalyst has been investigated for the hydroxylation of phenol. Wei Zhao *et al* reported the synthesis of highly ordered Fe-MCM-48 by a mixed templation method[1]. Its catalytic activity and selectivity was studied for phenol hydroxylation using hydrogen peroxide. The substituting element $Fe^{3+}$ is partially incorporated into the framework position forming a new type of active site, which raises the phenol conversion and the diphenol selectivity. Jun Wang *et al* reported $Cu^{2+}$ exchanged zeolites as efficient catalysts for phenol hydroxylation with hydrogen peroxide[2]. Both zeolite type and copper content in the zeolite catalyst were revealed to exert critical impact upon the catalytic activity in phenol hydroxylation reaction. A.Dubey *et al.* carried out the hydroxylation of phenol over CuM(II)M(III) ternary hydrotalcites, where M(II) is Ni or Co and M(III) is Al,Cr,or Fe and they studied the influence of various reaction parameters on the percentage phenol conversion and the selectivity of catechol and hydroquinone formed as the major products[3]. Hydroxylation of phenol was carried out over a series of CoNiAl ternary hydrotalcites having a (Co+Ni)/Al atomic ratio close to 2.6 and a Co:Ni atomic ratios ranging from 1:0 to 0:1 using $H_2O_2$ as oxidant and water as solvent[4]. Both end members of this series, namely CoAl-HT and NiAl-HT, showed negligible conversion of phenol while cooperative catalytic behaviour was noted when both the elements are present together. The catalytic activities towards phenol hydroxylation is carried out over intrazeolitic $Fe^{3+}$ prepared by chemical vapor deposition of $[(C_5H_5)Fe(CO)_2]_2$ inside NaY and FSM-16 zeolites. The higher activity of the Fe/NaY sample was attributed to the high dispersity of Fe ions that are located in framework positions and to the high crystallinity[5]. Mannar R. Mayura *et al* suggested that the coordination polymers have potential

catalytic activity for the liquid phase hydroxylation of phenol[6]. The α-$Fe_2O_3/SiO_2$ catalyst exhibited very good catalytic performance in phenol hydroxylation by $H_2O_2$ to dihydroxybenzene [7]. Fe supported catalysts containing 10 wt% of iron as oxide, on titania and alumina have been prepared and its catalytic activity was measured in a batch reactor using ozone as the oxidizing agent. The catalytic activity indicates that phenol is degraded with a low mineralisation to $CO_2$ [8].

Santos *et al* reported the aqueous phase oxidation of phenol using a series of commercial copper containing catalysts at elevated temperatures and oxygen pressures[9,10]. Catalytic wet peroxide oxidation of phenol over unpromoted $MnO_2/CeO_2$ revealed that even after complete removal of organic carbon from the solution was achieved, an important fraction of the initial carbon was transformed into a polymeric material strongly adsorbed on the surface of the catalyst[11-13]. This deposit was shown to be responsible for the catalyst deactivation *via* physical blockage of the active sites[12]. Waste water containing phenol is much toxic and on oxidation, the intermediates such as Catechol, hydroquinone, o-quinone and p-quinone were identified in the first stages of phenol oxidation. They are as toxic as phenol. With increasing reaction time, the colour of the solution gradually changes to dark brown due to the formation of benzoquinones (quinones). Catechol and hydroquinone are two of the many phenolic derivatives of high value. They are widely used as photography chemicals, anti-oxidants and polymerization inhibitors and are also used in pesticides, flavoring agents, and in medicine.

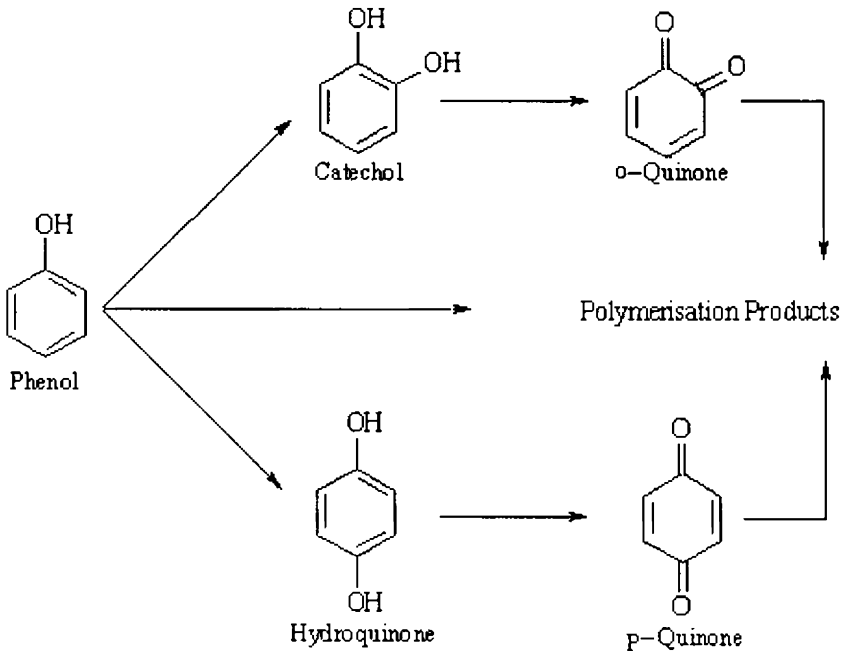


**Scheme 9.1 Reaction Pathway of phenol hydroxylation**

### 9.2.0 Mechanism of the Reaction

The appearance of an induction period and the exponential increase in the percentage conversion with time in the present study support the involvement of a free radical mechanism. Meyer et al. proposed a reaction mechanism suitable to the heterogeneous catalysis for the liquid phase oxidation **[14,15]**. An induction period was quite noticeable with all the systems, the time being dependent on the system chosen. This again suggests a free radical mechanism to be operating irrespective of the catalytic system selected. The high susceptibility of the aromatic ring of phenols towards oxidation can be attributed to the possible generation of the delocalised aryloxy radical *via.* the removal of a hydrogen atom. The generation of phenoxy radicals may occur on the catalyst surface. At the same instant, catalyst surface can also trigger the homolytic cleavage of the

hydrogen peroxide. A general mechanism of the reaction is sketched in scheme 9.2. The formation of catechol and hydroquinone is believed to occur *via.* the attack of $OH^{\bullet}$ on the benzene ring. The formation of phenoxy radicals occurs at the catalyst surface after which the propagation of the reaction can occur either in the liquid phase or on the catalyst surface. A further investigation into the course of the reaction is essential for a clear-cut prediction of the actual mechanism. The appearance of an induction period and the exponential increase in the percentage conversion with time in the present study support the involvement of a free radical mechanism. The generation of phenoxy radicals may occur on the catalyst surface. The catalysts surface can also trigger the homolytic cleavage of $H_2O_2$. All the experimental observations suggest that structural properties of the catalysts such as distribution of ions in the $TiO_2$ matrix and/or on the surface, aggregation/deaggregation and metal-assisted network formation as well as the dispersity of metal are important factors for the activity of these materials. The scheme below gives the complete mechanism of phenol hydroxylation with the products catechol and hydroquinone which further oxidizes to quinone.

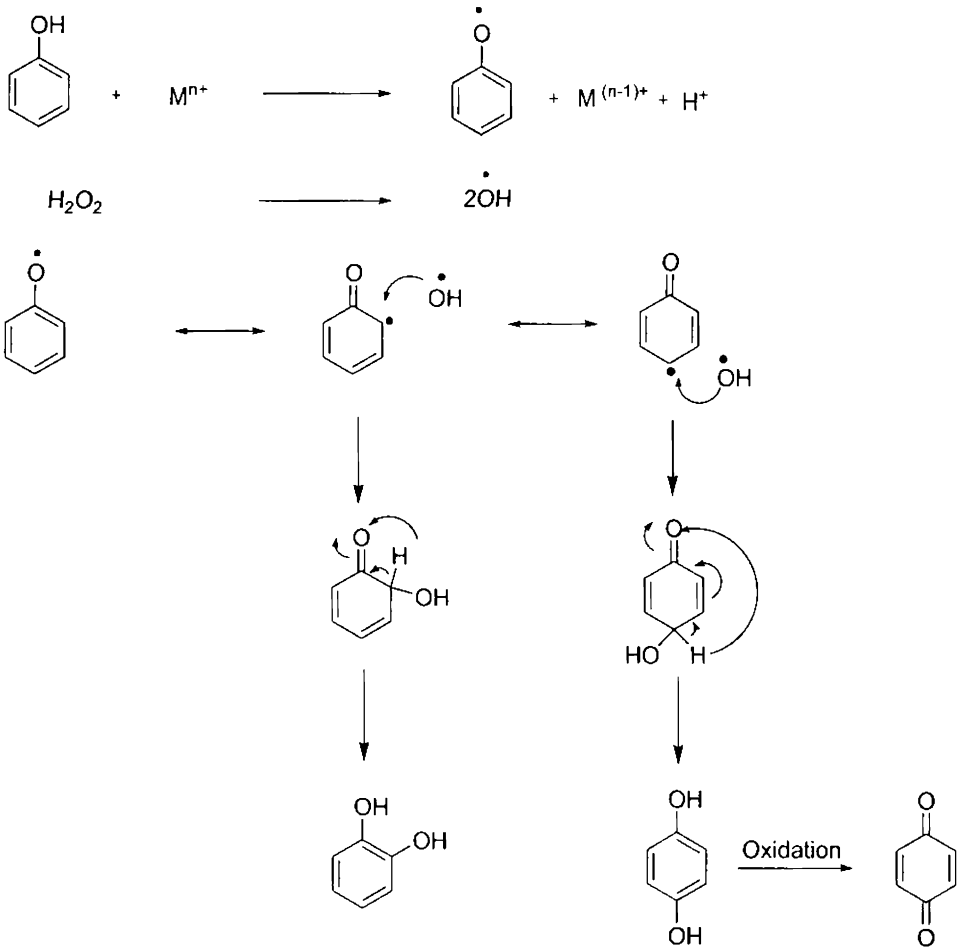


**Scheme 9.2 Proposed pathway for the phenol hydroxylation**

### 9.3.0 Procedure of the Reaction

Catalytic experiments were carried out in a round bottom flask equipped with a reflux condenser, a magnetic stirrer and a temperature controllable oil bath. The catalyst to be studied was added to start the reaction. For a typical run, 0.1 gm of the catalyst was added to 1:5 ratio of reactant : oxidant such as phenol: hydrogen peroxide and 10ml solvent water mixture and were stirred vigorously at 333K for 2h. The reaction mixture was then stirred at controlled temperature. The reaction products were analyzed at stipulated time using a Chemito 8610 gas chromatograph

using a FID detector and an OV-17 column by taking small aliquot out. Product identification was done by comparing the retention times with standards. It is well known that the solvent, reaction temperature, reaction time, catalyst size, catalyst amount, molar ratio of phenol to hydrogen peroxide are the main factors that influence the phenol hydroxylation and these factors are systematically investigated in the following sections.

The reaction is done using phenol and hydrogen peroxide in water solvent in the absence of a catalyst (blank run) and in the presence of the catalyst (0.1gm $Ti0_2$.Ce and $Ti0_2$.Cu) at 333K. Catechol (o-diphenol), hydroquinone (p-diphenol) and benzoquinons were the major products of this reaction despite the different conditions and catalysts used. We observed a percentage conversion of 2 and 52 after 60 minutes in the absence and presence of catalyst respectively.

### 9.4.0 Influence of reaction conditions

The reaction is conducted by varying the reaction parameters like the time of the reaction, temperature, mole ratio of reactant and oxidant, amount of the catalyst, different solvents and compared the activity of these systems under the same reaction conditions to get a favourable optimized state. Only hydroquinone selectivity is plotted in the graphs.

### 9.4.1 Effect of Time

Notably a relatively short reaction time resulted in incomplete conversion of phenol as well as undesirable product selectivity and the conversion increased with reaction time. There was an induction period of about 30 minutes where the systems gave marginal phenol conversion. After 30 minutes, a sharp rise was observed in the yield of diphenols. Suitably, a long reaction time was beneficial for the conversion of phenol,

but its deep oxidation of hydroquinone into benzoquinone and of benzoquinone into tar resulted in the completion of the reaction within 90 minutes. And observed that the reaction time of 60 minutes was suitable for the maximum conversion of phenol hydroxylation over the prepared systems. Only about 52wt% conversion is observed in the case of pure $TiO_2$ while $TiO_2$-Ce6 and $TiO_2$-Cu6 catalysts display 86 and 81 wt% conversion. This clearly indicates that the incorporated metals in titania matrix had a significant effect in the hydroxylation reaction.

**Reaction Conditions**

| | |
|---|---|
| Catalyst chosen | -0.1g $TiO_2$, $TiO_2$.Ce6, $TiO_2$.Cu6 |
| Phenol: $H_2O_2$ | -1: 5 |
| Temperature | -333K |
| Solvent | - 10ml Water |

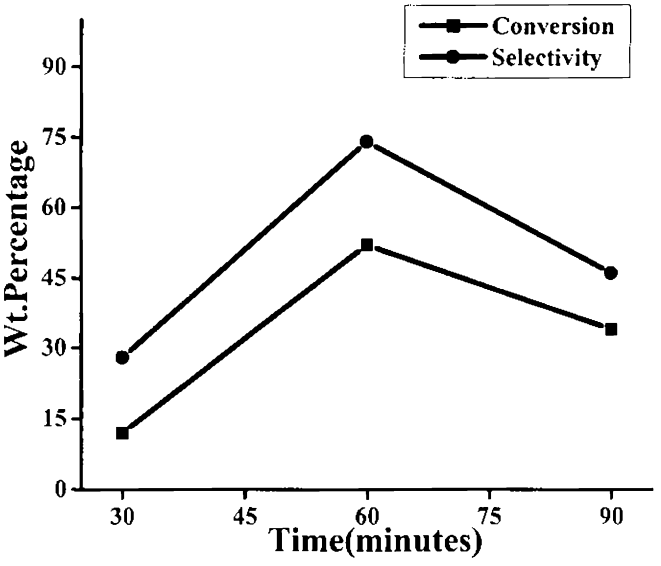


**Fig 9.1 Effect of time on the reaction by $TiO_2$**

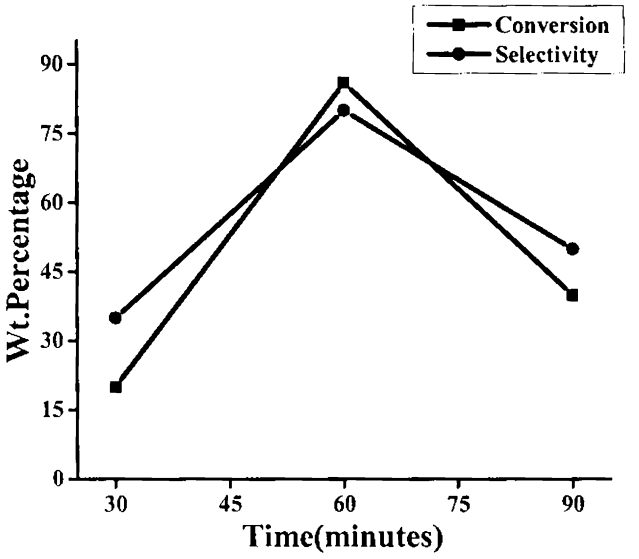


Fig 9.2 Effect of time on the reaction by $TiO_2$.Ce 6

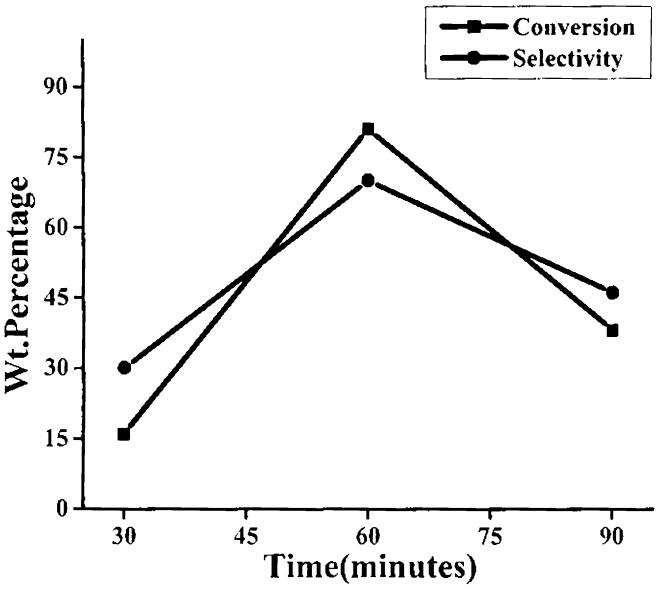


Fig 9.3 Effect of time on the reaction by $TiO_2$.Ce 6

### 9.4.2 Effect of Temperature

The activities and product selectivities in the temperature range of 323-343K for phenol hydroxylation with $H_2O_2$ over TiCe6 catalyst are presented in the figure 9.4. Obviously phenol conversion increased when the reaction temperature increases from 323 to 333K and when the temperature was above 333K, there is a remarkable reduction in phenol conversion. At 323K,phenol conversion was only 22% with a hydroquinone selectivity of 52%. When the temperature increased to 333K, phenol conversion increased to 86% with hydroquinone selectivity of 81%. Considering both conversion and selectivity, the reaction temperature chosen for hydroxylation reaction was 333K.

The decrease in phenol conversion with increase in reaction temperature is consistent with the exothermic nature of the reaction. The accelerated decomposition of $H_2O_2$ at elevated temperatures may also contribute to the drop off in the conversion. It has been reported that the activation energy for the decomposition of $H_2O_2$ is lower than that for the hydroxylation of phenol[16]. Above 343K, the amount of residual phenol in the reaction mixture was rather negligible. However, no peaks could be detected in the GC analysis corresponding to the products. This may be due to the overoxidation resulting in tarry products.

**Reaction Conditions**

| | |
|---|---|
| Catalyst chosen | -0.1g $TiO_2$-Ce6 |
| Phenol: $H_2O_2$ | -1: 5 |
| Duration | -60minutes |
| Solvent | - 10ml Water |

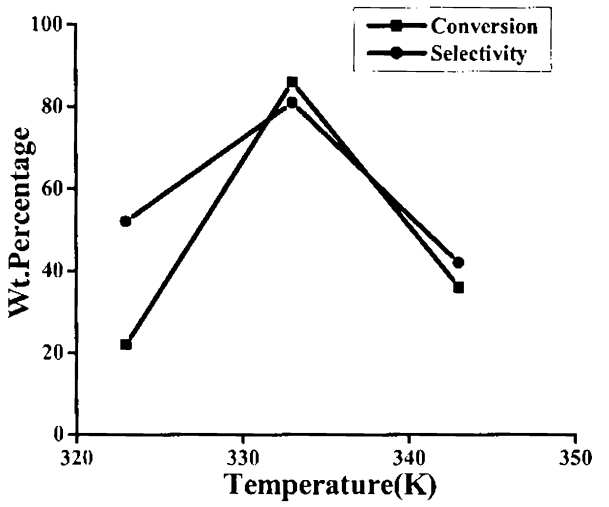


**Fig9.4 Effect of temperature on the reaction by $TiO_2$-Ce6**

### 9.4.3 Effect of Mole Ratio of Reactant:Oxidant

The influence of molar ratio of phenol to hydrogen peroxide in phenol hydroxylation over TiCe6 catalyst is summarized in figure . A larger molar ratio of hydrogen peroxide to phenol in the catalysis led to higher efficiency of utilization for $H_2O_2$. The phenol conversion first increases with the increase in the ratio to a certain extent and thereafter an increase in the phenol to $H_2O_2$ ratio causes a drastic reduction in the percentage conversion. The drastic reduction may be related to the overoxidation of phenol to tarry products at high peroxide concentration. The product selectivity is also influenced by the phenol to $H_2O_2$ molar ratio. At an optimum molar ratio of 1:5 the percentage selectivity is highest with a good product distribution.

**Reaction Conditions**

| | |
|---|---|
| Catalystchosen | -0.1g$TiO_2$-Ce6 |
| Temperature | -333K |
| Solvent | - 10ml Water |
| Duration | -60 minutes |

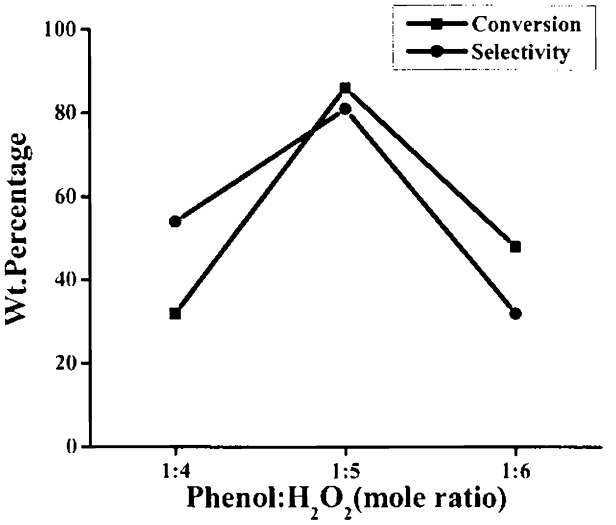


**Fig9.5 Effect of mole ratio on the reaction by $TiO_2$-Ce6**

### 9.4.4 Effect of catalyst amount

The effect of different amounts of the catalyst TiCe6 in phenol hydroxylation reaction is discussed here. Hydroxylation occurs very slowly in the absence of a catalyst. Phenol conversion increased with a catalyst amount up to 0.1g and then a further increase in catalyst amount decreases the phenol conversion. Addition of large amount of the catalyst to the reaction mixture had a negative effect in the prepared systems. This is because a larger amount of the catalyst hastened the decomposition of

hydrogen peroxide. Therefore a suitable amount of the catalyst in the catalysis was found to be 0.1gm.

**Reaction Conditions**

| | |
|---|---|
| Phenol: $H_2O_2$ | -1: 5 |
| Solvent | - 10ml Water |
| Temperature | -333K |
| Duration | -60 minutes |

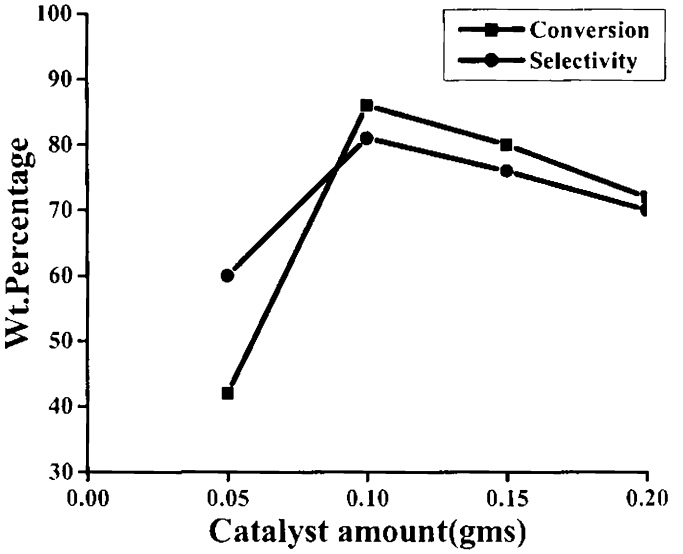


**Fig9.6 Effect of catalyst amount on the reaction by $TiO_2$-Ce6**

### 9.4.5 Effect of Solvent

It has been reported that the solvents in this reaction has a profound influence on the phenol conversion and the product selectivity. Table presents a summary of solvent influence in phenol hydroxylation over TiCe6 catalyst. When acetone is used as a solvent, the hydroxylation occurs at a slower rate even at temperatures up to 343K. Interestingly a change from organic solvents to water led to a significant increase in phenol conversion, indicating that water is the best solvent for this reaction over

the prepared systems. In the present study, water is used as a solvent. Water is safe, cheap and environmentally friendly solvent. However the amount of water strongly affected the phenol conversion and the product selectivity. At 333K, the catalytic activity was in the order water > acetonitrile > acetone.

**Reaction Conditions**

| | |
|---|---|
| Catalyst chosen | -0.1g $TiO_2$.Ce6 |
| Phenol: $H_2O_2$ | -1: 5 |
| Solvent volume | -10ml |
| Temperature | -333K |
| Duration | -60 minutes |

| Solvent | Conversion (wt %) | Selectivity (%) | |
|---|---|---|---|
| | | Catechol | Hydroquinone |
| Acetone | 12 | 16 | 84 |
| Water | 86 | 19 | 81 |
| Acetonitrile | 22 | 18 | 82 |

**Table9.1 Effect of solvent on the reaction by $TiO_2$-Ce6**

### 9.5.0 Catalytic activity of different systems in the reaction

**Optimized Reaction Conditions**

| | |
|---|---|
| Catalyst amount | -0.1g |
| Phenol: $H_2O_2$ | -1: 5 |
| Temperature | -333K |
| Solvent | - 10ml Water |
| Duration | -60 minutes |

| catalyst | Conversion (wt%) | Selectivity (%) | |
|---|---|---|---|
| | | Catechol | Hydroquinone |
| $TiO_2$ | 52 | 26 | 74 |
| $TiO_2$ -Ce 3 | 72 | 24 | 76 |
| $TiO_2$ -Ce 6 | 86 | 20 | 80 |
| TiO2 -Ce 9 | 78 | 22 | 78 |
| TiO2 -Cu 3 | 70 | 28 | 72 |
| TiO2 -Cu 6 | 81 | 30 | 70 |
| TiO2 -Cu 9 | 76 | 32 | 68 |

**Table 9.2 Effect of the catalysts in the reaction**

The table 9.2 presents the results of phenol hydroxylation over pure and metal loaded titania catalytic systems respectively. After optimization studies, catalytic activity of all the prepared systems were evaluated. Pure titania gave low conversion under the specified conditions and the metal loaded systems are highly effective in hydroxylating phenol.It is believed that the proximity of the hydroxylating agent and of the substrate molecule on or near the active catalyst site is essential for driving the reaction. In water, both phenol and hydrogen peroxide dissolve simultaneously and approach the active center, thereby generating hydroxy radicals, proposed to be the active species involved in the hydroxylation reaction. Moreover such an electrophile is easier produced and stabilized in water than in organic solvents. Possibly, the lack of hydroxylated nature for the other organic solvents may be responsible for the non-occurrence of this reaction. Furthermore when this reaction is carried out using different oxidants other than hydrogen peroxide, namely oxygen, air and tert-butyl hydroperoxide, none of them hydroxylate phenol to a significant extent under similar

reaction conditions, possibly due to the lack of generation of the active oxidant species and the solubility problems associated with the reactant and the oxidant. But no strict correlation is obtained between the catalytic activity and the catalyst properties. Among the metal incorporated systems, the individual effects created by the addition of the respective species may be playing a dominating role in deciding the catalytic activity. In all the systems, the percentage phenol conversion increases with the metal loading. This supports the active involvement of the incorporated metal in the reaction. Another interesting observation was that metal loaded systems gave good selectivity to hydroquinone(para product). To conclude, this study infer that a combined influence of various factors like the surface area, crystallite size and the electron accepting properties (redox properties) may be the driving force for the reaction. Ceria loaded titania systems showed higher phenol conversion and a good diphenol selectivity.

### 9.6.0 Reusability of the catalysts

The activity of the metal loaded systems were highly effective in hydroxylating phenol but the catalysts due to the high amount of tarry products formed and further the structural instability results in the deactivation of all the systems completely after the first cycle itself.

## References


1. Wei Zhao, Yunfei Luo, Peng Deng and Quanzhi Li, Catal Lett., 73(2001)199.
2. Jun Wang, Jung-Nam Park, HaCheol Jeong, Kwang-Sik Choi, Xian-Yong Wei, Suk-In Hong and Chul Wee Lee, Energy and fuels., 18(2004) 470.
3. A.Dubey, S.Kannan, S.Velu, K.Suzuki, Appl.Catal.A,Gen., 238(2003) 319.
4. Vicente Rives, Olga Prieto, Amit Dubey and Srinivavsan Kannan, J.Catal.,220(2003) 161.
5. Mohamed Mokhtar Mohamed, N.A.Eissa, Mat. Research Bulletin.,38(2003) 1993.
6. Mannar R.Mayura, Indu Jain, Salam J.J.Titinchi, Appl.Catal.A, Gen.,249(2003) 139.
7. Qingsheng Liu, Jianfeng Yu, Zhenlu Wang, Piaoping Yang and Tonghao Wu, React.Kinet.Catal.Lett.,73(2001) 179.
8. Gina Pecchi and Patrico Reyes, J. Sol-gel sci and Tech., 26 (2003) 865.
9. A.Santos, E.Barroso, F.G-Ochoa, Catal. Today., 48 (1999) 109.
10. A.Santos, P.Yustos, B.Durban, F.G-Ochoa., Catal. Today, 66 (2001) 511.
11. S.Hamoudi, F.Larachi, A.Sayari, J. Catal.., 177 (1998) 247.
12. S.Hamoudi, F.Larachi, A.Adnot, A.Sayari, J. Catal., 185 (1999) 333
13. S.Hamoudi, A.Sayari, K.Belkacemi, L.Bonneviot, L.Larachi, Catal. Toda.y, 62 (2000) 379
14. C.Meyer, G.Clement, J.C.Balaceanu, "Proc. 3rd Int. Congr. On Catalysis", Vol. 1 (1965) 184.
15. A.Sadana, J.R.Katzer, J. Catal., 35 (1974) 140.
16. R.Yu, F-S. Xiao, D.Wang, Y.Liu, G.Pang, S.Feng, S.Qiu, R.Xu, Catal. Lett., 49 (1997) 49

# Chapter 10

# Summary and conclusions

## 10.1.0 Summary

Scientists throughout the world are in search of a better methodology to reduce the use of environmentally hazardous chemicals common in industries .A significant contribution in this field is given by different redox catalysts in oxidation reactions. The oxidation of organic substrates represents one of the most important industrial chemical reactions, explaining the significant efforts invested in the research and development of new heterogeneous catalysts with increased activities and selectivities in these type reactions[1-4]. Hence liquid phase reactions like epoxidation of cylcohexene and hydroxylation of phenol were carried out with a new outlook in the challenge using $CeO_2/TiO_2$ and $CuO/TiO_2$ catalysts denoted as $TiO_2$-Ce as $TiO_2$-Cu respectively in this work. Also different wt% of metals incorporated titania catalysts like 3, 6, 9 wt% $CeO_2/TiO_2$ and $CuO/TiO_2$were subjected to the present study. But, in order to test the catalytic activity of the prepared systems, the experimental conditions were optimized using a particular catalyst, here, 6wt.% loaded $CeO_2/TiO_2$ catalyst denoted in the work as $TiO_2$-Ce6.This work also envisages the redox behaviour of ceria and copper due to its lattice defect structure, the importance of redox catalysis played by these catalysts, results of various characterization methods applied and the behaviour of the

strong acidic sites during heterogeneous catalysis which is still less reported, the surface as well as bulk characterization of supports and supported titania catalysts, in detail [5]. The interaction between metal oxides and the oxide supports have attracted much attention because of the wide applications of supported metal oxide systems. It is well known that supported metals oxides of titania were widely used as catalysts for various heterogeneous oxidation reactions. The oxidation products of these reactions are important in fine chemical industry, pharmaceuticals etc. In liquid phase reactions like epoxidation of cylcohexene and hydroxylation of phenol, many industrially important products are formed like cyclohexene epoxide could replace cyclohexenone as an intermediate in the synthesis of adipic acid, the precursor for Nylon 66 whereas Catechol and hydroquinone are two of the many phenolic derivatives of high value. Higher activity and selectivity of 6 wt% metals incorporated titania catalysts were observed, than the reported values[6]. The use of hydrogen peroxides in the oxidation of organic molecules is a major goal, both in academic and in industry, because of the environmental acceptability of this oxidant, which depends mainly on the nature of its by-product, water. Alkylated hydrogen peroxides like TBHP is a better oxidizing agent in certain type of oxidations. The catalytic behaviour is strongly influenced by the oxidants.

The interaction between metal oxides and the oxide supports have attracted much attention because of the wide applications of supported metal oxide systems[7,8]. It is well known that supported oxides of transition metals are widely used as catalysts for various reactions. Titania as well its metal modified catalysts systems afford high activity and selectivity in the liquid phase epoxidation of cyclohexene[9]. Cyclohexene epoxide is obtained as the major product during the reaction with small amounts of allylic substitution products. The catalytic behaviour is strongly

influenced by the reaction temperature, catalyst concentration, nature and amount of solvent as well as oxidant**[10]**.The excellent activity and selectivity in the epoxidation of cyclohexene is due to highly dispersed Lewis acidic titanium sites. The activity of the prepared catalysts and their stability with time in the epoxidation of cyclohexene by tert-butyl hydroperoxide hints that it might be possible to create cleaner nylon chemistry. The metallisation of $TiO_2$ photocatalyst induced Brønsted acidic sites and increased Lewis acidic sites on the $TiO_2$ surface which can be clearly understood by the ammonia TPD graphs. The strong acidities imparted a high reactivity on $TiO_2$ surface toward adsorbing reactant and oxygen molecules. Evidently, modification not only increased the number of strong Lewis acidic sites, but also induced an amount of Brønsted acidic sites on the surface of $TiO_2$. It suggests that the surface acidities of pure $TiO_2$ were too weak to react **[11]**. $TiO_2$-Ce6 catalyst exhibits strong Lewis acidic sites as well as Brønsted acidic sites and behaves as a strong redox catalyst, thus accepting electron, in the liquid phase oxidation reactions like epoxidation of cylcohexene and hydroxylation of phenol. Present systems show good conversion and selectivity when compared to the reported catalysts systems. It was recently demonstrated that a progressive increase of particle size will lead to a significant decrease in terms of activity, whereas in terms of selectivity, an increase in the selectivity **[12]**. This may be the reason for the detrimental effect of $Cu^{2+}$ loaded catalysts of titania in liquid phase oxidation reactions clear from the surface area determination. Apart from other catalysts, Cu metal loaded catalysts are very selective towards catechol. The reaction parameters that influence both conversion and selectivity can be optimized in such a way to get maximum catalytic efficiency.

Another interesting observation was that metal loaded systems of titania gave good selectivity to hydroquinone (para product) .This may be a consequence of some sort of association between the phenoxy radicals and the catalyst surface. Another possibility is that the diffusion of the radicals from the catalyst surface may be a slow process when compared with the attack of the hydroxy radicals. Thus, before the radical gets sufficient time to drift apart the attack by the $OH^{\cdot}$ occurs preferentially at the ortho position in case of metal loaded systems. From the above discussion, one can arrive at the conclusion that in liquid phase oxidation reactions, $CeO_2/TiO_2$ and $CuO/TiO_2$ catalysts were very active.

### 10.2.0 Conclusions

**Chapter 7**

This chapter gives an idea about the liquid phase oxidation reactions like epoxidation of cylcohexene and hydroxylation of phenol in which many industrially important products are formed. Here discusses about the redox properties of the ceria and copper incorporated titania catalysts .

**Chapter 8**

The epoxidation of cyclohexene is carried out efficiently over the prepared systems with the selective formation of cyclohexane epoxide. This reaction hints that it might be possible to create cleaner nylon chemistry. The total acidity of the prepared systems plays an important role in determining the catalytic activity in the dehydrogenation of cyclohexane and cyclohexene. The total acidity of the prepared systems plays an important role in determining the catalytic activity in the dehydrogenation of cyclohexane and cyclohexene.

## Chapter 9

A combined influence of various factors like redox properties, surface area, crystallite size, and the electron accepting properties may be the driving force for the reaction. The performance of the catalytic systems in the hydroxylation of phenol point to its potential in the degradation of phenolic wastes. Selection of an optimum reaction time also demands prime importance in order to achieve maximum activity and selectivity of the products. Metal modified titania catalysts seem to be a promising catalyst for the disposal of phenolic wastes. Pure titania gave low conversion under the specified conditions and the metal loaded systems are highly effective in hydroxylating phenol. In all the modified systems, the percentage phenol conversion increases up to 6%metal loading. This supports the active involvement of the incorporated metal in the reaction. Metal modified titania catalysts seem to be a promising catalyst for the disposal of phenolic wastes. Pure titania gave low conversion under the specified conditions and the metal loaded systems are highly effective in hydroxylating phenol. In all the modified systems, the percentage phenol conversion increases up to 6%metal loading. This supports the active involvement of the incorporated metal in the reaction. Metal modified titania catalysts seem to be a promising catalyst for the disposal of phenolic wastes. The appearance of an induction period and the exponential increase in the percentage conversion with time in the present study support the involvement of a free radical mechanism. The generation of phenoxy radicals may occur on the catalyst surface. The catalysts surface can also trigger the homolytic cleavage of $H_2O_2$.

### 10.3.0 Future Outlook

From the viewpoint of green chemistry, the use of heterogeneous catalysts like modified titania is desirable. The present investigation on the catalytic activity of modified titania catalysts reveal their high efficiency for various types of reaction like epoxidation of cyclohexene as well as hydroxylation of phenol. The work can be extended in the epoxidation of other cyclo olefins and the products of which are of independent significance and/or are valuable chemicals for synthesis of biologically active species. With its versatility and excellent control over products characteristics, hydrothermal processing has played an important role in catalyst preparation and no doubt will continue as a future oriented area. The application of the prepared catalysts makes the wet air oxidation process more attractive by achieving high conversion at considerably lower temperature and pressure. The higher activity and selectivity in the alkylation of aromatics carried out over the prepared systems is another important observation we got. Since the prepared catalysts are highly acidic, studies can be extended for various industrially important acid catalyzed alkylation and rearrangements of other aromatic molecules.

## References


1. A. Aguedach, S. Brosillon, J .Morvan, EK. Lhadi. Appl Catal B Environ.57(2005)55–62.
2. K. Bourikas, M .Stylidi, DI. Kondarides, XE. Verykios. Langmuir.21(2005)9222–30.
3. MD. Chadwick, JW. Goodwin, EJ .Lawson, PDA. Mills, B. Vincent.Colloids Surf A Physicochem Eng Asp.203(2002)229–36.
4. DN .Furlong, GD. Parfitt. J Colloid Interface Sci.65(1978)548–54.
5. L .Sun, Bolton JR. J Phys Chem;100(1996)4127–34.
6. K.Sato,M.Aoki,R.Noyri,Science,281(1998)1646.
7. A. Boonstra, C. Mutsaers, J. Phys. Chem. 79 (1975) 1694;
8. P. Salvador, C. Gutierrez, Chem. Phys. Lett. 86 (1982) 131;
9. M. Anpo, K. Chiba, M. Tomonari, S. Coluccia, M. Che, M.A. Fox,Bull.Chem. Soc. Jpn. 64 (1991) 543.
10. T. Yoshihara, R. Katoh, A. Furube, Y. Tamaki, M. Murai, K. Hara, S. Murata, H. Arakawa, A. Tachiya, J. Phys. Chem.B108(2004)3817
11. I.A. Shkrob, M.C. Sauer Jr., J. Phys. Chem. B 108 (2004) 12497
12. (12)N. Dimitratos, J.A. Lopez-Sanchez, D. Lennon, F. Porta, L. Prati, A. Villa,Catalysis Lett. 108 (2006) 147.

# PUBLICATIONS

**Journal Papers:-**

1. RATIONAL DISCOURSE ,National Journal of current research and studies, Vol. XIII. Published by Academic Cell, Mar Thoma College, Tiruvalla.

   SEMICONDUCTOR PHOTOCATALYSIS IN POLLUTION ABATEMENT

**International/National Conferences:-**

2. Oral presentation, National Symposium & Indo-US Seminar, IIP, Dehradun, April16-18, 2007.

   PHOTO CATALYTIC ACTIVITY OF TITANIA CATALYSTS BY HYDROTHERMAL ROUTE

3. Matcon-2007, International Conference, DAC,CUSAT, March 1-3, 2007.

   SYNTHESIS,CHARACTERIZATION AND PHOTOCATALYTIC ACTIVITY OF TITANIA CATALYSTS

4. National conference on smart electronics, C-met,Trichur ,March 8-9 ,2007.

   PHOTOCATALYTIC EFFICIENCY OF NANO-SILVER LOADED TITANIA CATALYSTS .

5. CTric-2008 , National Seminar ,DAC,CUSAT, January18-19, 2008.
   PLATINUM LOADED MESOPOROUS TITANIA WITH SURFACTANT TEMPLATE: PHOTOCATALYTIC ACTIVITY IN THE DEGRADATION OF DYES.

6. Orientation Programme on catalysis ,NCCR, IIT Madras, Nov17-Dec7, 2006.
   PHOTO CATALYTIC ACTIVITY OF TITANIA CATALYSTS PREPARED BY DIFFERENT ROUTES

7. FIC-06 , National seminar ,DAC, CUSAT, on March 24-25,2006.
   PHOTO CATALYTIC ACTIVITY OF TRANSITION METALS DOPED TITANIA PREPARED BY DIFFERENT ROUTES